2010

Synthesis and Characterization of Rare Earth-Nickel-Gallium Ternary Intermetallics

Kandace R. Thomas
Louisiana State University and Agricultural and Mechanical College, kthom55@lsu.edu

SYNTHESIS AND CHARACTERIZATION OF RARE EARTH-NICKEL-GALLIUM TERNARY INTERMETALLICS

A Dissertation

Submitted to the Graduate Faculty of the
Louisiana State University and
Agricultural and Mechanical College
in partial fulfillment of the
requirements for the degree of
Doctor of Philosophy

In

Department of Chemistry

By
Kandace R. Thomas
B.S., Southern University and A&M College, 2005
December 2010

DEDICATION

To my family

and

Those that helped me along the way

ACKNOWLEDGEMENTS

First, and foremost, I thank God. He has walked with me during this journey and when the load was too heavy to bear He carried me. His love for me has surpassed any obstacle that I have faced and I have faith that He has an extraordinary plan for my life.

I would like to thank my mother Shermaine M. Thomas for selflessly sacrificing to instill morals and values in myself and sisters. You have sown good seed and you shall reap a great harvest through your legacy. I thank my sisters Jasmine N. Millican and Angela C. Thomas for always believing in me. Our relationship is priceless and I could not have completed this journey without either of you. Thank you to my father Kemp Thomas, III for your spiritual guidance and constant prayer. Thank you to my step-father, Tyronne Perry, Sr. for your help and support throughout the years. Thank you to my aunt Stephanie H. Millican for always being there – you have been a continuous support for me and without you my godson would not exist. I thank my sister Scarlett M. Thomas – although time has separated us you have always been with me. To my brother Vernon Thomas – your time with us was very short, but I know that you loved me as much as a brother could love a sister. Thank you for the kind of love that will stay with me past a lifetime. I thank my younger siblings, cousins, nieces, and nephews for motivation, especially Justin M. Butler, Terrell D. Jones, Isis Francis, Joshua K. Thomas, and Tyronne Perry, Jr. I want all of you to be proud of me and I am expecting great things from you. To my loved ones that have passed away – Leola Bates Alexander, Steve B. Millican, Kemp Thomas, II, Luvinia Thomas, Nettie Millican, John W. Millican, Patricia Septh Armstead, Sara Thomas Victory, and Joseph Millican – I am proud to be a part of your legacy. Thank you for the stock of which I am made.

I thank Professor Julia Chan for guiding me through my graduate career and for supplying me with the tools I need to be successful. She saw something in me that no one else did and for that I am grateful. I would like to thank my committee members Professors George Stanley, Andrew Maverick, David Young and Jin-Woo Choi for their advice and support over the years. Special thanks go to my collaborators Professor David Young, Professor John Ditusa, Dr. Amar Karki, Dr. Monica Moldovan, and Dr. Cigdem Capan for our stimulating scientific discussions. This work would not be possible without you. I would also like to extend a warm thanks to Dr. Frank Fronczek for freely sharing his expert crystallographic knowledge.

The Chan group members past and present have been influential in this process, especially Jasmine N. Millican, Edem K. Okudzeto, Jung Y. Cho, and Dixie P. Geautreaux. They have provided both personal and professional support during this journey.

Last, but not least, I would like to thank the funding agencies that supported myself and my research: National Science Foundation – Division of Materials Research, Louisiana State University Bridge to Doctoral Fellowship, Graduate Alliance for Education in Louisiana, Sigma-Xi Grant-in-Aid, and Louisiana State University GK-12 Fellowship.

TABLE OF CONTENTS

LIST OF TABLES

LIST OF FIGURES

ABSTRACT

The structural and physical characterization of several early and latter rare earth *Ln*-Ni-Ga systems, which include Ln_2NiGa_{12} (*Ln* = Pr, Nd, Sm), α-*Ln*$NiGa_4$ (*Ln* = Y, Gd – Yb) and β-*Ln*$NiGa_4$ (*Ln* = Tb – Ho) will be presented in this work. These systems are thermodynamically located within a copious, robust phase space and provide a rich understanding of how slight modifications to synthetic preparations can yield the adoption of different structure types in a Ga-rich regime. Each of these phases is made up of well-studied substructures which lend an additional angle of apperception as to how their structure and properties are related.

Ln_2MGa_{12} (*Ln* = Pr, Nd, Sm; *M* = Ni, Cu) were studied to determine the evolution structure and properties as a function of rare earth and transition metal. These compounds are composed of alternating slabs of *Ln* surrounded by 14 Ga atoms and [NiGa/CuGa] rectangular prisms along the *c*-axis. Based on X-ray diffraction studies it was determined that the Ln_2CuGa_{12} analogues were Cu-deficient, with 90%, 78% and 77% Cu in Pr_2CuGa_{12}, Nd_2CuGa_{12}, and Sm_2CuGa_{12}, respectively.

Phases of α-*Ln*$NiGa_4$ (*Ln* = Y, Gd – Yb) and β-*Ln*$NiGa_4$ (*Ln* = Tb – Ho) were studied to determine how the crystal chemistry and properties change as a function of latter rare earth usage. α-*Ln*$NiGa_4$ (*Ln* = Y, Gd – Yb) is comprised of partial AlB_2 and distorted α-Fe substructures. Anisotropic magnetism is observed in these phases where a stronger coupling of the magnetic rare earth ions is present in the *ab*-plane. The variation of Curie-Weiss temperature as a function of *Ln*-*Ln* distance indicates RKKY-type magnetic interactions. β-*Ln*$NiGa_4$ (*Ln* = Tb – Ho), a polymorph of α-*Ln*$NiGa_4$, is composed of an inhomogeneous linear intergrowth of $BaAl_4$- and CaF_2-structure types. These phases are a disordered derivative of Ce_2NiGa_{10} and, based on previous work, are believed to be a modulated system within the Ni-Ga nets.

CHAPTER 1. INTRODUCTION

1.1 Motivation

New materials are needed now more than ever to propel the U.S. into the future of science and technology. The development of energy storage materials, microelectronics, and multifunctional structures is key for the U.S. to remain technologically competitive.[1] Crystal growth research is the footstool of innovation and discovery for materials research and has a rich history. From single crystal silicon used for microelectronics to single crystal superalloys used for jet engine turbine blades, the design and control of crystal growth has lead to technological advancements that have directly impacted our society. Although crystal growth is the fundamental basis of new materials research, it is on a decline in the U.S. Crystal growers are rarely recognized for their contributions to the materials research community. Without the synthesis of high-quality single crystals the advancement of alternative energy sources and technology development will decline.[1]

In a project to assess current work and new opportunities in the field of crystalline matter development, the National Academy of Sciences has summarized the study of crystalline systems into three grand challenges: (1) the development of next-generation of crystalline materials for future information and communications technologies, (2) the creation of new crystalline materials for energy production and conversion, and (3) evolution in the capacity to create crystalline materials by design.[1] Although intermetallic single crystals have made considerable contributions in each of the three areas, the study of these systems is on a decline in the U.S.,[1] as can be seen in Figure 1.1. Our research group works with intermetallic systems because the legacy of these materials is so vast and they offer a plethora of chemistry and physics to study.

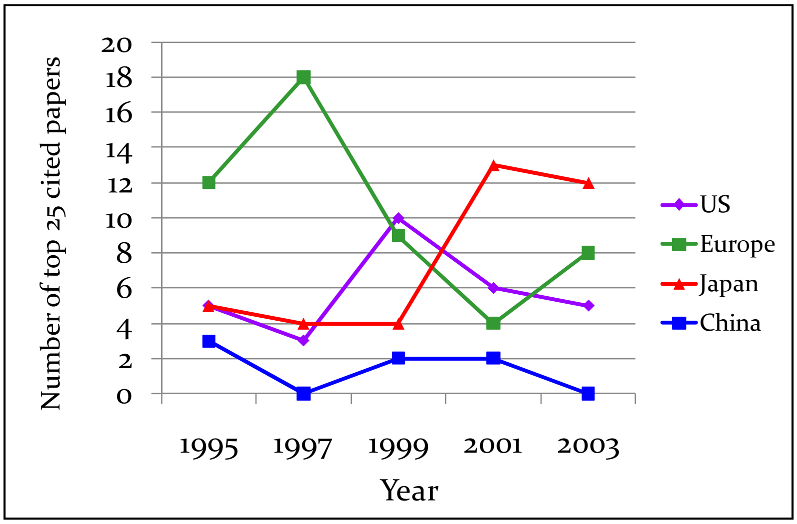

Figure 1.1 Number of top cited papers over ten years for high-temperature structural intermetallic single crystals. The graph demonstrates the location of research (which closely matches where the crystals were fabricated).[1] Adapted from reference 1.

1.2 The Focus of Our Group

Research scientists are working together to form interdisciplinary relationships in an effort to bring about advancements in next-generation technology. In our case, as solid state chemists, we work with condensed matter physicists to determine how the crystal chemistry of new phases is related to the physical properties. In particular, our streamlined focus is the growth of single crystalline materials as a tool for basic research and development. We can now consider the question "what is crystal growth?" A geologist may think of crystal growth as a naturally-occurring process in the lower surface of the Earth's crust to produce minerals and gem stones, such as quartz and ruby, respectively. A biologist may think of protein crystallization as a means to study structural biology and a pharmacologist may consider the crystalline formation of a drug for medicinal use. Although there are many different ways to grow crystals for various purposes there is a general knowledge among scientist that it can be difficult to determine the specific conditions necessary to obtain crystals with the desired phase and size. The perfect balance of materials, temperature, pressure, time, and space for optimal growth conditions is found in nature, but creating the balance for synthetic crystal growth in the laboratory requires skill and ingenuity. In the grand scheme of things we have only scratched the surface regarding all there is to be known about crystal formation processes and the design of new materials, but each experiment and each result gets us closer to the ultimate goal of structural tunability. Our motivation in particular is the search for highly correlated intermetallic systems that could potentially exhibit unusual magnetic and transport properties. We grow single crystalline materials, characterize, and collaborate with physicists to measure first-order physical properties of rare earth transition metal ternary intermetallic compounds. We study both the chemical and physical aspects of these new compounds to correlate structure and physical properties. We ask questions such as, "How will the physical properties change if we electron dope the structure?", "How does the structure change with substitution of an element?," and "How are these changes related?" In our research, it is common to grow a series of compounds to compare how the properties change as a function of small, but significant, variation of the structure. Specifically, in the study of the physical properties, we look for exotic magnetic and/or transport behavior in an effort to identify materials that will enable our understanding of chemistry and physics relevant in technology.

1.3 Materials and Methods

1.3.1 Synthesis

Self-flux growth is a synthetic method by which excess metal, usually incorporated into the compound, is used to lower the melting point of starting materials. Once the materials are in molten form they are able to react to form stable compounds upon cooling. Our starting materials consist of a lanthanide element, transition metal, and a main group element (*Ln*-*M*-*X*). An alumina crucible serves as the reaction vessel where the metals are layered with the excess metal (X) on the top. This stacking further ensures uniform melting of the other elements. After covering the crucible with quartz wool it is prepared for heat treatment by sealing it in an evacuated fused silica tube, which prevents oxidation during heating. Ampoules are then placed into a furnace for heat treatment. Heating profiles and reaction ratios are determined by: (1) the intent to avoid binary phases that are stable in that particular heating regime, and (2) previous work on similar systems containing the same elements. Once the heat treatment is complete, ampoules are inverted and centrifuged at temperatures higher than the melting point of X so that liquidus excess flux flows into the quartz wool. Once the ampoule is broken open, single crystalline product is left in the bottom of the alumina crucible and excess flux is removed by etching in dilute acid.

1.3.2 Structural Characterization - X-ray Diffraction

We utilize powder and single crystal X-ray diffraction to characterize crystalline materials, which are made up of a regular arrangement of atoms in three dimensions to form a unit cell. X-ray diffraction is a characterization technique that exploits Bragg's law $n\lambda = 2d\sin\theta$, where d is the spacing between planes of atoms, θ is the angle of incidence, and n is the diffraction order. Powder diffraction is primarily used for sample identification and to check homogeneity. A Bruker D8 Advance Powder X-ray Diffractometer equipped with Cu K_α (λ = 1.540562 Å) radiation is used for powder X-ray diffraction. Full structure determinations are performed with an Enraf Nonius Kappa CCD single crystal X-ray diffractometer equipped with Mo K_α (λ = 0.71073 Å) radiation. Low-temperature single crystal X-ray data collection is often used to evaluate the atomic displacement parameters. Temperature-dependent crystallographic studies are also useful to study systems that undergo phase transitions at a particular temperature. The types of phase transitions that we usually observe in our intermetallic systems are structural phase transitions, where a "shifting" of atoms occur when a more thermodynamically favorable arrangement exists at a given temperature. A phase transition can be evident by a change in the crystal system or a change in lattice parameters. In the context of the work presented in Chapter 4, a phase transition is evident by the formation of a superstructure, which gives rise to a second set of reflections that are associated with a periodic distortion of the basic structure.[2]

1.3.3 Physical Properties

1.3.3.1 Magnetism

The magnetic properties of rare earth intermetallic systems are usually governed by the lanthanide ions which have unpaired electrons. We typically perform temperature-dependent and field-dependent magnetization measurements to determine the magnetic properties of a new system. The applied magnetic field (H) and the magnetization (M) of the sample are related by the equation $B = H + 4\pi M$, where B is the flux density (or net local field). From the data collected the magnetic ordering type, such as ferromagnetic or antiferromagnetic, is determined.

The temperature dependence of the magnetic susceptibility (χ) is given by the Curie equation $\chi(T) = \frac{C}{T}$, where C is the Curie constant and T is the temperature. As shown in Figure 1.2, the susceptibility of a Curie-type paramagnet follows this law and the inverse susceptibility ($1/\chi$) should be linear with an intercept of zero. In the case of ferro- and antiferromagnets a third term, the Curie-Weiss temperature (θ), is used to account for the exchange interaction between magnetic moments and gives the equation $\chi = \frac{C}{T-\theta}$. A fit of the inverse susceptibility above the ordering temperature will give a Curie-Weiss temperature that is positive for a ferromagnetic interaction and negative for an antiferromagnetic interaction.[3] The experimental effective magnetic moment (μ_{eff}) is determined by an equation that relates the Curie constant and the effective magnetic moment: $\mu_{eff}^2 = \frac{3kC}{NB^2}$, where k is the Boltzmann constant, C is the Curie

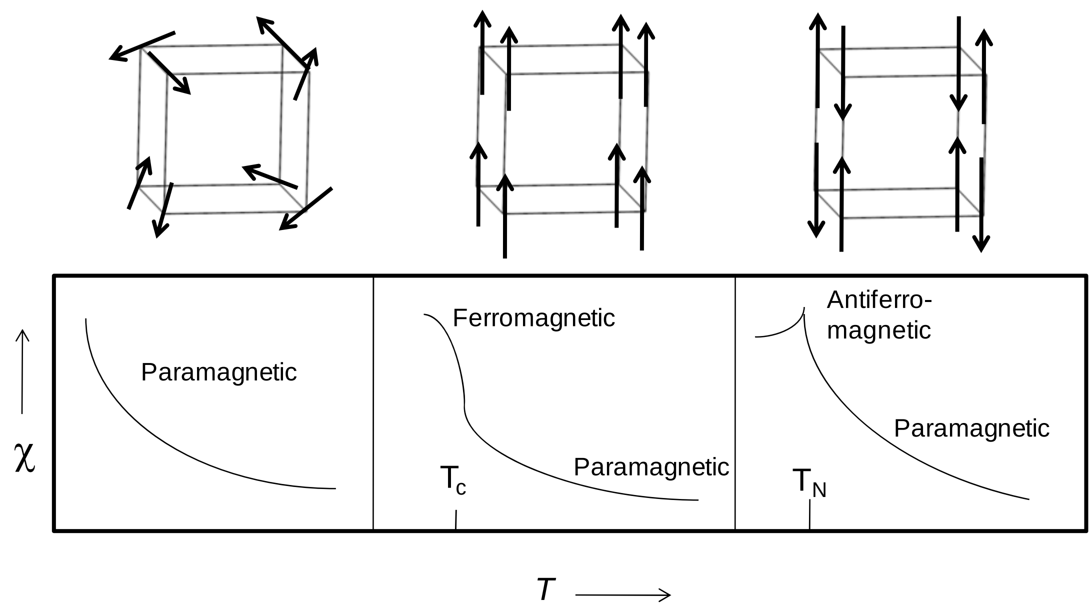

Figure 1.2 Susceptibility (χ) as a function of temperature (*T*). Arrows represent the orientation of magnetic ions in a primitive cubic cell.

constant, *N* is Avagadro's number, and *B* is Bohr magneton. The effective moment obtained from experiments can be compared to the calculated effective magneton number for a free ion and is given by $\mu_{eff} = g\sqrt{J(J+1)}$, where *g* is the gyromagnetic ratio and *J* is the total angular momentum. The value *g* is defined as $g = 1 + \frac{J(J+1) + S(S+1) - L(L+1)}{2J(J+1)}$, where *J* is the total angular momentum, *S* is the total spin angular momentum, and *L* is the total orbital angular momentum. Measurements of the magnetization as a function of field are performed to determine how the magnetic ions behave with increasing field. The calculated saturation moment is calculated by $\mu_{sat} = gJ$, where *g* is the gyromagnetic ratio and *J* is the total angular momentum.

In crystal systems that have unit cell axes that differ in dimensions, the exchange strength between magnetic moments may also differ in each crystallographic direction and can lead to anisotropic magnetism. This type of magnetic behavior is dependent upon the crystal orientation in an applied field. Measurements of $\chi(T)$ and $M(H)$ are performed with single crystals oriented parallel (||) and perpendicular (⊥) to the applied field. A stronger exchange between magnetic ions typically occurs in the crystallographic direction that has the shortest ion-ion distances and is reflected in the magnetic data.

1.3.3.2 Transport

Electrical resistivity measurements give information about how electrons travel through a material as a function of temperature. Resistivity (ρ) is inversely related to conductivity (σ) by the equation $\rho = \frac{1}{\sigma} = \frac{m}{ne^2\tau}$, where m is the mass, n is the number of electrons, e is the electron charge, and τ is time. Most of the materials presented in this work show metallic behavior where the resistivity increases with increasing temperature. Magnetoresistance (MR) is the change in resistance in an applied field and is defined as $MR(\%) = \frac{\rho_H - \rho_O}{\rho_O} \times 100$, where ρ_H is the resistance in an applied field and ρ_O is the resistance at zero field.

1.3.3.3 X-ray Photoelecton Spectroscopy

X-ray photoelectron spectroscopy (XPS) is a surface analysis technique used to study the composition and chemical state of organic and inorganic materials. A sample contained inside an ultra-high vacuum (UHV) chamber is irradiated with a beam of X-ray photons and energy is transferred to the surface atoms. This additional energy causes core electrons, now called photoelectrons, to be ejected from the atom. An energy analyzer measures the kinetic energy (KE) of the ejected photoelectron and the binding energy (BE) is determined by the equation $KE = hv - BE$, where h and v are the energy and velocity of the photon, respectively.[4]

1.4 Systems Studied in This Work

The focus of this dissertation is the crystal growth and characterization of *Ln*-Ni-Ga phases. Chapter 2 outlines work with the early lanthanides (*Ln* = Pr, Nd, Sm) which form Ln_2NiGa_{12}[5] and are isostructural to Ce_2NiGa_{12},[6] a phase that crystallizes in the tetragonal *P*4/*nbm* space group. These compounds order antiferromagnetically and from the magnetic susceptibility we have determined that only the lanthanide ions contribute to the magnetism. Latter lanthanides formed the polymorphs α-*Ln*NiGa$_4$ (*Ln* = Y, Gd – Yb)[7] and β-*Ln*NiGa$_4$ (*Ln* = Tb – Ho),[8] which are discussed in Chapters 3 and 4, respectively. Phases of α-*Ln*NiGa$_4$ (*Ln* = Y, Gd – Yb) crystallize in the orthorhombic *Cmcm* space group and have lattice parameters $a \sim 4$ Å, $b \sim 15$ Å, and $c \sim 6$ Å. The magnetism in these phases is anisotropic where there is a larger contribution from the conduction electrons in the *ab*-plane versus the *c*-axis. In this system, it was determined that there is a competition between RKKY and Kondo behavior that is directly related to *Ln*-*Ln* interatomic distance in the *ab*-plane. β-*Ln*NiGa$_4$ (*Ln* = Tb – Ho) crystallize in the tetragonal *I*4/*mmm* space group and is a disordered derivative of Ce_2NiGa_{10}, with an intergrowth of the $BaAl_4$[9] and CaF_2[10] structure types. The disorder is primarily due to the modulation of Ga in the Ni-Ga net substructures, as previously found in $YCo_{0.88}Ga_3Ge$[11] and $GdCo_{1-x}Ga_3Ge$.[12]

1.5 References

(1) *Frontiers in Crystalline Matter: From Discovery to Technology*. The National Academies Press: Washington, D.C., 2009.

(2) Bohm, H., Modulated structures at phase transitions. *Am. Mineral.* **1983,** *68*, 11-17.

(3) Kittel, C., *Introduction to Solid State Physics*. 8th ed.; John Wiley & Sons, Inc.: Hoboken, NJ, 2005.

(4) Seah, M. P.; Briggs, D., *Practical surface analysis by Auger and X-ray photoelectron spectroscopy*. 2nd ed.; Wiley & Sons: Chichester, UK, 1992.

(5) Thomas, K. R.; Cho, J. Y.; Millican, J. N.; Hembree, R. D.; Moldovan, M.; Karki, A.; Young, D. P.; Chan, J. Y., Crystal growth and physical properties of Ln_2MGa_{12} (Ln=Pr, Nd, and Sm; M=Ni, Cu). *J. Cryst. Growth* **2010,** *312*, 1098-1103.

(6) Yarmolyuk, Y. P.; Grin, Y.; Rozhdestvenskaya, I.; Usov, O.; Kuz'min, A.; Bruskov, V.; Gladyshevskii, R., Crystal chemical investigations of the series of inhomogeneous linear structures. 3. crystal structure of the $Ce_2Ga_{10}Ni$ and $La_2Ga_{10}Ni$ compounds. *Kristallografiya* **1982,** *27*, 999-1001.

(7) Thomas, K. R.; Hembree, R. D.; Karki, A. B.; Li, Y.; Young, D. P.; DiTusa, J.; Zhang, J.; Chan, J. Y., Anisotropic Magnetism in α-$LnNiGa_4$ (Ln = Y, Gd - Yb). **2010,** *In preparation*.

(8) Thomas, K. R.; Hembree, R. D.; Karki, A.; Young, D. P.; Chan, J. Y., *b*-*Ln*$NiGa_4$ (*Ln* = Tb, Dy, Ho): synthesis, structure, and physical properties of a new polymorph of *α*-*Ln*$NiGa_4$. *J. Solid State Chem.* **2010,** *Submitted*.

(9) Andress, K. R.; Alberti, E., Roentgenographische untersuchung der legierungsreihe Al-Ba. *Z. Metallkd.* **1935,** *27*, 125-126.

(10) Bragg, W. L., The analysis of crystals by the X-ray spectrometer. *P. Roy. Soc. Lond. A Mat.* **1914,** *89*, 468-489.

(11) Gray, D. L.; Francisco, M. C.; Kanatzidis, M. G., Distortion and charge density wave in the Ga square net coupled to the site occupancy wave in $YCo_{0.88}Ga_3Ge$. *Inorg. Chem.* **2008,** *47*, 7243-7248.

(12) Zhuravleva, M.; Evain, M.; Petricek, V.; Kanatzidis, M. G., $GdCo_{1-x}Ga_3Ge$: charge density wave in a Ga square net. *J. Am. Chem. Soc.* **2007,** *129*, 3082-3083.

CHAPTER 2. CRYSTAL GROWTH AND PHYSICAL PROPERTIES OF Ln_2MGa_{12} (Ln = Pr, Nd, and Sm; M = Ni, Cu)*

2.1 Introduction

In the search for highly-correlated systems, isostructural intermetallics are ideal candidates to study exotic phenomena due to the occurrence of unusual magnetic and transport properties. The synthesis of high-quality single crystals is necessary to measure the intrinsic properties of these materials. Through characterization of these intermetallic systems, we will gain knowledge about their structure-property relationships. A great example of this in the literature is the study of the Ce_nMIn_{3n+2} (n = 1, 2, ∞ and M = Co, Rh, Ir) phases, where $CeCoIn_5$ was first reported in the late 1980's, but later found to be a magnetically mediated heavy fermion superconducting system with a T_c = 2.3 K and $\gamma \sim$ 300 mJ/mol-K^2.[1, 2] Gamma (γ) is defined as the electronic contribution to heat capacity ($C_p = \gamma T + \alpha T^3$), where α is the phonon contribution and T is temperature. This finding immediately sparked interest in the Ce_nMIn_{3n+2} (n = 1, 2, ∞ and M = Co, Rh, Ir) class of compounds and led to the characterization of the Rh and Ir analogues, where a superconducting transition temperature (T_c) of 2.1 K (at 16 kbar) and $\gamma \sim$ 400 mJ/mol-K^2 and a T_c = 0.4 K and $\gamma \sim$ 750 mJ/mol-K^2 were observed for $CeRhIn_5$ and $CeIrIn_5$, respectively.[3-5] $CeIn_3$, the n = ∞ member, orders antiferromagnetically at T_N = 10 K and is also a moderate heavy fermion with $\gamma \sim$ 120 mJ/mol-K^2.[4,6] Interest in the Ce_nMIn_{3n+2} class of compounds has also motivated our group to grow Pd analogues. Our synthesis led to the discovery of a new heavy fermion, $CePdGa_6$, which orders antiferromagnetically at T_N = 5.5 K with $\gamma \sim$ 230-400 mJ/mol-Ce-K^2.[7] The moderate heavy fermion compound, Ce_2PdGa_{12} (T_N = 11 K and $\gamma \sim$ 170 mJ/mol-Ce-K^2), was later discovered and structurally compared to $CePdGa_6$.[8]

---

*Reprinted by permission of Elsevier: Thomas, K. R.; Cho, J. Y.; Millican, J. N.; Hembree, R. D.; Moldovan, M.; Karki, A.; Young, D. P.; Chan, J. Y. "Crystal growth and physical properties of Ln_2MGa_{12} (Ln =Pr, Nd, and Sm; M=Ni, Cu)", *J. Cryst. Growth* **2010**, *312*, 1098-1103.

Recently, large magnetoresistance (65 % at 9 Tesla) has been reported for Ce_2CuGa_{12},[9] a compound adopting the Sm_2NiGa_{12}[10] structure type. This structure can also be viewed as a repeating three-dimensional network of [CuGa], with Ce atoms occupying cavities made of Ga atoms. Ce_2CuGa_{12} exhibits an enhanced γ value ~ 69 mJ/mol-K^2, which led us to explore other *Ln*-Cu-Ga and *Ln*-Ni-Ga systems using Ga self-flux. In this paper we report the crystal growth and physical properties of Ln_2MGa_{12} (*Ln* = Pr, Nd, Sm; *M* = Ni, Cu).

2.2 Experimental

2.2.1 Synthesis

Single crystals of Ln_2MGa_{12} (*Ln* = Pr, Nd, Sm; *M* = Ni, Cu)) were synthesized by flux growth methods. Pr, Nd, or Sm ingot (3N Alfa Aesar), Cu powder (5N, Alfa Aesar), Ni powder (5N, Alfa Aesar) and Ga (6N, Alfa Aesar) were placed into an alumina crucible in a 1.5:1:15 reaction ratio. The crucible and its contents were then sealed into an evacuated fused silica tube and heated up to 1423 K for 7 h. After fast cooling to 673 K at a rate of 150 K/h, the tube was then slowly cooled to 573 K at a rate of 8 K/h and immediately inverted and spun with a centrifuge for the removal of excess Ga flux. Silver-color plate-like crystals were retrieved, and typical crystal size ranged from 1 × 2 × 2 to 1 × 2 × 5 mm^3. The crystals were not observed to degrade in air. Similar treatment was used to grow single crystals of Ln_2NiGa_{12} (*Ln* = Ce-Nd, Sm), where *Ln*, Ni and Ga were reacted in a 2:1:20 molar ratio inside an alumina tube.[10]

2.2.2 Single-crystal X-ray Diffraction

Silver-colored fragments, approximate size 0.025 × 0.025 × 0.05 mm^3, of Ln_2MGa_{12} (*Ln* = Pr, Nd, Sm; *M* = Ni, Cu) were mounted onto the goniometer of a Nonius KappaCCD diffractometer equipped with MoK_α radiation (λ = 0.71073 Å). Data were collected up to θ = 30.0° at 293 K. Further crystallographic parameters for Ln_2MGa_{12} (*Ln* = Pr, Nd, Sm; *M* = Ni, Cu) are provided in Table 2.1. The space group and atomic positions from Sm_2NiGa_{12} were used as an initial structural model for the structure determination of Ln_2MGa_{12} (*Ln* = Pr, Nd, Sm; *M* = Ni, Cu)) compound. The structural model was refined using SHELXL97.[11] In Ln_2CuGa_{12} analogues, the atomic displacement parameters were most well-behaved when Cu was modeled as partially occupied. Data were also corrected for extinction and refined with anisotropic displacement parameters. Atomic positions and displacement parameters for the compounds are provided in Table 2.2. The atomic displacement parameters for the Ga4 atom (8*m* site) in each phase are larger than those of the other Ga atoms. This was determined to be a form of statistical disorder in La_2CuGa_{12}. Using neutron powder diffraction, a model depicting an additional Ga atom on an 8*m* site with a partial occupancy of 0.60(4) was obtained.[9,10] In addition, a partial occupancy parameter of 0.42(4) for the original Ga4 atom was incorporated into the model to give a resultant stoichiometry of La_2CuGa_{12}. A fit of this model to our X-ray data did not result in a significant difference in the atomic displacement parameter for Ga4. The occupancy of the fifth Ga position was ~ 2 %, indicating very little electron density on the site. In addition, the electron density maps remained the same within a tenth of an electron-$Å^{-3}$. Attempts to model the Ga4 and Ga5 occupancies closer to those found in La_2CuGa_{12} resulted in a refinement divergence. Selected interatomic distances are located in Table 2.3.

2.2.3 Physical Property Measurements

Magnetization data were obtained using a Quantum Design Physical Property Measurement System. The temperature-dependent magnetization data were obtained under field-cooled (FC) conditions after cooling to 2 K under an applied field 0.1 T. Field-dependent measurements were collected at 3 K with H swept between 0 T and 9 T. Magnetic data were collected along the *c*-axis, i.e. with the magnetic field perpendicular to the single crystal plates. The electrical resistivity data were measured by the standard four-probe AC technique using 2-mil diameter Pt wires attached to the samples with a conductive silver epoxy.

Table 2.1 Crystallographic data for $Ln_2M\text{Ga}_{12}$ (Ln = Pr, Nd, Sm; M = Ni, Cu)

Crystal data					
Formula	Pr_2NiGa_{12}	Nd_2NiGa_{12}	$Pr_2Cu_{0.9}Ga_{12}$	$Nd_2Cu_{0.78}Ga_{12}$	$Sm_2Cu_{0.77}Ga_{12}$
a (Å)	6.008(4)	6.010(3)	6.078(5)	6.046(5)	6.010(5)
c (Å)	15.45(2)	15.445(5)	15.368(5)	15.334(5)	15.318(5)
V (Å^3)	557.8(5)	557.8(4)	567.7(7)	560.5(7)	553.2(7)
Z	2	2	2	2	2
Crystal system	tetragonal	tetragonal	tetragonal	tetragonal	tetragonal
Space group	$P4/nbm$	$P4/nbm$	$P4/nbm$	$P4/nbm$	$P4/nbm$
θ range (°)	3.96-27.89	3.96-29.98	2.65-30.01	2.66-30.01	2.66-30.03
μ (mm^{-1})	53.231	39.138	37.918	38.764	40.481
Data Collection					
Measured reflections	933	1250	1418	1198	1438
Independent reflections	346	466	477	472	466
R_{int}	0.1161	0.0460	0.0370	0.0520	0.0337
h	-7→7	-8→8	-8→8	-8→8	-8→8
k	-5→5	-5→5	-6→6	-6→6	-5→5
l	-17→15	-21→20	-21→16	-21→17	-19→21
Refinement					
$^aR^1[F^2>2\sigma(F^2)]$	0.0493	0.0442	0.0313	0.0386	0.0283
$^bwR^2(F^2)$	0.1063	0.1153	0.0749	0.0906	0.0721
Reflections	346	466	477	472	466
Parameters	26	26	27	27	27
$\Delta\rho_{max}$ (eÅ^{-3})	4.359	2.740	2.608	2.861	1.890
$\Delta\rho_{min}$ (eÅ^{-3})	-2.889	-2.868	-1.951	-2.122	-2.155

$^aR_1 = \Sigma||F_o| - |F_c||/\Sigma|F_o|$.
$^bwR_2 = [\Sigma[w(F_o^2-F_c^2)^2]/\Sigma[w(F_o^2)^2]]^{1/2}$; $w = 1/[\sigma^2F_o^2 + (0.0553P)^2 + 0.00P]$, $w = 1/[\sigma^2F_o^2 + (0.0638P)^2 + 6.8374P]$, $w = 1/[\sigma^2F_o^2 + (0.0337P)^2 + 3.6566P]$, $w = 1/[\sigma^2F_o^2 + (0.0431P)^2 + 3.8865P]$, and $w = 1/[\sigma^2F_o^2 + (0.0329P)^2 + 4.2364P]$ for Pr_2NiGa_{12}, Nd_2NiGa_{12}, $Pr_2Cu_{0.9}Ga_{12}$, $Nd_2Cu_{0.78}Ga_{12}$, and $Sm_2Cu_{0.77}Ga_{12}$, respectively.

2.3 Results and Discussion

2.3.1 Synthesis and Structure

We have reported the optimized synthesis route for Ce_2PdGa_{12} and Ce_2CuGa_{12} and realized that this structure type (we call it 2-1-12 for convenience) can be formed in low temperature ranges with a Ga rich reaction ratio. Because compounds adopting the $ThCr_2Si_2$[12] structure type in the Ln-M-X (Ln = lanthanide, M = transition metal, X = main group elements) ternary system are robust and readily form in a Ga-rich environment, several synthesis attempts to grow the 2-1-12 phase were required to eliminate minor impurities. $Ln_2M\text{Ga}_{12}$ (Ln = Pr, Nd, Sm; M = Ni, Cu) are isostructural to Sm_2NiGa_{12}. Along the crystallographic c-axis, this structure is composed of alternating slabs of [NiGa/CuGa] rectangular prisms and Ln (Ln = Pr, Nd, and Sm) atoms surrounded by Ga atoms as shown in Figure 2.1.

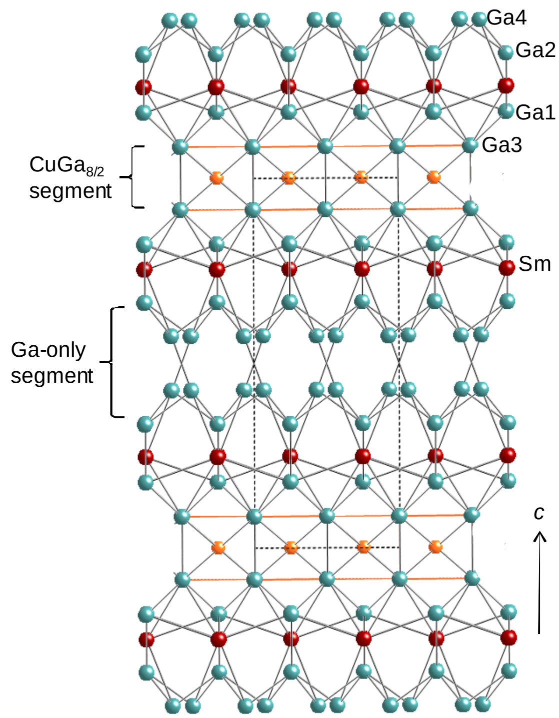

Figure 2.1 The crystal structure of Sm_2CuGa_{12}, where Sm, Cu, and Ga are represented by red, orange, and blue spheres, respectively. Dashed lines are used to show the unit cell.

The local Ln environment of Ln_2MGa_{12} (Ln = Pr, Nd, Sm; M = Ni, Cu) consists of 14 nearest neighbor Ga atoms. The decrease of Ln-Ga distances in the local Ln environment from Ce to Sm follows the trend of cell volumes for these phases and are in good agreement with those found in other binary and ternary systems such as LnGa$_6$,[13] Ln_3Ga,[14,15] LnCuGa$_3$ (Ln = Pr, Nd, Sm),[16,17] and LnNi$_x$Ga$_{4-x}$ (Ln = Pr, Nd, Sm).[18]

Table 2.2 Atomic positions and atomic displacement parameters for $Ln_2M\mathrm{Ga}_{12}$ (Ln = Pr, Nd, Sm; M = Ni, Cu)

atom	Wyckoff position	x	y	z	occ.[a]	U_{eq} (Å^2)[b]
Pr_2NiGa_{12}						
Pr	4*h*	3/4	1/4	0.24459(11)	1	0.0067(6)
Ni	2*c*	3/4	1/4	0	1	0.0047(13)
Ga1	4*g*	3/4	3/4	0.1816(2)	1	0.0088(10)
Ga2	4*g*	3/4	3/4	0.3394(3)	1	0.0120(10)
Ga3	8*m*	0.5006(3)	0.0006(3)	-0.08399(16)	1	0.0068(7)
Ga4	8*m*	0.5697(4)	0.0697(4)	0.4281(2)	1	0.0219(10)
Nd_2NiGa_{12}						
Nd	4*h*	3/4	1/4	0.24438(5)	1	0.0070(3)
Ni	2*c*	3/4	1/4	0	1	0.0072(6)
Ga1	4*g*	3/4	3/4	0.18242(10)	1	0.0081(4)
Ga2	4*g*	3/4	3/4	0.34007(11)	1	0.0113(5)
Ga3	8*m*	0.50032(14)	0.00032(14)	-0.08391(7)	1	0.0085(4)
Ga4	8*m*	0.57323(17)	0.07323(17)	0.42840(8)	1	0.0185(4)
$Pr_2Cu_{0.9}Ga_{12}$						
Pr	4*h*	3/4	1/4	0.24651(3)	1	0.0078(2)
Cu	2*c*	3/4	1/4	0	0.895(8)	0.0101(6)
Ga1	4*g*	3/4	3/4	0.17783(7)	1	0.0107(3)
Ga2	4*g*	3/4	3/4	0.33631(7)	1	0.0123(3)
Ga3	8*m*	0.50038(10)	0.00038(10)	-0.08516(5)	1	0.0130(3)
Ga4	8*m*	0.56341(14)	0.06341(14)	0.42637(7)	1	0.0247(3)
$Nd_2Cu_{0.78}Ga_{12}$						
Nd	4*h*	3/4	1/4	0.24682(4)	1	0.0106(3)
Cu	2*c*	3/4	1/4	0	0.781(10)	0.0171(10)
Ga1	4*g*	3/4	3/4	0.17737(9)	1	0.0137(4)
Ga2	4*g*	3/4	3/4	0.33574(9)	1	0.0154(4)
Ga3	8*m*	0.50061(14)	0.00061(14)	-0.08452(6)	1	0.0190(3)
Ga4	8*m*	0.56445(17)	0.06445(17)	0.42649(7)	1	0.0258(4)
$Sm_2Cu_{0.77}Ga_{12}$						
Sm	4*h*	3/4	1/4	0.24674(3)	1	0.0075(2)
Cu	2*c*	3/4	1/4	0	0.772(9)	0.0120(8)
Ga1	4*g*	3/4	3/4	0.17814(7)	1	0.0108(3)
Ga2	4*g*	3/4	3/4	0.33569(8)	1	0.0119(3)
Ga3	8*m*	0.50041(11)	0.00041(11)	-0.08522(5)	1	0.0155(3)
Ga4	8*m*	0.56722(13)	0.06722(13)	0.42651(6)	1	0.0207(3)

[a]Occupancy.
[b]U_{eq} is defined as one-third of the trace of the orthogonalized U_{ij} tensor.

Table 2.3 Selected interatomic distances (Å) for Ln_2MGa_{12} (Ln = Pr, Nd, Sm; M = Ni, Cu)

	Ln layer		MGa$_{8/2}$ segment		Ga-only segment	
Pr_2NiGa_{12}	Pr-Ga1 (×4)	3.1577(13)	Ni-Ga3 (×4)	2.485(3)	Ga2-Ga4 (×4)	2.597(3)
	Pr-Ga2 (×4)	3.3420(19)	NiGa3 (×4)	2.494(3)	Ga4-Ga4 (×1)	2.518(6)
	Pr-Ga3 (×2)	3.264(3)	Ga1-Ga3 (×4)	2.605(3)		
	Pr-Ga3 (×2)	3.270(3)				
	Pr-Ga4 (×2)	3.223(3)				
Nd_2NiGa_{12}	Nd-Ga1 (×4)	3.1537(6)	Ni-Ga3 (×4)	2.4866(12)	Ga2-Ga4 (×4)	2.6006(12)
	Nd-Ga2 (×4)	3.3488 (9)	NiGa3 (×4)	2.4912(12)	Ga4-Ga4 (×1)	2.538(3)
	Nd-Ga3 (×2)	3.2629(13)	Ga1-Ga3 (×4)	2.6134(12)		
	Nd-Ga3 (×2)	3.2664(13)				
	Nd-Ga4 (×2)	3.2148 (15)				
$Pr_2Cu_{0.9}Ga_{12}$	Pr-Ga1 (×4)	3.2171(5)	Cu-Ga3 (×4)	2.5134(10)	Ga2-Ga4 (×4)	2.6134(10)
	Pr-Ga2 (×4)	3.3378(7)	CuGa3 (×4)	2.519(10)	Ga4-Ga4 (×1)	2.511(2)
	Pr-Ga3 (×2)	3.2790(11)	Ga1-Ga3 (×4)	2.5778(9)		
	Pr-Ga3 (×2)	3.2833(11)				
	Pr-Ga4 (×2)	3.1960(12)				
$Nd_2Cu_{0.78}Ga_{12}$	Nd-Ga1 (×4)	3.2053(8)	Cu-Ga3 (×4)	2.4956(17)	Ga2-Ga4 (×4)	2.6101(15)
	Nd-Ga2 (×4)	3.3161(10)	CuGa3 (×4)	2.5044(17)	Ga4-Ga4 (×1)	2.508(3)
	Nd-Ga3 (×2)	3.2772(18)	Ga1-Ga3 (×4)	2.5679(14)		
	Nd-Ga3 (×2)	3.2840(18)				
	Nd-Ga4 (×2)	3.1798(18)				
$Sm_2Cu_{0.77}Ga_{12}$	Sm-Ga1 (×4)	3.1830(6)	Cu-Ga3 (×4)	2.4904(14)	Ga2-Ga4 (×4)	2.6048(12)
	Sm-Ga2 (×4)	3.2992(8)	CuGa3 (×4)	2.4963(14)	Ga4-Ga4 (×1)	2.521(3)
	Sm-Ga3 (×2)	3.2600(14)	Ga1-Ga3 (×4)	2.5589(11)		
	Sm-Ga3 (×2)	3.2645(14)				
	Sm-Ga4 (×2)	3.1632(15)				

2.3.2 Physical Properties

The magnetic susceptibilities of Ln_2NiGa_{12} (Ln = Pr and Nd) are presented in Figure 2.2. Pr_2NiGa_{12} and Nd_2NiGa_{12} order antiferromagnetically at ~ 18 K (θ = 5.37 K) and ~ 10 K (θ = -5.6 K), respectively. A modified Curie-Weiss equation $\chi(T) = \chi_0 + C/(T - \theta)$ was used to obtain the magnetic moments for each lanthanide ion, where χ_0 represents the temperature-independent

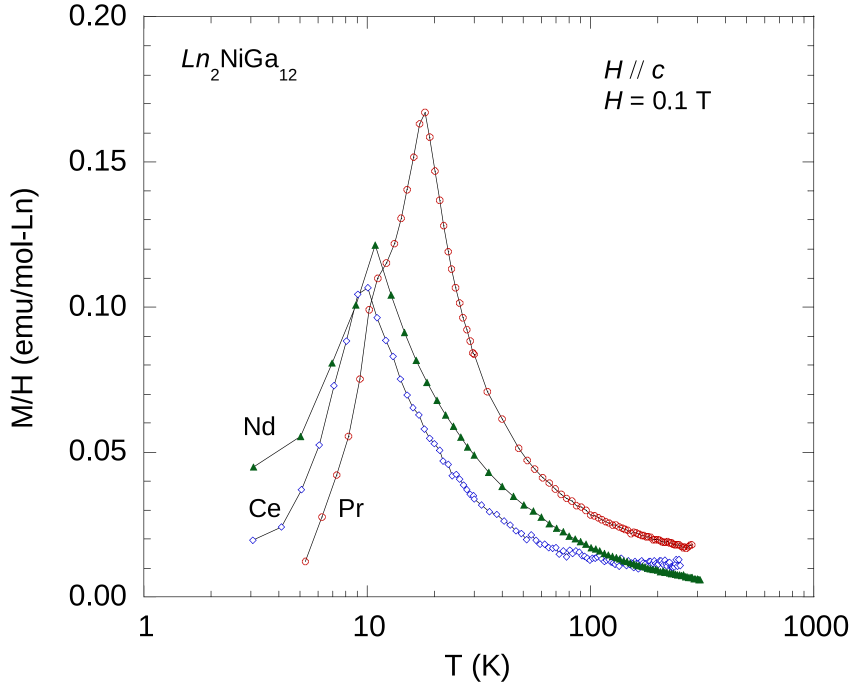

Figure 2.2 Magnetic susceptibility (emu/mol-*Ln*) of Ln_2NiGa_{12} as a function of temperature.

term, C is the Curie constant, and θ is the Weiss temperature. All fits are consistent with the spin-only moments of Ln^{3+} and magnetic data are summarized in Table 2.4.

The isothermal magnetization of Pr_2NiGa_{12}, as shown in Figure 2.3, is linear up to ~ 1 T, where a sharp metamagnetic transition occurs. A second stepwise increase in magnetization occurs around 2.5 T over a range of about 1 μ_B/Ln, where thereafter saturation of the moments begin around 1.7 μ_B/Ln, lower than the calculated saturation value for Pr^{3+} of 3.20 μ_B. Figure 2.3 shows the magnetization curves for Nd_2NiGa_{12} and Ce_2NiGa_{12},[9] where a meta-magnetic transition is also observed around 3.4 T. There is also an acute increase in magnetization for the Nd analogue close to 0 T, indicating that at low fields, the magnetization measurements may have begun in the middle of a metamagnetic transition. Saturation of this curve occurs around 1.4 μ_B, which is lower than the calculated saturation moment of 3.27 μ_B for Nd^{3+}. The meta-magnetic transitions observed in the field-dependent magnetization are again most likely due to a

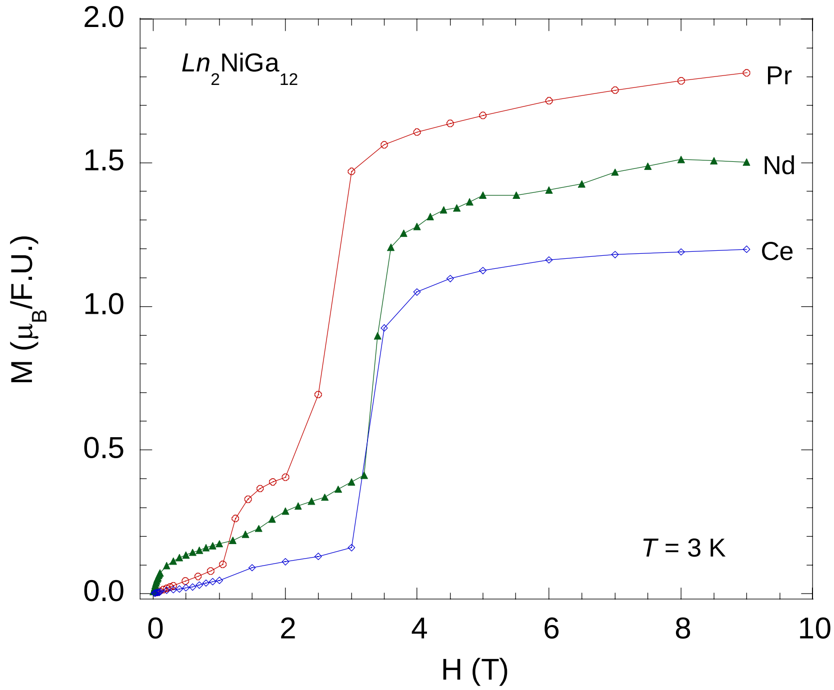

Figure 2.3 Magnetization of Ln_2NiGa_{12} (*Ln* = Ce, Pr, Nd) as a function of magnetic field.

spin-flop transition. The double transitions may result from spin-flop transitions between antiferromagnetic moments in-plane, and then a transition between planes.

The electrical resistivity of Ln_2NiGa_{12} (*Ln* = Pr, Nd, Sm, and Ce) along the *ab*-plane are presented in Figure 2.4. Each compound is metallic below room temperature, with RRR values ranging from 2 - 12. No signature of the antiferromagnetic ordering at the Néel temperatures was observed in the resistivity data for the current applied in the *ab*-plane. The magnetoresistance of Pr_2NiGa_{12}, Nd_2NiGa_{12}, and Sm_2NiGa_{12} are positive up to 100 % at H = 9 T and show classical MR behavior.

Magnetic susceptibility as a function of temperature under an applied field of 0.1 T along the crystallographic *c*-axis of single crystals of Ln_2CuGa_{12} (*Ln* = Pr, Nd, and Sm) are shown in Figure 2.5. Ln_2CuGa_{12} (*Ln* = Pr, Nd, and Sm) show antiferromagnetic ordering at 8.7 K, 2.9 K,

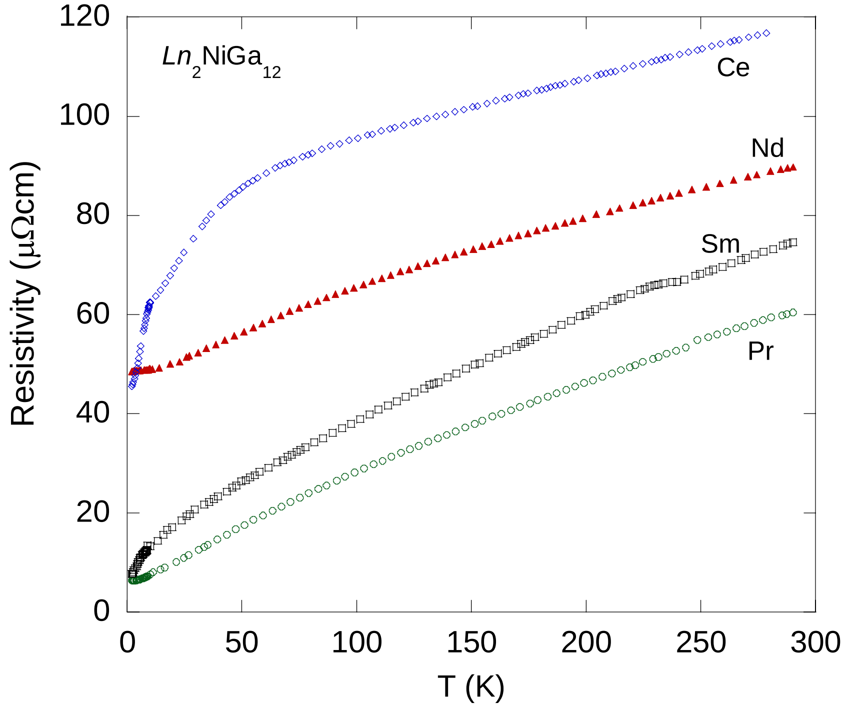

Figure 2.4 Electrical resistivity of Ln_2NiGa_{12} (*Ln* = Pr, Nd, Sm) as a function of temperature for current parallel to the *ab*-plane.

and 7.6 K for Pr_2CuGa_{12}, Nd_2CuGa_{12}, and Sm_2CuGa_{12}, respectively. The inset of Figure 2.5 shows the magnetic susceptibility of Sm_2CuGa_{12} for clarity. From fitting the magnetic susceptibility from 20 K to 250 K (from 20 K to 200 K for the Sm analogue), the effective moments (μ_{eff}) per *Ln* ion are 3.25 μ_B (Pr_2CuGa_{12}), 3.85 μ_B (Nd_2CuGa_{12}), and 0.52 μ_B (Sm_2CuGa_{12}). Figure 2.6 shows the isothermal magnetization in an applied field along the *c*-axis at 3 K. The magnetization of Pr_2CuGa_{12} increases linearly with field up to 1.5 T and then undergoes a sharp increase, i.e. meta-magnetic transition whose midpoint is ~1.75 T. Above the meta-magnetic transition (H > 2 T), the data are no longer linear, but appear paramagnetic, following a typical Brillouin curve. The data suggest that the linear increase in magnetization moments, and a spin-flop transition occurs at the metamagnetic transition, destroying the

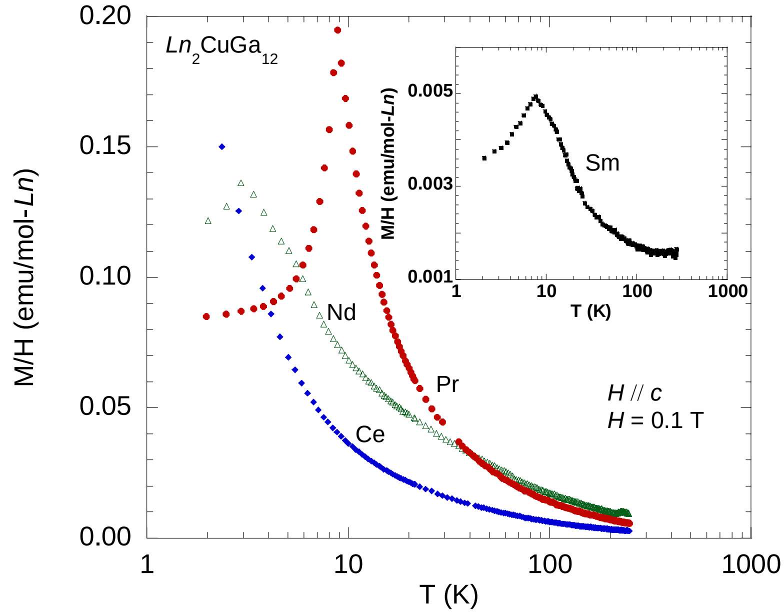

Figure 2.5 Magnetic susceptibility (emu/mol *Ln*) of Ln_2CuGa_{12} (*Ln* = Pr, Nd, Sm) as a function of temperature.

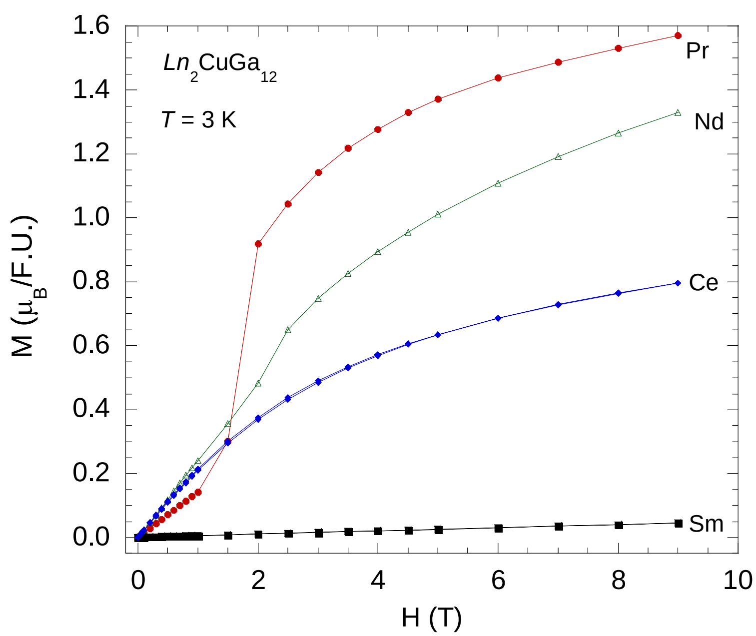

Figure 2.6 Magnetization of Ln_2CuGa_{12} (*Ln* = Ce, Pr, Nd, Sm) as a function of magnetic field.

antiferromagnetic ordering and resulting in paramagnetic moments. Also, Nd_2CuGa_{12} shows similar behavior (although not as sharp) to Pr_2CuGa_{12} with a meta-magnetic transition whose midpoint is ~2 T. Ce_2CuGa_{12} shows typical paramagnetic behavior over the entire field range from 0 to 9 T. The magnetization of Sm_2CuGa_{12} increases linearly up to 9 T, consistent with an antiferromagnet below its ordering temperature. A summary of the magnetic data can be found in Table 2.4.

Table 2.4 Magnetic properties of Ln_2MGa_{12} (Ln = Pr, Nd, Sm; M = Ni, Cu)

	fit range (K)	ordering T_N (K)	χ_o (× 10^{-2} emu/mol)	C	θ (K)	μ_{calc} (μ_B)	μ_{eff} (μ_B)
Ce_2NiGa_{12} [9]	20 – 200	10.0	5.6 × 10^{-3}	0.62	-6.67	2.54	2.23
Pr_2NiGa_{12}	20 – 278	10.0	1.10	1.67	5.37	3.58	3.58
Nd_2NiGa_{12}	50 – 278	17.9	0.07	1.73	-5.60	3.62	3.72
Sm_2NiGa_{12} [10]*	above T_N	9.0	----	----	----	0.84	0.54
Ce_2CuGa_{12} [9]	20 – 200	----	6.0 × 10^{-4}	0.65	-11.04	2.54	2.28
Pr_2CuGa_{12}	20 – 250	8.7	0.05	1.33	-1.06	3.58	3.25
Nd_2CuGa_{12}	20 – 250	2.9	0.20	1.85	-20.78	3.62	3.85
Sm_2CuGa_{12}	20 – 200	7.6	0.13	0.03	1.43	0.84	0.52

*The magnetic susceptibility of Sm_2NiGa_{12} was measured with an applied field 0.02 T.

The temperature-dependent electrical resistivity of single crystals of Ln_2CuGa_{12} (Ln = Pr, Nd, and Sm) for current applied along the *ab*-direction are shown in Figure 2.7, where the resistivity of Ce_2CuGa_{12} is shown for reference. All compounds show metallic behavior with RRR (residual resistivity ratio) values of 3.8, 2.0, and 4.6 for Pr_2CuGa_{12}, Nd_2CuGa_{12}, and Sm_2CuGa_{12}, respectively. No signature of the antiferromagnetic ordering at the Neel temperatures was observed in the resistivity data for the current applied in the *ab*-plane.

Figure 2.8 shows the magnetoresistance (MR % = $(\rho_H - \rho_0)/\rho_0 \times 100$) of a single crystal of Ln_2CuGa_{12} (Ln = Pr, Nd, and Sm) as a function of field at 3 K along the *ab*-plane. A large positive magnetoresistance is observed in the compounds that order antiferromagnetically: 35 %,

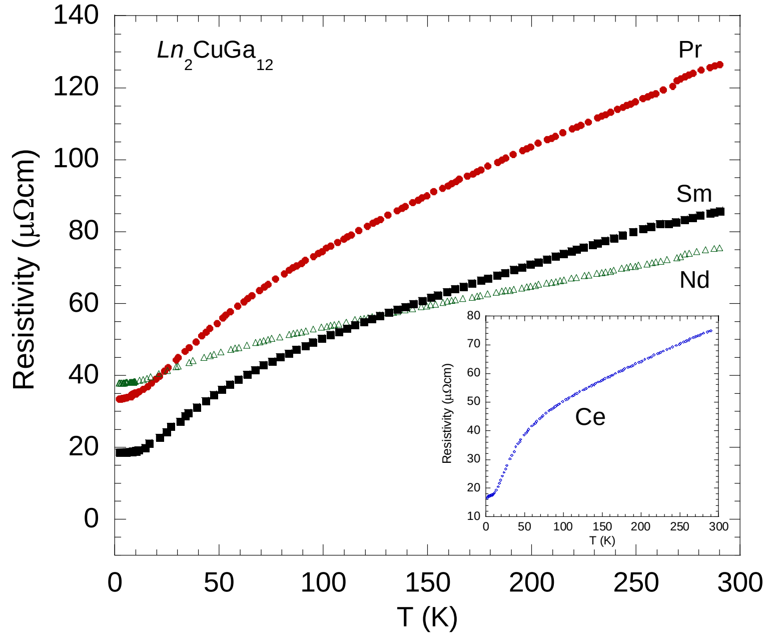

Figure 2.7 Electrical resistivity of Ln_2CuGa_{12} (Ln = Ce, Pr, Nd, Sm) as a function of temperature for current parallel to the *ab*-plane.

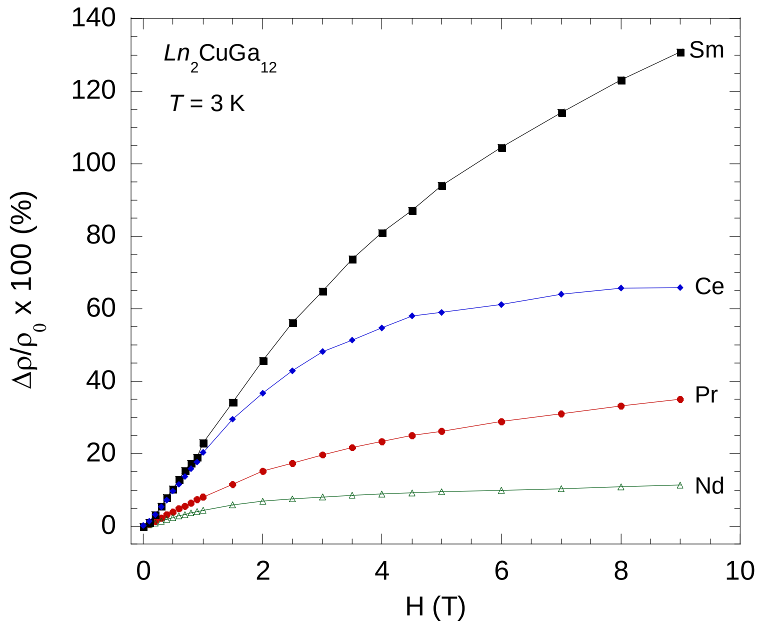

Figure 2.8 MR% of Ln_2CuGa_{12} (Ln = Ce, Pr, Nd, Sm) as a function of field.

10 % and 130 % at 9 T for Pr_2CuGa_{12}, Nd_2CuGa_{12}, and Sm_2CuGa_{12}, respectively. It is interesting to note that the in-plane magnetotransport is completely decoupled from the meta-magnetic transitions observed in the field-dependent magnetization (Figure 2.6), as the MR varies smoothly with field. The magnetoresistance of the Ce compound is ~ 65 %.

2.4 References

(1) Kalychak, Y. M.; Zaremba, V. I.; Baranyak, V. M.; Bruskov, V. A.; Zavalii, P. Y., Crystalline-structures of compounds $CeCoIn_5$, $PrCoIn_5$, $NdCoIn_5$, $SmCoIn_5$, $GdCoIn_5$, $TbCoIn_5$, $DyCoIn_5$, $HoCoIn_5$, $YCoIn_5$, $CeCoIn_8$, $PrCoIn_8$, $NdCoIn_8$, $SmCoIn_8$, $GdCoIn_8$, $DyCoIn_8$, $HoCoIn_8$, $ErCoIn_8$, $TmCoIn_8$, $YCoIn_8$. *Russ. Metall.* **1989,** *1*, 213-215.

(2) Petrovic, C.; Pagliuso, P. G.; Hundley, M. F.; Movshovich, R.; Sarrao, J. L.; Thompson, J. D.; Fisk, Z.; Monthoux, P., Heavy-fermion superconductivity in $CeCoIn_5$ at 2.3 K. *J. Phys.-Condens. Mat.* **2001,** *13*, L337-L342.

(3) Hegger, H.; Petrovic, C.; Moshopoulou, E. G.; Hundley, M. F.; Sarrao, J. L.; Fisk, Z.; Thompson, J. D., Pressure-induced superconductivity in quasi-2D $CeRhIn_5$. *Phys. Rev. Lett.* **2000,** *84*, 4986-4989.

(4) Mathur, N. D.; Grosche, F. M.; Julian, S. R.; Walker, I. R.; Freye, D. M.; Haselwimmer, R. K. W.; Lonzarich, G. G., Magnetically mediated superconductivity in heavy fermion compounds. *Nature* **1998,** *394*, 39-43.

(5) Petrovic, C.; Movshovich, R.; Jaime, M.; Pagliuso, P. G.; Hundley, M. F.; Sarrao, J. L.; Fisk, Z.; Thompson, J. D., A new heavy-fermion superconductor $CeIrIn_5$: a relative of the cuprates? *Europhys. Lett.* **2001,** *53*, 354-359.

(6) Buschow, K. H. J.; Dewijn, H. W.; Vandiepe.Am, Magnetic susceptibilities of rare-earth-indium compounds - RIn_3. *J. Chem. Phys.* **1969,** *50*, 137-141.

(7) Macaluso, R. T.; Nakatsuji, S.; Lee, H.; Fisk, Z.; Moldovan, M.; Young, D. P.; Chan, J. Y., Synthesis, structure, and magnetism of a new heavy-fermion antiferromagnet, $CePdGa_6$. *J. Solid State Chem.* **2003,** *174*, 296-301.

(8) Macaluso, R. T.; Millican, J. N.; Nakatsuji, S.; Lee, H. O.; Carter, B.; Moreno, N. O.; Fisk, Z.; Chan, J. Y., A comparison of the structure and localized magnetism in Ce_2PdGa_{12} with the heavy fermion $CePdGa_6$. *J. Solid State Chem.* **2005,** *178*, 3547-3553.

(9) Cho, J. Y.; Millican, J. N.; Capan, C.; Sokolov, D. A.; Moldovan, M.; Karki, A. B.; Young, D. P.; Aronson, M. C.; Chan, J. Y., Crystal growth, structure, and physical properties of Ln_2MGa_{12} (Ln = La, Ce; M = Ni, Cu). *Chem. Mater.* **2008,** *20*, 6116-6123.

(10) Chen, X. Z.; Small, P.; Sportouch, S.; Zhuravleva, M.; Brazis, P.; Kannewurf, C. R.; Kanatzidis, M. G., Molten Ga as a solvent for exploratory synthesis: the new ternary polygallide Sm_2NiGa_{12}. *Chem. Mater.* **2000,** *12*, 2520-2522.

(11) Sheldrick, G. M., A short history of SHELX. *Acta Cryst.* **2008,** *A64*, 112-122.

(12) Ban, Z.; Sikirica, M., Crystal structure of ternary silicides ThM_2Si_2 (M - Cr, Mn, Fe, Co, Ni and Cu). *Acta Cryst.* **1965,** *18*, 594-599.

(13) Pelleg, J.; Kimmel, G.; Dayan, D., RGa_6 (R=rare-earth atom), a common intermetallic compound of the R-Ga systems. *J. Less-Common Met.* **1981,** *81*, 33-44.

(14) Manory, R.; Pelleg, J.; Grill, A., Neodymium-gallium system. *J. Less-Common Met.* **1978,** *61*, 293-299.

(15) Yatsenko, S. P.; Semyannikov, A. A.; Semenov, B. G.; Chuntonov, K. A., Phase-diagrams of rare-earth metals with gallium. *J. Less-Common Met.* **1979,** *64*, 185-199.

(16) Grin, Y. N.; Hiebl, K.; Rogl, P.; Noel, H., Magnetic behavior and structural chemistry of ternary gallides $RECu_xGa_{4-x}$ (RE=La, Ce, Pr, Nd, Sm,Gd). *J. Less-Common Met.* **1990,** *162*, 371-377.

(17) Hulliger, F., On rare-earth gold aluminides $LnAuAl_3$ and related-compounds. *J. Alloy Compd.* **1995,** *218*, 255-258.

(18) Grin, Y. N.; Hiebl, K.; Rogl, P.; Noel, H., Magnetism and structural chemistry of ternary gallides $RENi_xGa_{4-x}$ (RE=La, Ce, Pr, Nd, Sm, Gd, Tb) and $LaCo_{0.5}Ga_{3.5}$. *J. Less-Common Met.* **1990,** *162*, 361-369.

CHAPTER 3. ANISOTROPIC MAGNETISM IN α-*Ln*NiGa$_4$ (*Ln* = Y, Gd – Yb)

3.1 Introduction

The discovery of the heavy fermion antiferromagnet CePdGa$_6$[1] with $T_N \sim 6$ K and $\gamma \sim 230$-400 mJ/mol-Ce-K^2 has led us to study related intermetallic phases, such as Ce$_2$PdGa$_{10}$,[2] Ce$_2$PdGa$_{12}$,[3] and Ln_2MGa$_{12}$ (*Ln* = La, Ce; *M* = Ni, Cu).[4] The ternary phases of the Ce-Pd-Ga system allowed us to study the competition between RKKY and Kondo effects. The fact that Ce$_2$PdGa$_{12}$ orders at a higher ordering temperature (11 K) is attributed to the extra Ga layers in the crystal structure. In addition, this antiferromagnet was found to exhibit an enhanced mass with $\gamma \sim 170$ mJ/mol-Ce-K^2. Isomorphic phases Ln_2MGa$_{12}$ (*Ln* = La, Ce; *M* = Ni, Cu) were investigated to determine how the properties change with substitution of Cu for Ni and Pd. Kondo-like behavior was observed in the resistivity of the isoelectronic Ce$_2$NiGa$_{12}$ analogue which shows enhanced mass with $\gamma \sim 191$ mJ/mol-Ce-K^2. The corresponding Cu analogue also shows enhanced electronic behavior with a $\gamma \sim 69$ mJ/mol-Ce-K^2.

To probe the magnetic exchange interactions in relation to rare earth element, we grew high quality single crystals of a series of *Ln*-Ni-Ga compounds. These phases, where *Ln* = Y, Gd - Yb, are isostructural to the parent structure type YNiAl$_4$,[5] crystallize in the orthorhombic *Cmcm* space group with lattice parameters $a \sim 4$ Å, $b \sim 15$ Å, and $c \sim 6$ Å. Along the crystallographic *b*-axis, slabs of Ni@Ga$_7$$Ln_2$ and non-magnetic slabs of Ga atoms alternate throughout the lattice. Single crystals of the *Ln*NiGa$_4$ (*Ln* = Y, Sm, Gd – Yb) phases of this structure type were first synthesized by Yarmolyuk and coworkers, in which stoichiometric ratios of the constituent elements were arc melted under argon and then annealed at 600 °C for sample homogeneity.[6] The magnetic susceptibility of TmNiGa$_4$ was investigated at high temperature from 300 K to 700 K, but did not show ordering in this temperature range. Romaka *et al*. measured the magnetic susceptibilities of *Ln*NiGa$_4$ (*Ln* = Y, Gd – Tm), but ordering was not observed down to 70 K.[7]

The temperature dependent magnetic susceptibility of $YbNiGa_4$ was reported for temperatures between 4.2 and 300 K at 0.01 and 0.007 T,[8] and a deviation from Curie-Weiss behavior was observed in the susceptibility due to the intermediate valence state of Yb. X-ray absorption measurements in field show a continuous conversion of Yb^{2+} to Yb^{3+} as a function of pressure up to 25.4 GPa. Herein, we report the crystal growth, full-structure determination, and low temperature physical properties of $LnNiGa_4$ $LnNiGa_4$ (Ln = Y, Gd – Yb) to systematically investigate the magnetic behavior across this isostructural series.

3.2 Experimental

3.2.1 Synthesis

Single crystals of $LnNiGa_4$ (Ln = Y, Gd – Yb) were prepared via the flux growth method. Pieces of Y, Gd, Tb, Dy, Ho, Er, Tm, and Yb (3*N*, Alfa Aesar), Ni powder (5*N*, Alfa Aesar) and Ga shot (7*N*, Alfa Aesar) were placed into alumina crucibles, covered with quartz wool, sealed in an evacuated silica tube, and placed into a high temperature furnace for heating. The $LnNiGa_4$ (Ln = Y, Gd – Er) samples were prepared by combining the constituent elements in a 1.5:1:15 ratio, heating to 1423 K at 170 K/h, and annealing at that temperature for 24 h. They were then cooled to 973 K at 150 K/h and further cooled to 873 K at 8 K/h. Each ampoule was then inverted and centrifuged for up to 8 min to remove excess Ga flux. This method yielded needle-like crystals with lengths up to ~ 6 mm, as shown in Figure 3.1. However, a slightly different stoichiometric ratio of starting materials and heat treatment were employed to obtain larger single crystals of $TmNiGa_4$, as the previous synthetic method yielded smaller crystals only up to ~ 2 mm in length. In addition to eliminating the fast-cool step in the temperature profile, a 2:1:15 stoichiometric ratio of *Ln*: Ni: Ga was employed to obtain $TmNiGa_4$. After dwelling, the ampoule was slow cooled from 1423 K to 873 K at 10 K/h. The sample was fast-cooled to 973 K

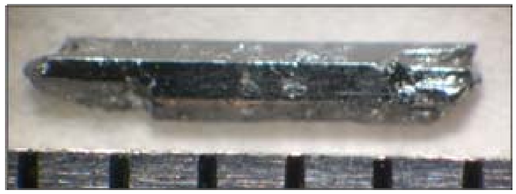

Figure 3.1 A single crystal of $TmNiGa_4$. Surface roughness is due to etching and crystal deformities incurred when separating the crystals.

at 200 K/h, and then slow-cooled to 873 K at 8 K/h. Single crystals of $YbNiGa_4$ were also synthesized to note trends within the series. The process was similar except the dwell temperature for $YbNiGa_4$ was lowered to 1123 K to account for the low vapor pressure of elemental Yb. Samples were fast-cooled to 973 K at 200 K/h, and then slow-cooled to 873 K at 8 K/h. Centrifugation followed at 873 K to remove excess flux which resulted in silver-coloured, spindle-like crystals up to ~ 8 mm in length. Excess flux was further removed from the surface of the crystals by etching in diluted HCl (6 M). The phase purity of each material was confirmed using powder X-ray diffraction, and the structural characterization of these phases was obtained using single crystal X-ray diffraction.

3.2.2 Experimental

A suitable needle-like crystal of each sample was positioned onto a thin, glass fibre, mounted onto a goniometer head with an extender, and then loaded onto a Nonius Kappa CCD X-ray diffractometer equipped with a Mo K_α radiation tube of wavelength 0.71073 Å. Preliminary lattice checks revealed an orthorhombic cell for each phase with $a \sim 4$ Å, $b \sim 15$ Å, $c \sim 6$ Å, $V \sim 400$ Å^3, and point group symmetry *mmm*. Based on these cell parameters, it was determined that these phases were isostructural to the previously reported structure type, $YNiAl_4$.[5] Data were collected, and the structural models were refined by direct methods using SHELXL97,[9] where the atomic parameters of $YNiAl_4$ were used as starting values for refinement. Cell refinement and data reduction were completed using Denzo and Scalepack.[10] A parameter to correct for absorption was applied to the model, and the extinction parameter was refined. Crystallographic parameters are presented in Table 3.1 and 3.2. Atomic positions and anisotropic displacement parameters are shown in Table 3.3.

Table 3.1 Crystallographic parameters of *Ln*$NiGa_4$ (*Ln* = Y, Gd – Dy), orthorhombic, *Cmcm.*

Formula	$YNiGa_4$	$GdNiGa_4$	$TbNiGa_4$	$DyNiGa_4$
a (Å)	4.076(5)	4.093(5)	4.080(5)	4.069(5)
b (Å)	15.245 (5)	15.355(5)	15.286(5)	15.230 (5)
c (Å)	6.552 (5)	6.548(5)	6.542(5)	6.529 (5)
V (Å^3)	407.1(6)	411.5(6)	408.0(6)	404.6 (6)
Z	4	4	4	4
Size (mm^3)	0.025/0.03/0.05	0.03/0.03/0.05	0.025/0.025/0.05	0.025/0.025/0.05
θ range(°)	2.67 – 30.04	4.09 – 29.95	4.10 – 29.99	2.67 – 30.04
μ (mm^{-1})	44.477	45.946	47.421	48.808
R_{int}	0.0242	0.0256	0.0221	0.0362
h	-5 → 5	-5 → 5	-5 → 5	-5 → 5
k	-21 → 21	-21 → 21	-20 → 21	-19 →21
l	-9 → 9	-9 → 9	-9 → 9	-8 →9
$^aR_1[F^2 > 2\sigma(F^2)]$	0.0362	0.0281	0.0284	0.0398
$^b wR_2(F^2)$	0.0871	0.0699	0.0723	0.0989
Reflections	363	362	363	361
Parameters	24	24	24	24
GooF	1.167	1.100	1.204	1.111
$\Delta\rho_{max}$ (eÅ^{-3})	1.606	2.536	2.227	2.883
$\Delta\rho_{min}$ (eÅ^{-3})	-3.221	-2.366	-2.694	-2.544
Extinction coeff.	0.0109(10)	0.0043(4)	0.0117(7)	0.0042(5)

$^aR_1 = \Sigma\|F_o| - |F_c\|/\Sigma|F_o|$.

$^b wR_2 = [\Sigma[w(F_o^2-F_c^2)^2]/\Sigma[w(F_o^2)^2]]^{1/2}$; $w = 1/[\sigma^2F_o^2 + (0.0476P)^2 + 4.5788P]$, $w = 1/[\sigma^2F_o^2 + (0.0343P)^2 + 6.8134P]$, $w = 1/[\sigma^2F_o^2 + (0.0308P)^2 + 4.2582P]$, $w = 1/[\sigma^2F_o^2 + (0.0538P)^2 + 11.096P]$ for $YNiGa_4$, $GdNiGa_4$, $TbNiGa_4$, and $DyNiGa_4$,.

Table 3.2 Crystallographic parameters of *Ln*NiGa$_4$ (*Ln* = Ho – Yb), orthorhombic, *Cmcm.*

Formula	$HoNiGa_4$	$ErNiGa_4$	$TmNiGa_4$	$YbNiGa_4$
a (Å)	4.062 (5)	4.0578 (5)	4.0472(2)	4.046(1)
b (Å)	15.185 (5)	15.135(5)	15.088(4)	15.083(5)
c (Å)	6.534 (5)	6.536 (5)	6.551(2)	6.545(3)
V (Å^3)	403.0 (6)	401.4(6)	400.1(2)	399.5(2)
Z	4	4	4	4
Size (mm^3)	0.025/0.03/0.05	0.03/0.05/0.05	0.05/0.05/0.08	0.25/0.05/0.05
θ range(°)	2.68 – 29.98	4.12 – 30.05	4.12 – 29.96	2.70 – 30.03
μ (mm^{-1})	50.091	51.486	52.851	54.130
R_{int}	0.0300	0.0173	0.0370	0.0267
h	-5 → 5	-5 → 5	-5 → 5	-5 → 5
k	-19 → 21	-19 → 21	-19 → 20	-19 → 20
l	-9 → 9	-9 → 9	-9 → 9	-9 → 9
$^aR_1[F^2 > 2\sigma(F^2)]$	0.0300	0.0192	0.0340	0.0275
^{b}w$R_2(F^2)$	0.0700	0.0496	0.0904	0.0628
Reflections	360	358	356	358
Parameters	24	24	24	24
GooF	1.149	1.216	1.189	1.159
$\Delta\rho_{max}$ (eÅ^{-3})	1.816	1.733	3.832	1.622
$\Delta\rho_{min}$ (eÅ^{-3})	-2.527	-1.547	-2.468	-2.475
Extinction coeff.	0.0042(4)	0.0048(3)	0.0048(5)	0.0098(5)

$^aR_1 = \Sigma\|F_o| - |F_c\|/\Sigma|F_o|$.
^{b}w$R_2 = [\Sigma[w(F_o^2 - F_c^2)^2]/\Sigma[w(F_o^2)^2]]^{1/2}$; $w = 1/[\sigma^2F_o^2 + (0.0276P)^2 + 4.1795P]$, $w = 1/[\sigma^2F_o^2 + (0.0138P)^2 + 8.2897P]$, $w = 1/[\sigma^2F_o^2 + (0.0437P)^2 + 15.0319P]$, and $w = 1/[\sigma^2F_o^2 + (0.0208P)^2 + 5.1750P]$ for $HoNiGa_4$, $ErNiGa_4$, $TmNiGa_4$, and $YbNiGa_4$, respectively.

Table 3.3 Atomic positions and anisotropic displacement parameters for *Ln*NiGa$_4$ (*Ln* = Y, Gd – Yb)

Atom	Wyckoff position	x	y	z	U_{eq}(Å^2)^a
Y	4*c*	0	0.61842(6)	1/4	0.0064(3)
Ni	4c	0	0.27492(8)	1/4	0.0098(4)
Ga1	4*a*	0	0	0	0.0101(3)
Ga2	4*c*	0	0.42719(8)	1/4	0.0108(3)
Ga3	8*f*	0	0.81393(5)	0.05148(13)	0.0077(3)
Gd	4*c*	0	0.61739(3)	1/4	0.0088(2)
Ni	4*c*	0	0.27549(9)	1/4	0.0108(3)
Ga1	4*a*	0	0	0	0.0130(3)
Ga2	4*c*	0	0.42713(8)	1/4	0.0124(3)
Ga3	8*f*	0	0.81352(5)	0.05165(14)	0.0115(3)

Table 3.3 (cont.)

Atom	Wyckoff position	x	y	z	U_{eq}(Å^2)^a
Tb	4*c*	0	0.61744(3)	1/4	0.0076(2)
Ni	4*c*	0	0.27510(9)	1/4	0.0109(4)
Ga1	4*a*	0	0	0	0.0114(3)
Ga2	4*c*	0	0.42689(9)	1/4	0.0120(3)
Ga3	8*f*	0	0.81372(6)	0.05107(14)	0.0100(3)
Dy	4*c*	0	0.61803(5)	1/4	0.0082(3)
Ni	4*c*	0	0.27498(16)	1/4	0.0121(6)
Ga1	4*a*	0	0	0	0.0117(5)
Ga2	4*c*	0	0.42764(14)	1/4	0.0124(5)
Ga3	8*f*	0	0.81413(9)	0.0508(2)	0.0105(4)
Ho	4*c*	0	0.61873(4)	1/4	0.0076(2)
Ni	4*c*	0	0.2749711)	1/4	0.0117(4)
Ga1	4*a*	0	0	0	0.0116(4)
Ga2	4*c*	0	0.42793(10)	1/4	0.0115(4)
Ga3	8*f*	0	0.81444(6)	0.05087(17)	0.0099(3)
Er	4*c*	0	0.61933(2)	1/4	0.0054(9)
Ni	4*c*	0	0.27484(12)	1/4	0.0083(3)
Ga1	4*a*	0	0	0	0.0090(2)
Ga2	4*c*	0	0.42828(8)	1/4	0.0095(2)
Ga3	8*f*	0	0.81473(5)	0.05085(11)	0.0066(2)
Tm	4*c*	0	0.61996(4)	1/4	0.0076(3)
Ni	4*c*	0	0.27440(12)	1/4	0.0102(4)
Ga1	4*a*	0	0	0	0.0111(4)
Ga2	4*c*	0	0.42890(12)	1/4	0.0111(4)
Ga3	8*f*	0	0.81496(7)	0.05095(18)	0.0088(3)
Yb	4*c*	0	0.62004(3)	1/4	0.0064(2)
Ni	4*c*	0	0.27451(10)	1/4	0.0084(4)
Ga1	4*a*	0	0	0	0.0086(3)
Ga2	4*c*	0	0.42885(9)	1/4	0.0092(3)
Ga3	8*f*	0	0.81505(6)	0.05098(14)	0.0061(3)

$^a U_{eq}$ is defined as one-third of the trace of the orthogonalized U_{ij} tensor.

3.2.3 Physical Property Measurements

Magnetization and in-plane electrical resistance data were collected on multiple single crystals of $YNiGa_4$ (8.2 mg), $GdNiGa_4$ (7.8 mg), $TbNiGa_4$ (164.0 mg), $DyNiGa_4$ (170.0 mg), $HoNiGa_4$ (21.0 mg), $ErNiGa_4$ (6.1 mg), $TmNiGa_4$ (6.6 mg), and $YbNiGa_4$ (16.0 mg) using a

Quantum Design Physical Properties Measurement System (PPMS). Magnetization was measured from 0 to 9 T at 3 K, where care was taken to align either the c-axis or the ab-plane of the crystal with the magnetic field. Zero-field cool (ZFC) susceptibility was then measured from 2 K to 278 K at 0.1 T, with magnetic field parallel to the *ab*- and *c*-directions of the crystals. Electrical resistance was measured using the standard four-probe technique. Magnetoresistance (MR) measurements were obtained at 3 K from 0 to 9 T with field perpendicular to the current. The current direction was applied along the *c*-axis.

3.2.4 X-ray Photoelectron Spectroscopy Measurements

The as-grown sample surface of $TmNiGa_4$ was cleaned at room temperature using methanol and immediately transferred into the μ metal-shielded analysis chamber equipped with an X-ray photoelectron spectroscopy (XPS) system. XPS measurements were carried out with a Phoibos 150 MCD Energy Hemispherical Analyzer by using a monochromated Al α X-ray source with photon energy of 1486.7 eV. The overall energy resolution is 0.16 eV. The Au $4f_{7/2}$ peak energy was used as a reference for the binding energy calibration. The base pressure of our system during the measurements was 2×10^{-9} Torr.

3.3 Results and Discussion

3.3.1 Structure

Ln$NiGa_4$ (*Ln*= Y, Gd – Yb) crystallize in the orthorhombic *Cmcm* space group ($Z = 4$) and adopt the $YNiAl_4$ structure type.[5] Figure 3.2(a) shows the crystal structure of $YbNiGa_4$ as a model for *Ln*$NiGa_4$ (*Ln* = Y, Gd – Yb), where the unit cell is emphasized with dashed lines. There are two substructures present within the unit cell: (1) a partial AlB_2 system with an *Ln* atom at the center surrounded by Ni and Ga atoms, and (2) a distorted α-Fe net composed only of Ga atoms, which are shown in the top left and top right corners of the unit cell, respectively. *Ln* atoms are located inside of cages (19-corner polyhedral) formed by two *Ln* atoms, four Ni atoms, and thirteen Ga atoms. The *Ln*-polyhedra are face-sharing along the [100] direction and are edge-sharing along the [001] direction. Ni atoms have nine nearest neighbors: seven Ga atoms and two *Ln* atoms, which form a distorted trigonal prism with a Ga3 atom at each of its six corners. Two of the side faces are capped with *Ln* atoms, and the third with a Ga2 atom. This Ni@Ga_7Ln_2 framework translates through the lattice along the *c*-axis and alternates with Ga-only layers in the [010] direction as shown in Figure 3.2(b). As expected, the structural properties of our $YbNiGa_4$ compound are similar to those published by Vasylechko *et al*.[8] X-ray absorption spectroscopy measurements revealed that the Yb in the reported phase was intermediate with an effective valence of 2.48 (52% of Yb $4f^{14}$). Selected interatomic distances are provided in Table 3.4.

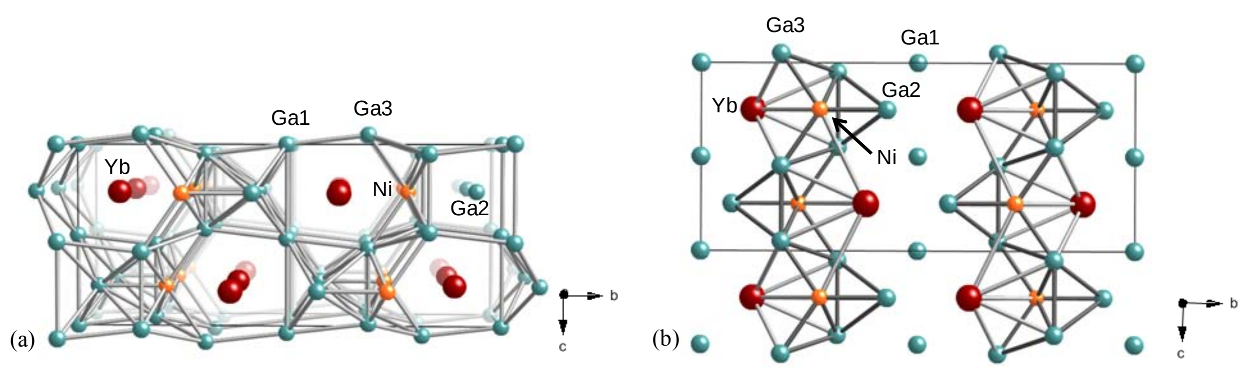

Figure 3.2 (a) The crystal structure of $YbNiGa_4$ is presented as a model for *Ln*$NiGa_4$ and is shown along the *a*-axis where *Ln* is presented as a red sphere, Ni as orange, and Ga atoms are shown as blue. (b) The local coordination environment of Ni is shown as it relates to the unit cell. A layering of Ni@Ga_7Ln_2 and Ga atoms translate through the lattice in the [010] direction. Ga-Ga bonds have been omitted for clarity.

Table 3.4 Selected interatomic distances (Å) for $LnNiGa_4$ (Ln = Y, Gd – Yb)

	Ln-Ga1	*Ln*-Ga2	*Ln*-Ga3	*Ln*-Ni	Ni-Ga2	Ni-Ga3
$YNiGa_4$	3.1774(18) ×4	2.9152(18) 3.349(2) ×2	3.020(2) ×4 3.2520(15) ×2	3.138(2) ×2 3.658(13) ×2	2.321(2)	2.3951(17) ×2 2.490(2) ×4
$GdNiGa_4$	3.1807(18) ×4	2.9214(16) 3.345(2) ×2	3.036(2) ×4 3.2798(14) ×2	3.175(2) ×2 3.664(14) ×2	2.328(2)	2.4019(17) ×2 2.493(2) ×4
$TbNiGa_4$	3.1716(18) ×4	2.9127(17) 3.340(2) ×2	3.025(2) ×4 3.2703(14) ×2	3.157(2) ×2 3.660(15) ×2	2.320(2)	2.3922(18) ×2 2.491(2) ×4
$DyNiGa_4$	3.1678(18) ×4	2.900(2) 3.338(2) ×2	3.011(2) ×4 3.2575(19) ×2	3.139(3) ×2 3.649(2)×2	2.325(3)	2.387(2) ×2 2.487(2) ×4
$HoNiGa_4$	3.1692(18) ×4	2.8974(18) 3.343(2) ×2	3.003(2) ×4 3.2441(15) ×2	3.123(2) ×2 3.644(15) ×2	2.323(2)	2.3891(19) ×2 2.485(2) ×4
$ErNiGa_4$	3.1699(18) ×4	2.8914(15) 3.347(2) ×2	2.997(2) ×4 3.2312(13) ×2	3.107(2) ×2 3.641(15) ×2	2.3224(19)	2.3883(16) ×2 2.485(2) ×4
$TmNiGa_4$	3.1710(3) ×4	2.8828(18) 3.3578(5) ×2	2.9913(9) ×4 3.2183(12) ×2	3.0865(15)×2 3.641(2)×2	2.331(3)	2.3886(16) ×2 2.4842(8) ×4
$YbNiGa_4$	3.1703(5) ×4	2.8841(15) 3.3550(10)×2	2.9891(9) ×4 3.2169(11) ×2	3.0859(13)×2 3.639(13) ×2	2.328(2)	2.3888(14) ×2 2.4831(8) ×4

3.3.2 Physical Properties

3.3.2.1 Magnetism

(a) $YNiGa_4$ - The magnetic susceptibility of $YNiGa_4$ is small and diamagnetic.

(b) $GdNiGa_4$ - The magnetic susceptibility of $GdNiGa_4$ with field applied along the *ab*-direction of the crystal (Figure 3.3) follows a Curie-Weiss law until ~ 16.5 K, where a sharp antiferromagnetic transition occurs. A modified Curie-Weiss fit of the susceptibility, gives an experimental effective moment of 8.3(1.2) μ_B for Gd^{3+} and a Weiss constant (θ) of -36.7(1.6) K with a fit from $50 < T < 200$ K. The susceptibility curve with the magnetic field applied along the *c*-direction has the same trend with the exception of the antiferromagnetic transition occurring at a slightly higher temperature (T_N ~ 18.3 K). An effective moment of 7.9(1.1) μ_B /Gd is obtained and is in agreement with the calculated value of 7.9 μ_B for the free Hund's rule moment of Gd^{3+}. Also, a Weiss constant of -33.4(1.3) K was obtained with a fit from 50 < T < 200 K, indicating strong antiferromagnetic correlations along both crystallographic directions.

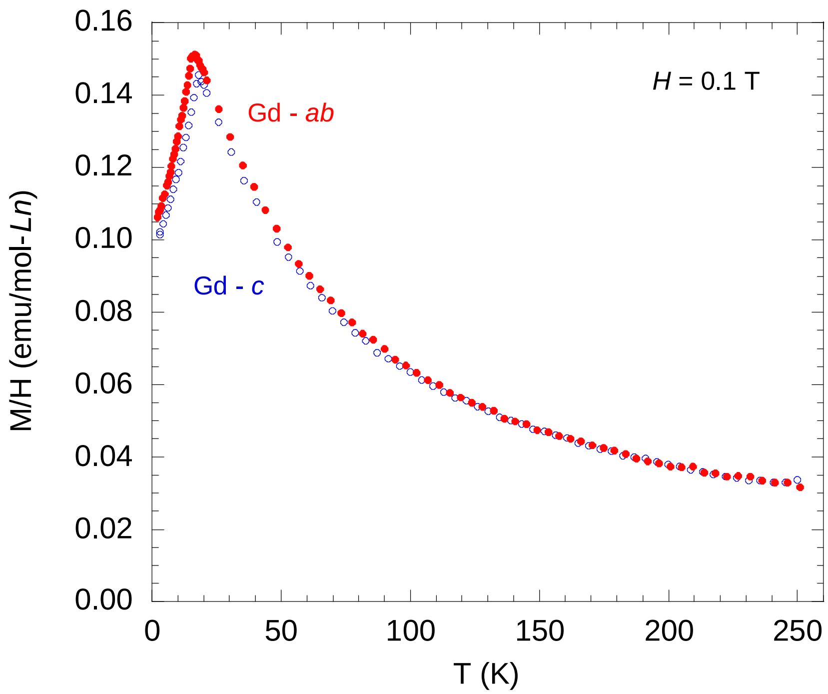

Figure 3.3 Magnetic susceptibility of $GdNiGa_4$ with field of 0.1 T applied parallel to the *ab*- and *c*-directions of the crystal.

The field-dependent magnetization of $GdNiGa_4$ is shown in Figure 3.4. For the field applied along the *ab*-direction, a small linear increase in magnetization with field is observed, typical of an antiferromagnet, with the exception of a small, possibly metamagnetic transition near 3.5 T. The magnetization curve for the field applied along the *c*-direction is also typical for an antiferromagnet, and a small metamagnetic transition is also observed, but this time at a much higher field (~ 7 T).

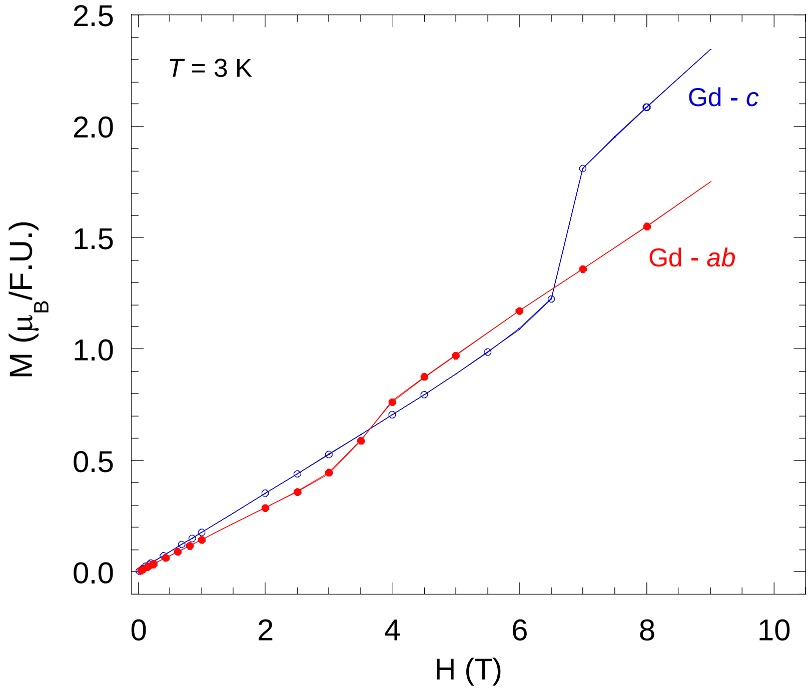

Figure 3.4 Field dependent magnetization data for $GdNiGa_4$ at field up to 9 T.

(c) $TbNiGa_4$ - There are two antiferromagnetic transitions present in the magnetic susceptibilities of $TbNiGa_4$ in both the *ab*- and *c*-directions (Figure 3.5). The first transition occurs ~ 26 K and the second ~15 K. The effective moments obtained with a fit from 50 K < *T* < 200 K are 14.3(1.6) μ_B and 14.6(2.3) μ_B in the *ab*- and *c*-directions, respectively. The calculated value for a free Tb^{3+} ion is 9.7 μ_B, and thus, the experimental values are significantly higher. Both θ-values, -13.8(0.7) K in the *ab*-direction and -66.8(1.8) K in the *c*-direction, indicate antiferromagnetic correlations.

The magnetization curves in the *ab*- and *c*-directions are very different (Figure 3.6). In the *c*-direction, the curve does not saturate in field up to 9 T but increases linearly with field, consistent with antiferromagnetism. For field applied along the *ab*-direction, two sharp metamagnetic transitions occur at 3.5 T and 6.5 T, with a significant hysteresis associated with

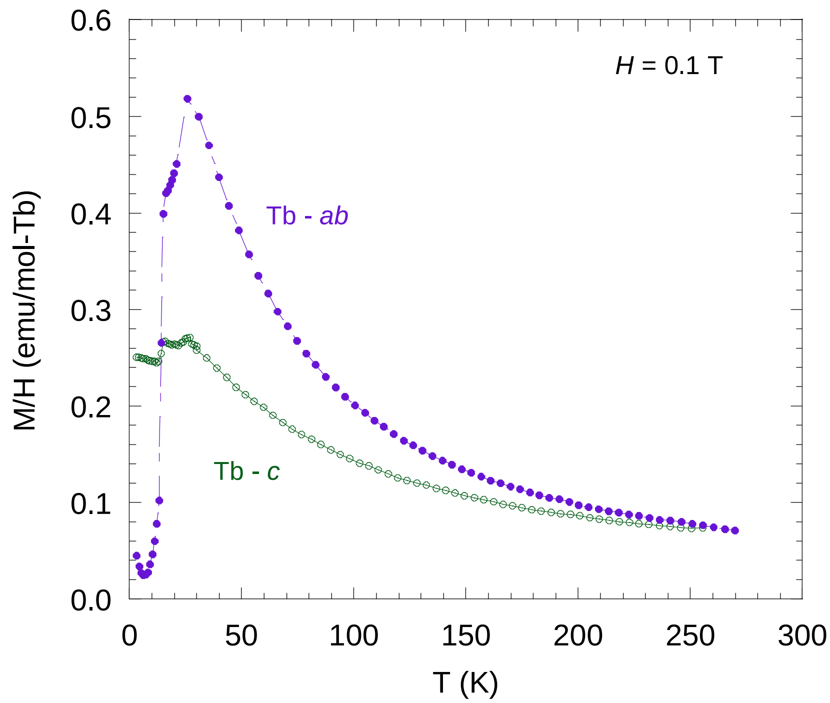

Figure 3.5 Magnetic susceptibility of $TbNiGa_4$ with field of 0.1 T applied parallel to the *ab*- and *c*-directions of the crystal.

the lower field transition. The saturation magnetization in the *ab*-direction is large (~ 11.5 μ_B), which is much higher than the calculated saturation moment of 9.0 μ_B for Tb^{3+}. The hysteretic curve suggests ferromagnetic correlations at low field and the metamagnetic transition thereafter identifies a spin reorientation at slightly higher field.

We decided to measure the magnetic susceptibility with field parallel to the *ab*-direction of the crystal at 3 T and 8 T to ascertain which type of correlations dominate the system before and after the metamagnetic transition at ~ 3.5 T. These curves are presented in Figure 3.7. With applied field at 3 T, the antiferromagnetic transitions are suppressed to ~24.0 K and ~6.0 K. For an applied field of 8 T, which is above the upper metamagnetic transition shown in Figure 3.6, both antiferromagnetic transitions are completely suppressed. No magnetic ordering is observed in the susceptibility curve down to 2 K. This suggests that the two metamagnetic transitions observed in $TbNiGa_4$ at 3.5 T and 6.5 T are associated with the two Neel transitions at 15 K and 26 K, respectively.

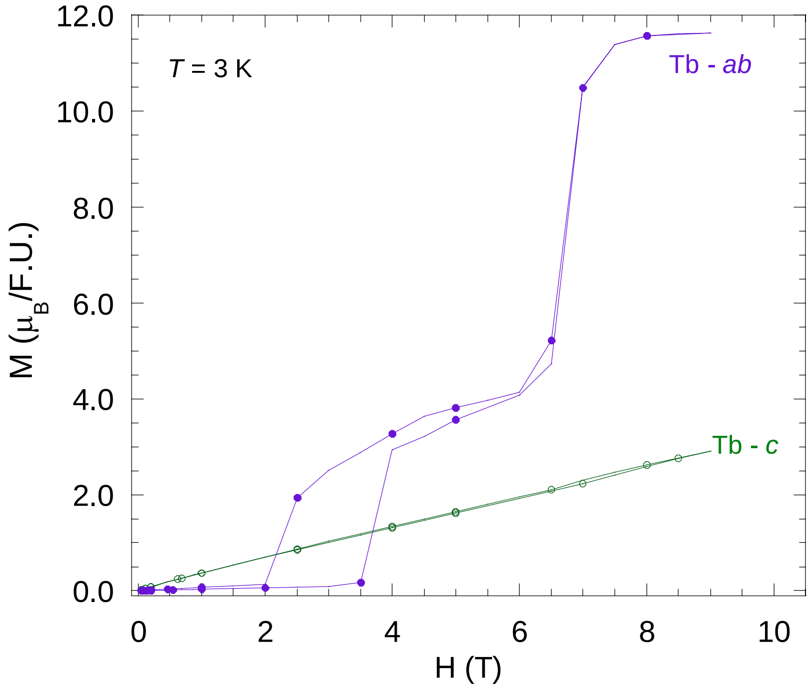

Figure 3.6 Field dependent magnetization data for $TbNiGa_4$ at field up to 9 T.

(d) $DyNiGa_4$ - The magnetic susceptibility of $DyNiGa_4$ in the *c*-direction of the crystal has an antiferromagnetic transition ~ 21.6 K (Figure 3.8). A modified Curie-Weiss fit gives an experimental effective moment of 7.3(1.0) μ_B for Dy^{3+} and a Weiss constant of -46.5(1.6) K. The experimental value is much lower than the calculated moment for a free Dy^{3+} ion which is 10.6 μ_B. Conversely, in the *ab*-direction the susceptibility curve looks essentially paramagnetic, with a small transition near 6.8 K. A fit to the data from 50 K < T < 200 K gives a Weiss constant of -4.8(0.4) K and an effective moment of 12.6(1.2) μ_B.

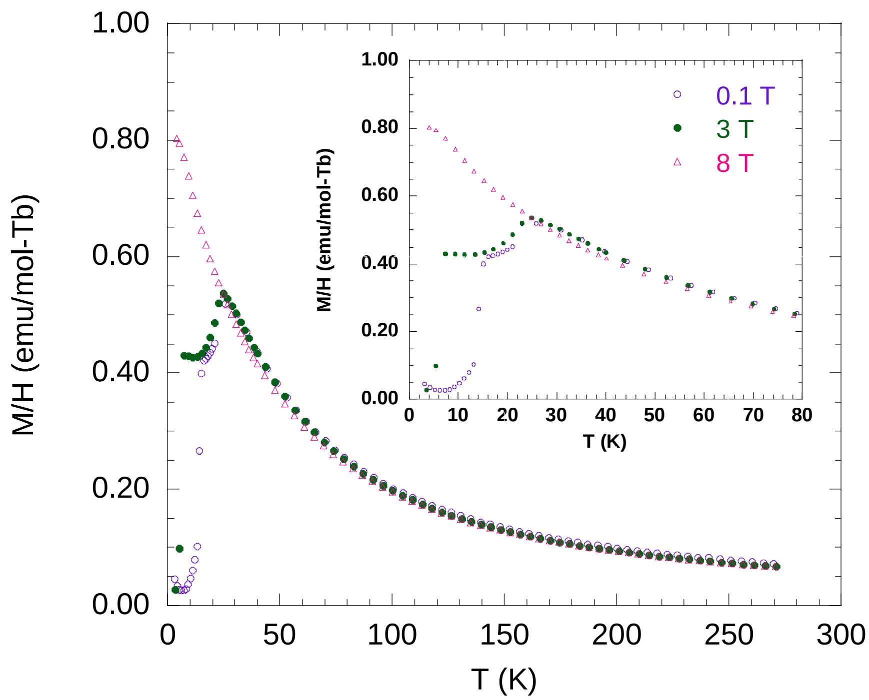

Figure 3.7 Magnetic susceptibility of $TbNiGa_4$ with field applied in the *ab*-direction at $H = 2.9$ T and $H = 7.9$ T, with the susceptibility at 0.1 T shown for reference.

The magnetization curve of $DyNiGa_4$ for the field applied in the *ab*-plane (Figure 3.9), increases with increasing field, typical of a Brillouin function for a paramagnetic material. Near 3.5 T, a sharp metamagnetic transition is observed. At higher fields the magnetization quickly saturates to a value near 9.0 μ_B, which is close to the 10.0 μ_B expected for Dy^{3+}. For field applied along the *c*-axis, the magnetization is smaller and varies linearly with the field, typical of an antiferromagnet. $TbNiGa_4$ and $DyNiGa_4$ share very similar magnetic qualities. Both are antiferromagnetic along the *c*-axis, and both demonstrate very sharp metamagnetic transitions for the field applied in the *ab*-plane, with their magnetization quickly saturating above the transition.

(e) $HoNiGa_4$ - The susceptibilities of $HoNiGa_4$ in both the *ab*- and *c*-directions show transitions ~ 5.1 K (Figure 3.10). At this temperature there is a slight decrease in the magnetization along both directions, akin to antiferromagnetic ordering, albeit not very pronounced. Larger than expected effective moments are obtained from a Curie-Weiss fit of the

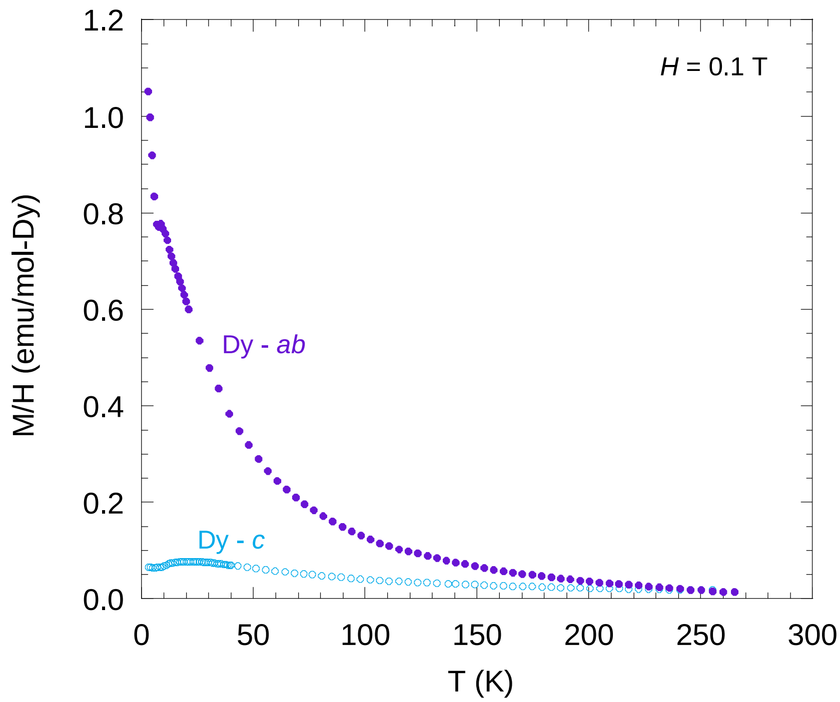

Figure 3.8 Magnetic susceptibility of $DyNiGa_4$ with field of 0.1 T applied parallel to the *ab*- and *c*-directions of the crystal.

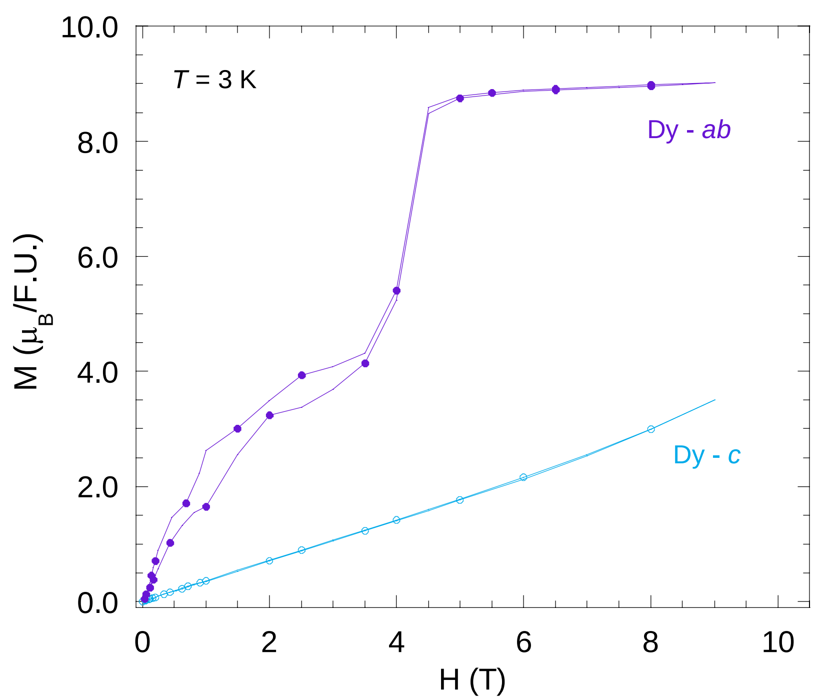

Figure 3.9 Field dependent magnetization data for $DyNiGa_4$ at field up to 9 T.

susceptibility, where values of 13.6(1.2) μ_B and 11.3(1.1) μ_B are calculated for the *ab*- and *c*-direction, respectively. A free Ho^{3+} ion has an effective moment of 10.6 μ_B. Both susceptibilities show antiferromagnetic correlations with θ = -2.4(0.2) K in the *ab*-direction and θ = -5.4(0.4) K in the *c*-direction.

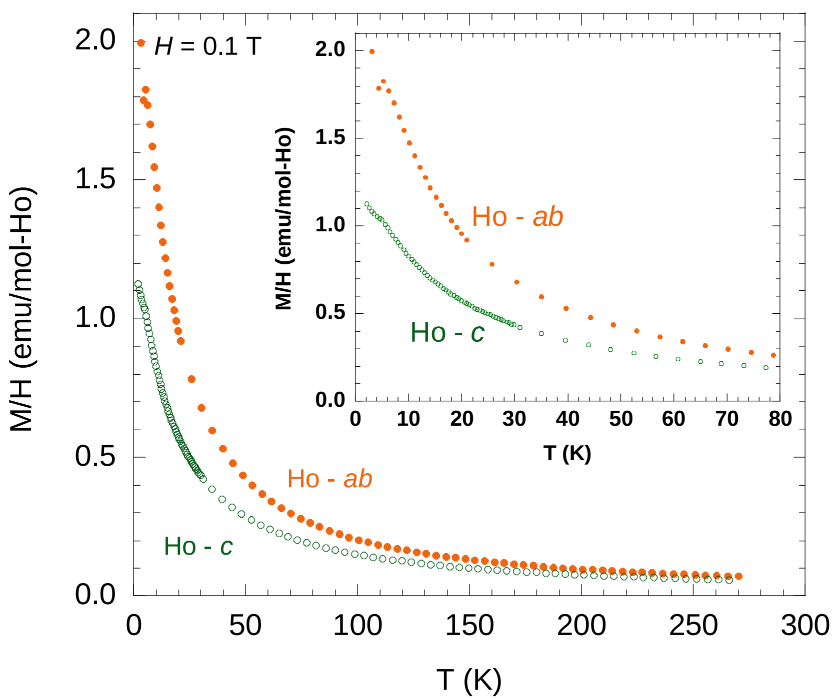

Figure 3.10 Magnetic susceptibility of $HoNiGa_4$ with field of 0.1 T applied parallel to the *ab*- and *c*-directions of the crystal.

The magnetizations in both directions are shown in Figure 3.11. Both vary linearly with field for small fields (consistent with antiferromagnetism), before approaching saturation values between 8 – 10 μ_B at high field. The magnetization in the *ab*-direction approaches the saturation value gradually, while the *c*-axis data shows a metamagnetic transition at ~ 1 T, and possibly another transition near 8 T. Both are much smaller than what was observed in the Tb sample, for example, and both of these transitions are hysteretic, as they are no longer present upon reducing the field.

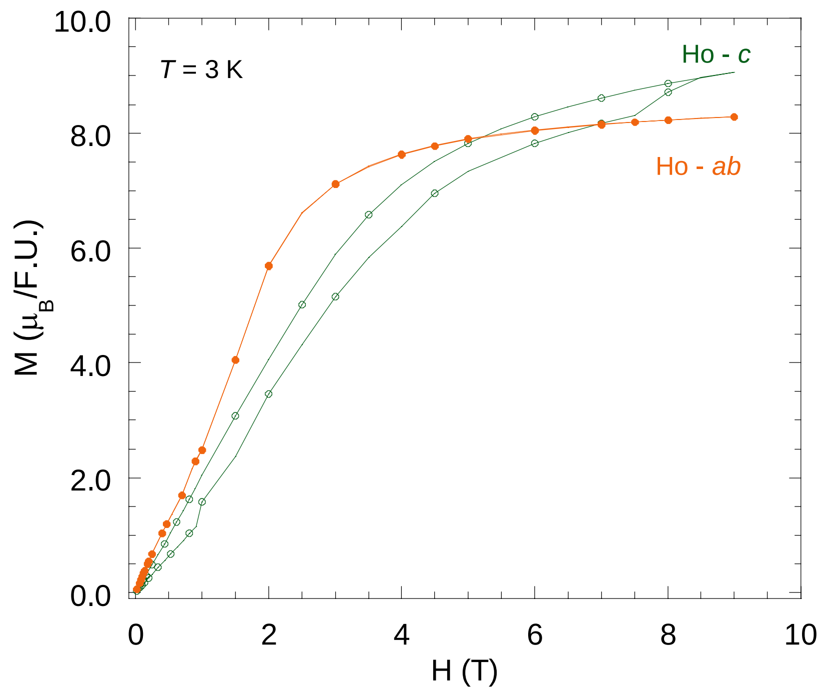

(b)

Figure 3.11 Field dependent magnetization data for $HoNiGa_4$ at field up to 9 T.

(f) $ErNiGa_4$ – This compound displays very similar magnetic behavior to the Tb sample. Two small, broad antiferromagnetic-like transitions are observed at ~ 4.0 K and 4.5 K in the susceptibilities of $ErNiGa_4$ in the *ab*- and *c*-directions, respectively, and are shown in Figure 3.12. The experimental effective moments calculated from fits to the data are 10.4(0.8) μ_B in the *ab*-direction and 9.0(1.2) μ_B in the *c*-direction, respectively. The free ion moment for Er^{3+} is 9.5 μ_B. Although the experimental moments are not largely different, the Weiss constants associated with the susceptibility curves are much different, where θ = 2.7(0.2) K in the *ab*-direction and θ = -34.5(1.1) K in the *c*-direction.

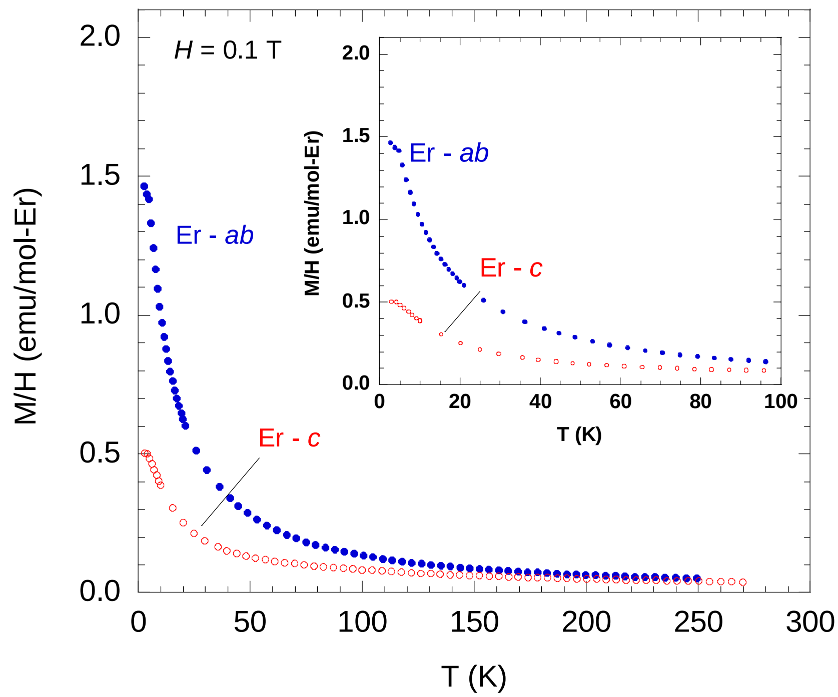

Figure 3.12 Magnetic susceptibility of $ErNiGa_4$ with field of 0.1 T applied parallel to the *ab*- and *c*-directions of the crystal.

The magnetization of $ErNiGa_4$ (Figure 3.13) in the *ab*-direction increases linearly at small fields (antiferromagnetic) and then saturates at fields up to 9 T at 7.5 μ_B, which is slightly lower than the expected magnetization saturation of 9.0 μ_B for Er^{3+}. Another small, hysteretic metamagnetic transition is observed at 4.5 T. In the *c*-direction, the magnetization looks paramagnetic and is tending toward a saturation value well below that of Er^{3+}. And unlike the Ho sample, no metamagnetic transition or hysteresis is observed for field applied along this direction.

(g) $TmNiGa_4$ - The susceptibility of $TmNiGa_4$ (Figure 3.14) in the *ab*-direction is significantly higher than that in the *c*-direction, where the experimental effective moment of Tm^{3+} in the *ab*-direction is 11.6(1.4) μ_B as compared to 6.6(2.3) μ_B in the *c*-direction. Both values are higher than the calculated magnetic contribution of 7.5 μ_B from a free Tm^{3+} ion. We see positive ordering temperatures (Curie temperatures) in both susceptibilities, 3.3 K in the *ab*-direction and 7.3 K in the *c*-direction (see inset, Figure 7). The positive Weiss constants of 3.4(0.6) K and 6.2(1.1) K for the *ab*- and *c*-directions respectively, were obtained with a modified fit.

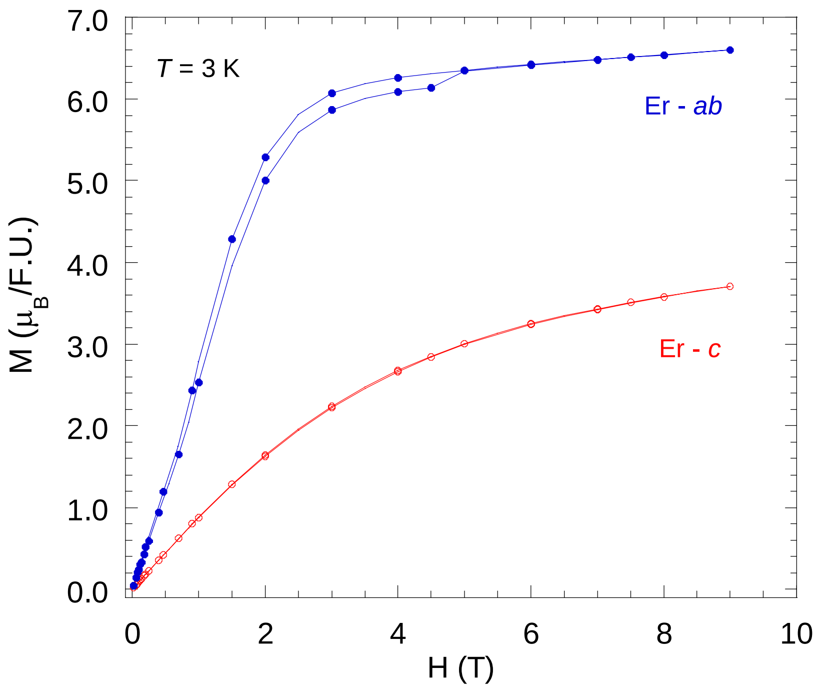

Figure 3.13 Field dependent magnetization data for $ErNiGa_4$ at field up to 9 T.

As a parallel, the magnetization curves in both directions saturate within the calculated value of 7.0 μ_B and are shown in Figure 3.15. In the *ab*-direction, the up-field and down-field curves mirror each other in trend with saturation occurring ~ 2.5 T. In the opposite direction, the up-field magnetization curve is linear until ~ 7.0 T where a large metamagnetic transition occurs and then saturates around 6.8 μ_B. The magnetization of the down-field curve remains close to 6.8 μ_B until around 2.0 T.

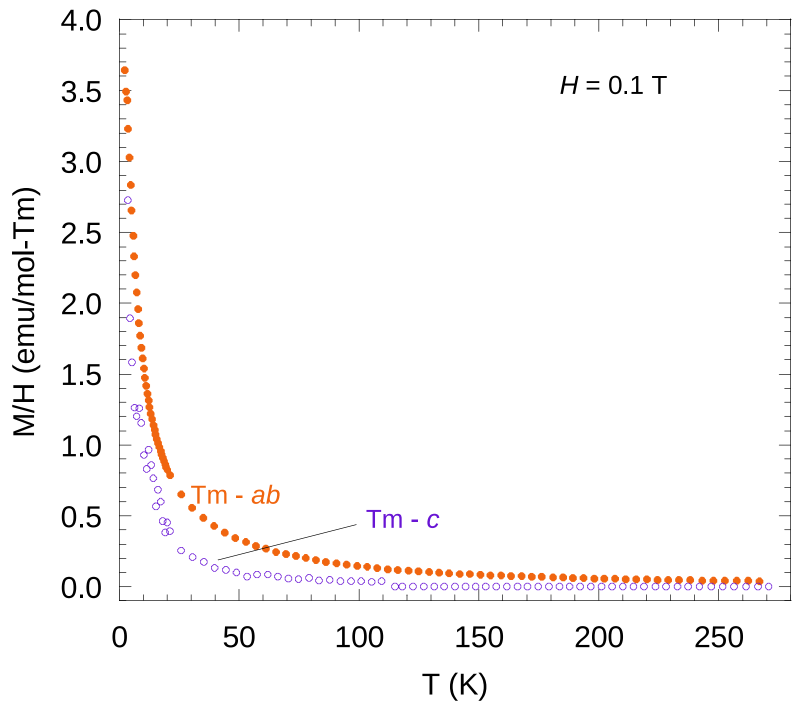

Figure 3.14 Magnetic susceptibility of $TmNiGa_4$ with field of 0.1 T applied parallel to the *ab*- and *c*-directions of the crystal.

(h) $YbNiGa_4$. The susceptibility curves of $YbNiGa_4$ are presented in Figure 3.16. Both directions have the same shape, but the susceptibility is much higher in the *ab*-direction than in the c-direction. Ordering is not seen down to 2 K in either susceptibility and both show ferromagnetic correlations from the Weiss constant, 5.1(0.5) K and 1.5(0.3) K in the *ab*- and *c*-directions. From the susceptibility curves, we expect that the effective moment in the *ab*-direction to be higher than that in the *c*-direction, where the experimental value is 11.0(1.2) μ_B in the *ab*-direction and 8.1(0.6) μ_B in the c-direction. Both values are much higher compared to the calculated value of 4.5 μ_B for a free Yb^{3+} ion.

Similarly, the magnetization curves of $YbNiGa_4$ (Figure 3.17) in the *ab*-direction is higher than that in the *c*-direction. As expected, saturation occurs ~ 6.8 μ_B in the *ab*-direction and ~ 5.8 μ_B in the *c*-direction due to stronger spin correlations in the *ab*-direction. Theoretically, the

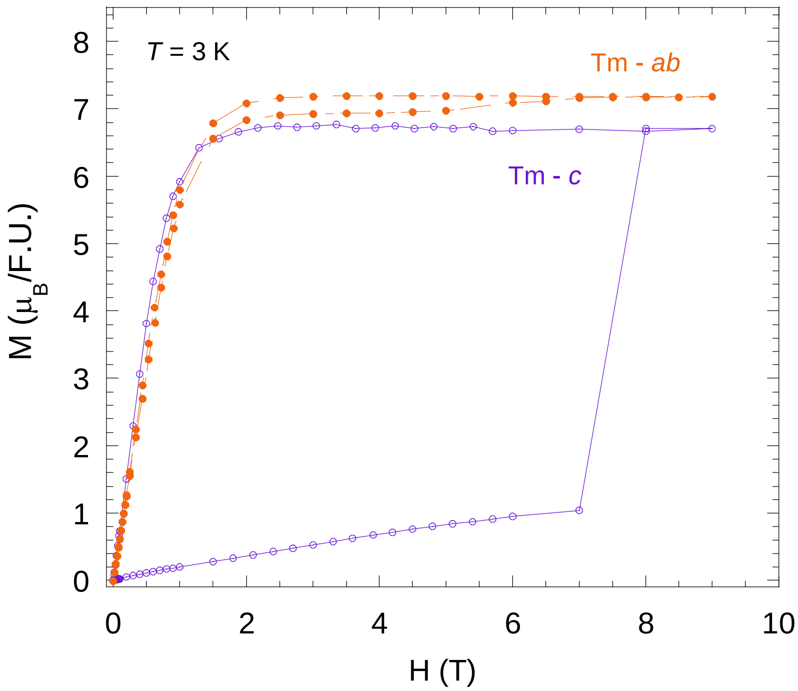

Figure 3.15 Field dependent magnetization data for $TmNiGa_4$ at field up to 9 T.

magnetic saturation of a free Yb^{3+} ion should occur around 4.0 μ_B. We believe the saturation in the *c*-direction to be higher due to a sudden change in the magnetic structure of $YbNiGa_4$ ~ 5 T, from antiferromagnetic (low magnetization) to ferromagnetic (high magnetization) and is similar to $TbNiGa_4$. Although there are not large changes in the magnetization in the *ab*-direction, there are step-wise changes when field is increased. As the field is decreased there is a smooth curve, creating a hysteretic loop.

The physical properties of our $YbNiGa_4$ compound are different than those published by Vasylechko *et al.*[8] The susceptibility of their $YbNiGa_4$ compound did not follow Curie-Weiss behavior and was approximately three orders of magnitude lower. X-ray absorption spectroscopy measurements revealed that Yb in their phase was intermediate with an effective valence of 2.48 (52% of Yb $4f^{14}$). Based on cell volume (Figure 3.18) and magnetic behavior that is similar to $TmNiGa_4$, where Tm was shown to be in the 3+ state, we believe that our phase contains Yb that is closer to the $4f^{13}$ state.

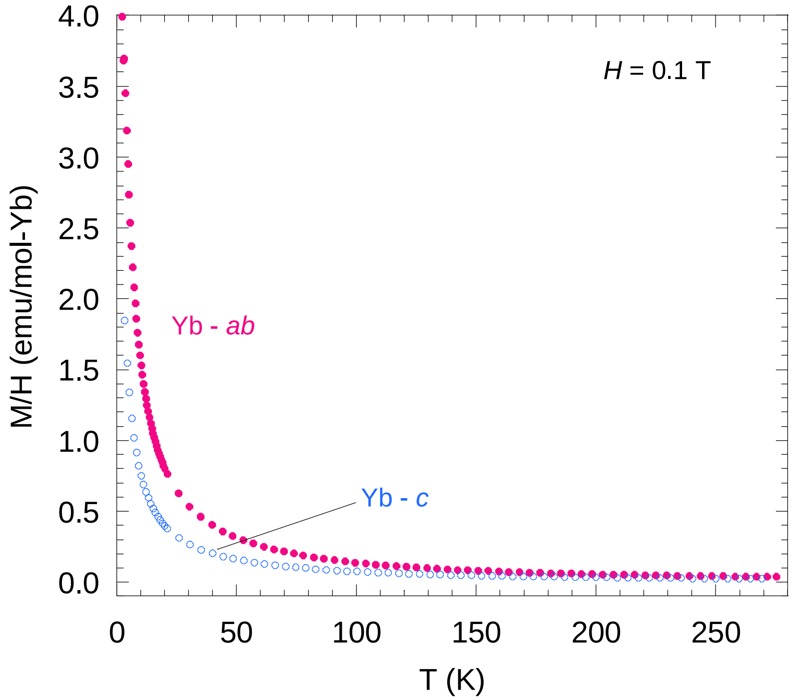

Figure 3.16 Magnetic susceptibility of $YbNiGa_4$.

To determine if the differences were consistent, we re-grew α-$YbNiGa_4$ and structurally characterized the sample with powder and single crystal X-ray diffraction. A comparison of this sample (KT054) to our previous sample (RDH036) yielded very different results. Overall, the sample KT054 was most like that of Grin's when volume and magnetic susceptibilities are compared as shown in Figures 3.19 and 3.20. Several lattice checks from different crystals within each batch reveal that each is homogenous. The single crystal XRD structure solutions are the same for Grin, RDH036, and KT054. When the powder X-ray diffraction patterns of RDH036 and KT054 are compared there is a systematic increase of +0.22 in 2θ for RDH036, which is in agreement with the smaller cell dimensions obtained in single crystal XRD experiments. Several attempts to re-synthesize RDH036 were unsuccessful.

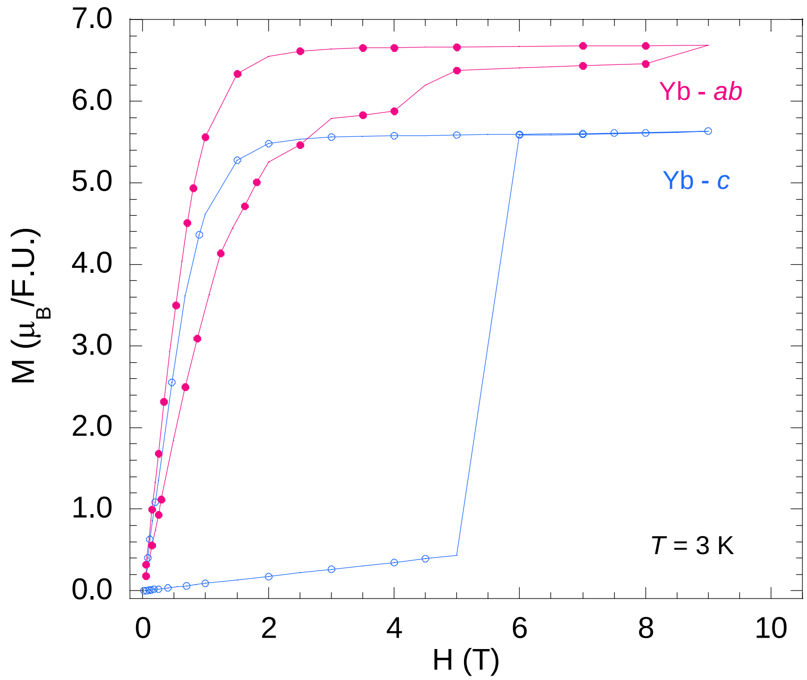

Figure 3.17 Magnetization of $YbNiGa_4$ at 3 K.

(i) The relationship between θ (K) and *Ln*-*Ln* distances are presented in Figure 3.21. We were able to use a cosine function to fit the θ-values obtained from the magnetic susceptibility of *Ln*$NiGa_4$ (*Ln* = Gd-Yb) in the *ab*-direction. This trend of theta as a function of *Ln*-*Ln* distance suggests a dominance of RKKY in this family of compounds, where the closest *Ln*-*Ln* contacts lead to magnetic ordering via conduction electrons. A summary of magnetic data is presented in Tables 3.5 and 3.6.

3.3.2.2 Transport

The resistivity of each analogue is presented in Figures 3.22 and 3.23. Each maintains a linear relationship as a function of temperature down to temperatures of 16.1 K, 13.3 K, 10.5 K,

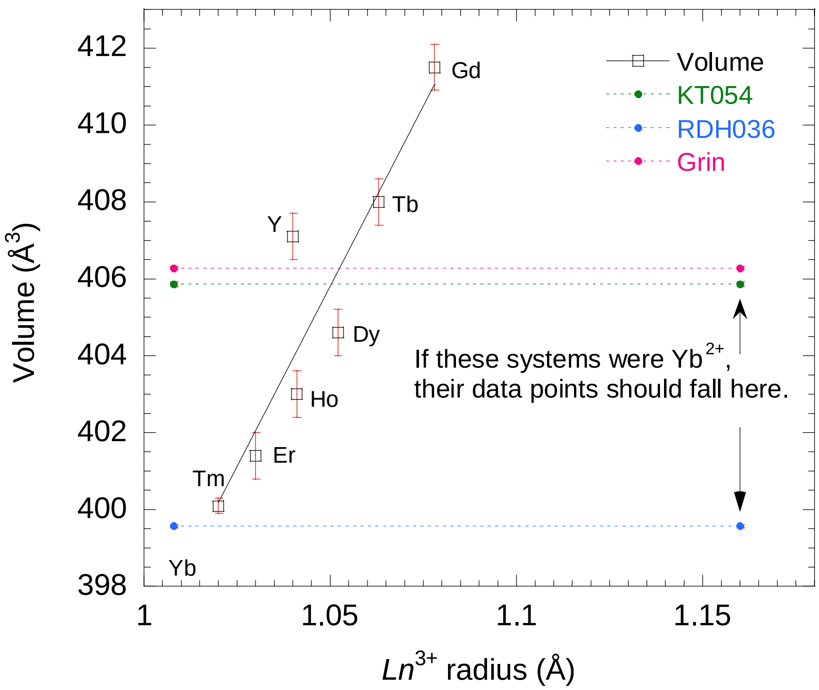

Figure 3.18 A plot of volume versus rare earth radii.

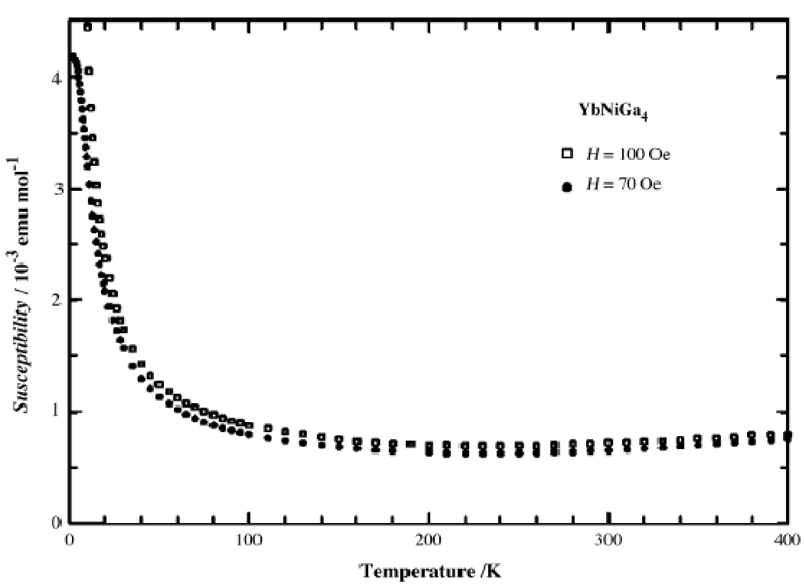

Figure 3.19 Magnetic susceptibility of $YbNiGa_4$ in fields of 100 Oe and 7 kOe, as obtained from reference [8].

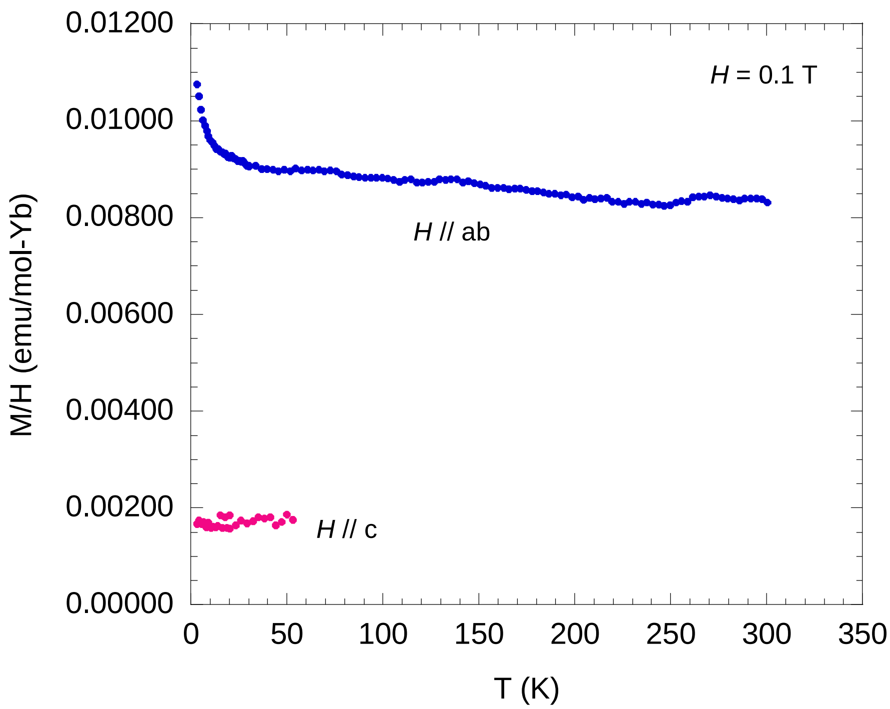

Figure 3.20 A quick scan of the magnetic susceptibility of KT054.

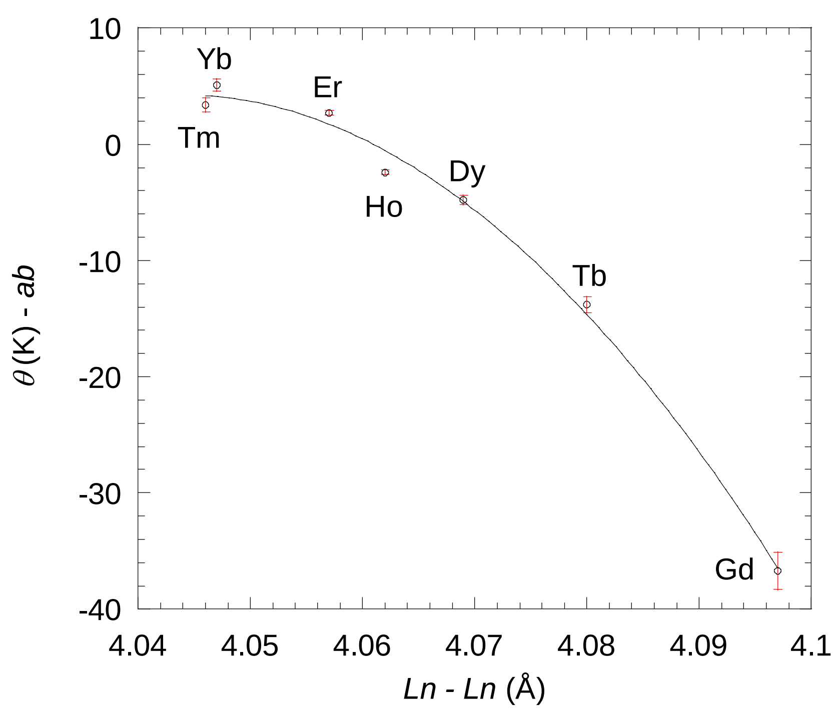

Figure 3.21 The Weiss constant (θ) varies as a function of *Ln*-*Ln* distance.

5.0 K, 9.5 K, 8.3 K, and 3.0 K for $GdNiGa_4$, $TbNiGa_4$, $DyNiGa_4$, $HoNiGa_4$, $ErNiGa_4$, $TmNiGa_4$, and $YbNiGa_4$, respectively, where a transition is observed. The residual resistivity ratio (RRR = $\rho_{278\ K}/\rho_{2\ K}$) for each analogue is less than ~ 50, with the exception of $ErNiGa_4$ where RRR ~ 3100. The magnetoresistance for $ErNiGa_4$ is greater than ~ 150 %, while the MR% of the other analogues is positive up to ~ 30 % (Figure 3.24).

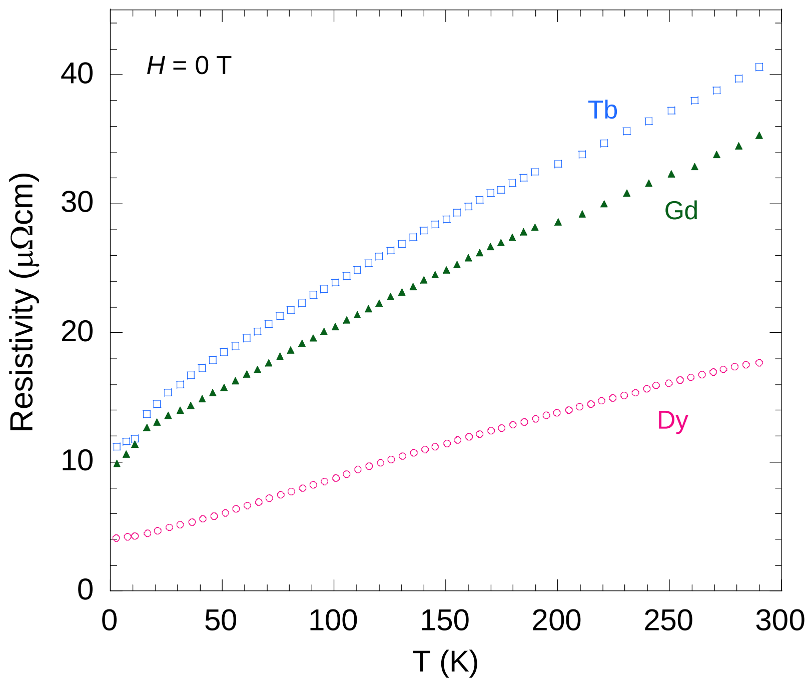

Figure 3.22 Resistivity curves of $GdNiGa_4$, $TbNiGa_4$, and $DyNiGa_4$.

3.3.2.3 X-ray Photoelectron Spectroscopy of $TmNiGa_4$

Surface studies were conducted to determine the electronic state of each element in $TmNiGa_4$. We chose to study $TmNiGa_4$ because crystals of this phase have the best crystal quality. This phase also has an effective magnetic moment much higher than expected for a free ion of Tm^{3+}. We were mainly concerned with the state of Ni and wanted to establish if Ni was contributing to the magnetism by resolving its electronic configuration. The oxidation state of

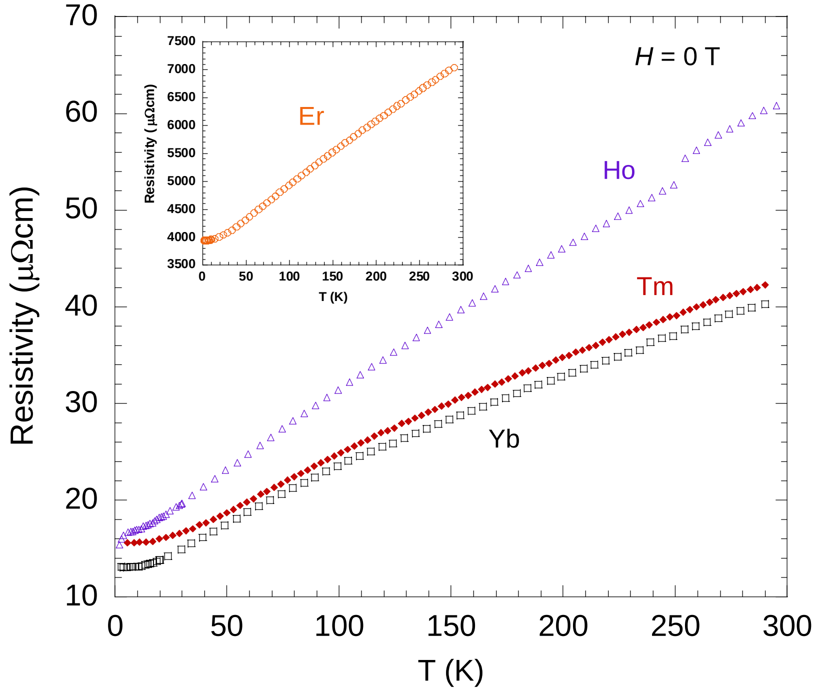

Figure 3.23 Resistivity curves of $HoNiGa_4$,$TmNiGa_4$, and $ErNiGa_4$ (inset).

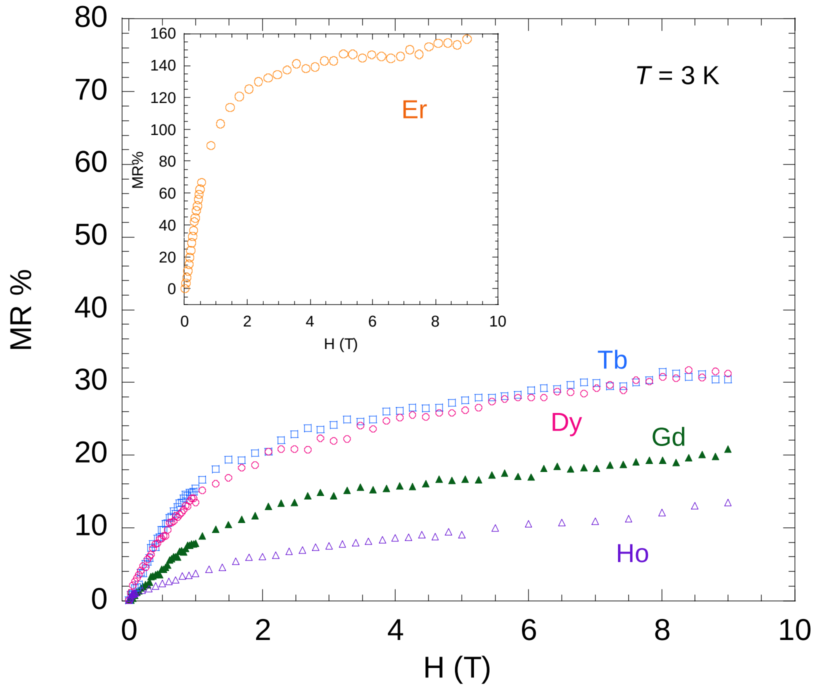

Figure 3.24 Magnetoresistance of $GdNiGa_4$, $TbNiGa_4$, $DyNiGa_4$, $HoNiGa_4$, and $ErNiGa_4$ (inset).

Table 3.5 Summary of magnetic data (*H* // *ab*-direction) for *Ln*$NiGa_4$ (*Ln* = Gd – Yb).

	T_N (K)	T_C (K)	μ_{eff} (μ_B) experimental	μ_{eff} (μ_B) calculated	θ (K)	μ_{sat} (μ_B)	T (K)
$GdNiGa_4$	16.5	------	8.3(1.2)	7.9	-36.7(1.6)	------	50 - 200
$TbNiGa_4$	25.8, 15.8	------	14.3(1.6)	9.7	-13.8(0.7)	11.8	50 - 200
$DyNiGa_4$	6.8	------	12.6(1.2)	10.6	-4.8(0.4)	9.0	50 - 200
$HoNiGa_4$	------	5.1	13.6(1.2)	10.6	-2.4(0.2)	8.0	30 - 200
$ErNiGa_4$	------	4.0	10.4(0.8)	9.5	2.7(0.2)	------	50 - 200
$TmNiGa_4$	------	3.3	11.6(1.4)	7.5	3.4(0.6)	7.0	50 - 200
$YbNiGa_4$	------	------	11.0(1.2)	4.5	5.1(0.5)	6.8	50 - 200

Table 3.6 Summary of magnetic data (*H* // *c*-direction) *Ln*$NiGa_4$ (*Ln* = Gd – Yb).

	T_N (K)	T_C (K)	μ_{eff} (μ_B) experimental	μ_{eff} (μ_B) calculated	θ (K)	μ_{sat} (μ_B)	T (K)
$GdNiGa_4$	18.3	------	7.9(1.1)	7.9	-33.4(1.3)	------	50 - 200
$TbNiGa_4$	26.9, 15.2	------	14.6(2.3)	9.7	-66.8(1.8)	------	50 - 200
$DyNiGa_4$	21.6	------	7.3(1.0)	10.6	-46.5(1.6)	------	50 - 200
$HoNiGa_4$	------	5.1	11.3(1.1)	10.6	-5.4(0.4)	9.0	50 - 200
$ErNiGa_4$	------	4.5	9.0(1.2)	9.5	-34.5(1.1)	6.5	50 - 200
$TmNiGa_4$	------	7.3	6.6(2.3)	7.5	6.2(1.1)	6.8	20 - 110
$YbNiGa_4$	------	------	8.1(0.6)	4.5	1.5(0.3)	5.6	50 - 200

Ni would give us more insight into how or if Ni is contributing to the magnetism, as Ni could be magnetically ordering or only contributing paramagnetically. Table 3.7 summarizes the Tm, Ni, and Ga energies in $TmNiGa_4$.

After the Shirley background subtraction,[11] we fitted out the binding energy position for Ni $2p_{1/2}$ and Ni $2p_{3/2}$ core levels as shown in Figure 3.25. The spin-orbit coupling value determined from the XPS spectra of $2p_{1/2}$ and $2p_{3/2}$ is 17.1 eV. Comparing the binding energy with pure Ni metal, we can conclude this material has metallic character because the binding energy for Ni $2p_{3/2}$ peak in $TmNiGa_4$ is 853.08 eV, while that of the pure Ni metal is 852.9 eV. Another very well investigated feature is the 6-eV shake up satellite in terms of final state effect. We observed that the satellite is weaker and more broadened than that in pure Ni metal. The binding energy for the satellite feature is 857.8 eV, which is smaller than that in Ni. Neither of those findings conflict with our proposed semi-itinerant model.

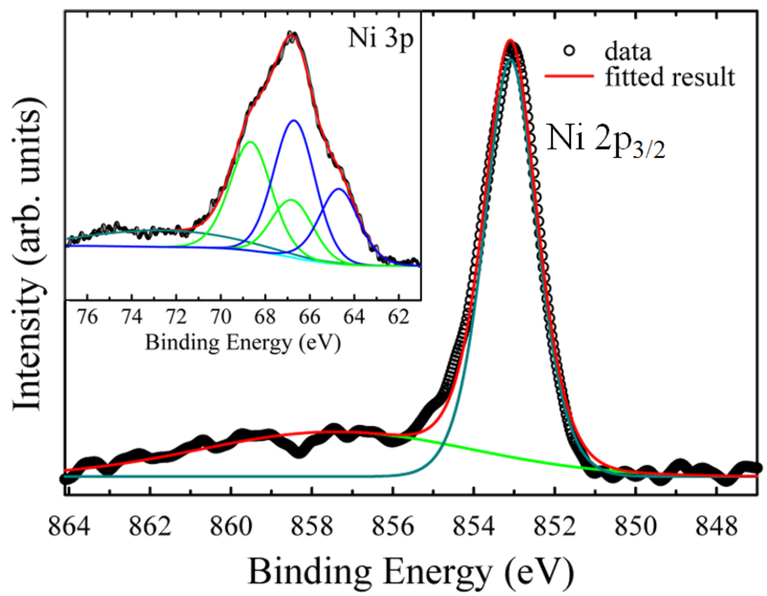

Figure 3.25 XPS spectra of Ni core levels in $TmNiGa_4$ crystal measured at room temperature. Ni $2p_{3/2}$ is fitted to a single standard core peak with a broad satellite. The Ni shallow core $3p_{1/2}$ and $3p_{3/2}$, which are fitted to two distinct components, respectively, are shown in the inset.

In this system, Ga1, Ga2 and Ga3 atoms are in a 1:1:2 ratio, respectively. This is reflected in the Ga $2p_{1/2}$ and Ga $2p_{3/2}$ spectra, where a 1:1:2 intensity ratio is also observed. The binding energies, where Ga2 > Ga3 > Ga1, reflect the atomic environments within the system. Indeed, as shown in Figure 3.26 and based on our simple fitting with standard core level spectral function after the Shirley background subtraction, the Ga $2p_{1/2}$ and $2p_{3/2}$ core spectra exhibit a three peak structure, separated by a total energy difference of ~ 2.51 ± 0.16 eV for Ga $2p_{1/2}$ and ~ 2.64 ± 0.16 eV for Ga $2p_{3/2}$ cores, respectively (see Table 3.7). These shifts are almost identical considering the resolution. The intensity ratio of the high binding energy major peak (Ga3) to each of the lower binding energy minor peaks (Ga1 and Ga2) is about 2:1, which is consistent

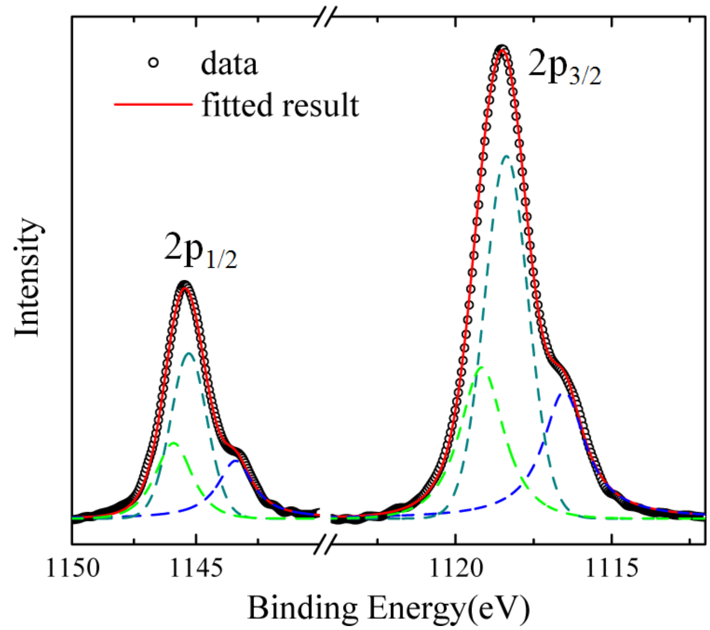

Figure 3.26 XPS spectra of Ga $2p_{1/2}$ and $2p_{3/2}$ core levels in $TmNiGa_4$ crystal measured at room temperature. Each spin-orbital splitting peak is fitted to the convolution of three components associated with the three distinct Ga sites in the compound.

with the results of the structural refinement from X-ray diffraction. It is reasonable to assign the major 2*p* peaks to the emission from Ga3 atoms while the minor 2p peaks to the emissions from Ga1 and Ga2 atoms. Further structural studies revealed that each Ga atom is surrounded by 12 nearest neighbors to form a distorted bcc-like cube with four of its six faces capped. The type of atoms that lie on the faces of the cube more strongly affect the binding energy than the interatomic distances of the neighboring atoms. The largest areas where a photon can enter the cube to excite an electron from the core Ga atom are the faces. With four faces capped, the available area is already limited. In addition, larger caps, such as *Ln* atoms, hinder the entry of the photon. In this system, Ga2 has three faces capped with Tm atoms and as a result has the largest binding energy. Ga3 and Ga1 atoms have one and zero faces capped by Tm atoms, respectively.

Table 3.7 Energies of Ni and Ga in $TmNiGa_4$.

Core levels	Binding energy (eV)	Intensity
Ni		
Ni $2p_{3/2}$	853.088	3931.283
Ni $2p_{3/2}$ satellite	857.405	2062.122(broad)
Ni $3p_{1/2}$ major	68.654	725.651
Ni $3p_{1/2}$ minor	66.694	367.359
Ni $3p_{3/2}$ major	66.787	897.129
Ni $3p_{3/2}$ minor	64.683	469.766
Ga		
Ga1 $2p_{1/2}$	1145.900	5941.209
Ga3 $2p_{1/2}$	1145.286	11930.810
Ga2 $2p_{1/2}$	1143.399	5935.497
Ga1 $2p_{3/2}$	1119.160	11848.680
Ga3 $2p_{3/2}$	1118.371	24972.996
Ga2 $2p_{1/2}$	1116.520	12427.480

3.4 Conclusion

We have grown and structurally characterized single crystals of *Ln*$NiGa_4$ (*Ln* = Y, Gd-Yb). These phases crystallize in the orthorhombic $YNiAl_4$ structure type and are magnetically anisotropic. A plot of Weiss temperatures as a function of *Ln-Ln* distance corresponds well to an RKKY-type relationship. The larger effective moments obtained from the susceptibilities of some analogues may possibly be attributed to either the fact that Ni can carry a moment or to the itinerant nature of the Ni conduction electrons. Other anomalous behavior includes the large metamagnetic transitions observed in the magnetizations of $DyNiGa_4$ and $TmNiGa_4$ at moderate magnetic fields. Additional experimental work is needed to determine the source of the large magnetic moment arising in some analogues. These compounds have small RRR and residual resistivities of 10 - 20 μΩcm, with the exception of the Er analogue. The Er compound is semimetallic having a RRR of less than 2, a residual resistivity of 4 mΩcm, and a positive MR of 150% in a 9 T field.

3.5 References

(1) Macaluso, R. T.; Nakatsuji, S.; Lee, H.; Fisk, Z.; Moldovan, M.; Young, D. P.; Chan, J. Y., Synthesis, structure, and magnetism of a new heavy-fermion antiferromagnet, $CePdGa_6$. *J. Solid State Chem.* **2003,** *174*, 296-301.

(2) Millican, J. N.; Macaluso, R. T.; Young, D. P.; Moldovan, M.; Chan, J. Y., Synthesis, structure, and physical properties of Ce_2PdGa_{10}. *J. Solid State Chem.* **2004,** *177*, 4695-4700.

(3) Macaluso, R. T.; Millican, J. N.; Nakatsuji, S.; Lee, H. O.; Carter, B.; Moreno, N. O.; Fisk, Z.; Chan, J. Y., A comparison of the structure and localized magnetism in Ce_2PdGa_{12} with the heavy fermion $CePdGa_6$. *J. Solid State Chem.* **2005,** *178*, 3547-3553.

(4) Cho, J. Y.; Millican, J. N.; Capan, C.; Sokolov, D. A.; Moldovan, M.; Karki, A. B.; Young, D. P.; Aronson, M. C.; Chan, J. Y., Crystal growth, structure, and physical properties of Ln_2MGa_{12} (Ln = La, Ce; M = Ni, Cu). *Chem. Mater.* **2008,** *20*, 6116-6123.

(5) Rykhal, R. M.; Zarechny, O.; Yarmolyuk, Y., Crystal-structure of compounds $YNiAl_4$ and $YNiAl_2$. *Kristallografiya* **1972,** *17*, 521-&.

(6) Yarmolyuk, Y. P.; Grin, Y. N., Intermetallic compounds RGa_2Ni and RGa_4Ni in (Y,Sm,Gd,Tb,Dy,Ho,Er,Tm,Yb,Lu)-Ga-Ni Systems. *Russ. Metall.* **1981,** *5*, 179-183.

(7) Romaka, V. A.; Grin, Y. N.; Yarmolyuk, Y. P., Magnetic and crystallographic characteristics of $RNiGa_4$ compounds (R=rare-earth metal). *Ukr. Fiz. Zh.* **1983,** *28*, 1095-1097.

(8) Vasylechko, L.; Schnelle, W.; Schmidt, M.; Burkhardt, U.; Borrmann, H.; Schwarz, U.; Grin, Y., Valence behaviour of ytterbium in $YbNiGa_4$. *J. Alloy Compd.* **2006,** *416*, 35-42.

(9) Sheldrick, G. M., A short history of SHELX. *Acta Cryst.* **2008,** *A64*, 112-122.

(10) Otwinowski, Z.; Minor, W., Processing of X-ray diffraction data collected in oscillation mode. In *Methods in Enzymology*, Carter, J., C. W.; Sweet, R. M., Eds. Academic Press: 1997; Vol. 276, pp 307-326.

(11) Shirley, D. A., High resolution X-ray photoemission spectrum of valence bands of gold. *Phys. Rev. B* **1972,** *5*, 4709-&.

(12) Thomas, K. R.; Hembree, R. D.; Karki, A.; Li, Y.; Zhang, J.; Young, D. P.; DiTusa, J. F.; Chan, J. Y., Anisotropic magnetism in α-$LnNiGa_4$. *J. Phys.: Condens. Matter* **2010**, to be submitted.

CHAPTER 4. *β*-*Ln*NiGa$_4$ (*Ln* = Tb – Ho): SYNTHESIS, STRUCTURE AND PROPERTIES OF A NEW POLYMORPH OF *α*-*Ln*NiGa$_4$

4.1 Introduction

The exploratory synthesis of *Ln*-Ni-Ga systems led us to characterize a number of intermetallic phases, including Ln_2NiGa_{12} (*Ln* = La-Nd, Sm) and *α*-*Ln*NiGa$_4$ (*Ln* = Y, Gd – Yb) [1-3]. The tetragonal Ln_2NiGa_{12} phases crystallize in the *P*4/*nbm* space group, with *Ln* atoms in cavities made by Ga atoms. Ce_2NiGa_{12} magnetically orders ~ 10 K and was shown to have enhanced electronic mass with $\gamma \approx 191$ mJ/mol^{-1} K^{-2} [1]. A large positive magnetoresistance ~ 216 % at 9 T was observed for La_2NiGa_{12} [1]. *α*-*Ln*NiGa$_4$ phases crystallize in the orthorhombic *Cmcm* space group and have lattice parameters *a* ~ 4 Å, *b* ~ 15 Å, and *c* ~ 6 Å. In addition to magnetic anisotropy, susceptibility measurements in the *ab*-direction reveal a switch from antiferromagnetic to ferromagnetic correlations across the rare earth series [3]. In this manuscript, we report the synthesis of *β*-*Ln*NiGa$_4$ (*Ln* = Tb, Dy, Ho). We have found these phases to be structurally similar to the previously studied modulated, charge density wave compounds YCo_xGa_3Ge [4] and $GdCo_{1-x}Ga_3Ge$ [5,6]. The disorder in the Ga-square nets of $GdCo_{1-x}Ga_3Ge$ was first identified by the presence of a supercell, which was observed through selected area electron diffraction experiments [6]. Further investigation with the use of a (3+1)*D* superspace technique revealed that the superstructure is present in the *ab*-plane of YCo_xGa_3Ge and $GdCo_{1-x}Ga_3Ge$ and is incommensurate with the tetragonal lattice. In both phases, the site occupancy for Co is inversely coupled with the site occupancy of Ga in the $[CoGa]_2$ net. We also observe disorder within the Ga nets of *β*-*Ln*NiGa$_4$ (*Ln* = Tb, Dy, Ho) and this leads us to believe that these compounds are possibly modulated structures as well. Here we present the single crystal X-ray diffraction studies, magnetic, and electrical properties of *β*-*Ln*NiGa$_4$ (*Ln* = Tb, Dy, Ho).

4.2 Experimental

4.2.1 Synthesis

Single crystals of *β*-*Ln*$NiGa_4$ (*Ln* = Tb, Dy, Ho) were synthesized using the self-flux method where *Ln* (3*N*, Alfa Aesar), Ni powder (5*N*, Alfa Aesar) and Ga shot (7*N*, Alfa Aesar) were placed into an alumina crucible in a 1.5:1:15 reaction ratio. Each crucible was covered with quartz wool, sealed in an evacuated silica tube, and placed into a high temperature furnace for heat treatment. The ampoules were heated to 1423 K at 170 K/h, and annealed at that temperature for 24 h. They were then cooled to 773 K at 150 K/h and further cooled to 723 K at 8 K/h. Each ampoule was inverted and centrifuged for up to 8 min to remove excess Ga flux, which flowed into the quartz wool that initially covered the sample. Plate-like aggregates contained single crystals up to 2 mm × 1 mm × 0.025 mm and did not show signs of degradation in air. This method also yielded less than 5 % of *α*-*Ln*$NiGa_4$, an orthorhombic phase that can be isolated by slow-cooling from 973 K to 873 K. When the heat treatment was modified to slow-cool from 823 K to 723 K there was about 10 % of *α*-*Ln*$NiGa_4$ present [3], indicating that the optimal range for *β*-*Ln*$NiGa_4$ formation is from 773 to 723 K. Slow-cooling below 723 K would most likely lead to the formation of the binary *Ln*Ga_6, a very robust compound that often forms at low-temperatures in this phase space. The *α*-*Ln*$NiGa_4$ and *β*-*Ln*$NiGa_4$ phases are easily separated by morphology, since *α*-*Ln*$NiGa_4$ grew as thin needles. Powder diffraction was used to confirm the purity of *β*-*Ln*$NiGa_4$ single crystals and *α*-*Ln*$NiGa_4$ was not found as an impurity.

4.2.2 Single Crystal X-ray Diffraction

Silver-colored fragments with approximate dimensions 0.025 × 0.05 × 0.08 mm^3 were cleaved from aggregates of *β*-*Ln*$NiGa_4$ (*Ln* = Tb, Dy, Ho) and were mounted onto the goniometer of a Nonius KappaCCD diffractometer equipped with MoK_α radiation (λ = 0.71073 Å). Data were collected up to θ = 30.0° at 298 K. In addition, data were collected on *β*-$TbNiGa_4$ at 200 K, 240 K, and 340 K to observe how the structure changes as a function of temperature. Each collection encompassed a hemisphere of reciprocal space and the raw data were scaled in the triclinic *P*1 space group to ensure that all collected intensities were included for structural refinement. Further crystallographic parameters for β-*Ln*NiGa$_4$ (*Ln* = Tb, Dy, Ho) are provided in Table 4.1.

The space group (*I*4/*mmm*) and atomic positions of YNiGa$_3$Ge[12] were used as an initial model for the structure determination of each phase. The structural model was refined using SHELXL97 and absorption corrections were applied using a multi-scan method that modifies redundancies in the data-set. Data were also corrected for extinction and refined with anisotropic displacement parameters. After we obtained a good structural model with low residual electron densities and R-values, weighting schemes (*w*) were applied. The results were comparable to those found for YNiGa$_3$Ge, where the *RE*MGa$_3$Ge (*RE* = Y, Gd, Sm; *M* = Co, Ni) structure-type was found to contain superstructures through transmission electron microscopy (TEM) studies using selected area electron diffraction (SAED). In addition to the strong Bragg subcell reflections, the authors also observed supercell reflections in the SAED patterns at 0 1 0, -1 0 0, 0 -1 0, and 1 0 0 in the [001] zone axis for SmNiGa$_3$Ge, SmCoGa$_3$Ge, and GdCoGa$_3$Ge. These supercell reflections are symmetry forbidden according to the conditions that limit the possible reflections for the *I*4/*mmm* space group, which state that every *hkl* reflection must give an even number for $h + k + l$. This condition is more clearly stated as *hkl*: $h + k + l = 2n$, where *n* is an integer. This structure type was later found to be modulated through studies of the GdCo$_{1-x}$Ga$_3$Ge[9] and YCo$_{0.88}$Ga$_3$Ge[11] analogues which crystallize in the orthorhombic *Immm*(α00)00*s* superspace group with $a \sim 4.1$, $b \sim 4.1$, and $c \sim 23$ Å. A modulation vector of $q = 0.3200(4)a^*$ and $q = 0.3043(12)a^*$ for GdCo$_{1-x}$Ga$_3$Ge and YCo$_{0.88}$Ga$_3$Ge, respectively, were obtained using a (3+1)*D* superspace technique.

Table 4.1 Crystallographic parameters for *β-Ln*NiGa$_4$ in the tetragonal *I*4/*mmm* space group

Crystal data				
Formula	β-TbNiGa$_{3.9}$	β-TbNiGa$_{3.8}$	β-DyNi$_{0.9}$Ga$_{3.9}$	β-HoNi$_{0.9}$Ga$_{3.9}$
a (Å)	4.207(5)	4.201(5)	4.191(2)	4.181(2)
c (Å)	23.838(5)	23.805(5)	23.699(5)	23.612(5)
V (Å^3)	421.9(7)	420.1(7)	416.3(3)	412.7(4)
Z	4	4	4	4
Crystal size (mm^3)	0.03×0.08×0.13	0.03×0.08×0.13	0.03×0.05×0.08	0.05×0.08×0.08
θ range (°)	3.42-30.04	1.71-30.09	1.72-29.88	3.45-29.95
μ (mm^{-1})	45.859	46.053	47.438	48.907
Data Collection				
Temperature (K)	298	200	298	298
Measured reflections	627	2220	572	562
Independent reflections	231	232	227	225
R_{int}	0.0302	0.1124	0.0733	0.0558
h	-5→5	-5→5	-5→5	-5→5
k	-4→4	-5→5	-4→4	-4→4
l	-33→33	-33→33	-32→31	-26→32
Refinement				
$^aR^1[F^2>2\sigma(F^2)]$	0.0338	0.0435	0.0578	0.0422
$^bwR^2(F^2)$	0.0913	0.1065	0.1525	0.1055
Reflections	231	232	227	225
Parameters	27	27	27	27
$\Delta\rho_{max}$ (eÅ^{-3})	3.419	3.464	3.123	3.420
$\Delta\rho_{min}$ (eÅ^{-3})	-2.460	-2.204	-5.814	-5.062
GooF	1.129	1.141	1.185	1.084

$^aR_1 = \Sigma\| F_o| - |F_c\| / \Sigma|F_o|$.
$^bwR_2 = [\Sigma[w(F_o^2-F_c^2)^2]/\Sigma[w(F_o^2)^2]]^{1/2}$; $w = 1/[\sigma^2F_o^2 + (0.0491P)^2 + 17.8401P]$, $w = 1/[\sigma^2F_o^2 + (0.0559P)^2 + 21.4803P]$, $w = 1/[\sigma^2F_o^2 + (0.0988P)^2 + 8.6374P]$, and $w = 1/[\sigma^2F_o^2 + (0.0557P)^2 + 13.7088P]$ for β-TbNiGa$_{3.9}$, β-TbNiGa$_{3.8}$, β-DyNi$_{0.9}$Ga$_{3.9}$, and β-HoNi$_{0.9}$Ga$_{3.9}$, respectively.

Based on these findings, we have modeled our systems to account for the disorder observed in our original structural refinement by modifying the occupancies of several atoms. Although weighting schemes improved we still observed enlarged thermal ellipsoids that did not scale well, which indicated that the system was very disordered. Data collections at 200 K for β-TbNiGa$_4$ did not have any significant impact on the anisotropic displacement parameters, but we did observe additional symmetry forbidden *hkl* reflections that were not present at 240 K, 298 K, and 340 K. In agreement with the work conducted on *REM*Ga$_3$Ge (*RE* = Y, Gd, Sm; *M* = Co, Ni), we see forbidden reflections in the reciprocal lattice for *β*-$TbNiGa_4$ at *hkl* 0 1 0, -1 0 0, 0 -1 0, and 1 0 0. We attribute these additional, or satellite, reflections to a supercell but are not able elucidate a modulation vector given that we do not possess the (3+1)*D* superspace technique. Attempts to solve the structure within the same space group with a doubled *c*-axis, doubled *a*- and *b*-axes, and a doubled cell were unsuccessful. The same number of reflections was used for the solution of each doubling attempt since the space group was kept the same. The only way to incorporate the additional reflections into the refinement was to switch to a primitive cell setting (*P*4/*mmm*), where twice as many reflections were needed for a solution. Modeling the unit cell within this space group was unsuccessful due to the very low intensity of the supercell reflections.

Our final model was solved within *I*4/*mmm* space group. Atomic positions and displacement parameters for each compound are provided in Table 4.2, and selected interatomic distances are presented in Table 4.3. The Ga4' position in our structure solution represents the movement (or modulation) of Ga4 within the Ni2-Ga4 nets, therefore the Ga4 and Ga4' positions were restrained to have the same atomic displacement parameter (ADP) value. If ADPs were unconstrained for Ga4 and Ga4' a non-positive definite ADP was obtained for Ga4', indicating that the two could not have independent thermal fluctuations. Attempts to completely remove Ga4' from the model resulted in a residual electron density ~ 10 e/Å^3. A refinement of *β*-$TbNiGa_4$ at 200 K was modeled without the Ga4' position to determine the direction of the motion of Ga4 within the Ni2-Ga4 nets. Atomic positions and displacement parameters for this model are located in Table 4.4. The ADP of Ga4 more than triples when the Ga4' position is not included in the refinement as shown in Table 4.5. The ADP value changed from approximately 0.022(5) Å^2 to 0.08716(337) Å^2. Also, the Ga4 position is fully occupied when Ga4' is not present. The occupancy of Ni2 remains the same within the error of the experiment. From Table

Table 4.2 Atomic positions and thermal parameters for *β-Ln*$NiGa_4$ (Ln = Tb, Dy, Ho)

Atom	Wyckoff position	*x*	*y*	*z*	Occ.[b]	U_{eq} ($Å^2$)[a]
β-$TbNiGa_{3.9}$						
T = 298 K						
Tb	4*e*	0	0	0.14720(3)	1	0.0095(4)
Ni1	2*a*	0	0	0	1	0.0094(7)
Ni2	4*e*	0	0	0.2834(3)	0.504(16)	0.037(2)
Ga1	8*g*	1/2	0	0.44524(6)	1	0.0144(5)
Ga2	4*d*	0	1/2	1/4	0.367(5)	0.0283(17)
Ga3	4*e*	0	0	0.3574(17)	0.53(6)	0.025(5)
Ga4	4*e*	0	0	0.3834(13)	0.47(6)	0.017(3)
Ga4’	16*n*	0	0.618(4)	0.7384(6)	0.133(5)	0.0283(17)
β-$TbNiGa_{3.8}$						
T = 200 K						
Tb	4*e*	0	0	0.14720(4)	1	0.0107(5)
Ni1	2*a*	0	0	0	1	0.0094(10)
Ni2	4*e*	0	0	0.2836(3)	0.518(19)	0.040(3)
Ga1	8*g*	1/2	0	0.44522(8)	1	0.0146(6)
Ga2	4*d*	0	1/2	1/4	0.378(5)	0.024(2)
Ga3	4*e*	0	0	0.354(2)	0.41(9)	0.014(5)
Ga4	4*e*	0	0	0.380(2)	0.59(9)	0.022(5)
Ga4’	16*n*	0	0.618(4)	0.7390(9)	0.122(5)	0.024(2)
β-$DyNi_{0.9}Ga_{3.9}$						
T = 298 K						
Dy	4*e*	0	0	0.14748(3)	1	0.0099(7)
Ni1	2*a*	0	0	0	1	0.0099(11)
Ni2	4*e*	0	0	0.2822(4)	0.48(2)	0.039(4)
Ga1	8*g*	1/2	0	0.44485(8)	1	0.0144(8)
Ga2	4*d*	0	1/2	1/4	0.357(6)	0.028(2)
Ga3	4*e*	0	0	0.3522(10)	0.40(6)	0.014(3)
Ga4	4*e*	0	0	0.3783(13)	0.60(6)	0.026(5)
Ga4’	16*n*	0	0.588(6)	0.7408(10)	0.143(6)	0.028 (2)
β-$HoNi_{0.9}Ga_{3.9}$						
T = 298 K						
Ho	4*e*	0	0	0.14766(4)	1	0.0089(5)
Ni1	2*a*	0	0	0	1	0.0080(9)
Ni2	4*e*	0	0	0.2823(3)	0.043(10)	0.032(3)
Ga1	8*g*	1/2	0	0.44448(7)	1	0.0119(6)
Ga2	4*d*	0	1/2	1/4	0.343(6)	0.029(2)
Ga3	4*e*	0	0	0.3535(12)	0.54(6)	0.014(3)
Ga4	4*e*	0	0	0.3794(18)	0.46(6)	0.019(5)
Ga4’	16*n*	0	0.568(8)	0.7420(16)	0.157(6)	0.029 (2)

[a]U_{eq} is defined as one-third of the trace of the orthogonalized U_{ij} tensor.

[b]Occupancy.

Table 4.3 Selected interatomic distances (Å) for *β-Ln*$NiGa_4$ (*Ln* = Tb – Ho)

	Ln-Ga plane		$[NiGa_6]$ slab		$[Ni\text{-}Ga]_2$ net	
β-$TbNiGa_{3.9}$	Tb-Ga2 (×4)	3.063(8)	Ni1-Ga1 (×8)	2.476(2)	Ni2-Ga4 (×4)	2.249(3)
T = 298 K	Tb-Ga3 (×4)	2.977(4)			Ni2-Ga4' (×4)	1.728(14)
					Ni2-Ga4' (×4)	2.404(7)
					Ni2-Ga4' (×4)	2.611(17)
β-$TbNiGa_{3.8}$	Tb-Ga2 (×4)	3.043(11)	Ni1-Ga1 (×8)	2.472(2)	Ni2-Ga4 (×4)	2.247(4)
T = 200 K	Tb-Ga3 (×4)	2.971(4)			Ni2-Ga4' (×4)	1.691(16)
					Ni2-Ga4' (×4)	2.405(9)
					Ni2-Ga4' (×4)	2.65(2)
β-$DyNiGa_4$	Dy -Ga2 (×4)	3.026(6)	Ni1-Ga1 (×8)	2.4697(10)	Ni2-Ga4 (×4)	2.230(3)
T = 298 K	Dy -Ga3 (×4)	2.9636(2)			Ni2-Ga4' (×4)	1.811(18)
					Ni2-Ga4' (×4)	2.343(9)
					Ni2-Ga4' (×4)	2.52(3)
β-$HoNiGa_4$	Ho -Ga2 (×4)	3.025(9)	Ni1-Ga1 (×8)	2.4676(9)	Ni2-Ga4 (×4)	2.225(3)
T = 298 K	Ho -Ga3 (×4)	2.9566(4)			Ni2-Ga4' (×4)	1.89(2)
					Ni2-Ga4' (×4)	2.314(13)
					Ni2-Ga4' (×4)	2.44 (4)

4.5 it can be seen that Ga4 and Ni2 are moving more in the *ab*- than in the *c*-direction. As a result, the Ga2 and Ga3 atoms move more in the *c*-direction to compensate for the modulation of Ga in the Ni2-Ga4 net. This type of motion is in agreement with that seen in $GdCo_{1-x}Ga_3Ge$ and $YCo_{1-x}Ga_3Ge$ where modulation occurs within the Ga nets of the structure. The diameter of the Ga4 thermal ellipsoid is 0.90 Å in the crystallographic *a*- and *b*- directions, and is approximately 0.68 Å in the *c*-direction. For comparison, the diameters of the Ga2 and Ga3 ellipsoids are as follows: 0.11 Å in the *a*- and *b*-directions and 0.29 Å in the *c*-direction. Each diameter length is relative to the cell dimensions.

Table 4.4 Atomic positions and thermal parameters of β-$TbNiGa_4$ modeled without the Ga4' position

Atom	Wyckoff position	*x*	*y*	*z*	Occ.[b]	U_{eq} (Å^2)[a]
β-$TbNiGa_4$						
T = 200 K						
Tb	4*e*	0	0	0.14723(7)	1	0.0116(8)
Ni1	2*a*	0	0	0	1	0.0108(14)
Ni2	4*e*	0	0	0.2837(5)	0.49(3)	0.036(5)
Ga1	8*g*	1/2	0	0.44528(12)	1	0.0155(9)
Ga2	4*d*	0	1/2	1/4	1	0.087(3)
Ga3	4*e*	0	0	0.3548(7)	0.476(16)	0.0181(19)
Ga4	4*e*	0	0	0.3812(6)	0.524(16)	0.0181(19)

Table 4.5 Anisotropic displacement parameters (Å^2) of β-$TbNiGa_4$ at 200 K modeled without the Ga4' position

	U_{11}	U_{22}	U_{33}	U_{eq}
Tb	0.0128(9)	0.0128(9)	0.0090(1)	0.011(8)
Ni1	0.011(2)	0.011(2)	0.009(3)	0.010(2)
Ni2	0.044(6)	0.044(6)	0.020(7)	0.036(5)
Ga1	0.023(2)	0.010(2)	0.030(5)	0.0155(9)
Ga2	0.011(2)	0.011(2)	0.030(5)	0.018(2)
Ga3	0.011(2)	0.011(2)	0.030(5)	0.018(2)
Ga4	0.094(5)	0.094(5)	0.072(6)	0.087(3)

*U_{12}, U_{13}, and U_{23} are zero for each atom.

4.2.3 Physical Property Measurements

Aggregates of β-LnNiGa$_4$ (*Ln* = Tb, Dy, Ho) were prepared by etching in dilute hydrochloric acid to remove excess flux. Sample purity was confirmed via powder X-ray diffraction. Magnetization data were obtained using a Quantum Design Physical Property Measurement System. The temperature-dependent magnetization data were obtained from 2 K to 300 K with an applied field 0.1 T. Field-dependent measurements were collected at 3 K with field swept between 0 T and 9 T. The electrical resistance data were measured using the standard four-probe AC technique.

4.3 Results and Discussion

4.3.1 Structure

In an effort to synthesize latter rare earth phases of the Sm_2NiGa_{12}[13] structure type, we have found three new analogues in the *Ln*-Ni-Ga phase space. Single crystals of β-*Ln*$NiGa_4$ (*Ln* = Tb, Dy, Ho) were formed, most likely due to Ln_2NiGa_{12} phase instability with smaller rare earth elements. These phases crystallize in the tetragonal *I*4/*mmm* space group with lattice parameters $a \sim 4$ Å and $c \sim 23$ Å, $Z = 4$, $V \sim 400$ Å^3 as shown in Figure 4.1. β-*Ln*$NiGa_4$ (*Ln* = Tb, Dy, Ho) are isostructural to $YNiGa_3Ge$,[12] a disordered derivative of the Ce_2NiGa_{10}[14] structure type. In our analogues, a substitution of Ge with Ga changes the structure formula from $RE_4M_2[M_2\square_2Ga''_{12}Ge_4]$ to $RE_4M_2[\mathrm{M}_2\square_2Ga''_{12}Ga_4]$, where ($\square$) represents vacancies not found in the Ce_2NiGa_{10} structure type. β-$TbNiGa_4$, β-$DyNiGa_4$, and β-$HoNiGa_4$ are related to the linear inhomogeneous $BaAl_4$ – CaF_2 intergrowth series, which also include Ce_2NiGa_{10}[14] and $Ce_4Ni_2Ga_{17}$.[15] The unit cell volume decreases from β-$TbNiGa_4$ to β-$HoNiGa_4$ and is consistent with lanthanide contraction.

The crystal structure of β-*Ln*$NiGa_4$ (*Ln* = Tb, Dy, Ho) is composed of *Ln*-Ga planes, $[NiGa_6]$ slabs, and $[Ni\text{-}Ga]_2$ nets. *Ln*-Ga planes contain *Ln* surrounded by disordered Ga atoms, where four Ga2 and four Ga3 atoms are positionally disorderd. *Ln*-*Ln* interatomic distances are equal to the length of the crystallographic *a*-axis of the unit cell and are not within bonding distance. *Ln*-Ga interatomic distances are in good agreement with those found in $TbGa_3$,[16] Dy_5Ga_3,[17] and $HoGa_2$.[18]

Slabs of [$NiGa_4'Ga_2''$], where Ga′ and Ga″ represent Ga1 and Ga3 atoms, respectively, traverse through the *ab*-plane of the structure. Ni1 has 8 nearest neighbor Ga1 atoms and 8 next nearest neighbor Ga4 atoms, where Ga1 atoms are located on the faces of the cell and Ga4 atoms are positioned on the edges of the cell. In the *ab*-plane of the structure, $NiGa_4'$ rectangular prisms are edge-sharing ($NiGa_{8/2}$). A second sub-structure, a puckered net of $[Ni\text{-}Ga]_2$, also extends through the *ab*-plane of the cell and is formed by alternating Ni and Ga atoms in an *ABAB*... arrangement, where *A* is Ni2 and *B* represents Ga4 atoms. Ni2 – Ga4 interatomic distances are 2.249(3) Å in β-$TbNiGa_4$, 2.230(3) Å in β-$DyNiGa_4$, and 2.225(3) in β-$HoNiGa_4$,

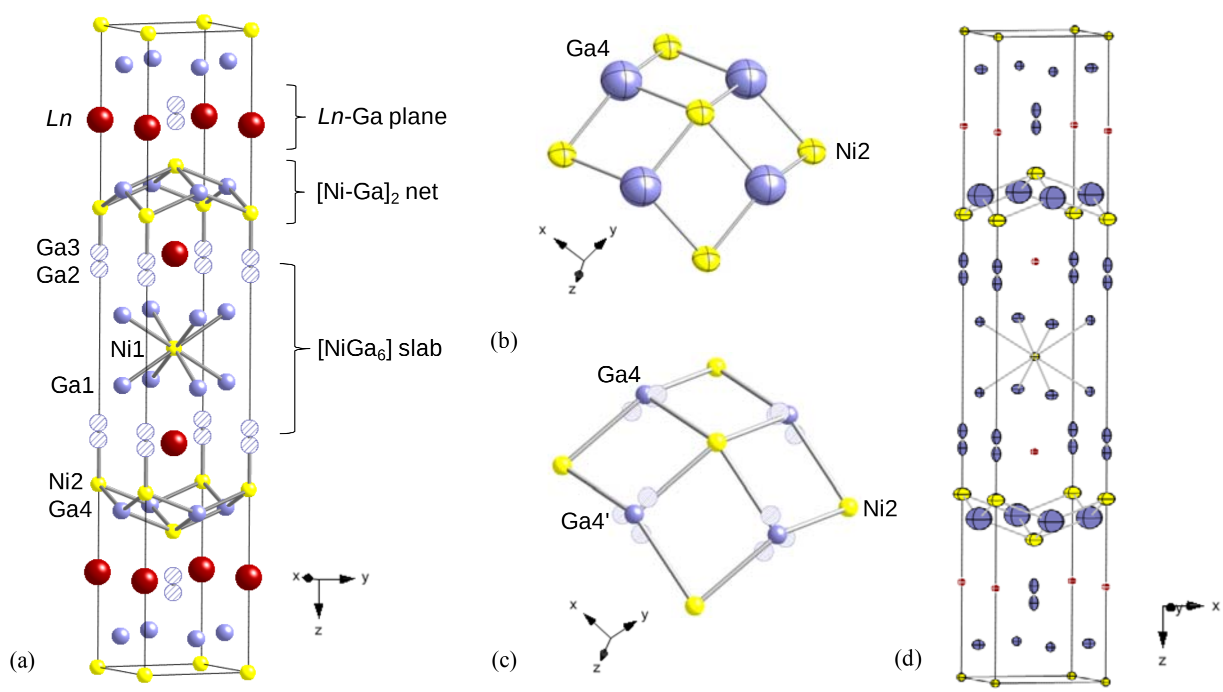

Figure 4.1 The crystal structure of β-$TbNiGa_4$ is presented as a model for β-*Ln*$NiGa_4$ (*Ln* = Dy, Ho). (a) The unit cell is shown where *Ln* atoms are red spheres, Ni atoms are yellow spheres, and Ga atoms are purple spheres. The striped, purple spheres represent Ga atoms that are positionally disordered. Ga4' atoms have been omitted from this model for clarity. (b) A model depicting the enlarged thermal ellipsoids of Ga4. (c) A Ni2-Ga4 net is shown with Ga4' atoms included to depict the modulation of electron density of Ga4 within the net. Ga4 atoms are filled spheres and Ga4' atoms are hatched spheres. (d) A thermal ellipsoid plot of the unit cell is presented to show the size of the Ga4 ellipsoid as compared to the other Ga atoms, and to show that Ga2, Ga3, and Ga4 ellipsoids are highly directional.

and are within expected *Ln*-Ga interatomic distances. The disorder of Ga4 within the nets is modeled by a Ga4' position as shown in the top-right of Figure 4.1.

4.3.2 Magnetic and Transport Properties

The magnetic susceptibilities of β-*Ln*$NiGa_4$ (*Ln* = Tb, Dy, Ho), which are presented in Figure 4.2, were measured under an applied field of 0.1 T with field parallel to the *c*-direction of the crystals. β-$TbNiGa_4$, β-$DyNiGa_4$, and β-$HoNiGa_4$ each shows paramagnetic behavior at high temperatures, and each has a magnetic transition ~ 5 K. Fitting the data to a Curie-Weiss law with a temperature-independent background term [$\chi = C/(T-\theta) + \chi_0$] returns Weiss constants (θ)

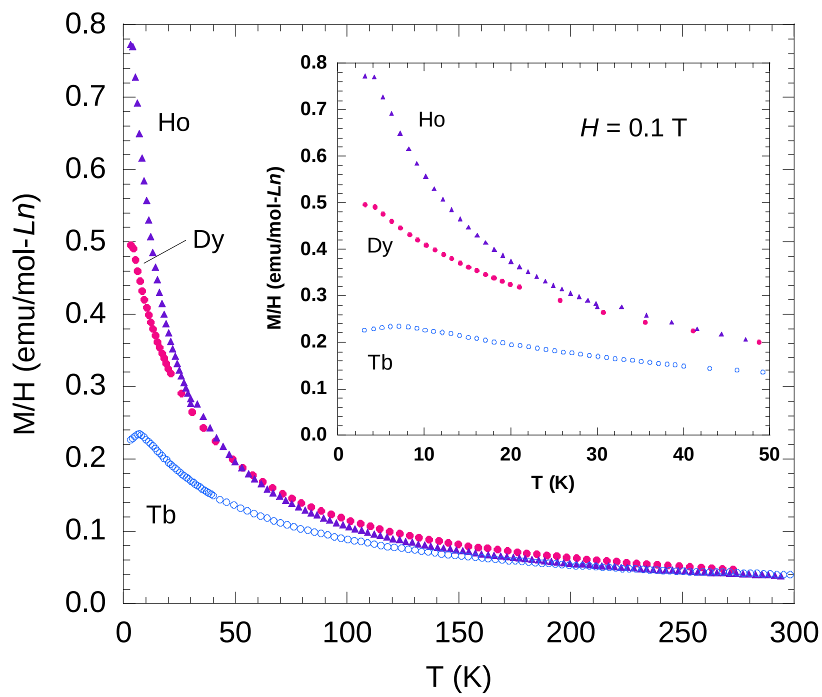

Figure 4.2 Magnetic susceptibility of β-*Ln*$NiGa_4$ (*Ln* = Tb, Dy, Ho) with an applied field of 0.1 T. The inset shows susceptibility up to 50 K.

of -43.2(6) K, -21.9(2) K, and -12.4(1) K for β-$TbNiGa_4$, β-$DyNiGa_4$, and β-$HoNiGa_4$, respectively, suggesting antiferromagnetic correlations at low temperature. A definite Neel transition is observed in the Tb-analogue ~ 6 K, and there is evidence for long-range order in the other analogues near 5 K (see inset of Figure 4.2). Since the onset of the transitions in the susceptibility data occur near the base temperature of our magnetometer, additional magnetic measurements, or specific heat measurements, below 5 K will be necessary to definitively verify long-range order.

The relationship between θ (K) and *Ln-Ln* (Å) for the α-*Ln*$NiGa_4$ (*Ln* = Gd – Yb) and β-*Ln*$NiGa_4$ (*Ln* = Tb – Dy) series is presented in Figure 4.3. The trend for the β-*Ln*$NiGa_4$ (*Ln* = Tb – Dy) series is similar to that of the α-*Ln*$NiGa_4$ (*Ln* = Gd – Yb) series, which show a dominance of RKKY-type behavior [3]. Effective magnetic moments per *Ln* atom of 9.9(8) μ_B, 10.6(6) μ_B, and 9.6(4) μ_B were obtained for β-$TbNiGa_4$, β-$DyNiGa_4$, and β-$HoNiGa_4$ respectively, from the Curie-Weiss fits between 50 K – 278 K. The experimental magnetic moments obtained for each are in good agreement with the calculated magnetic moment of 9.7 μ_B, 10.6 μ_B, and 10.6 μ_B for a free Tb^{3+}, Dy^{3+}, and Ho^{3+} ion, respectively.

The field dependence of the magnetization at 3 K of each analogue is shown in Figure 4.4. The curve for β-$TbNiGa_4$ is linear in field up to 9 T and does not saturate. A free ion of Tb^{3+} ion is calculated to saturate around 9.0 μ_B and in this phase reaches a maximum ~ 4.6 μ_B at 9 T, which corresponds to ~ 50 % of the full saturation value. The magnetization of β-$DyNiGa_4$ increases linearly at low fields (below ~ 2 T), typical of an antiferromagnet, and then exhibits behavior similar to a paramagnetic material. The magnetization reaches a maximum value of ~ 5.2 μ_B at 9 T, as compared to the calculated saturation value for Dy^{3+} of 10.0 μ_B. The curve for β-$HoNiGa_4$ begins to saturate around 3 T and reaches ~ 5.5 μ_B/mol at 9 T. Full magnetic saturation for a free Ho^{3+} ion is 10.0 μ_B.

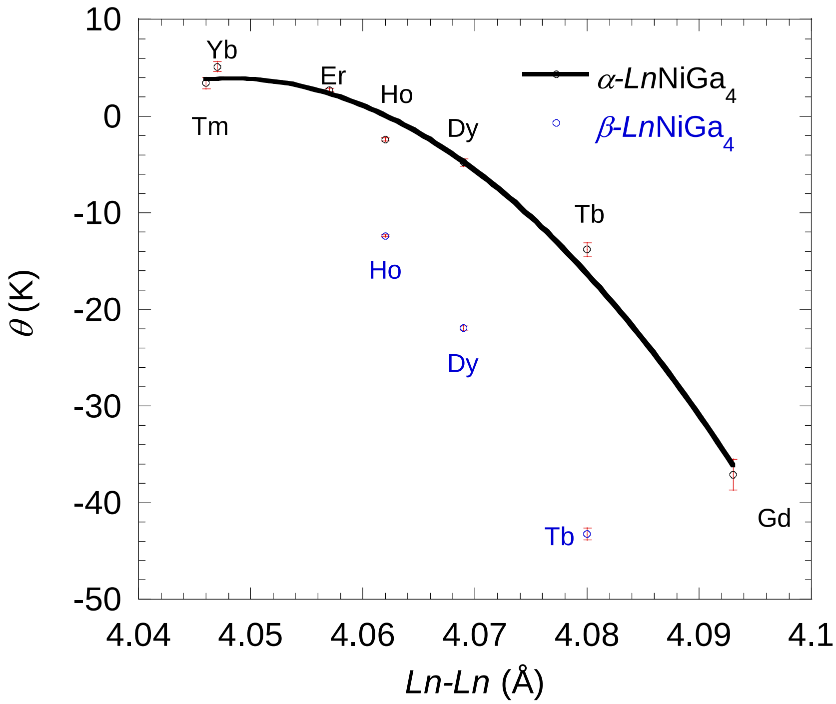

Figure 4.3 The variation of θ (K) as a function of *Ln-Ln* distance for the α-*Ln*NiGa$_4$ (*Ln* = Gd – Yb) and β-*Ln*NiGa$_4$ (*Ln* = Tb – Dy) series.

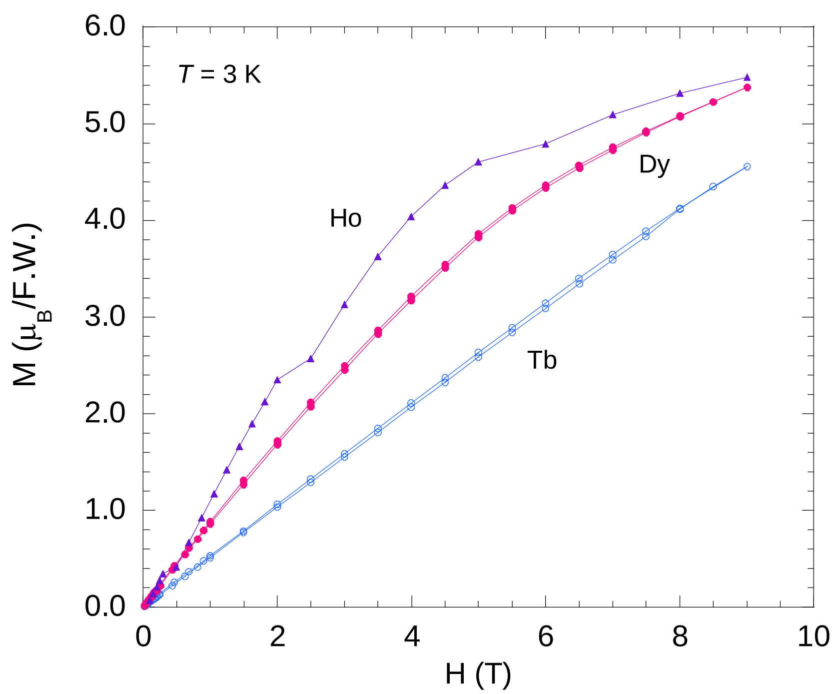

Figure 4.4 The isothermal magnetization of β-*Ln*NiGa$_4$ (*Ln* = Tb, Dy, Ho) at 3 K.

The resistance curves of β-*Ln*NiGa$_4$ (*Ln* = Tb, Dy, Ho) are presented in Figure 4.5 and show metallic behavior at high temperatures. Below ~ 6 K, each sample displays a small kink in its resistivity (Figure 4.5 inset). This feature provides further evidence that the samples are undergoing a long-range magnetic ordering transition at this temperature, and the drop in the resistivity below the kink would correspond to a decrease in the spin-disorder scattering. β-TbNiGa$_4$ and β-DyNiGa$_4$ also show a transition in their resistivity at ~ 240 and 280 K. This

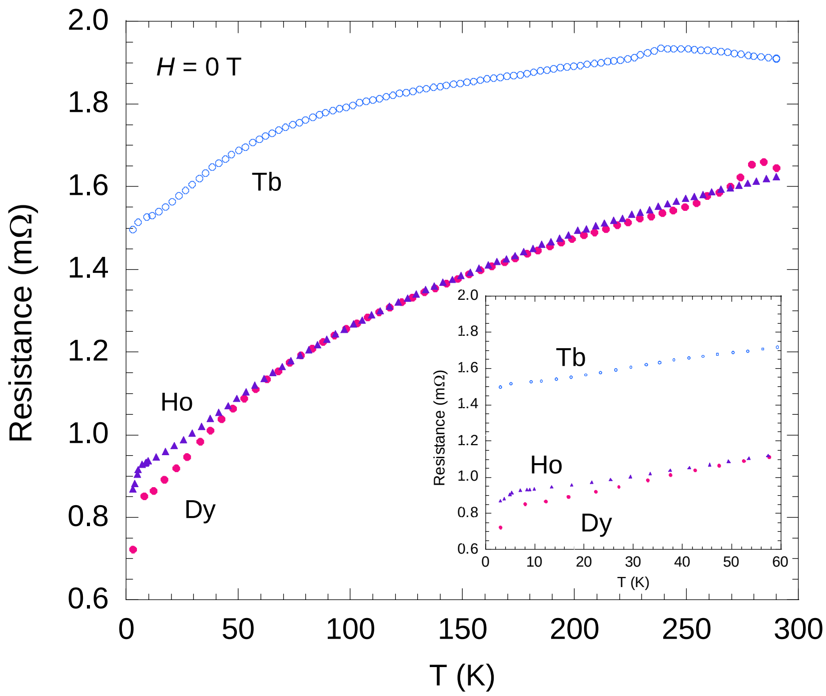

Figure 4.5 The electrical resistance of β-*Ln*NiGa$_4$ (*Ln* = Tb, Dy, Ho) as a function of temperature is shown.

transition is a reproducible feature in the resistance and was measured over 2-3 samples for β-TbNiGa$_4$ and β-DyNiGa$_4$. We believe this signature in the transport data is associated with a phase transition related to the appearance of a supercell below room temperature based on the temperature-dependent single crystal X-ray diffraction studies of β-TbNiGa$_4$. Supercell reflections are not observed at or above the temperature of the phase transition seen in the resistance, but are only observed in data collected below the transition temperature.

The magnetoresistance (MR % = $(\rho_H - \rho_0)/\rho_0 \times 100$) of β-*Ln*$NiGa_4$ (*Ln* = Tb, Dy, Ho) is presented in Figure 4.6, where measurements were collected at 3 K. Positive magnetoresistance, less than 50% for β-$TbNiGa_4$, β-$DyNiGa_4$, and β-$HoNiGa_4$, is observed in field up to 9 T. The MR of these compounds is unusually sensitive to low field. We observe steep increases in the MR below 0.03 T, especially in the Dy-analogue, and at higher field we see a monotonic, positive MR.

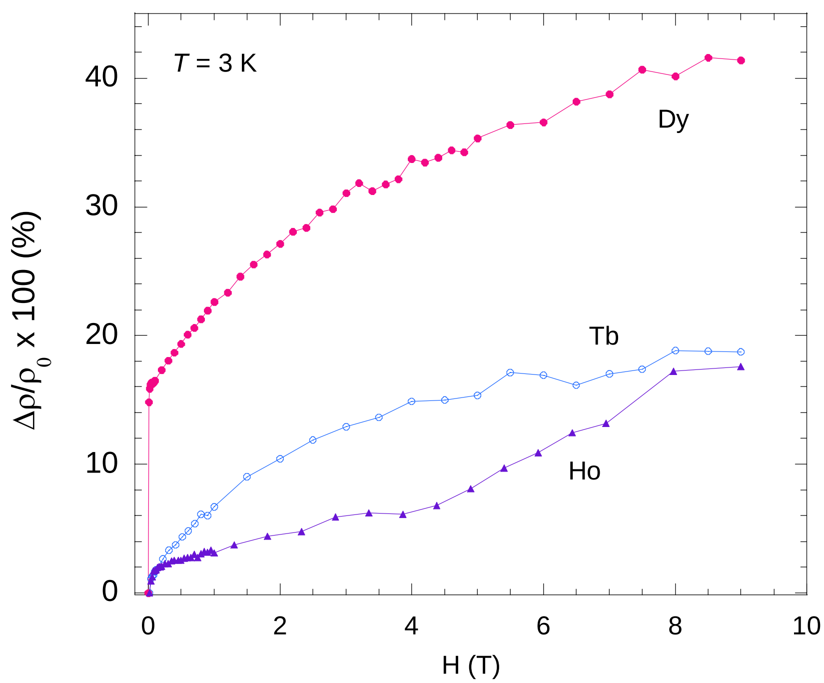

Figure 4.6 The MR% of β-*Ln*$NiGa_4$ (*Ln* = Tb, Dy, Ho) at 3 K is shown.

4.4 References

(1) Bohm, H., Modulated structures at phase transitions. *Am. Mineral.* **1983,** *68*, 11-17.

(2) Zhuravleva, M. A.; Bilc, D.; Pcionek, R. J.; Mahanti, S. D.; Kanatzidis, M. G., Tb4FeGe8 grown in liquid gallium: Trans-cis chains from the distortion of a planar Ge square net. *Inorg. Chem.* **2005,** *44*, 2177-2188.

(3) Shelton, R. N.; Hausermann-Berg, L. S.; Klavins, P.; Yang, H. D.; Anderson, M. S.; Swenson, C. A., *Phys. Rev. B* **1986,** *34*.

(4) Yang, H. D.; Shelton, R. N.; Braun, H. F., *Phys. Rev. B* **1986,** *33*.

(5) Galli, F.; Feyerherm, R.; Hendrikx, R. W. A.; Dudzik, E.; Nieuwenhuys, G. J.; Ramakrishnan, S.; Brown, S. D.; van Smaalen, S.; Mydosh, J. A., *J. Phys.-Condes. Matter* **2002,** *14*.

(6) DiMasi, E.; Aronson, M. C.; Mansfield, J. F.; Foran, B.; Lee, S., Chemical pressure and charge-density waves in rare-earth tritellurides. *Phys. Rev. B* **1995,** *52*, 14516-14525.

(7) Ru, N.; Chu, J.-H.; Fisher, I. R., Magnetic properties of the charge density wave compounds RTe3 (R=Y, La, Ce, Pr, Nd, Sm, Gd, Tb, Dy, Ho, Er, and Tm). *Phys. Rev. B* **2008,** *78*, 012410.

(8) van Smaalen, S.; Shaz, M.; Palatinus, L.; Daniels, P.; Galli, F.; Nieuwenhuys, G. J.; Mydosh, J. A., Mutiple charge-density waves in R5Ir4Si10 (R=Ho, Er, Tm and Lu). *Phys. Rev. B* **2004,** *69*, 014103-1 - 01403-11.

(9) Zhuravleva, M.; Evain, M.; Petricek, V.; Kanatzidis, M. G., $GdCo_{1-x}Ga_3Ge$: charge density wave in a Ga square net. *J. Am. Chem. Soc.* **2007,** *129*, 3082-3083.

(10) Malliakas, C.; Billinge, S. J. L.; Kim, H. J.; Kanatzidis, M. G., Square nets of tellurium: rare-earth dependent variation in the charge-density wave of RETe3 (RE= Rare-earth element). *J. Am. Chem. Soc.* **2005,** *127*, 6510-6511.

(11) Gray, D. L.; Francisco, M. C.; Kanatzidis, M. G., Distortion and charge density wave in the Ga square net coupled to the site occupancy wave in $YCo_{0.88}Ga_3Ge$. *Inorg. Chem.* **2008,** *47*, 7243-7248.

(12) Zhuravleva, M.; Pcionek, R. J.; Wang, X.; Schultz, A. J.; Kanatzidis, M. G., $REMGa_3Ge$ and $RE_3Ni_3Ga_8Ge_3$ (M=Ni, Co; RE=rare-earth element): new intermetallics synthesized in liquid gallium. X-ray, electron and neutron structure determination and magnetism. *Inorg. Chem.* **2003,** *42*, 6412-6424.

(13) Chen, X. Z.; Small, P.; Sportouch, S.; Zhuravleva, M.; Brazis, P.; Kannewurf, C. R.; Kanatzidis, M. G., Molten Ga as a solvent for exploratory synthesis: the new ternary polygallide Sm_2NiGa_{12}. *Chem. Mater.* **2000,** *12*, 2520-2522.

(14) Yarmolyuk, Y. P.; Grin, Y.; Rozhdestvenskaya, I.; Usov, O.; Kuz'min, A.; Bruskov, V.; Gladyshevskii, R., Crystal chemical investigations of the series of inhomogeneous linear structures. 3. crystal structure of the $Ce_2Ga_{10}Ni$ and $La_2Ga_{10}Ni$ compounds. *Kristallografiya* **1982,** *27*, 999-1001.

(15) Grin, Y. N.; Yarmolyuk, Y. P.; Usev, O. A.; Kuzmin, A. M.; Burkov, V. A., Investigation of the series of inhomogeneous linear structures from crystal chemical-data. 5. crystal-structure of $Ce_4Ga_{17}Ni$ and $Nd_4Ga_{17}Ni_2$ compounds. *Kristallografiya* **1983,** *28*, 1207-1209.

(16) Cirafici, S.; Franceschi, E., Stacking of close-packed AB_3 layers in RGa_3 compounds (R=heavy rare-earth). *J. Less-Common Met.* **1981,** *77*, 269-280.

(17) Palenzona, A.; Franceschi, E., Crystal structure of rare-earth gallides (RE_5Ga_3). *J. Less-Common Met.* **1968,** *14*, 47-53.

(18) Haszko, S. E., Rare-earth gallium compounds having the aluminum-boride structure. *T. Metall. Soc. Aime* **1961,** *221*, 201-202.

CHAPTER 5. CONCLUSION

5.1 A Synopsis of This Dissertation Work

The goal of this dissertation was to present the structural and physical characterization results of several *Ln*-Ni-Ga phases. The growth of high-quality single crystals has enabled the study of three new systems: Ln_2MGa_{12} (*Ln* = Pr, Nd, Sm; *M* = Ni, Cu),[1] α-LnNiGa$_4$ (*Ln* = Y, Gd – Yb),[2] and β-LnNiGa$_4$ (*Ln* = Tb – Ho).[3] Each system was studied as a series to draw comparisons from both the structure and properties, which include the study of sub-structural motifs, lanthanide environments, magnetic ordering, etc. It was also pertinent to compare new phases with those that have been previously studied to obtain a better overall understanding of their chemical and physical behavior.

The three systems presented in this work were synthesized in a Ga-rich regime. The temperature profiles to obtain these phases are very similar and only varied in the cool step(s), with Ln_2MGa_{12} (*Ln* = Pr, Nd, Sm; *M* = Ni, Cu), β-LnNiGa$_4$ (*Ln* = Tb – Ho), and α-LnNiGa$_4$ (*Ln* = Y, Gd – Yb) forming at low, mid, and high temperature ranges, respectively. Phases of Ln_2MGa_{12} (*Ln* = Pr, Nd, Sm; *M* = Ni, Cu) were investigated to determine how replacing Ni for Cu as the transition metal atom affected the structure and physical properties. It was found that the transition metal site was only partially occupied in the Cu-containing analogues, and this is not unexpected given the coordination preferences of Cu.[1] Each phase orders antiferromagnetically at low temperatures with effective moments that are close to the calculated values for a free, trivalent lanthanide ion. α-LnNiGa$_4$ (*Ln* = Y, Gd – Yb) compounds also order at low temperatures and are magnetically anisotropic with a stronger coupling of magnetic ions in the *ab*-plane. The coupling strength of the magnetic ions is directly related to the *Ln*-*Ln* distance in the *a*-direction and is indicative of RKKY-type interactions.[2] β-LnNiGa$_4$ (*Ln* = Tb – Ho), a polymorph of α-LnNiGa$_4$, was found to contain a superstructure below room temperatures.[3] Based on the analysis of atomic displacement parameters the modulation of this phase occurs in the Ni-Ga nets and is consistent with the previously published studies of a similar compound.

The crystal structure of each system differs in how the atoms are arranged, but are similar in that each is composed of at least one structural motif that is found as a binary in the low-temperature (100 – 800 °C), Ga-rich region of the *Ln*-Ga phase diagrams shown in Figure 5.1, such as the $PuGa_6$,[4] AlB_2,[5] $BaAl_4$,[6] and CaF_2[7] structure types. These binary phases can be thought of as the

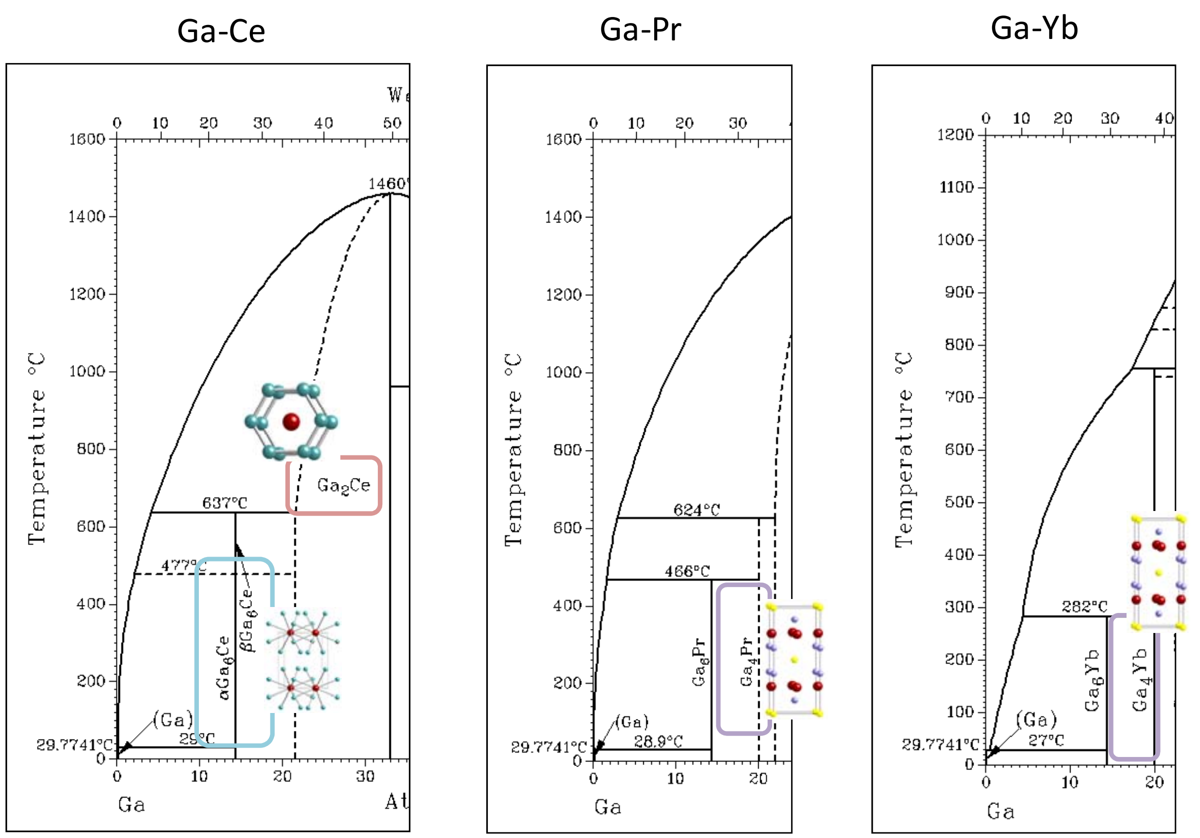

Figure 5.1 Partial binary *Ln*-Ga phase diagrams which show the low-temperature, Ga-rich region and the binary structure types that form in those regions. Phase diagrams as obtained from reference 8.

building blocks of our ternary phases. Phases of Ln_2MGa_{12} (Ln = Pr, Nd, Sm; M = Ni, Cu) are composed of alternating slabs of $PuGa_6$ and CaF_2 units as is depicted in Figure 5.2. α-LnNiGa$_4$ (Ln = Y, Gd – Yb) phases contain partial AlB_2 subunits, and β-LnNiGa$_4$ (Ln = Tb – Ho) is made up of $BaAl_4$ and CaF_2 motifs. Based on the commonalities between Ln-Ga binaries and ternary-phase substructures, we can potentially identify possible structural features that will be present in ternary phases based on the structure types located in the flux-rich region of the phase diagrams.

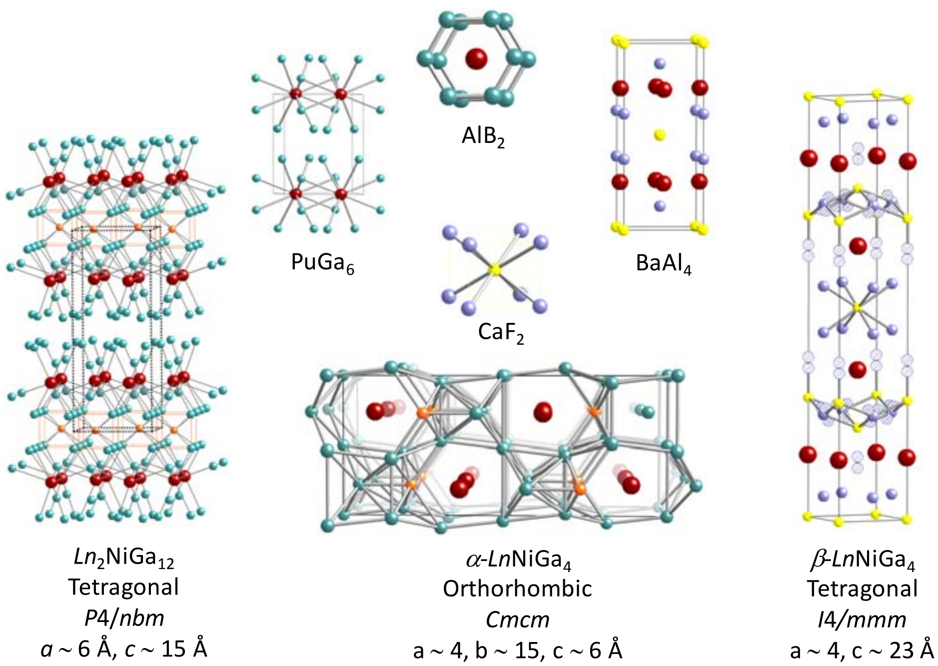

Figure 5.2 The crystal structures of the ternary compounds studied in this work and the related binary structure types of which they are composed.

5.2 Outlook

The α-LnNiGa$_4$ system is so magnetically rich that it would be of interest to see how changing the transition metal atom would affect the physical properties. Based on a literature search we have noted that the properties of other reported isostructural phases do not show the same magnetic behavior that we observe in our compounds. [9-21] Although no work has been published to the best of our knowledge on Fe-containing compounds in this structure type, there has been work in our group which provides evidence that Fe can be doped onto the Ni-site to give α-*Ln*(Ni,Fe)Ga_4. This work will need to be in conjunction with careful elemental analysis of Ni and Fe content.

5.3 References

(1) Thomas, K. R.; Cho, J. Y.; Millican, J. N.; Hembree, R. D.; Moldovan, M.; Karki, A.; Young, D. P.; Chan, J. Y., Crystal growth and physical properties of Ln_2MGa_{12} (Ln=Pr, Nd, and Sm; M=Ni, Cu). *J. Cryst. Growth* **2010,** *312*, 1098-1103.

(2) Thomas, K. R.; Hembree, R. D.; Karki, A. B.; Li, Y.; Young, D. P.; DiTusa, J.; Zhang, J.; Chan, J. Y., Anisotropic Magnetism in α-$LnNiGa_4$ (Ln = Y, Gd - Yb). **2010,** *In preparation*.

(3) Thomas, K. R.; Hembree, R. D.; Karki, A.; Young, D. P.; Chan, J. Y., β-*Ln*$NiGa_4$ (*Ln* = Tb, Dy, Ho): synthesis, structure, and physical properties of a new polymorph of α-*Ln*$NiGa_4$. *J. Solid State Chem.* **2010,** *Submitted*.

(4) Ellinger, F. H.; Zachariasen, W. H., Crystal structures of $PuGa_4$ and $PuGa_6$. *Acta Crys.* **1965,** *19*, 281-283.

(5) Hofmann, W.; Janiche, W., The structural type of aluminium boride (AlB_2). *Naturwissenschaften* **1935,** *23*, 851-851.

(6) Andress, K. R.; Alberti, E., Roentgenographische untersuchung der legierungsreihe Al-Ba. *Z. Metallkd.* **1935,** *27*, 125-126.

(7) Bragg, W. L., The analysis of crystals by the X-ray spectrometer. *P. Roy. Soc. Lond. A Mat.* **1914,** *89*, 468-489.

(8) Massalski, T. B.; Okamoto, H., *Binary alloy phase diagrams*. 2nd ed.; ASM International: Materials Park, OH, 1990.

(9) Galadzhun, Y. V.; Pottgen, R., Platinum-indium polyanions in the structures of $LaPtIn_4$ and $LnPtIn_3$ (Ln = La, Ce, Pr, Nd, Sm) and structure refinement of Ce_2Pt_2In. *Z. Anorg. Allg. Chem.* **1999,** *625*, 481-487.

(10) Hoffmann, R. D.; Pottgen, R., Distorted bcc indium cubes as structural motifs in Ca[TIn_4] (T=Rh, Pd, Ir). *Chem. Eur. J.* **2000,** *6*, 600-607.

(11) Hoffmann, R. D.; Pottgen, R.; Zaremba, V. I.; Kalychak, Y. M., New indides $EuAuIn_2$, $EuPdIn_4$, $GdRhIn_2$, $YbRhIn_4$, and $YbPdIn_4$. *Z. Naturforsch. (B)* **2000,** *55*, 834-840.

(12) Jia, Y. Z.; Belin, C.; Tillard, M.; Lacroix-Orio, L.; Zitoun, D.; Feng, G. H., Three novel phases in the Sm-Co-Ga system. Syntheses, crystal and electronic structures, and electrical and magnetic properties. *Inorg. Chem.* **2007,** *46*, 4177-4186.

(13) Mizushima, T.; Isikawa, Y.; Sakurai, J.; Mori, K., Magnetic properties of $PrNiAl_4$. *J. Magn. Magn. Mater.* **1995,** *140*, 925-926.

(14) Muts, I.; Zaremba, V. I.; Baran, V. V.; Pottgen, R., New indium-rich indides $SrTIn_4$ (T = Ni, Pd, Pt). *Z.Naturforsch.(B)* **2007,** *62*, 1407-1410.

(15) Nesterenko, S. N.; Tursina, A. L.; Shtepa, D. V.; Noel, H.; Seropegin, Y. D., Single crystal investigation of the ternary indides $Ce_2Pd_4In_5$ and $CePdIn_4$. *J. Alloy Compd.* **2007,** *442*, 93-95.

(16) Pottgen, R., Crystal-structure and physical-properties of $CeNiIn_4$. *J. Mater. Chem.* **1995,** *5*, 769-772.

(17) Pottgen, R.; Mullmann, R.; Mosel, B. D.; Eckert, H., Structure refinement, magnetic susceptibility, electrical conductivity and europium-151 Mossbauer spectroscopy of $EuNiIn_4$. *J. Mater. Chem.* **1996,** *6*, 801-805.

(18) Rykhal, R. M.; Zarechny.Os; Yarmolyu.Yp, Crystal-structure of compounds $YNiAl_4$ and $YNiAl_2$. *Kristallografiya* **1972,** *17*, 521-&.

(19) Vasylechko, L.; Schnelle, W.; Schmidt, M.; Burkhardt, U.; Borrmann, H.; Schwarz, U.; Grin, Y., Valence behaviour of ytterbium in $YbNiGa_4$. *J. Alloy Compd.* **2006,** *416*, 35-42.

(20) Wawryk, R.; Stepien-Damm, J.; Henkie, Z.; Cichorek, T.; Steglich, F., The crystal structure, transport and thermodynamic properties of $ThCoGa_4$ single crystals. *J. Phys.-Condes. Matter* **2004,** *16*, 5427-5434.

(21) Zaremba, V. I.; Rodewald, U. C.; Hoffmann, R. D.; Kalychak, Y. M.; Pottgen, R., The indium-rich intermetallics $YbCoIn_5$, $YbRhIn_5$, and $YbPtIn_4$. *Z. Anorg. Allg. Chem.* **2003,** *629*, 1157-1161.

APPENDIX 1. STUDIES OF TWO NON-CENTROSYMMETRIC SUPERCONDUCTORS

A1.1 Introduction

Recently we have conducted structural studies on the non-centrosymmetric superconductors $La_3Bi_4Pt_3$[1] and Mo_3Al_2C,[2] which have T_c ~ 1.2 K and 9.2 K, respectively. $La_3Bi_4Pt_3$ crystallizes in the cubic *I*-43*d* (No. 220) space group and our goal was to probe the crystal chemical differences between samples with slightly different superconducting temperatures. A correlation between synthetic conditions and T_c was observed by our collaborators, but we wanted to know how the stoichiometry changed as a function of these conditions. Polycrystalline samples of Mo_3Al_2C were investigated using powder X-ray diffraction to confirm phase formation and to determine homogeneity

A1.2 $La_3Bi_4Pt_3$

A1.2.1 Single Crystal X-ray Diffraction

Single crystals of $La_3Bi_4Pt_3$ were previously prepared by collaborators and used as received. Crystals were cut to 0.025 × 0.025 × 0.025 mm to minimize the absorption of X-rays by heavy elements. Samples were mounted onto the goniometer of an Enraf Nonius Kappa CCD diffractometer equipped with MoK_α radiation (λ = 0.71073 Å). Data were collected up to θ = 30.0° at ambient temperature. Crystallographic parameters are shown in Table A1.1. The space group and atomic positions of $Y_3Au_3Sb_4$ were used as an initial structural model for the structure determination of $La_3Bi_4Pt_3$.[3] The structural model was refined using SHELXL97.[4] Since Pt and Bi have similar atomic scattering factors several structural refinements were completed to obtain the best model. It was found that Pt and Bi each occupy a single Wyckoff site with no mixing. Attempts to model Bi in the Pt position, and vice-versa, resulted in a divergence of the model. In the case of CC030 the Pt site could be modeled as partially occupied and is in agreement with

SEM analysis done by our collaborators. A partially occupied Pt site in GS29 was not supported by our model as the occupancy parameter remained close to unity. Data were corrected for extinction and refined with anisotropic displacement parameters. Atomic positions and displacement parameters for two compounds are provided in Table A1.2.

Table A1.1 Crystallographic parameters for $La_3Bi_4Pt_{2.8}$ and $La_3Bi_4Pt_3$

Sample	CC030	GS29
Formula	$La_3Bi_4Pt_{2.8}$	$La_3Bi_4Pt_3$
a (Å)	10.119(7)	10.144(4)
V (Å^3)	1036.1(2)	1043.8(6)
Z	4	4
Crystal size (mm^3)	0.025 x 0.025 x 0.025	0.025 x 0.025 x 0.025
Crystal System	cubic	cubic
Space group	I-43d	I-43d
θ range(°)	4.93 – 29.94	4.92 – 30.35
μ (mm^{-1})	179.97	178.65
h	-14 → 14	-14 → 14
k	-9 → 10	-9 → 10
l	-9 → 9	-9 → 9
$^aR_1[F^2 > 2\sigma(F^2)]$	4.00	2.84
$^b wR_2(F^2)$	7.41	9.56
Reflections	454	269
Parameters	10	9
$\Delta\rho_{max}$ (eÅ^{-3})	2.847	3.605
$\Delta\rho_{min}$ (eÅ^{-3})	-2.524	-2.265
GOF	1.055	1.110
Extinction coeff.	0.00087(13)	0.0034(5)

$^aR_1 = \Sigma\|F_o| - |F_c\|/\Sigma|F_o|$.
$^b wR_2 = [\Sigma[w(F_o^2-F_c^2)^2]/\Sigma[w(F_o^2)^2]]^{1/2}$; $w = 1/[\sigma^2F_o^2 + (0.0189P)^2 + 0.0P]$ and $w = 1/[\sigma^2F_o^2 + (0.0P)^2 + 0.0P]$ for $La_3Bi_4Pt_{2.8}$ and $La_3Bi_4Pt_3$, respectively.

A1.2.2 Results and Discussion

Compounds of $La_3Bi_4Pt_3$ are isostructural to $Y_3Au_3Sb_4$[3] and can be viewed as a network of La and Pt traversing through the lattice in each crystallographic direction as shown in Figure A1.1(a). The local environment of each atom is presented in Figure A1.1(b). Each La atom is

Table A1.2 Atomic positions and displacement parameters for $La_3Bi_4Pt_{2.8}$ and $La_3Bi_4Pt_3$

Atom	Wyckoff site	x	y	z	Occ.	U_{eq}(Å^2)^a
CC030	$La_3Pt_{2.8}Bi_4$					
La	12*a*	0	1/4	3/8	1	0.0164(10)
Pt	12*b*	7/8	0	1/4	0.950(9)	0.0166(11)
Bi	16*c*	0.08393(10)	0.08393(10)	0.08393(10)	1	0.0181(5)
GS29	$La_3Pt_3Bi_4$					
La	12*a*	0	1/4	3/8	1	0.0131(6)
Pt	12*b*	7/8	0	1/4	1	0.0157(6)
Bi	16*c*	0.08408(7)	0.08408(7)	0.08408(7)	1	0.0127(5)

$^aU_{eq}$ is defined as one-third of the trace of the orthogonalized U_{ij} tensor.

surrounded by eight Bi atoms to form two interpenetrating tetrahedra (bisdisphenoid). In the *c*-direction four of the Bi atoms are axial and four are equatorial, with the axial atoms having a larger La-Bi inter-atomic distance. The 8-coordinate La polyhedra are face-sharing in each crystallographic direction. Similarly, Ni atoms are coordinated to four Bi atoms to form a tetrahedron. Selected inter-atomic distances are listed in Table A1.3. We have found that the difference between compounds with different superconducting transition temperatures is the concentration of Pt on the 12*b* site. A small enhancement in T_c is observed in the Pt-deficient analogue, as experimental work reported by our collaborators on these compounds indicate that $La_3Bi_4Pt_3$ and $La_3Bi_4Pt_{2.8}$ exhibit superconductivity at T_c = 1.2 K and 1.4 K, respectively. Superconductivity was not observed in the transport of $La_3Bi_4Pt_3$ down to 2 K in previous work by Hundley, *et al*.[5]

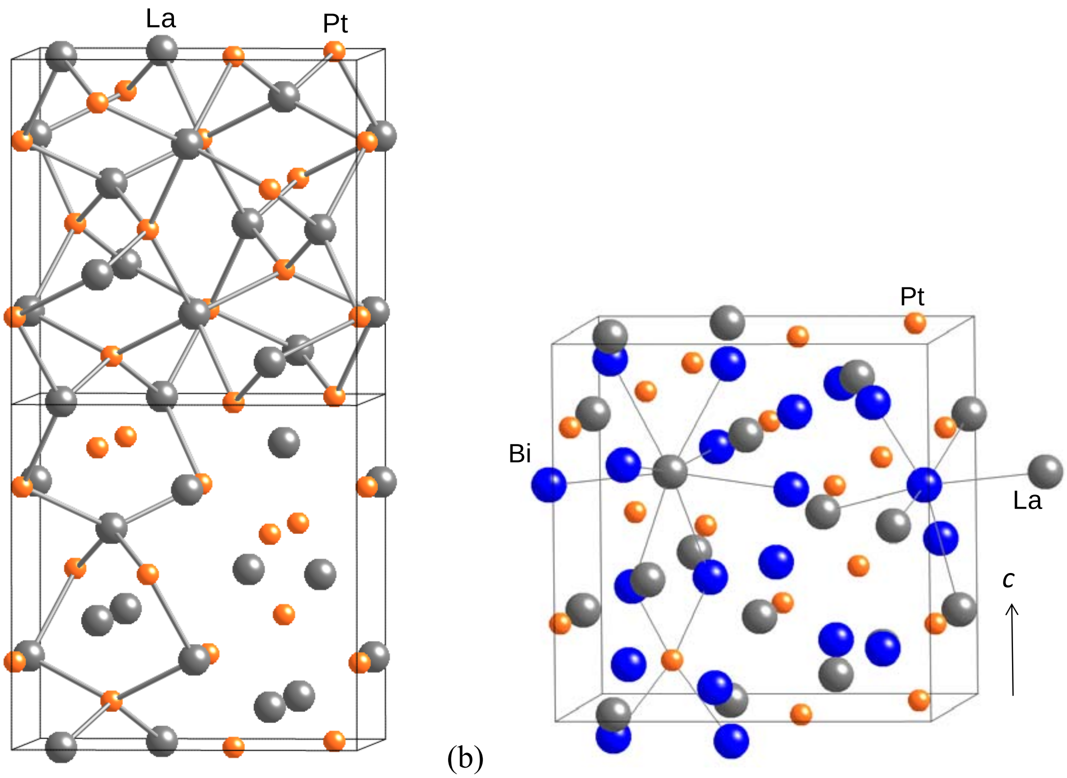

(a) (b)

Figure A1.1 The crystal structure of $La_3Bi_4Pt_3$ is presented, where La, Bi, and Pt are represented by grey, blue, and orange spheres, respectively. (a) Two unit cells are shown to depict the La-Pt network in the crystallographic *c*-direction. (b) The local environments of La, Pt, and Bi are highlighted in this view of the unit cell.

Table A1.3 Selected inter-atomic distances (Å) of $La_3Bi_4Pt_{2.8}$ and $La_3Bi_4Pt_3$

	La–Bi	La–Pt	Pt–Bi
CC030	3.496(3) ×4	3.098(2) ×4	2.831(2) ×4
$La_3Bi_4Pt_{2.8}$	3.509(3) ×4		
GS29	3.502(4) ×4	3.106(2) ×4	2.838(2) ×4
$La_3Bi_4Pt_3$	3.519(4) ×4		

A1.3 Mo_3Al_2C

A1.3.1 Powder X-ray Diffraction Results

Powder analysis was performed on polycrystalline samples of Mo_3Al_2C. Samples of Mo_3Al_2C were prepared by arc melting stoichiometric amounts of the substituent elements.

Samples were ground with mortar and pestle for at least eight minutes and then mounted onto a sample plate. Data were collected at ambient temperature from 2θ = 20 to 80°. As shown in Figure A1.2, powder X-ray diffraction results reveal that the sample is single phase with a small amount of Mo and Mo_3Al_8. This phase crystallizes in the cubic $P4_132$ space group with lattice parameter a ~ 6.8 Å and is presented in the inset of Figure A1.2.

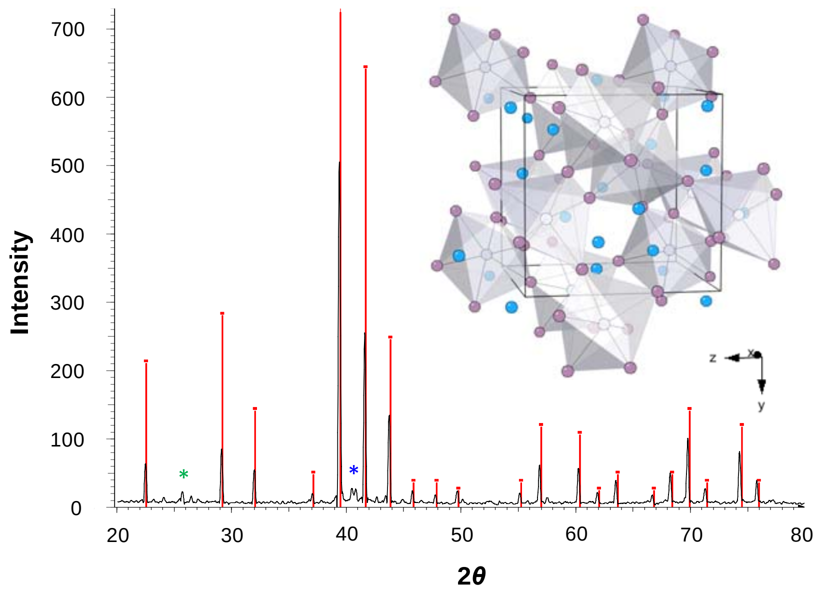

Figure A1.2 The experimental (black) and calculated (red) powder X-ray diffraction pattern of Mo_3Al_2C. The green and blue stars indicate impurity peaks from Mo_3Al_8 and Mo, respectively. The crystal structure of Mo_3Al_2C is presented with Mo atoms, Al atoms, and C atoms represented as purple, blue, and gray spheres, respectively. The figure is adopted from reference 2 and the atomic coordinates were obtained from reference [6].

A1.4 References

(1) Seyfarth, G.; Thomas, K. R.; Chan, J. Y.; Capan, C., **2010,** *To be submitted*.

(2) Karki, A. B.; Xiong, Y. M.; Vekhter, I.; Browne, D.; Adams, P. W.; Young, D. P.; Thomas, K. R.; Chan, J. Y.; Prozorov, R.; Kim, H., Structure and physical properties of the noncentrosymmetric superconductor Mo_3Al_2C. *Phys. Rev. B* **2010,** *86*, 064512.

(3) Dwight, A. E., Yttrium-Gold-Antimony $Y_3Au_3Sb_4$. *Acta Cryst.* **1977,** *B33*, 1579-1581.

(4) Sheldrick, G. M., A short history of SHELX. *Acta Cryst.* **2008,** *A64*, 112-122.

(5) Hundley, M. F.; Canfield, P. C.; Thompson, J. D.; Fisk, Z.; Lawrence, J. M., Hybridization gap in $Ce_3Bi_4Pt_3$. *Phys. Rev. B* **1990,** *42*, 6842-6845.

(6) Jeitschko, W.; Nowotny, H.; Benesovsky, F., Ein beitrag zum dreistoff - molybdan-aluminium-kohlenstoff. *Monatsh. Chem.* **1963,** *94*, 247-&.

APPENDIX 2. UNPUBLISHED CRYSTALLOGRAPHIC INFORMATION FILES

A2.1 Ce_2RhGa_{12}

```
data_shelxl

_audit_creation_method            SHELXL-97
_chemical_name_systematic
;
 ?
;
_chemical_name_common             ?
_chemical_melting_point           ?
_chemical_formula_moiety          ?
_chemical_formula_sum
 'Ce2 Ga12 Rh'
_chemical_formula_weight          1219.79

loop_
 _atom_type_symbol
 _atom_type_description
 _atom_type_scat_dispersion_real
 _atom_type_scat_dispersion_imag
 _atom_type_scat_source
 'Ce'  'Ce'  -0.2486   2.6331
 'International Tables Vol C Tables 4.2.6.8
and 6.1.1.4'
 'Rh'  'Rh'  -1.1178   0.9187
 'International Tables Vol C Tables 4.2.6.8
and 6.1.1.4'
 'Ga'  'Ga'   0.2307   1.6083
 'International Tables Vol C Tables 4.2.6.8
and 6.1.1.4'

_symmetry_cell_setting            ?
_symmetry_space_group_name_H-M    ?

loop_
 _symmetry_equiv_pos_as_xyz
 'x, y, z'
 '-x+1/2, -y+1/2, z'
 'x, -y+1/2, -z'
 '-x+1/2, y, -z'
 '-y+1/2, -x+1/2, -z'
 'y, x, -z'
 'y, -x+1/2, z'
 '-y+1/2, x, z'
 '-x, -y, -z'
 'x-1/2, y-1/2, -z'
 '-x, y-1/2, z'
 'x-1/2, -y, z'
 'y-1/2, x-1/2, z'
 '-y, -x, z'
 '-y, x-1/2, -z'
 'y-1/2, -x, -z'

_cell_length_a                    6.0560(3)
_cell_length_b                    6.0560(3)
_cell_length_c                    15.7060(9)
_cell_angle_alpha                 90.00
_cell_angle_beta                  90.00
_cell_angle_gamma                 90.00
_cell_volume                      576.02(5)
_cell_formula_units_Z             2
_cell_measurement_temperature     298(2)
_cell_measurement_reflns_used     ?
_cell_measurement_theta_min       ?
_cell_measurement_theta_max       ?

_exptl_crystal_description        ?
_exptl_crystal_colour             ?
_exptl_crystal_size_max           0.05
_exptl_crystal_size_mid           0.05
_exptl_crystal_size_min           0.03
_exptl_crystal_density_meas       ?
_exptl_crystal_density_diffrn     7.033
_exptl_crystal_density_method           'not
measured'
_exptl_crystal_F_000              1066
_exptl_absorpt_coefficient_mu     36.592
_exptl_absorpt_correction_type    ?
_exptl_absorpt_correction_T_min   0.2620
_exptl_absorpt_correction_T_max   0.4615
_exptl_absorpt_process_details    ?

_exptl_special_details
;
 ?
;

_diffrn_ambient_temperature       298(2)
_diffrn_radiation_wavelength      0.71073
_diffrn_radiation_type            MoK\a
_diffrn_radiation_source               'fine-
focus sealed tube'
_diffrn_radiation_monochromator   graphite
_diffrn_measurement_device_type   ?
_diffrn_measurement_method        ?
_diffrn_detector_area_resol_mean  ?
_diffrn_standards_number          ?
_diffrn_standards_interval_count  ?
_diffrn_standards_interval_time   ?
_diffrn_standards_decay_%         ?
_diffrn_reflns_number             1212
_diffrn_reflns_av_R_equivalents   0.0439
_diffrn_reflns_av_sigmaI/netI     0.0438
_diffrn_reflns_limit_h_min        -8
_diffrn_reflns_limit_h_max        8
_diffrn_reflns_limit_k_min        -6
_diffrn_reflns_limit_k_max        6
_diffrn_reflns_limit_l_min        -22
_diffrn_reflns_limit_l_max        17
_diffrn_reflns_theta_min          2.59
_diffrn_reflns_theta_max          30.00
_reflns_number_total              482
_reflns_number_gt                 436
_reflns_threshold_expression      >2sigma(I)

_computing_data_collection        ?
_computing_cell_refinement        ?
_computing_data_reduction         ?
_computing_structure_solution      'SHELXS-97
(Sheldrick, 1990)'
_computing_structure_refinement    'SHELXL-97
(Sheldrick, 1997)'
_computing_molecular_graphics     ?
_computing_publication_material   ?

_refine_special_details
;
 Refinement of F^2^ against ALL reflections.
The weighted R-factor wR and
 goodness  of  fit  S  are  based  on  F^2^,
conventional R-factors R are based
 on F, with F set to zero for negative F^2^.
The threshold expression of
```

```
 F^2^ > 2sigma(F^2^) is used only for
calculating R-factors(gt) etc. and is
 not relevant to the choice of reflections
for refinement.  R-factors based
 on F^2^ are statistically about twice as
large as those based on F, and R-
 factors based on ALL data will be even
larger.
;

_refine_ls_structure_factor_coef  Fsqd
_refine_ls_matrix_type            full
_refine_ls_weighting_scheme       calc
_refine_ls_weighting_details
 'calc
w=1/[\s^2^(Fo^2^)+(0.0338P)^2^+4.4336P]
where P=(Fo^2^+2Fc^2^)/3'
_atom_sites_solution_primary      direct
_atom_sites_solution_secondary    difmap
_atom_sites_solution_hydrogens    geom
_refine_ls_hydrogen_treatment     mixed
_refine_ls_extinction_method      SHELXL
_refine_ls_extinction_coef        0.0023(4)
_refine_ls_extinction_expression
 'Fc^*^=kFc[1+0.001xFc^2^\l^3^/sin(2\q)]^-
1/4^'
_refine_ls_number_reflns          482
_refine_ls_number_parameters      26
_refine_ls_number_restraints      0
_refine_ls_R_factor_all           0.0356
_refine_ls_R_factor_gt            0.0322
_refine_ls_wR_factor_ref          0.0813
_refine_ls_wR_factor_gt           0.0793
_refine_ls_goodness_of_fit_ref    1.126
_refine_ls_restrained_S_all       1.126
_refine_ls_shift/su_max           0.000
_refine_ls_shift/su_mean          0.000

loop_
 _atom_site_label
 _atom_site_type_symbol
 _atom_site_fract_x
 _atom_site_fract_y
 _atom_site_fract_z
 _atom_site_U_iso_or_equiv
 _atom_site_adp_type
 _atom_site_occupancy
 _atom_site_symmetry_multiplicity
 _atom_site_calc_flag
 _atom_site_refinement_flags
 _atom_site_disorder_assembly
 _atom_site_disorder_group
Ce1 Ce 0.7500 0.2500 0.24416(3) 0.0106(2)
Uani 1 4 d S . .
Rh1 Rh 0.7500 0.2500 0.0000 0.0101(3) Uani 1
8 d S . .
Ga1 Ga 0.7500 0.7500 0.18518(7) 0.0116(3)
Uani 1 4 d S . .
Ga2 Ga 0.7500 0.7500 0.34139(7) 0.0149(3)
Uani 1 4 d S . .
Ga3 Ga 0.50012(9) 0.00012(9) -0.08581(4)
0.0120(3) Uani 1 2 d S . .
Ga4 Ga 0.56849(13) 0.06849(13) 0.42882(5)
0.0241(3) Uani 1 2 d S . .

loop_
 _atom_site_aniso_label
 _atom_site_aniso_U_11
 _atom_site_aniso_U_22
 _atom_site_aniso_U_33
 _atom_site_aniso_U_23
 _atom_site_aniso_U_13
 _atom_site_aniso_U_12
Ce1 0.0110(3) 0.0110(3) 0.0098(3) 0.000
0.000 -0.00039(18)
Rh1 0.0109(4) 0.0109(4) 0.0085(4) 0.000
0.000 0.000
Ga1 0.0127(4) 0.0127(4) 0.0092(5) 0.000
0.000 0.000
Ga2 0.0176(4) 0.0176(4) 0.0093(5) 0.000
0.000 0.000
Ga3 0.0135(3) 0.0135(3) 0.0090(4)
0.00018(18) 0.00018(18) -0.0013(3)
Ga4 0.0293(4) 0.0293(4) 0.0139(4) 0.0053(3)
0.0053(3) 0.0108(4)

_geom_special_details
;
 All esds (except the esd in the dihedral
angle between two l.s. planes)
 are estimated using the full covariance
matrix.  The cell esds are taken
 into account individually in the estimation
of esds in distances, angles
 and torsion angles; correlations between
esds in cell parameters are only
 used when they are defined by crystal
symmetry.  An approximate (isotropic)
 treatment of cell esds is used for
estimating esds involving l.s. planes.
;

loop_
 _geom_bond_atom_site_label_1
 _geom_bond_atom_site_label_2
 _geom_bond_distance
 _geom_bond_site_symmetry_2
 _geom_bond_publ_flag
Ce1 Ga1 3.1665(4) 11_755 ?
Ce1 Ga1 3.1665(4) . ?
Ce1 Ga1 3.1665(4) 11_655 ?
Ce1 Ga1 3.1665(4) 1_545 ?
Ce1 Ga3 3.2810(8) 4_655 ?
Ce1 Ga3 3.2810(8) 3 ?
Ce1 Ga3 3.2824(8) 10_665 ?
Ce1 Ga3 3.2824(8) 9_655 ?
Ce1 Ga4 3.2907(10) 2_655 ?
Ce1 Ga4 3.2907(10) . ?
Ce1 Ga2 3.3913(6) . ?
Ce1 Ga2 3.3913(6) 11_755 ?
Rh1 Ga3 2.5291(8) 4_655 ?
Rh1 Ga3 2.5291(8) 3 ?
Rh1 Ga3 2.5291(8) 2_655 ?
Rh1 Ga3 2.5291(8) . ?
Rh1 Ga3 2.5309(8) 10_665 ?
Rh1 Ga3 2.5309(8) 9_655 ?
Rh1 Ga3 2.5309(8) 12_655 ?
Rh1 Ga3 2.5309(8) 11_665 ?
Ga1 Ga2 2.4535(15) . ?
Ga1 Ga3 2.6495(7) 4_665 ?
Ga1 Ga3 2.6495(7) 10_665 ?
Ga1 Ga3 2.6495(7) 9_665 ?
Ga1 Ga3 2.6495(7) 3 ?
Ga1 Ce1 3.1665(4) 11_765 ?
Ga1 Ce1 3.1665(4) 1_565 ?
Ga1 Ce1 3.1666(4) 11_665 ?
Ga2 Ga4 2.6104(8) 11_665 ?
Ga2 Ga4 2.6104(8) 2_655 ?
Ga2 Ga4 2.6104(8) 1_565 ?
Ga2 Ga4 2.6104(8) 12_665 ?
Ga2 Ce1 3.3913(6) 11_765 ?
Ga2 Ce1 3.3913(6) 1_565 ?
Ga2 Ce1 3.3913(6) 11_665 ?
Ga3 Rh1 2.5309(8) 9_655 ?
```

```
Ga3 Ga1 2.6495(7) 3 ?
Ga3 Ga1 2.6495(7) 9_665 ?
Ga3 Ga3 2.6955(14) 9_655 ?
Ga3 Ce1 3.2810(8) 3 ?
Ga3 Ce1 3.2824(8) 9_655 ?
Ga4 Ga4 2.5249(17) 9_656 ?
Ga4 Ga2 2.6104(8) 11_655 ?
Ga4 Ga2 2.6104(8) 1_545 ?

loop_
 _geom_angle_atom_site_label_1
 _geom_angle_atom_site_label_2
 _geom_angle_atom_site_label_3
 _geom_angle
 _geom_angle_site_symmetry_1
 _geom_angle_site_symmetry_3
 _geom_angle_publ_flag
Ga1 Ce1 Ga1 85.090(12) 11_755 . ?
Ga1 Ce1 Ga1 145.98(4) 11_755 11_655 ?
Ga1 Ce1 Ga1 85.090(12) . 11_655 ?
Ga1 Ce1 Ga1 85.090(12) 11_755 1_545 ?
Ga1 Ce1 Ga1 145.98(4) . 1_545 ?
Ga1 Ce1 Ga1 85.090(12) 11_655 1_545 ?
Ga1 Ce1 Ga3 48.487(16) 11_755 4_655 ?
Ga1 Ce1 Ga3 102.67(2) . 4_655 ?
Ga1 Ce1 Ga3 102.67(2) 11_655 4_655 ?
Ga1 Ce1 Ga3 48.487(16) 1_545 4_655 ?
Ga1 Ce1 Ga3 102.67(2) 11_755 3 ?
Ga1 Ce1 Ga3 48.487(16) . 3 ?
Ga1 Ce1 Ga3 48.487(16) 11_655 3 ?
Ga1 Ce1 Ga3 102.67(2) 1_545 3 ?
Ga3 Ce1 Ga3 81.42(3) 4_655 3 ?
Ga1 Ce1 Ga3 48.475(16) 11_755 10_665 ?
Ga1 Ce1 Ga3 48.475(16) . 10_665 ?
Ga1 Ce1 Ga3 102.69(2) 11_655 10_665 ?
Ga1 Ce1 Ga3 102.69(2) 1_545 10_665 ?
Ga3 Ce1 Ga3 54.948(12) 4_655 10_665 ?
Ga3 Ce1 Ga3 54.948(12) 3 10_665 ?
Ga1 Ce1 Ga3 102.69(2) 11_755 9_655 ?
Ga1 Ce1 Ga3 102.69(2) . 9_655 ?
Ga1 Ce1 Ga3 48.475(16) 11_655 9_655 ?
Ga1 Ce1 Ga3 48.475(16) 1_545 9_655 ?
Ga3 Ce1 Ga3 54.948(12) 4_655 9_655 ?
Ga3 Ce1 Ga3 54.948(12) 3 9_655 ?
Ga3 Ce1 Ga3 81.48(3) 10_665 9_655 ?
Ga1 Ce1 Ga4 86.47(2) 11_755 2_655 ?
Ga1 Ce1 Ga4 86.47(2) . 2_655 ?
Ga1 Ce1 Ga4 125.26(2) 11_655 2_655 ?
Ga1 Ce1 Ga4 125.26(2) 1_545 2_655 ?
Ga3 Ce1 Ga4 131.919(14) 4_655 2_655 ?
Ga3 Ce1 Ga4 131.919(14) 3 2_655 ?
Ga3 Ce1 Ga4 111.07(2) 10_665 2_655 ?
Ga3 Ce1 Ga4 167.45(3) 9_655 2_655 ?
Ga1 Ce1 Ga4 125.26(2) 11_755 . ?
Ga1 Ce1 Ga4 125.26(2) . . ?
Ga1 Ce1 Ga4 86.47(2) 11_655 . ?
Ga1 Ce1 Ga4 86.47(2) 1_545 . ?
Ga3 Ce1 Ga4 131.919(14) 4_655 . ?
Ga3 Ce1 Ga4 131.919(14) 3 . ?
Ga3 Ce1 Ga4 167.45(3) 10_665 . ?
Ga3 Ce1 Ga4 111.07(2) 9_655 . ?
Ga4 Ce1 Ga4 56.38(4) 2_655 . ?
Ga1 Ce1 Ga2 97.570(9) 11_755 . ?
Ga1 Ce1 Ga2 43.77(2) . . ?
Ga1 Ce1 Ga2 97.570(9) 11_655 . ?
Ga1 Ce1 Ga2 170.25(3) 1_545 . ?
Ga3 Ce1 Ga2 138.863(14) 4_655 . ?
Ga3 Ce1 Ga2 85.958(18) 3 . ?
Ga3 Ce1 Ga2 85.937(18) 10_665 . ?
Ga3 Ce1 Ga2 138.870(14) 9_655 . ?
Ga4 Ce1 Ga2 45.962(17) 2_655 . ?
Ga4 Ce1 Ga2 84.34(3) . . ?
Ga1 Ce1 Ga2 43.77(2) 11_755 11_755 ?
Ga1 Ce1 Ga2 97.570(9) . 11_755 ?
Ga1 Ce1 Ga2 170.25(3) 11_655 11_755 ?
Ga1 Ce1 Ga2 97.570(9) 1_545 11_755 ?
Ga3 Ce1 Ga2 85.958(18) 4_655 11_755 ?
Ga3 Ce1 Ga2 138.863(14) 3 11_755 ?
Ga3 Ce1 Ga2 85.937(18) 10_665 11_755 ?
Ga3 Ce1 Ga2 138.870(14) 9_655 11_755 ?
Ga4 Ce1 Ga2 45.961(17) 2_655 11_755 ?
Ga4 Ce1 Ga2 84.34(3) . 11_755 ?
Ga2 Ce1 Ga2 78.301(15) . 11_755 ?
Ga3 Rh1 Ga3 115.60(3) 4_655 3 ?
Ga3 Rh1 Ga3 106.498(15) 4_655 2_655 ?
Ga3 Rh1 Ga3 106.498(15) 3 2_655 ?
Ga3 Rh1 Ga3 106.498(15) 4_655 . ?
Ga3 Rh1 Ga3 106.498(15) 3 . ?
Ga3 Rh1 Ga3 115.60(3) 2_655 . ?
Ga3 Rh1 Ga3 73.514(12) 4_655 10_665 ?
Ga3 Rh1 Ga3 73.514(12) 3 10_665 ?
Ga3 Rh1 Ga3 64.38(3) 2_655 10_665 ?
Ga3 Rh1 Ga3 179.97(3) . 10_665 ?
Ga3 Rh1 Ga3 73.514(12) 4_655 9_655 ?
Ga3 Rh1 Ga3 73.514(12) 3 9_655 ?
Ga3 Rh1 Ga3 179.97(3) 2_655 9_655 ?
Ga3 Rh1 Ga3 64.38(3) . 9_655 ?
Ga3 Rh1 Ga3 115.65(3) 10_665 9_655 ?
Ga3 Rh1 Ga3 64.38(3) 4_655 12_655 ?
Ga3 Rh1 Ga3 179.98(3) 3 12_655 ?
Ga3 Rh1 Ga3 73.514(12) 2_655 12_655 ?
Ga3 Rh1 Ga3 73.514(12) . 12_655 ?
Ga3 Rh1 Ga3 106.474(15) 10_665 12_655 ?
Ga3 Rh1 Ga3 106.474(15) 9_655 12_655 ?
Ga3 Rh1 Ga3 179.98(3) 4_655 11_665 ?
Ga3 Rh1 Ga3 64.38(3) 3 11_665 ?
Ga3 Rh1 Ga3 73.514(12) 2_655 11_665 ?
Ga3 Rh1 Ga3 73.514(12) . 11_665 ?
Ga3 Rh1 Ga3 106.475(15) 10_665 11_665 ?
Ga3 Rh1 Ga3 106.474(15) 9_655 11_665 ?
Ga3 Rh1 Ga3 115.65(3) 12_655 11_665 ?
Ga2 Ga1 Ga3 126.09(2) . 4_665 ?
Ga2 Ga1 Ga3 126.09(2) . 10_665 ?
Ga3 Ga1 Ga3 69.70(2) 4_665 10_665 ?
Ga2 Ga1 Ga3 126.09(2) . 9_665 ?
Ga3 Ga1 Ga3 69.70(2) 4_665 9_665 ?
Ga3 Ga1 Ga3 107.83(4) 10_665 9_665 ?
Ga2 Ga1 Ga3 126.09(2) . 3 ?
Ga3 Ga1 Ga3 107.83(4) 4_665 3 ?
Ga3 Ga1 Ga3 69.70(2) 10_665 3 ?
Ga3 Ga1 Ga3 69.70(2) 9_665 3 ?
Ga2 Ga1 Ce1 72.99(2) . 11_765 ?
Ga3 Ga1 Ce1 68.048(17) 4_665 11_765 ?
Ga3 Ga1 Ce1 68.015(17) 10_665 11_765 ?
Ga3 Ga1 Ce1 135.97(2) 9_665 11_765 ?
Ga3 Ga1 Ce1 135.93(2) 3 11_765 ?
Ga2 Ga1 Ce1 72.99(2) . 1_565 ?
Ga3 Ga1 Ce1 68.015(17) 4_665 1_565 ?
Ga3 Ga1 Ce1 135.93(2) 10_665 1_565 ?
Ga3 Ga1 Ce1 68.048(17) 9_665 1_565 ?
Ga3 Ga1 Ce1 135.97(2) 3 1_565 ?
Ce1 Ga1 Ce1 85.090(12) 11_765 1_565 ?
Ga2 Ga1 Ce1 72.99(2) . . ?
Ga3 Ga1 Ce1 135.97(2) 4_665 . ?
Ga3 Ga1 Ce1 68.047(17) 10_665 . ?
Ga3 Ga1 Ce1 135.93(2) 9_665 . ?
Ga3 Ga1 Ce1 68.014(17) 3 . ?
Ce1 Ga1 Ce1 85.090(12) 11_765 . ?
Ce1 Ga1 Ce1 145.98(4) 1_565 . ?
Ga2 Ga1 Ce1 72.99(2) . 11_665 ?
Ga3 Ga1 Ce1 135.93(2) 4_665 11_665 ?
Ga3 Ga1 Ce1 135.97(2) 10_665 11_665 ?
Ga3 Ga1 Ce1 68.015(17) 9_665 11_665 ?
Ga3 Ga1 Ce1 68.048(17) 3 11_665 ?
```

```
Ce1 Ga1 Ce1 145.98(4) 11_765 11_665 ?
Ce1 Ga1 Ce1 85.090(12) 1_565 11_665 ?
Ce1 Ga1 Ce1 85.090(12) . 11_665 ?
Ga1 Ga2 Ga4 121.74(3) . 11_665 ?
Ga1 Ga2 Ga4 121.74(3) . 2_655 ?
Ga4 Ga2 Ga4 73.93(2) 11_665 2_655 ?
Ga1 Ga2 Ga4 121.74(3) . 1_565 ?
Ga4 Ga2 Ga4 73.93(2) 11_665 1_565 ?
Ga4 Ga2 Ga4 116.52(5) 2_655 1_565 ?
Ga1 Ga2 Ga4 121.74(3) . 12_665 ?
Ga4 Ga2 Ga4 116.52(5) 11_665 12_665 ?
Ga4 Ga2 Ga4 73.93(2) 2_655 12_665 ?
Ga4 Ga2 Ga4 73.93(2) 1_565 12_665 ?
Ga1 Ga2 Ce1 63.238(18) . 11_765 ?
Ga4 Ga2 Ce1 153.72(2) 11_665 11_765 ?
Ga4 Ga2 Ce1 82.00(2) 2_655 11_765 ?
Ga4 Ga2 Ce1 127.80(2) 1_565 11_765 ?
Ga4 Ga2 Ce1 64.99(2) 12_665 11_765 ?
Ga1 Ga2 Ce1 63.238(18) . 1_565 ?
Ga4 Ga2 Ce1 127.80(2) 11_665 1_565 ?
Ga4 Ga2 Ce1 153.72(2) 2_655 1_565 ?
Ga4 Ga2 Ce1 64.98(2) 1_565 1_565 ?
Ga4 Ga2 Ce1 82.00(2) 12_665 1_565 ?
Ce1 Ga2 Ce1 78.302(15) 11_765 1_565 ?
Ga1 Ga2 Ce1 63.238(18) . 11_665 ?
Ga4 Ga2 Ce1 64.99(2) 11_665 11_665 ?
Ga4 Ga2 Ce1 127.80(2) 2_655 11_665 ?
Ga4 Ga2 Ce1 82.00(2) 1_565 11_665 ?
Ga4 Ga2 Ce1 153.72(2) 12_665 11_665 ?
Ce1 Ga2 Ce1 126.48(4) 11_765 11_665 ?
Ce1 Ga2 Ce1 78.302(15) 1_565 11_665 ?
Ga1 Ga2 Ce1 63.237(18) . . ?
Ga4 Ga2 Ce1 82.00(2) 11_665 . ?
Ga4 Ga2 Ce1 64.99(2) 2_655 . ?
Ga4 Ga2 Ce1 153.72(2) 1_565 . ?
Ga4 Ga2 Ce1 127.80(2) 12_665 . ?
Ce1 Ga2 Ce1 78.301(15) 11_765 . ?
Ce1 Ga2 Ce1 126.48(4) 1_565 . ?
Ce1 Ga2 Ce1 78.301(15) 11_665 . ?
Rh1 Ga3 Rh1 115.62(3) . 9_655 ?
Rh1 Ga3 Ga1 108.31(2) . 3 ?
Rh1 Ga3 Ga1 108.26(2) 9_655 3 ?
Rh1 Ga3 Ga1 108.31(2) . 9_665 ?
Rh1 Ga3 Ga1 108.26(2) 9_655 9_665 ?
Ga1 Ga3 Ga1 107.82(4) 3 9_665 ?
Rh1 Ga3 Ga3 57.84(3) . 9_655 ?
Rh1 Ga3 Ga3 57.78(3) 9_655 9_655 ?
Ga1 Ga3 Ga3 126.09(2) 3 9_655 ?
Ga1 Ga3 Ga3 126.09(2) 9_665 9_655 ?
Rh1 Ga3 Ce1 81.49(2) . 3 ?
Rh1 Ga3 Ce1 162.89(3) 9_655 3 ?
Ga1 Ga3 Ce1 63.499(18) 3 3 ?
Ga1 Ga3 Ce1 63.499(18) 9_665 3 ?
Ga3 Ga3 Ce1 139.33(4) 9_655 3 ?
Rh1 Ga3 Ce1 162.94(3) . 9_655 ?
Rh1 Ga3 Ce1 81.44(2) 9_655 9_655 ?
Ga1 Ga3 Ce1 63.477(18) 3 9_655 ?
Ga1 Ga3 Ce1 63.477(18) 9_665 9_655 ?
Ga3 Ga3 Ce1 139.22(4) 9_655 9_655 ?
Ce1 Ga3 Ce1 81.45(2) 3 9_655 ?
Ga4 Ga4 Ga2 111.19(4) 9_656 11_655 ?
Ga4 Ga4 Ga2 111.19(4) 9_656 1_545 ?
Ga2 Ga4 Ga2 110.21(5) 11_655 1_545 ?
Ga4 Ga4 Ce1 179.50(7) 9_656 . ?
Ga2 Ga4 Ce1 69.05(3) 11_655 . ?
Ga2 Ga4 Ce1 69.05(3) 1_545 . ?

_diffrn_measured_fraction_theta_max    0.996
_diffrn_reflns_theta_full              30.00
_diffrn_measured_fraction_theta_full   0.996
_refine_diff_density_max    2.688
_refine_diff_density_min   -2.205
_refine_diff_density_rms    0.417
```

A2.2 Ce_2IrGa_{12}

```
data_shelxl

_audit_creation_method            SHELXL-97
_chemical_name_systematic
;
 ?
;
_chemical_name_common             ?
_chemical_melting_point           ?
_chemical_formula_moiety          ?
_chemical_formula_sum
 'Ce2 Ga12 Ir'
_chemical_formula_weight          1309.08

loop_
 _atom_type_symbol
 _atom_type_description
 _atom_type_scat_dispersion_real
 _atom_type_scat_dispersion_imag
 _atom_type_scat_source
 'Ce'  'Ce'  -0.2486   2.6331
 'International Tables Vol C Tables 4.2.6.8
and 6.1.1.4'
 'Ir'  'Ir'  -1.4442   7.9887
 'International Tables Vol C Tables 4.2.6.8
and 6.1.1.4'
 'Ga'  'Ga'   0.2307   1.6083
 'International Tables Vol C Tables 4.2.6.8
and 6.1.1.4'

_symmetry_cell_setting            ?
_symmetry_space_group_name_H-M    ?

loop_
 _symmetry_equiv_pos_as_xyz
 'x, y, z'
 '-x+1/2, -y+1/2, z'
 'x, -y+1/2, -z'
 '-x+1/2, y, -z'
 '-y+1/2, -x+1/2, -z'
 'y, x, -z'
 'y, -x+1/2, z'
 '-y+1/2, x, z'
 '-x, -y, -z'
 'x-1/2, y-1/2, -z'
 '-x, y-1/2, z'
 'x-1/2, -y, z'
 'y-1/2, x-1/2, z'
 '-y, -x, z'
 '-y, x-1/2, -z'
 'y-1/2, -x, -z'

_cell_length_a                    6.0730(4)
_cell_length_b                    6.0730(4)
_cell_length_c
15.6970(13)
_cell_angle_alpha                 90.00
_cell_angle_beta                  90.00
_cell_angle_gamma                 90.00
_cell_volume                      578.93(7)
_cell_formula_units_Z             3
_cell_measurement_temperature     298(2)
_cell_measurement_reflns_used     ?
_cell_measurement_theta_min       ?
_cell_measurement_theta_max       ?

_exptl_crystal_description        ?
_exptl_crystal_colour             ?
_exptl_crystal_size_max           0.05
_exptl_crystal_size_mid           0.05
_exptl_crystal_size_min           0.03
_exptl_crystal_density_meas       ?
_exptl_crystal_density_diffrn     11.265
_exptl_crystal_density_method           'not
measured'
_exptl_crystal_F_000              1695
_exptl_absorpt_coefficient_mu     69.698
_exptl_absorpt_correction_type    ?
_exptl_absorpt_correction_T_min   0.1283
_exptl_absorpt_correction_T_max   0.2747
_exptl_absorpt_process_details    ?

_exptl_special_details
;
 ?
;

_diffrn_ambient_temperature       298(2)
_diffrn_radiation_wavelength      0.71073
_diffrn_radiation_type            MoK\a
_diffrn_radiation_source              'fine-
focus sealed tube'
_diffrn_radiation_monochromator   graphite
_diffrn_measurement_device_type   ?
_diffrn_measurement_method        ?
_diffrn_detector_area_resol_mean  ?
_diffrn_standards_number          ?
_diffrn_standards_interval_count  ?
_diffrn_standards_interval_time   ?
_diffrn_standards_decay_%         ?
_diffrn_reflns_number             1262
_diffrn_reflns_av_R_equivalents   0.0700
_diffrn_reflns_av_sigmaI/netI     0.0632
_diffrn_reflns_limit_h_min        -8
_diffrn_reflns_limit_h_max        8
_diffrn_reflns_limit_k_min        -6
_diffrn_reflns_limit_k_max        6
_diffrn_reflns_limit_l_min        -13
_diffrn_reflns_limit_l_max        22
_diffrn_reflns_theta_min          2.60
_diffrn_reflns_theta_max          30.03
_reflns_number_total              484
_reflns_number_gt                 400
_reflns_threshold_expression      >2sigma(I)

_computing_data_collection        ?
_computing_cell_refinement        ?
_computing_data_reduction         ?
_computing_structure_solution      'SHELXS-97
(Sheldrick, 1990)'
_computing_structure_refinement    'SHELXL-97
(Sheldrick, 1997)'
_computing_molecular_graphics     ?
_computing_publication_material   ?

_refine_special_details
;
 Refinement of F^2^ against ALL reflections.
The weighted R-factor wR and
 goodness  of  fit  S  are  based  on  F^2^,
conventional R-factors R are based
 on F, with F set to zero for negative F^2^.
The threshold expression of
 F^2^  >  2sigma(F^2^)  is  used  only  for
calculating R-factors(gt) etc. and is
 not relevant to the choice of reflections
for refinement.  R-factors based
 on  F^2^  are  statistically  about  twice  as
large as those based on F, and R-
```

```
 factors based on ALL data will be even
larger.
;

_refine_ls_structure_factor_coef  Fsqd
_refine_ls_matrix_type            full
_refine_ls_weighting_scheme       calc
_refine_ls_weighting_details
 'calc
w=1/[\s^2^(Fo^2^)+(0.0688P)^2^+8.1015P]
where P=(Fo^2^+2Fc^2^)/3'
_atom_sites_solution_primary      direct
_atom_sites_solution_secondary    difmap
_atom_sites_solution_hydrogens    geom
_refine_ls_hydrogen_treatment     mixed
_refine_ls_extinction_method      SHELXL
_refine_ls_extinction_coef        0.0021(5)
_refine_ls_extinction_expression
 'Fc^*^=kFc[1+0.001xFc^2^\l^3^/sin(2\q)]^-
1/4^'
_refine_ls_number_reflns          484
_refine_ls_number_parameters      25
_refine_ls_number_restraints      0
_refine_ls_R_factor_all           0.0546
_refine_ls_R_factor_gt            0.0458
_refine_ls_wR_factor_ref          0.1303
_refine_ls_wR_factor_gt           0.1234
_refine_ls_goodness_of_fit_ref    1.119
_refine_ls_restrained_S_all       1.119
_refine_ls_shift/su_max           0.000
_refine_ls_shift/su_mean          0.000

loop_
 _atom_site_label
 _atom_site_type_symbol
 _atom_site_fract_x
 _atom_site_fract_y
 _atom_site_fract_z
 _atom_site_U_iso_or_equiv
 _atom_site_adp_type
 _atom_site_occupancy
 _atom_site_symmetry_multiplicity
 _atom_site_calc_flag
 _atom_site_refinement_flags
 _atom_site_disorder_assembly
 _atom_site_disorder_group
Ir1 Ir 0.7500 0.2500 0.5000 0.0097(4) Uani 1
8 d S . .
Ce2 Ce 0.7500 0.2500 0.25752(7) 0.0106(4)
Uani 1 4 d S . .
Ga3 Ga 0.5000 0.0000 0.41394(9) 0.0120(4)
Uani 1 2 d S . .
Ga4 Ga 0.5699(2) 0.0699(2) 0.07103(11)
0.0254(5) Uani 1 2 d S . .
Ga5 Ga 0.7500 0.7500 0.31381(15) 0.0110(5)
Uani 1 4 d S . .
Ga6 Ga 0.7500 0.7500 0.15795(15) 0.0157(5)
Uani 1 4 d S . .

loop_
 _atom_site_aniso_label
 _atom_site_aniso_U_11
 _atom_site_aniso_U_22
 _atom_site_aniso_U_33
 _atom_site_aniso_U_23
 _atom_site_aniso_U_13
 _atom_site_aniso_U_12
Ir1 0.0077(4) 0.0077(4) 0.0136(6) 0.000
0.000 0.000
Ce2 0.0085(4) 0.0085(4) 0.0147(6) 0.000
0.000 -0.0001(3)
Ga3 0.0110(5) 0.0110(5) 0.0141(8) 0.0000(3)
0.0000(3) -0.0009(5)
Ga4 0.0275(6) 0.0275(6) 0.0212(8) -0.0061(5)
-0.0061(5) 0.0098(7)
Ga5 0.0099(6) 0.0099(6) 0.0133(10) 0.000
0.000 0.000
Ga6 0.0157(7) 0.0157(7) 0.0155(10) 0.000
0.000 0.000

_geom_special_details
;
 All esds (except the esd in the dihedral
angle between two l.s. planes)
 are estimated using the full covariance
matrix.  The cell esds are taken
 into account individually in the estimation
of esds in distances, angles
 and torsion angles; correlations between
esds in cell parameters are only
 used when they are defined by crystal
symmetry.  An approximate (isotropic)
 treatment of cell esds is used for
estimating esds involving l.s. planes.
;

loop_
 _geom_bond_atom_site_label_1
 _geom_bond_atom_site_label_2
 _geom_bond_distance
 _geom_bond_site_symmetry_2
 _geom_bond_publ_flag
Ir1 Ga3 2.5368(8) 10_666 ?
Ir1 Ga3 2.5368(8) 2_655 ?
Ir1 Ga3 2.5368(8) 9_656 ?
Ir1 Ga3 2.5368(8) 12_655 ?
Ir1 Ga3 2.5368(8) 4_656 ?
Ir1 Ga3 2.5368(8) 3_556 ?
Ir1 Ga3 2.5368(8) 11_665 ?
Ir1 Ga3 2.5368(8) . ?
Ce2 Ga5 3.1624(8) 11_755 ?
Ce2 Ga5 3.1624(8) 11_655 ?
Ce2 Ga5 3.1624(8) 1_545 ?
Ce2 Ga5 3.1624(8) . ?
Ce2 Ga3 3.2616(14) . ?
Ce2 Ga3 3.2616(14) 2_655 ?
Ce2 Ga3 3.2616(14) 11_665 ?
Ce2 Ga3 3.2616(14) 12_655 ?
Ce2 Ga4 3.311(2) 2_655 ?
Ce2 Ga4 3.311(2) . ?
Ce2 Ga6 3.4151(12) 11_655 ?
Ce2 Ga6 3.4151(12) 1_545 ?
Ga3 Ir1 2.5367(8) 9_656 ?
Ga3 Ga5 2.6609(16) 11_655 ?
Ga3 Ga5 2.6609(16) 1_545 ?
Ga3 Ga3 2.702(3) 9_656 ?
Ga3 Ce2 3.2616(14) 11_655 ?
Ga4 Ga4 2.533(3) 9_655 ?
Ga4 Ga6 2.6140(15) 11_655 ?
Ga4 Ga6 2.6140(15) 1_545 ?
Ga5 Ga6 2.447(3) . ?
Ga5 Ga3 2.6609(16) 12_665 ?
Ga5 Ga3 2.6609(16) 2_655 ?
Ga5 Ga3 2.6609(16) 1_565 ?
Ga5 Ga3 2.6609(16) 11_665 ?
Ga5 Ce2 3.1624(8) 11_665 ?
Ga5 Ce2 3.1624(8) 11_765 ?
Ga5 Ce2 3.1624(8) 1_565 ?
Ga6 Ga4 2.6140(15) 11_665 ?
Ga6 Ga4 2.6140(15) 2_655 ?
Ga6 Ga4 2.6140(15) 12_665 ?
Ga6 Ga4 2.6140(15) 1_565 ?
Ga6 Ce2 3.4152(12) 11_765 ?
```

```
Ga6 Ce2 3.4152(12) 1_565 ?
Ga6 Ce2 3.4152(12) 11_665 ?

loop_
 _geom_angle_atom_site_label_1
 _geom_angle_atom_site_label_2
 _geom_angle_atom_site_label_3
 _geom_angle
 _geom_angle_site_symmetry_1
 _geom_angle_site_symmetry_3
 _geom_angle_publ_flag
Ga3 Ir1 Ga3 64.35(5) 10_666 2_655 ?
Ga3 Ir1 Ga3 115.65(5) 10_666 9_656 ?
Ga3 Ir1 Ga3 180.0 2_655 9_656 ?
Ga3 Ir1 Ga3 106.48(3) 10_666 12_655 ?
Ga3 Ir1 Ga3 73.52(3) 2_655 12_655 ?
Ga3 Ir1 Ga3 106.48(3) 9_656 12_655 ?
Ga3 Ir1 Ga3 73.52(3) 10_666 4_656 ?
Ga3 Ir1 Ga3 106.48(3) 2_655 4_656 ?
Ga3 Ir1 Ga3 73.52(3) 9_656 4_656 ?
Ga3 Ir1 Ga3 64.35(5) 12_655 4_656 ?
Ga3 Ir1 Ga3 73.52(3) 10_666 3_556 ?
Ga3 Ir1 Ga3 106.48(3) 2_655 3_556 ?
Ga3 Ir1 Ga3 73.52(3) 9_656 3_556 ?
Ga3 Ir1 Ga3 180.00(5) 12_655 3_556 ?
Ga3 Ir1 Ga3 115.65(5) 4_656 3_556 ?
Ga3 Ir1 Ga3 106.48(3) 10_666 11_665 ?
Ga3 Ir1 Ga3 73.52(3) 2_655 11_665 ?
Ga3 Ir1 Ga3 106.48(3) 9_656 11_665 ?
Ga3 Ir1 Ga3 115.65(5) 12_655 11_665 ?
Ga3 Ir1 Ga3 180.00(5) 4_656 11_665 ?
Ga3 Ir1 Ga3 64.35(5) 3_556 11_665 ?
Ga3 Ir1 Ga3 180.0 10_666 . ?
Ga3 Ir1 Ga3 115.64(5) 2_655 . ?
Ga3 Ir1 Ga3 64.36(5) 9_656 . ?
Ga3 Ir1 Ga3 73.52(3) 12_655 . ?
Ga3 Ir1 Ga3 106.48(3) 4_656 . ?
Ga3 Ir1 Ga3 106.48(3) 3_556 . ?
Ga3 Ir1 Ga3 73.52(3) 11_665 . ?
Ga5 Ce2 Ga5 147.55(9) 11_755 11_655 ?
Ga5 Ce2 Ga5 85.52(3) 11_755 1_545 ?
Ga5 Ce2 Ga5 85.52(3) 11_655 1_545 ?
Ga5 Ce2 Ga5 85.52(3) 11_755 . ?
Ga5 Ce2 Ga5 85.52(3) 11_655 . ?
Ga5 Ce2 Ga5 147.55(9) 1_545 . ?
Ga5 Ce2 Ga3 103.69(5) 11_755 . ?
Ga5 Ce2 Ga3 48.91(3) 11_655 . ?
Ga5 Ce2 Ga3 48.91(3) 1_545 . ?
Ga5 Ce2 Ga3 103.69(5) . . ?
Ga5 Ce2 Ga3 48.91(3) 11_755 2_655 ?
Ga5 Ce2 Ga3 103.69(5) 11_655 2_655 ?
Ga5 Ce2 Ga3 103.69(5) 1_545 2_655 ?
Ga5 Ce2 Ga3 48.91(3) . 2_655 ?
Ga3 Ce2 Ga3 82.34(4) . 2_655 ?
Ga5 Ce2 Ga3 103.69(5) 11_755 11_665 ?
Ga5 Ce2 Ga3 48.91(3) 11_655 11_665 ?
Ga5 Ce2 Ga3 103.69(5) 1_545 11_665 ?
Ga5 Ce2 Ga3 48.91(3) . 11_665 ?
Ga3 Ce2 Ga3 55.48(3) . 11_665 ?
Ga3 Ce2 Ga3 55.48(3) 2_655 11_665 ?
Ga5 Ce2 Ga3 48.91(3) 11_755 12_655 ?
Ga5 Ce2 Ga3 103.69(5) 11_655 12_655 ?
Ga5 Ce2 Ga3 48.91(3) 1_545 12_655 ?
Ga5 Ce2 Ga3 103.69(5) . 12_655 ?
Ga3 Ce2 Ga3 55.48(3) . 12_655 ?
Ga3 Ce2 Ga3 55.48(3) 2_655 12_655 ?
Ga3 Ce2 Ga3 82.34(4) 11_665 12_655 ?
Ga5 Ce2 Ga4 85.98(5) 11_755 2_655 ?
Ga5 Ce2 Ga4 124.34(5) 11_655 2_655 ?
Ga5 Ce2 Ga4 124.34(5) 1_545 2_655 ?
Ga5 Ce2 Ga4 85.98(5) . 2_655 ?
Ga3 Ce2 Ga4 166.67(4) . 2_655 ?
Ga3 Ce2 Ga4 110.98(4) 2_655 2_655 ?
Ga3 Ce2 Ga4 131.73(2) 11_665 2_655 ?
Ga3 Ce2 Ga4 131.73(2) 12_655 2_655 ?
Ga5 Ce2 Ga4 124.34(5) 11_755 . ?
Ga5 Ce2 Ga4 85.98(5) 11_655 . ?
Ga5 Ce2 Ga4 85.98(5) 1_545 . ?
Ga5 Ce2 Ga4 124.34(5) . . ?
Ga3 Ce2 Ga4 110.98(4) . . ?
Ga3 Ce2 Ga4 166.67(4) 2_655 . ?
Ga3 Ce2 Ga4 131.73(2) 11_665 . ?
Ga3 Ce2 Ga4 131.73(2) 12_655 . ?
Ga4 Ce2 Ga4 55.69(7) 2_655 . ?
Ga5 Ce2 Ga6 168.99(7) 11_755 11_655 ?
Ga5 Ce2 Ga6 43.46(5) 11_655 11_655 ?
Ga5 Ce2 Ga6 97.35(2) 1_545 11_655 ?
Ga5 Ce2 Ga6 97.35(2) . 11_655 ?
Ga3 Ce2 Ga6 86.02(3) . 11_655 ?
Ga3 Ce2 Ga6 139.32(3) 2_655 11_655 ?
Ga3 Ce2 Ga6 86.02(3) 11_665 11_655 ?
Ga3 Ce2 Ga6 139.32(3) 12_655 11_655 ?
Ga4 Ce2 Ga6 83.63(5) 2_655 11_655 ?
Ga4 Ce2 Ga6 45.71(3) . 11_655 ?
Ga5 Ce2 Ga6 97.35(2) 11_755 1_545 ?
Ga5 Ce2 Ga6 97.35(2) 11_655 1_545 ?
Ga5 Ce2 Ga6 43.46(5) 1_545 1_545 ?
Ga5 Ce2 Ga6 168.99(7) . 1_545 ?
Ga3 Ce2 Ga6 86.02(3) . 1_545 ?
Ga3 Ce2 Ga6 139.32(3) 2_655 1_545 ?
Ga3 Ce2 Ga6 139.32(3) 11_665 1_545 ?
Ga3 Ce2 Ga6 86.02(3) 12_655 1_545 ?
Ga4 Ce2 Ga6 83.63(5) 2_655 1_545 ?
Ga4 Ce2 Ga6 45.71(3) . 1_545 ?
Ga6 Ce2 Ga6 77.91(3) 11_655 1_545 ?
Ir1 Ga3 Ir1 115.65(5) 9_656 . ?
Ir1 Ga3 Ga5 108.333(19) 9_656 11_655 ?
Ir1 Ga3 Ga5 108.334(19) . 11_655 ?
Ir1 Ga3 Ga5 108.333(19) 9_656 1_545 ?
Ir1 Ga3 Ga5 108.334(19) . 1_545 ?
Ga5 Ga3 Ga5 107.59(9) 11_655 1_545 ?
Ir1 Ga3 Ga3 57.82(3) 9_656 9_656 ?
Ir1 Ga3 Ga3 57.82(3) . 9_656 ?
Ga5 Ga3 Ga3 126.20(5) 11_655 9_656 ?
Ga5 Ga3 Ga3 126.20(5) 1_545 9_656 ?
Ir1 Ga3 Ce2 81.006(17) 9_656 11_655 ?
Ir1 Ga3 Ce2 163.35(5) . 11_655 ?
Ga5 Ga3 Ce2 63.60(4) 11_655 11_655 ?
Ga5 Ga3 Ce2 63.60(4) 1_545 11_655 ?
Ga3 Ga3 Ce2 138.83(2) 9_656 11_655 ?
Ir1 Ga3 Ce2 163.35(5) 9_656 . ?
Ir1 Ga3 Ce2 81.007(17) . . ?
Ga5 Ga3 Ce2 63.60(4) 11_655 . ?
Ga5 Ga3 Ce2 63.60(4) 1_545 . ?
Ga3 Ga3 Ce2 138.83(2) 9_656 . ?
Ce2 Ga3 Ce2 82.34(4) 11_655 . ?
Ga4 Ga4 Ga6 110.52(7) 9_655 11_655 ?
Ga4 Ga4 Ga6 110.52(7) 9_655 1_545 ?
Ga6 Ga4 Ga6 110.45(9) 11_655 1_545 ?
Ga4 Ga4 Ce2 179.53(12) 9_655 . ?
Ga6 Ga4 Ce2 69.25(5) 11_655 . ?
Ga6 Ga4 Ce2 69.25(5) 1_545 . ?
Ga6 Ga5 Ga3 126.20(5) . 12_665 ?
Ga6 Ga5 Ga3 126.20(5) . 2_655 ?
Ga3 Ga5 Ga3 69.58(5) 12_665 2_655 ?
Ga6 Ga5 Ga3 126.20(5) . 1_565 ?
Ga3 Ga5 Ga3 69.58(5) 12_665 1_565 ?
Ga3 Ga5 Ga3 107.59(9) 2_655 1_565 ?
Ga6 Ga5 Ga3 126.20(5) . 11_665 ?
Ga3 Ga5 Ga3 107.59(9) 12_665 11_665 ?
Ga3 Ga5 Ga3 69.58(5) 2_655 11_665 ?
Ga3 Ga5 Ga3 69.58(5) 1_565 11_665 ?
Ga6 Ga5 Ce2 73.78(5) . 11_665 ?
Ga3 Ga5 Ce2 135.47(4) 12_665 11_665 ?
```

```
Ga3 Ga5 Ce2 135.47(4) 2_655 11_665 ?
Ga3 Ga5 Ce2 67.49(2) 1_565 11_665 ?
Ga3 Ga5 Ce2 67.49(2) 11_665 11_665 ?
Ga6 Ga5 Ce2 73.78(5) . 11_765 ?
Ga3 Ga5 Ce2 67.49(2) 12_665 11_765 ?
Ga3 Ga5 Ce2 67.49(2) 2_655 11_765 ?
Ga3 Ga5 Ce2 135.47(4) 1_565 11_765 ?
Ga3 Ga5 Ce2 135.47(4) 11_665 11_765 ?
Ce2 Ga5 Ce2 147.55(9) 11_665 11_765 ?
Ga6 Ga5 Ce2 73.78(5) . 1_565 ?
Ga3 Ga5 Ce2 67.49(2) 12_665 1_565 ?
Ga3 Ga5 Ce2 135.47(4) 2_655 1_565 ?
Ga3 Ga5 Ce2 67.49(2) 1_565 1_565 ?
Ga3 Ga5 Ce2 135.47(4) 11_665 1_565 ?
Ce2 Ga5 Ce2 85.52(3) 11_665 1_565 ?
Ce2 Ga5 Ce2 85.52(3) 11_765 1_565 ?
Ga6 Ga5 Ce2 73.78(5) . . ?
Ga3 Ga5 Ce2 135.47(4) 12_665 . ?
Ga3 Ga5 Ce2 67.49(2) 2_655 . ?
Ga3 Ga5 Ce2 135.47(4) 1_565 . ?
Ga3 Ga5 Ce2 67.49(2) 11_665 . ?
Ce2 Ga5 Ce2 85.52(3) 11_665 . ?
Ce2 Ga5 Ce2 85.52(3) 11_765 . ?
Ce2 Ga5 Ce2 147.55(9) 1_565 . ?
Ga5 Ga6 Ga4 121.47(5) . 11_665 ?
Ga5 Ga6 Ga4 121.47(5) . 2_655 ?
Ga4 Ga6 Ga4 74.19(5) 11_665 2_655 ?
Ga5 Ga6 Ga4 121.47(5) . 12_665 ?
Ga4 Ga6 Ga4 117.07(10) 11_665 12_665 ?
Ga4 Ga6 Ga4 74.19(5) 2_655 12_665 ?
Ga5 Ga6 Ga4 121.47(5) . 1_565 ?
Ga4 Ga6 Ga4 74.19(5) 11_665 1_565 ?
Ga4 Ga6 Ga4 117.07(10) 2_655 1_565 ?
Ga4 Ga6 Ga4 74.19(5) 12_665 1_565 ?
Ga5 Ga6 Ce2 62.76(4) . . ?
Ga4 Ga6 Ce2 82.35(4) 11_665 . ?
Ga4 Ga6 Ce2 65.04(4) 2_655 . ?
Ga4 Ga6 Ce2 127.65(4) 12_665 . ?
Ga4 Ga6 Ce2 154.13(4) 1_565 . ?
Ga5 Ga6 Ce2 62.76(4) . 11_765 ?
Ga4 Ga6 Ce2 154.13(4) 11_665 11_765 ?
Ga4 Ga6 Ce2 82.36(4) 2_655 11_765 ?
Ga4 Ga6 Ce2 65.04(4) 12_665 11_765 ?
Ga4 Ga6 Ce2 127.65(4) 1_565 11_765 ?
Ce2 Ga6 Ce2 77.91(3) . 11_765 ?
Ga5 Ga6 Ce2 62.76(4) . 1_565 ?
Ga4 Ga6 Ce2 127.65(4) 11_665 1_565 ?
Ga4 Ga6 Ce2 154.13(4) 2_655 1_565 ?
Ga4 Ga6 Ce2 82.36(4) 12_665 1_565 ?
Ga4 Ga6 Ce2 65.04(4) 1_565 1_565 ?
Ce2 Ga6 Ce2 125.53(8) . 1_565 ?
Ce2 Ga6 Ce2 77.91(3) 11_765 1_565 ?
Ga5 Ga6 Ce2 62.76(4) . 11_665 ?
Ga4 Ga6 Ce2 65.04(4) 11_665 11_665 ?
Ga4 Ga6 Ce2 127.65(4) 2_655 11_665 ?
Ga4 Ga6 Ce2 154.13(4) 12_665 11_665 ?
Ga4 Ga6 Ce2 82.36(4) 1_565 11_665 ?
Ce2 Ga6 Ce2 77.91(3) . 11_665 ?
Ce2 Ga6 Ce2 125.53(8) 11_765 11_665 ?
Ce2 Ga6 Ce2 77.91(3) 1_565 11_665 ?

_diffrn_measured_fraction_theta_max    0.994
_diffrn_reflns_theta_full              30.03
_diffrn_measured_fraction_theta_full   0.994
_refine_diff_density_max    3.295
_refine_diff_density_min   -2.975
_refine_diff_density_rms    0.616
```

A2.3 Er_2NiGa_8

```
data_erni2ga2

_audit_creation_method            SHELXL-97
_chemical_name_systematic
;
 ?
;
_chemical_name_common             ?
_chemical_melting_point           ?
_chemical_formula_moiety          ?
_chemical_formula_sum
 'Er2 Ga8 Ni'
_chemical_formula_weight          950.99

loop_
 _atom_type_symbol
 _atom_type_description
 _atom_type_scat_dispersion_real
 _atom_type_scat_dispersion_imag
 _atom_type_scat_source
 'Ni'  'Ni'   0.3393   1.1124
 'International Tables Vol C Tables 4.2.6.8
and 6.1.1.4'
 'Ga'  'Ga'   0.2307   1.6083
 'International Tables Vol C Tables 4.2.6.8
and 6.1.1.4'
 'Er'  'Er'  -0.2586   4.9576
 'International Tables Vol C Tables 4.2.6.8
and 6.1.1.4'

_symmetry_cell_setting            ?
_symmetry_space_group_name_H-M    ?

loop_
 _symmetry_equiv_pos_as_xyz
 'x, y, z'
 '-x, -y, z'
 'x, -y, -z'
 '-x, y, -z'
 '-y, -x, -z'
 'y, x, -z'
 'y, -x, z'
 '-y, x, z'
 '-x, -y, -z'
 'x, y, -z'
 '-x, y, z'
 'x, -y, z'
 'y, x, z'
 '-y, -x, z'
 '-y, x, -z'
 'y, -x, -z'

_cell_length_a                    4.2248(5)
_cell_length_b                    4.2248(5)
_cell_length_c                    10.9144(7)
_cell_angle_alpha                 90.00
_cell_angle_beta                  90.00
_cell_angle_gamma                 90.00
_cell_volume                      194.81(3)
_cell_formula_units_Z             1
_cell_measurement_temperature     298(2)
_cell_measurement_reflns_used     ?
_cell_measurement_theta_min       ?
_cell_measurement_theta_max       ?

_exptl_crystal_description        ?
_exptl_crystal_colour             ?
_exptl_crystal_size_max           0.05
_exptl_crystal_size_mid           0.03
_exptl_crystal_size_min           0.03
_exptl_crystal_density_meas       ?
_exptl_crystal_density_diffrn     8.106
_exptl_crystal_density_method          'not
measured'
_exptl_crystal_F_000              412
_exptl_absorpt_coefficient_mu     50.701
_exptl_absorpt_correction_type    ?
_exptl_absorpt_correction_T_min   0.1860
_exptl_absorpt_correction_T_max   0.3638
_exptl_absorpt_process_details    ?

_exptl_special_details
;
 ?
;

_diffrn_ambient_temperature       298(2)
_diffrn_radiation_wavelength      0.71073
_diffrn_radiation_type            MoK\a
_diffrn_radiation_source               'fine-
focus sealed tube'
_diffrn_radiation_monochromator   graphite
_diffrn_measurement_device_type   ?
_diffrn_measurement_method        ?
_diffrn_detector_area_resol_mean  ?
_diffrn_standards_number          ?
_diffrn_standards_interval_count  ?
_diffrn_standards_interval_time   ?
_diffrn_standards_decay_%         ?
_diffrn_reflns_number             527
_diffrn_reflns_av_R_equivalents   0.0674
_diffrn_reflns_av_sigmaI/netI     0.0519
_diffrn_reflns_limit_h_min        -5
_diffrn_reflns_limit_h_max        5
_diffrn_reflns_limit_k_min        -4
_diffrn_reflns_limit_k_max        4
_diffrn_reflns_limit_l_min        -11
_diffrn_reflns_limit_l_max        15
_diffrn_reflns_theta_min          3.73
_diffrn_reflns_theta_max          30.01
_reflns_number_total              218
_reflns_number_gt                 195
_reflns_threshold_expression      >2sigma(I)

_computing_data_collection        ?
_computing_cell_refinement        ?
_computing_data_reduction         ?
_computing_structure_solution     ?
_computing_structure_refinement    'SHELXL-97
(Sheldrick, 1997)'
_computing_molecular_graphics     ?
_computing_publication_material   ?

_refine_special_details
;
 Refinement of F^2^ against ALL reflections.
The weighted R-factor wR and
 goodness of fit S are based on F^2^,
conventional R-factors R are based
 on F, with F set to zero for negative F^2^.
The threshold expression of
 F^2^ > 2sigma(F^2^) is used only for
calculating R-factors(gt) etc. and is
 not relevant to the choice of reflections
for refinement.  R-factors based
 on F^2^ are statistically about twice as
large as those based on F, and R-
 factors based on ALL data will be even
larger.
```

```
;

_refine_ls_structure_factor_coef  Fsqd
_refine_ls_matrix_type            full
_refine_ls_weighting_scheme       calc
_refine_ls_weighting_details
 'calc
w=1/[\s^2^(Fo^2^)+(0.0694P)^2^+3.3764P]
where P=(Fo^2^+2Fc^2^)/3'
_atom_sites_solution_primary      direct
_atom_sites_solution_secondary    difmap
_atom_sites_solution_hydrogens    geom
_refine_ls_hydrogen_treatment     mixed
_refine_ls_extinction_method      SHELXL
_refine_ls_extinction_coef        0.037(5)
_refine_ls_extinction_expression
 'Fc^*^=kFc[1+0.001xFc^2^\l^3^/sin(2\q)]^-
1/4^'
_refine_ls_number_reflns          218
_refine_ls_number_parameters      17
_refine_ls_number_restraints      0
_refine_ls_R_factor_all           0.0574
_refine_ls_R_factor_gt            0.0503
_refine_ls_wR_factor_ref          0.1245
_refine_ls_wR_factor_gt           0.1194
_refine_ls_goodness_of_fit_ref    1.130
_refine_ls_restrained_S_all       1.130
_refine_ls_shift/su_max           3.231
_refine_ls_shift/su_mean          0.506

loop_
 _atom_site_label
 _atom_site_type_symbol
 _atom_site_fract_x
 _atom_site_fract_y
 _atom_site_fract_z
 _atom_site_U_iso_or_equiv
 _atom_site_adp_type
 _atom_site_occupancy
 _atom_site_symmetry_multiplicity
 _atom_site_calc_flag
 _atom_site_refinement_flags
 _atom_site_disorder_assembly
 _atom_site_disorder_group
Er01 Er 0.0000 0.0000 0.30889(10) 0.0049(5)
Uani 1 8 d S . .
Ni02 Ni 0.0000 0.0000 0.0000 0.0066(9) Uani
1 16 d S . .
Ga03 Ga 0.0000 0.5000 0.1196(2) 0.0089(6)
Uani 1 4 d S . .
Ga05 Ga 0.0000 0.5000 0.5000 0.0136(9) Uani
1 8 d S . .
Ga04 Ga 0.5000 0.5000 0.3019(3) 0.0110(8)
Uani 1 8 d S . .

loop_
 _atom_site_aniso_label
 _atom_site_aniso_U_11
 _atom_site_aniso_U_22
 _atom_site_aniso_U_33
 _atom_site_aniso_U_23
 _atom_site_aniso_U_13
 _atom_site_aniso_U_12
Er01 0.0074(6) 0.0074(6) 0.0000(7) 0.000
0.000 0.000
Ni02 0.0099(13) 0.0099(13) 0.000(2) 0.000
0.000 0.000
Ga03 0.0182(11) 0.0084(10) 0.0000(10) 0.000
0.000 0.000
Ga05 0.033(2) 0.0082(14) 0.0000(16) 0.000
0.000 0.000
Ga04 0.0102(10) 0.0102(10) 0.0125(18) 0.000
0.000 0.000

_geom_special_details
;
 All esds (except the esd in the dihedral
angle between two l.s. planes)
 are estimated using the full covariance
matrix.  The cell esds are taken
 into account individually in the estimation
of esds in distances, angles
 and torsion angles; correlations between
esds in cell parameters are only
 used when they are defined by crystal
symmetry.  An approximate (isotropic)
 treatment of cell esds is used for
estimating esds involving l.s. planes.
;

loop_
 _geom_bond_atom_site_label_1
 _geom_bond_atom_site_label_2
 _geom_bond_distance
 _geom_bond_site_symmetry_2
 _geom_bond_publ_flag
Er01 Ga03 2.9547(16) 13_455 ?
Er01 Ga03 2.9547(16) 1_545 ?
Er01 Ga03 2.9547(16) . ?
Er01 Ga03 2.9547(16) 13 ?
Er01 Ga05 2.9687(8) 5_656 ?
Er01 Ga05 2.9687(8) . ?
Er01 Ga05 2.9687(8) 5_556 ?
Er01 Ga05 2.9687(8) 1_545 ?
Er01 Ga04 2.9884(4) 1_445 ?
Er01 Ga04 2.9884(4) . ?
Er01 Ga04 2.9884(4) 1_455 ?
Er01 Ga04 2.9884(4) 1_545 ?
Ni02 Ga03 2.4832(13) 13 ?
Ni02 Ga03 2.4832(13) 5 ?
Ni02 Ga03 2.4832(13) 9 ?
Ni02 Ga03 2.4832(13) . ?
Ni02 Ga03 2.4832(13) 13_455 ?
Ni02 Ga03 2.4832(13) 5_655 ?
Ni02 Ga03 2.4832(13) 9_565 ?
Ni02 Ga03 2.4832(13) 1_545 ?
Ni02 Er01 3.3714(11) 9 ?
Ga03 Ni02 2.4832(13) 1_565 ?
Ga03 Ga03 2.611(5) 9_565 ?
Ga03 Ga04 2.902(2) . ?
Ga03 Ga04 2.902(2) 1_455 ?
Ga03 Er01 2.9547(16) 1_565 ?
Ga03 Ga03 2.9874(4) 13_455 ?
Ga03 Ga03 2.9874(4) 13_565 ?
Ga03 Ga03 2.9874(4) 13 ?
Ga03 Ga03 2.9874(4) 13_465 ?
Ga05 Er01 2.9687(8) 9_566 ?
Ga05 Er01 2.9687(8) 1_565 ?
Ga05 Er01 2.9687(8) 9_556 ?
Ga05 Ga05 2.9874(4) 5_666 ?
Ga05 Ga05 2.9874(4) 5_556 ?
Ga05 Ga05 2.9874(4) 5_656 ?
Ga05 Ga05 2.9874(4) 5_566 ?
Ga04 Ga03 2.902(2) 13 ?
Ga04 Ga03 2.902(2) 13_565 ?
Ga04 Ga03 2.902(2) 1_655 ?
Ga04 Er01 2.9884(4) 1_665 ?
Ga04 Er01 2.9884(4) 1_655 ?
Ga04 Er01 2.9884(4) 1_565 ?

loop_
 _geom_angle_atom_site_label_1
 _geom_angle_atom_site_label_2
```

```
 _geom_angle_atom_site_label_3
 _geom_angle
 _geom_angle_site_symmetry_1
 _geom_angle_site_symmetry_3
 _geom_angle_publ_flag
Ga03 Er01 Ga03 60.73(4) 13_455 1_545 ?
Ga03 Er01 Ga03 60.73(4) 13_455 . ?
Ga03 Er01 Ga03 91.27(6) 1_545 . ?
Ga03 Er01 Ga03 91.27(6) 13_455 13 ?
Ga03 Er01 Ga03 60.73(4) 1_545 13 ?
Ga03 Er01 Ga03 60.73(4) . 13 ?
Ga03 Er01 Ga05 179.73(4) 13_455 5_656 ?
Ga03 Er01 Ga05 119.425(19) 1_545 5_656 ?
Ga03 Er01 Ga05 119.424(19) . 5_656 ?
Ga03 Er01 Ga05 89.00(3) 13 5_656 ?
Ga03 Er01 Ga05 119.425(19) 13_455 . ?
Ga03 Er01 Ga05 179.73(4) 1_545 . ?
Ga03 Er01 Ga05 89.00(3) . . ?
Ga03 Er01 Ga05 119.424(19) 13 . ?
Ga05 Er01 Ga05 60.418(17) 5_656 . ?
Ga03 Er01 Ga05 89.00(3) 13_455 5_556 ?
Ga03 Er01 Ga05 119.424(19) 1_545 5_556 ?
Ga03 Er01 Ga05 119.424(19) . 5_556 ?
Ga03 Er01 Ga05 179.73(4) 13 5_556 ?
Ga05 Er01 Ga05 90.73(3) 5_656 5_556 ?
Ga05 Er01 Ga05 60.418(17) . 5_556 ?
Ga03 Er01 Ga05 119.424(19) 13_455 1_545 ?
Ga03 Er01 Ga05 89.00(3) 1_545 1_545 ?
Ga03 Er01 Ga05 179.73(4) . 1_545 ?
Ga03 Er01 Ga05 119.424(19) 13 1_545 ?
Ga05 Er01 Ga05 60.418(17) 5_656 1_545 ?
Ga05 Er01 Ga05 90.73(3) . 1_545 ?
Ga05 Er01 Ga05 60.418(17) 5_556 1_545 ?
Ga03 Er01 Ga04 58.45(5) 13_455 1_445 ?
Ga03 Er01 Ga04 58.45(5) 1_545 1_445 ?
Ga03 Er01 Ga04 119.18(5) . 1_445 ?
Ga03 Er01 Ga04 119.18(5) 13 1_445 ?
Ga05 Er01 Ga04 121.39(5) 5_656 1_445 ?
Ga05 Er01 Ga04 121.39(5) . 1_445 ?
Ga05 Er01 Ga04 60.98(5) 5_556 1_445 ?
Ga05 Er01 Ga04 60.98(5) 1_545 1_445 ?
Ga03 Er01 Ga04 119.18(5) 13_455 . ?
Ga03 Er01 Ga04 119.18(5) 1_545 . ?
Ga03 Er01 Ga04 58.45(5) . . ?
Ga03 Er01 Ga04 58.45(5) 13 . ?
Ga05 Er01 Ga04 60.98(5) 5_656 . ?
Ga05 Er01 Ga04 60.98(5) . . ?
Ga05 Er01 Ga04 121.39(5) 5_556 . ?
Ga05 Er01 Ga04 121.39(5) 1_545 . ?
Ga04 Er01 Ga04 177.07(12) 1_445 . ?
Ga03 Er01 Ga04 58.45(5) 13_455 1_455 ?
Ga03 Er01 Ga04 119.18(5) 1_545 1_455 ?
Ga03 Er01 Ga04 58.45(5) . 1_455 ?
Ga03 Er01 Ga04 119.18(5) 13 1_455 ?
Ga05 Er01 Ga04 121.39(5) 5_656 1_455 ?
Ga05 Er01 Ga04 60.98(5) . 1_455 ?
Ga05 Er01 Ga04 60.98(5) 5_556 1_455 ?
Ga05 Er01 Ga04 121.39(5) 1_545 1_455 ?
Ga04 Er01 Ga04 89.963(3) 1_445 1_455 ?
Ga04 Er01 Ga04 89.963(3) . 1_455 ?
Ga03 Er01 Ga04 119.18(5) 13_455 1_545 ?
Ga03 Er01 Ga04 58.45(5) 1_545 1_545 ?
Ga03 Er01 Ga04 119.18(5) . 1_545 ?
Ga03 Er01 Ga04 58.45(5) 13 1_545 ?
Ga05 Er01 Ga04 60.98(5) 5_656 1_545 ?
Ga05 Er01 Ga04 121.39(5) . 1_545 ?
Ga05 Er01 Ga04 121.39(5) 5_556 1_545 ?
Ga05 Er01 Ga04 60.98(5) 1_545 1_545 ?
Ga04 Er01 Ga04 89.963(3) 1_445 1_545 ?
Ga04 Er01 Ga04 89.963(3) . 1_545 ?
Ga04 Er01 Ga04 177.07(12) 1_455 1_545 ?
Ga03 Ni02 Ga03 180.00(9) 13 5 ?
Ga03 Ni02 Ga03 106.04(4) 13 9 ?
Ga03 Ni02 Ga03 73.96(4) 5 9 ?
Ga03 Ni02 Ga03 73.96(4) 13 . ?
Ga03 Ni02 Ga03 106.04(4) 5 . ?
Ga03 Ni02 Ga03 180.00(9) 9 . ?
Ga03 Ni02 Ga03 116.57(9) 13 13_455 ?
Ga03 Ni02 Ga03 63.43(9) 5 13_455 ?
Ga03 Ni02 Ga03 106.04(4) 9 13_455 ?
Ga03 Ni02 Ga03 73.96(4) . 13_455 ?
Ga03 Ni02 Ga03 63.43(9) 13 5_655 ?
Ga03 Ni02 Ga03 116.57(9) 5 5_655 ?
Ga03 Ni02 Ga03 73.96(4) 9 5_655 ?
Ga03 Ni02 Ga03 106.04(4) . 5_655 ?
Ga03 Ni02 Ga03 180.00(9) 13_455 5_655 ?
Ga03 Ni02 Ga03 106.04(4) 13 9_565 ?
Ga03 Ni02 Ga03 73.96(4) 5 9_565 ?
Ga03 Ni02 Ga03 116.57(9) 9 9_565 ?
Ga03 Ni02 Ga03 63.43(9) . 9_565 ?
Ga03 Ni02 Ga03 106.04(4) 13_455 9_565 ?
Ga03 Ni02 Ga03 73.96(4) 5_655 9_565 ?
Ga03 Ni02 Ga03 73.96(4) 13 1_545 ?
Ga03 Ni02 Ga03 106.04(4) 5 1_545 ?
Ga03 Ni02 Ga03 63.43(9) 9 1_545 ?
Ga03 Ni02 Ga03 116.57(9) . 1_545 ?
Ga03 Ni02 Ga03 73.96(4) 13_455 1_545 ?
Ga03 Ni02 Ga03 106.04(4) 5_655 1_545 ?
Ga03 Ni02 Ga03 180.00(9) 9_565 1_545 ?
Ga03 Ni02 Er01 58.29(5) 13 . ?
Ga03 Ni02 Er01 121.71(5) 5 . ?
Ga03 Ni02 Er01 121.71(5) 9 . ?
Ga03 Ni02 Er01 58.29(5) . . ?
Ga03 Ni02 Er01 58.29(5) 13_455 . ?
Ga03 Ni02 Er01 121.71(5) 5_655 . ?
Ga03 Ni02 Er01 121.71(5) 9_565 . ?
Ga03 Ni02 Er01 58.29(5) 1_545 . ?
Ga03 Ni02 Er01 121.71(5) 13 9 ?
Ga03 Ni02 Er01 58.29(5) 5 9 ?
Ga03 Ni02 Er01 58.29(5) 9 9 ?
Ga03 Ni02 Er01 121.71(5) . 9 ?
Ga03 Ni02 Er01 121.71(5) 13_455 9 ?
Ga03 Ni02 Er01 58.29(5) 5_655 9 ?
Ga03 Ni02 Er01 58.29(5) 9_565 9 ?
Ga03 Ni02 Er01 121.71(5) 1_545 9 ?
Er01 Ni02 Er01 180.0 . 9 ?
Ni02 Ga03 Ni02 116.57(9) . 1_565 ?
Ni02 Ga03 Ga03 58.29(5) . 9_565 ?
Ni02 Ga03 Ga03 58.29(5) 1_565 9_565 ?
Ni02 Ga03 Ga04 111.13(3) . . ?
Ni02 Ga03 Ga04 111.13(3) 1_565 . ?
Ga03 Ga03 Ga04 133.29(5) 9_565 . ?
Ni02 Ga03 Ga04 111.13(3) . 1_455 ?
Ni02 Ga03 Ga04 111.13(3) 1_565 1_455 ?
Ga03 Ga03 Ga04 133.29(5) 9_565 1_455 ?
Ga04 Ga03 Ga04 93.43(10) . 1_455 ?
Ni02 Ga03 Er01 167.35(8) . 1_565 ?
Ni02 Ga03 Er01 76.08(2) 1_565 1_565 ?
Ga03 Ga03 Er01 134.36(3) 9_565 1_565 ?
Ga04 Ga03 Er01 61.35(4) . 1_565 ?
Ga04 Ga03 Er01 61.35(4) 1_455 1_565 ?
Ni02 Ga03 Er01 76.08(2) . . ?
Ni02 Ga03 Er01 167.35(8) 1_565 . ?
Ga03 Ga03 Er01 134.36(3) 9_565 . ?
Ga04 Ga03 Er01 61.35(4) . . ?
Ga04 Ga03 Er01 61.35(4) 1_455 . ?
Er01 Ga03 Er01 91.27(6) 1_565 . ?
Ni02 Ga03 Ga03 53.02(2) . 13_455 ?
Ni02 Ga03 Ga03 126.98(2) 1_565 13_455 ?
Ga03 Ga03 Ga03 90.0 9_565 13_455 ?
Ga04 Ga03 Ga03 120.98(3) . 13_455 ?
Ga04 Ga03 Ga03 59.02(3) 1_455 13_455 ?
Er01 Ga03 Ga03 120.366(18) 1_565 13_455 ?
Er01 Ga03 Ga03 59.634(18) . 13_455 ?
```

```
Ni02 Ga03 Ga03 126.98(2) . 13_565 ?
Ni02 Ga03 Ga03 53.02(2) 1_565 13_565 ?
Ga03 Ga03 Ga03 90.0 9_565 13_565 ?
Ga04 Ga03 Ga03 59.02(3) . 13_565 ?
Ga04 Ga03 Ga03 120.98(3) 1_455 13_565 ?
Er01 Ga03 Ga03 59.634(18) 1_565 13_565 ?
Er01 Ga03 Ga03 120.366(18) . 13_565 ?
Ga03 Ga03 Ga03 180.0 13_455 13_565 ?
Ni02 Ga03 Ga03 53.02(2) . 13 ?
Ni02 Ga03 Ga03 126.98(2) 1_565 13 ?
Ga03 Ga03 Ga03 90.0 9_565 13 ?
Ga04 Ga03 Ga03 59.02(3) . 13 ?
Ga04 Ga03 Ga03 120.98(3) 1_455 13 ?
Er01 Ga03 Ga03 120.366(18) 1_565 13 ?
Er01 Ga03 Ga03 59.634(18) . 13 ?
Ga03 Ga03 Ga03 90.0 13_455 13 ?
Ga03 Ga03 Ga03 90.0 13_565 13 ?
Ni02 Ga03 Ga03 126.98(2) . 13_465 ?
Ni02 Ga03 Ga03 53.02(2) 1_565 13_465 ?
Ga03 Ga03 Ga03 90.0 9_565 13_465 ?
Ga04 Ga03 Ga03 120.98(3) . 13_465 ?
Ga04 Ga03 Ga03 59.02(3) 1_455 13_465 ?
Er01 Ga03 Ga03 59.634(18) 1_565 13_465 ?
Er01 Ga03 Ga03 120.366(18) . 13_465 ?
Ga03 Ga03 Ga03 90.0 13_455 13_465 ?
Ga03 Ga03 Ga03 90.0 13_565 13_465 ?
Ga03 Ga03 Ga03 180.0 13 13_465 ?
Er01 Ga05 Er01 180.0 9_566 . ?
Er01 Ga05 Er01 89.27(3) 9_566 1_565 ?
Er01 Ga05 Er01 90.73(3) . 1_565 ?
Er01 Ga05 Er01 90.73(3) 9_566 9_556 ?
Er01 Ga05 Er01 89.27(3) . 9_556 ?
Er01 Ga05 Er01 180.0 1_565 9_556 ?
Er01 Ga05 Ga05 59.791(9) 9_566 5_666 ?
Er01 Ga05 Ga05 120.209(9) . 5_666 ?
Er01 Ga05 Ga05 59.791(9) 1_565 5_666 ?
Er01 Ga05 Ga05 120.209(9) 9_556 5_666 ?
Er01 Ga05 Ga05 120.209(9) 9_566 5_556 ?
Er01 Ga05 Ga05 59.791(9) . 5_556 ?
Er01 Ga05 Ga05 120.209(9) 1_565 5_556 ?
Er01 Ga05 Ga05 59.791(9) 9_556 5_556 ?
Ga05 Ga05 Ga05 180.0 5_666 5_556 ?
Er01 Ga05 Ga05 120.209(9) 9_566 5_656 ?
Er01 Ga05 Ga05 59.791(9) . 5_656 ?
Er01 Ga05 Ga05 120.209(9) 1_565 5_656 ?
Er01 Ga05 Ga05 59.791(9) 9_556 5_656 ?
Ga05 Ga05 Ga05 90.0 5_666 5_656 ?
Ga05 Ga05 Ga05 90.0 5_556 5_656 ?
Er01 Ga05 Ga05 59.791(9) 9_566 5_566 ?
Er01 Ga05 Ga05 120.209(9) . 5_566 ?
Er01 Ga05 Ga05 59.791(9) 1_565 5_566 ?
Er01 Ga05 Ga05 120.209(9) 9_556 5_566 ?
Ga05 Ga05 Ga05 90.0 5_666 5_566 ?
Ga05 Ga05 Ga05 90.0 5_556 5_566 ?
Ga05 Ga05 Ga05 180.0 5_656 5_566 ?
Ga03 Ga04 Ga03 61.96(6) . 13 ?
Ga03 Ga04 Ga03 61.96(6) . 13_565 ?
Ga03 Ga04 Ga03 93.43(10) 13 13_565 ?
Ga03 Ga04 Ga03 93.43(10) . 1_655 ?
Ga03 Ga04 Ga03 61.96(6) 13 1_655 ?
Ga03 Ga04 Ga03 61.96(6) 13_565 1_655 ?
Ga03 Ga04 Er01 122.14(7) . 1_665 ?
Ga03 Ga04 Er01 122.14(7) 13 1_665 ?
Ga03 Ga04 Er01 60.19(3) 13_565 1_665 ?
Ga03 Ga04 Er01 60.19(3) 1_655 1_665 ?
Ga03 Ga04 Er01 60.19(3) . . ?
Ga03 Ga04 Er01 60.19(3) 13 . ?
```

```
Ga03 Ga04 Er01 122.14(7) 13_565 . ?
Ga03 Ga04 Er01 122.14(7) 1_655 . ?
Er01 Ga04 Er01 177.07(12) 1_665 . ?
Ga03 Ga04 Er01 122.14(7) . 1_655 ?
Ga03 Ga04 Er01 60.19(3) 13 1_655 ?
Ga03 Ga04 Er01 122.14(7) 13_565 1_655 ?
Ga03 Ga04 Er01 60.19(3) 1_655 1_655 ?
Er01 Ga04 Er01 89.963(3) 1_665 1_655 ?
Er01 Ga04 Er01 89.963(3) . 1_655 ?
Ga03 Ga04 Er01 60.19(3) . 1_565 ?
Ga03 Ga04 Er01 122.14(7) 13 1_565 ?
Ga03 Ga04 Er01 60.19(3) 13_565 1_565 ?
Ga03 Ga04 Er01 122.14(7) 1_655 1_565 ?
Er01 Ga04 Er01 89.963(3) 1_665 1_565 ?
Er01 Ga04 Er01 89.963(3) . 1_565 ?
Er01 Ga04 Er01 177.07(12) 1_655 1_565 ?

_diffrn_measured_fraction_theta_max    0.995
_diffrn_reflns_theta_full              30.01
_diffrn_measured_fraction_theta_full   0.995
_refine_diff_density_max    4.866
_refine_diff_density_min   -8.626
_refine_diff_density_rms    0.813
```

A2.4 $HoNi_3Ga_9$

```
data_honi3ga9

_audit_creation_method            SHELXL-97
_chemical_name_systematic
;
 ?
;
_chemical_name_common             ?
_chemical_melting_point           ?
_chemical_formula_moiety          ?
_chemical_formula_sum
 'Ga9 Ho Ni3'
_chemical_formula_weight          968.54

loop_
 _atom_type_symbol
 _atom_type_description
 _atom_type_scat_dispersion_real
 _atom_type_scat_dispersion_imag
 _atom_type_scat_source
 'Ni'  'Ni'   0.3393   1.1124
 'International Tables Vol C Tables 4.2.6.8
and 6.1.1.4'
 'Ga'  'Ga'   0.2307   1.6083
 'International Tables Vol C Tables 4.2.6.8
and 6.1.1.4'
 'Ho'  'Ho'  -0.2175   4.6783
 'International Tables Vol C Tables 4.2.6.8
and 6.1.1.4'

_symmetry_cell_setting            ?
_symmetry_space_group_name_H-M    ?

loop_
 _symmetry_equiv_pos_as_xyz
 'x, y, z'
 '-y, x-y, z'
 '-x+y, -x, z'
 'x-y, -y, -z'
 '-x, -x+y, -z'
 'y, x, -z'
 'x+2/3, y+1/3, z+1/3'
 '-y+2/3, x-y+1/3, z+1/3'
 '-x+y+2/3, -x+1/3, z+1/3'
 'x-y+2/3, -y+1/3, -z+1/3'
 '-x+2/3, -x+y+1/3, -z+1/3'
 'y+2/3, x+1/3, -z+1/3'
 'x+1/3, y+2/3, z+2/3'
 '-y+1/3, x-y+2/3, z+2/3'
 '-x+y+1/3, -x+2/3, z+2/3'
 'x-y+1/3, -y+2/3, -z+2/3'
 '-x+1/3, -x+y+2/3, -z+2/3'
 'y+1/3, x+2/3, -z+2/3'

_cell_length_a                    7.2368(3)
_cell_length_b                    7.2368(3)
_cell_length_c
27.3841(19)
_cell_angle_alpha                 90.00
_cell_angle_beta                  90.00
_cell_angle_gamma                 120.00
_cell_volume
1242.00(11)
_cell_formula_units_Z             6
_cell_measurement_temperature     293(2)
_cell_measurement_reflns_used     ?
_cell_measurement_theta_min       ?
_cell_measurement_theta_max       ?

_exptl_crystal_description        ?
_exptl_crystal_colour             ?
_exptl_crystal_size_max           ?
_exptl_crystal_size_mid           ?
_exptl_crystal_size_min           ?
_exptl_crystal_density_meas       ?
_exptl_crystal_density_diffrn     7.770
_exptl_crystal_density_method            'not
measured'
_exptl_crystal_F_000              2580
_exptl_absorpt_coefficient_mu     44.739
_exptl_absorpt_correction_type    ?
_exptl_absorpt_correction_T_min   ?
_exptl_absorpt_correction_T_max   ?
_exptl_absorpt_process_details    ?

_exptl_special_details
;
 ?
;

_diffrn_ambient_temperature       293(2)
_diffrn_radiation_wavelength      0.71073
_diffrn_radiation_type            MoK\a
_diffrn_radiation_source               'fine-
focus sealed tube'
_diffrn_radiation_monochromator   graphite
_diffrn_measurement_device_type   ?
_diffrn_measurement_method        ?
_diffrn_detector_area_resol_mean  ?
_diffrn_standards_number          ?
_diffrn_standards_interval_count  ?
_diffrn_standards_interval_time   ?
_diffrn_standards_decay_%         ?
_diffrn_reflns_number             1171
_diffrn_reflns_av_R_equivalents   0.0578
_diffrn_reflns_av_sigmaI/netI     0.0675
_diffrn_reflns_limit_h_min        -10
_diffrn_reflns_limit_h_max        10
_diffrn_reflns_limit_k_min        -8
_diffrn_reflns_limit_k_max        8
_diffrn_reflns_limit_l_min        -38
_diffrn_reflns_limit_l_max        23
_diffrn_reflns_theta_min          2.23
_diffrn_reflns_theta_max          29.93
_reflns_number_total              797
_reflns_number_gt                 732
_reflns_threshold_expression      >2sigma(I)

_computing_data_collection        ?
_computing_cell_refinement        ?
_computing_data_reduction         ?
_computing_structure_solution     ?
_computing_structure_refinement    'SHELXL-97
(Sheldrick, 1997)'
_computing_molecular_graphics     ?
_computing_publication_material   ?

_refine_special_details
;
 Refinement of F^2^ against ALL reflections.
The weighted R-factor wR and
 goodness  of  fit  S  are  based  on  F^2^,
conventional R-factors R are based
 on F, with F set to zero for negative F^2^.
The threshold expression of
 F^2^  >  2sigma(F^2^)  is  used  only  for
calculating R-factors(gt) etc. and is
```

```
 not relevant to the choice of reflections
for refinement.  R-factors based
 on F^2^ are statistically about twice as
large as those based on F, and R-
 factors based on ALL data will be even
larger.
;

_refine_ls_structure_factor_coef  Fsqd
_refine_ls_matrix_type            full
_refine_ls_weighting_scheme       calc
_refine_ls_weighting_details
 'calc
w=1/[\s^2^(Fo^2^)+(0.1000P)^2^+0.0000P]
where P=(Fo^2^+2Fc^2^)/3'
_atom_sites_solution_primary      direct
_atom_sites_solution_secondary    difmap
_atom_sites_solution_hydrogens    geom
_refine_ls_hydrogen_treatment     mixed
_refine_ls_extinction_method      SHELXL
_refine_ls_extinction_coef        0.0046(4)
_refine_ls_extinction_expression
 'Fc^*^=kFc[1+0.001xFc^2^\l^3^/sin(2\q)]^-
1/4^'
_refine_ls_abs_structure_details
 'Flack H D (1983), Acta Cryst. A39, 876-
881'
_refine_ls_abs_structure_Flack    1.07(14)
_refine_ls_number_reflns          797
_refine_ls_number_parameters      42
_refine_ls_number_restraints      0
_refine_ls_R_factor_all           0.0644
_refine_ls_R_factor_gt            0.0589
_refine_ls_wR_factor_ref          0.1578
_refine_ls_wR_factor_gt           0.1535
_refine_ls_goodness_of_fit_ref    1.190
_refine_ls_restrained_S_all       1.190
_refine_ls_shift/su_max           0.016
_refine_ls_shift/su_mean          0.004

loop_
 _atom_site_label
 _atom_site_type_symbol
 _atom_site_fract_x
 _atom_site_fract_y
 _atom_site_fract_z
 _atom_site_U_iso_or_equiv
 _atom_site_adp_type
 _atom_site_occupancy
 _atom_site_symmetry_multiplicity
 _atom_site_calc_flag
 _atom_site_refinement_flags
 _atom_site_disorder_assembly
 _atom_site_disorder_group
Ga1  Ga  0.0000  0.0000  0.38466(13)  0.0082(6)
Uani 1 3 d S . .
Ga2  Ga  0.0000  0.0000  0.28375(13)  0.0074(6)
Uani 1 3 d S . .
Ga3  Ga  0.0000  0.0000  0.05034(13)  0.0072(6)
Uani 1 3 d S . .
Ga4  Ga  0.3333(3)  0.0000  0.0000  0.0096(6)
Uani 1 2 d S . .
Ga5  Ga  0.2098(3)  0.0000  0.5000  0.0084(5)
Uani 1 2 d S . .
Ho1  Ho  0.0000  0.0000  0.16698(3)  0.0065(4)
Uani 1 3 d S . .
Ni1   Ni   0.3399(3)   0.0000(3)   0.41834(11)
0.0070(6) Uani 1 1 d . . .
Ga6   Ga   0.3298(3)   0.3298(3)   0.43381(14)
0.0078(5) Uani 1 1 d . . .

loop_
 _atom_site_aniso_label
 _atom_site_aniso_U_11
 _atom_site_aniso_U_22
 _atom_site_aniso_U_33
 _atom_site_aniso_U_23
 _atom_site_aniso_U_13
 _atom_site_aniso_U_12
Ga1  0.0066(8)  0.0066(8)  0.0115(14)  0.000
0.000 0.0033(4)
Ga2  0.0062(8)  0.0062(8)  0.0098(14)  0.000
0.000 0.0031(4)
Ga3  0.0059(8)  0.0059(8)  0.0099(14)  0.000
0.000 0.0029(4)
Ga4   0.0114(9)   0.0116(11)   0.0059(16)   -
0.0001(7) 0.0000(3) 0.0058(5)
Ga5    0.0081(8)    0.0080(10)    0.0092(10)
0.0002(9) 0.0001(5) 0.0040(5)
Ho1  0.0043(4)  0.0043(4)  0.0108(6)  0.000
0.000 0.0022(2)
Ni1    0.0051(10)    0.0065(11)    0.0100(14)
0.0007(6) 0.0008(6) 0.0035(7)
Ga6 0.0051(9) 0.0048(9) 0.0139(10) 0.0007(6)
0.0001(6) 0.0027(7)

_geom_special_details
;
 All esds (except the esd in the dihedral
angle between two l.s. planes)
 are estimated using the full covariance
matrix.  The cell esds are taken
 into account individually in the estimation
of esds in distances, angles
 and torsion angles; correlations between
esds in cell parameters are only
 used when they are defined by crystal
symmetry.  An approximate (isotropic)
 treatment of cell esds is used for
estimating esds involving l.s. planes.
;

loop_
 _geom_bond_atom_site_label_1
 _geom_bond_atom_site_label_2
 _geom_bond_distance
 _geom_bond_site_symmetry_2
 _geom_bond_publ_flag
Ga1 Ni1 2.627(2) . ?
Ga1 Ni1 2.627(2) 3 ?
Ga1 Ni1 2.627(2) 2 ?
Ga1 Ga6 2.740(3) . ?
Ga1 Ga6 2.740(3) 2 ?
Ga1 Ga6 2.740(3) 3 ?
Ga1 Ga2 2.763(6) . ?
Ga1 Ga4 2.792(2) 9 ?
Ga1 Ga4 2.792(2) 8_445 ?
Ga1 Ga4 2.792(2) 7_455 ?
Ga2 Ni1 2.579(3) 17 ?
Ga2 Ni1 2.579(3) 16_445 ?
Ga2 Ni1 2.579(3) 18_545 ?
Ga2 Ga4 2.7684(19) 9 ?
Ga2 Ga4 2.7684(19) 8_445 ?
Ga2 Ga4 2.7684(19) 7_455 ?
Ga2 Ga6 2.797(3) 18_445 ?
Ga2 Ga6 2.797(3) 16 ?
Ga2 Ga6 2.797(3) 17_545 ?
Ga2 Ho1 3.198(4) . ?
Ga3 Ni1 2.570(2) 15_554 ?
Ga3 Ni1 2.570(3) 13_444 ?
Ga3 Ni1 2.570(2) 14_544 ?
Ga3 Ga3 2.757(7) 4 ?
Ga3 Ga4 2.778(3) 3 ?
Ga3 Ga4 2.778(3) . ?
```

```
Ga3 Ga4 2.778(3) 2 ?
Ga3 Ga6 2.787(3) 13_444 ?
Ga3 Ga6 2.787(3) 15_554 ?
Ga3 Ga6 2.787(3) 14_544 ?
Ga3 Ho1 3.194(4) . ?
Ga4 Ni1 2.328(3) 14_544 ?
Ga4 Ni1 2.328(3) 11 ?
Ga4 Ga2 2.7684(19) 10 ?
Ga4 Ga2 2.7684(19) 13_544 ?
Ga4 Ga3 2.778(3) 4 ?
Ga4 Ga1 2.792(2) 10 ?
Ga4 Ga1 2.792(2) 13_544 ?
Ga5 Ni1 2.426(3) 4_556 ?
Ga5 Ni1 2.426(3) . ?
Ga5 Ga5 2.630(4) 3 ?
Ga5 Ga5 2.630(4) 2 ?
Ga5 Ga6 2.768(3) 4_556 ?
Ga5 Ga6 2.768(3) . ?
Ga5 Ga6 2.768(3) 6_556 ?
Ga5 Ga6 2.768(3) 3 ?
Ga5 Ho1 2.9622(15) 7 ?
Ga5 Ho1 2.9622(15) 16_545 ?
Ho1 Ga5 2.9621(15) 15_554 ?
Ho1 Ga5 2.9622(15) 13_444 ?
Ho1 Ga5 2.9622(15) 14_544 ?
Ho1 Ga6 3.023(3) 18_445 ?
Ho1 Ga6 3.023(3) 16 ?
Ho1 Ga6 3.023(3) 17_545 ?
Ho1 Ga6 3.033(3) 13_444 ?
Ho1 Ga6 3.033(3) 15_554 ?
Ho1 Ga6 3.033(3) 14_544 ?
Ho1 Ni1 3.266(3) 17 ?
Ni1 Ga4 2.328(3) 9 ?
Ni1 Ga6 2.428(2) 2_655 ?
Ni1 Ga6 2.460(2) . ?
Ni1 Ga6 2.461(2) 3 ?
Ni1 Ga3 2.570(3) 7 ?
Ni1 Ga2 2.579(3) 16_545 ?
Ni1 Ho1 3.267(3) 16_545 ?
Ni1 Ho1 3.278(3) 7 ?
Ga6 Ni1 2.428(2) 3_665 ?
Ga6 Ni1 2.461(2) 2 ?
Ga6 Ga5 2.768(3) 2 ?
Ga6 Ga3 2.787(3) 7 ?
Ga6 Ga2 2.797(3) 16 ?
Ga6 Ho1 3.023(3) 16 ?
Ga6 Ho1 3.033(3) 7 ?

loop_
 _geom_angle_atom_site_label_1
 _geom_angle_atom_site_label_2
 _geom_angle_atom_site_label_3
 _geom_angle
 _geom_angle_site_symmetry_1
 _geom_angle_site_symmetry_3
 _geom_angle_publ_flag
Ni1 Ga1 Ni1 108.37(10) . 3 ?
Ni1 Ga1 Ni1 108.37(10) . 2 ?
Ni1 Ga1 Ni1 108.37(10) 3 2 ?
Ni1 Ga1 Ga6 54.53(6) . . ?
Ni1 Ga1 Ga6 130.03(16) 3 . ?
Ni1 Ga1 Ga6 54.54(6) 2 . ?
Ni1 Ga1 Ga6 130.03(16) . 2 ?
Ni1 Ga1 Ga6 54.54(6) 3 2 ?
Ni1 Ga1 Ga6 54.53(6) 2 2 ?
Ga6 Ga1 Ga6 97.94(10) . 2 ?
Ni1 Ga1 Ga6 54.54(6) . 3 ?
Ni1 Ga1 Ga6 54.53(6) 3 3 ?
Ni1 Ga1 Ga6 130.03(16) 2 3 ?
Ga6 Ga1 Ga6 97.94(10) . 3 ?
Ga6 Ga1 Ga6 97.94(10) 2 3 ?
Ni1 Ga1 Ga2 110.55(10) . . ?
Ni1 Ga1 Ga2 110.55(10) 3 . ?
Ni1 Ga1 Ga2 110.55(10) 2 . ?
Ga6 Ga1 Ga2 119.42(8) . . ?
Ga6 Ga1 Ga2 119.42(8) 2 . ?
Ga6 Ga1 Ga2 119.42(8) 3 . ?
Ni1 Ga1 Ga4 50.78(7) . 9 ?
Ni1 Ga1 Ga4 125.54(6) 3 9 ?
Ni1 Ga1 Ga4 125.54(6) 2 9 ?
Ga6 Ga1 Ga4 82.58(6) . 9 ?
Ga6 Ga1 Ga4 179.19(13) 2 9 ?
Ga6 Ga1 Ga4 82.59(6) 3 9 ?
Ga2 Ga1 Ga4 59.77(6) . 9 ?
Ni1 Ga1 Ga4 125.54(6) . 8_445 ?
Ni1 Ga1 Ga4 50.78(7) 3 8_445 ?
Ni1 Ga1 Ga4 125.54(6) 2 8_445 ?
Ga6 Ga1 Ga4 179.19(13) . 8_445 ?
Ga6 Ga1 Ga4 82.59(6) 2 8_445 ?
Ga6 Ga1 Ga4 82.58(6) 3 8_445 ?
Ga2 Ga1 Ga4 59.78(6) . 8_445 ?
Ga4 Ga1 Ga4 96.89(8) 9 8_445 ?
Ni1 Ga1 Ga4 125.54(6) . 7_455 ?
Ni1 Ga1 Ga4 125.54(6) 3 7_455 ?
Ni1 Ga1 Ga4 50.78(7) 2 7_455 ?
Ga6 Ga1 Ga4 82.59(6) . 7_455 ?
Ga6 Ga1 Ga4 82.58(6) 2 7_455 ?
Ga6 Ga1 Ga4 179.19(13) 3 7_455 ?
Ga2 Ga1 Ga4 59.78(6) . 7_455 ?
Ga4 Ga1 Ga4 96.89(8) 9 7_455 ?
Ga4 Ga1 Ga4 96.89(8) 8_445 7_455 ?
Ni1 Ga2 Ni1 106.72(10) 17 16_445 ?
Ni1 Ga2 Ni1 106.72(10) 17 18_545 ?
Ni1 Ga2 Ni1 106.72(10) 16_445 18_545 ?
Ni1 Ga2 Ga1 112.10(10) 17 . ?
Ni1 Ga2 Ga1 112.10(10) 16_445 . ?
Ni1 Ga2 Ga1 112.10(10) 18_545 . ?
Ni1 Ga2 Ga4 126.88(6) 17 9 ?
Ni1 Ga2 Ga4 125.19(6) 16_445 9 ?
Ni1 Ga2 Ga4 51.48(7) 18_545 9 ?
Ga1 Ga2 Ga4 60.63(6) . 9 ?
Ni1 Ga2 Ga4 125.19(6) 17 8_445 ?
Ni1 Ga2 Ga4 51.48(7) 16_445 8_445 ?
Ni1 Ga2 Ga4 126.88(6) 18_545 8_445 ?
Ga1 Ga2 Ga4 60.63(6) . 8_445 ?
Ga4 Ga2 Ga4 98.00(8) 9 8_445 ?
Ni1 Ga2 Ga4 51.48(7) 17 7_455 ?
Ni1 Ga2 Ga4 126.88(6) 16_445 7_455 ?
Ni1 Ga2 Ga4 125.19(6) 18_545 7_455 ?
Ga1 Ga2 Ga4 60.63(6) . 7_455 ?
Ga4 Ga2 Ga4 98.00(8) 9 7_455 ?
Ga4 Ga2 Ga4 98.00(8) 8_445 7_455 ?
Ni1 Ga2 Ga6 53.51(6) 17 18_445 ?
Ni1 Ga2 Ga6 54.30(6) 16_445 18_445 ?
Ni1 Ga2 Ga6 128.01(15) 18_545 18_445 ?
Ga1 Ga2 Ga6 119.88(8) . 18_445 ?
Ga4 Ga2 Ga6 179.32(10) 9 18_445 ?
Ga4 Ga2 Ga6 81.99(6) 8_445 18_445 ?
Ga4 Ga2 Ga6 82.68(6) 7_455 18_445 ?
Ni1 Ga2 Ga6 54.30(6) 17 16 ?
Ni1 Ga2 Ga6 128.01(15) 16_445 16 ?
Ni1 Ga2 Ga6 53.51(6) 18_545 16 ?
Ga1 Ga2 Ga6 119.88(8) . 16 ?
Ga4 Ga2 Ga6 82.68(6) 9 16 ?
Ga4 Ga2 Ga6 179.32(10) 8_445 16 ?
Ga4 Ga2 Ga6 81.99(6) 7_455 16 ?
Ga6 Ga2 Ga6 97.33(11) 18_445 16 ?
Ni1 Ga2 Ga6 128.01(15) 17 17_545 ?
Ni1 Ga2 Ga6 53.51(6) 16_445 17_545 ?
Ni1 Ga2 Ga6 54.30(6) 18_545 17_545 ?
Ga1 Ga2 Ga6 119.88(8) . 17_545 ?
Ga4 Ga2 Ga6 81.99(6) 9 17_545 ?
Ga4 Ga2 Ga6 82.68(6) 8_445 17_545 ?
Ga4 Ga2 Ga6 179.32(11) 7_455 17_545 ?
```

```
Ga6 Ga2 Ga6 97.33(11) 18_445 17_545 ?
Ga6 Ga2 Ga6 97.33(11) 16 17_545 ?
Ni1 Ga2 Ho1 67.90(10) 17 . ?
Ni1 Ga2 Ho1 67.90(10) 16_445 . ?
Ni1 Ga2 Ho1 67.90(10) 18_545 . ?
Ga1 Ga2 Ho1 180.0 . . ?
Ga4 Ga2 Ho1 119.37(6) 9 . ?
Ga4 Ga2 Ho1 119.37(6) 8_445 . ?
Ga4 Ga2 Ho1 119.37(6) 7_455 . ?
Ga6 Ga2 Ho1 60.12(8) 18_445 . ?
Ga6 Ga2 Ho1 60.12(8) 16 . ?
Ga6 Ga2 Ho1 60.12(8) 17_545 . ?
Ni1 Ga3 Ni1 107.18(10) 15_554 13_444 ?
Ni1 Ga3 Ni1 107.18(10) 15_554 14_544 ?
Ni1 Ga3 Ni1 107.18(10) 13_444 14_544 ?
Ni1 Ga3 Ga3 111.67(10) 15_554 4 ?
Ni1 Ga3 Ga3 111.67(10) 13_444 4 ?
Ni1 Ga3 Ga3 111.67(10) 14_544 4 ?
Ni1 Ga3 Ga4 125.08(5) 15_554 3 ?
Ni1 Ga3 Ga4 51.43(7) 13_444 3 ?
Ni1 Ga3 Ga4 126.77(5) 14_544 3 ?
Ga3 Ga3 Ga4 60.25(6) 4 3 ?
Ni1 Ga3 Ga4 126.77(5) 15_554 . ?
Ni1 Ga3 Ga4 125.07(5) 13_444 . ?
Ni1 Ga3 Ga4 51.43(7) 14_544 . ?
Ga3 Ga3 Ga4 60.25(6) 4 . ?
Ga4 Ga3 Ga4 97.50(8) 3 . ?
Ni1 Ga3 Ga4 51.43(7) 15_554 2 ?
Ni1 Ga3 Ga4 126.77(5) 13_444 2 ?
Ni1 Ga3 Ga4 125.08(5) 14_544 2 ?
Ga3 Ga3 Ga4 60.25(6) 4 2 ?
Ga4 Ga3 Ga4 97.50(8) 3 2 ?
Ga4 Ga3 Ga4 97.50(8) . 2 ?
Ni1 Ga3 Ga6 53.71(6) 15_554 13_444 ?
Ni1 Ga3 Ga6 54.50(6) 13_444 13_444 ?
Ni1 Ga3 Ga6 128.82(15) 14_544 13_444 ?
Ga3 Ga3 Ga6 119.51(8) 4 13_444 ?
Ga4 Ga3 Ga6 81.99(5) 3 13_444 ?
Ga4 Ga3 Ga6 179.48(8) . 13_444 ?
Ga4 Ga3 Ga6 82.69(5) 2 13_444 ?
Ni1 Ga3 Ga6 54.50(6) 15_554 15_554 ?
Ni1 Ga3 Ga6 128.82(15) 13_444 15_554 ?
Ni1 Ga3 Ga6 53.71(6) 14_544 15_554 ?
Ga3 Ga3 Ga6 119.51(8) 4 15_554 ?
Ga4 Ga3 Ga6 179.48(8) 3 15_554 ?
Ga4 Ga3 Ga6 82.68(5) . 15_554 ?
Ga4 Ga3 Ga6 81.99(5) 2 15_554 ?
Ga6 Ga3 Ga6 97.82(10) 13_444 15_554 ?
Ni1 Ga3 Ga6 128.82(15) 15_554 14_544 ?
Ni1 Ga3 Ga6 53.71(6) 13_444 14_544 ?
Ni1 Ga3 Ga6 54.50(6) 14_544 14_544 ?
Ga3 Ga3 Ga6 119.51(8) 4 14_544 ?
Ga4 Ga3 Ga6 82.69(5) 3 14_544 ?
Ga4 Ga3 Ga6 81.99(5) . 14_544 ?
Ga4 Ga3 Ga6 179.48(8) 2 14_544 ?
Ga6 Ga3 Ga6 97.82(10) 13_444 14_544 ?
Ga6 Ga3 Ga6 97.82(10) 15_554 14_544 ?
Ni1 Ga3 Ho1 68.33(10) 15_554 . ?
Ni1 Ga3 Ho1 68.33(10) 13_444 . ?
Ni1 Ga3 Ho1 68.33(10) 14_544 . ?
Ga3 Ga3 Ho1 180.0 4 . ?
Ga4 Ga3 Ho1 119.75(6) 3 . ?
Ga4 Ga3 Ho1 119.75(6) . . ?
Ga4 Ga3 Ho1 119.75(6) 2 . ?
Ga6 Ga3 Ho1 60.49(8) 13_444 . ?
Ga6 Ga3 Ho1 60.49(8) 15_554 . ?
Ga6 Ga3 Ho1 60.49(8) 14_544 . ?
Ni1 Ga4 Ni1 178.85(13) 14_544 11 ?
Ni1 Ga4 Ga2 60.05(8) 14_544 10 ?
Ni1 Ga4 Ga2 120.53(9) 11 10 ?
Ni1 Ga4 Ga2 120.53(9) 14_544 13_544 ?
Ni1 Ga4 Ga2 60.05(8) 11 13_544 ?
Ga2 Ga4 Ga2 128.32(9) 10 13_544 ?
Ni1 Ga4 Ga3 119.17(10) 14_544 4 ?
Ni1 Ga4 Ga3 59.68(8) 11 4 ?
Ga2 Ga4 Ga3 128.45(5) 10 4 ?
Ga2 Ga4 Ga3 97.76(8) 13_544 4 ?
Ni1 Ga4 Ga3 59.68(8) 14_544 . ?
Ni1 Ga4 Ga3 119.17(10) 11 . ?
Ga2 Ga4 Ga3 97.76(8) 10 . ?
Ga2 Ga4 Ga3 128.45(5) 13_544 . ?
Ga3 Ga4 Ga3 59.50(13) 4 . ?
Ni1 Ga4 Ga1 119.64(8) 14_544 10 ?
Ni1 Ga4 Ga1 60.93(8) 11 10 ?
Ga2 Ga4 Ga1 59.60(12) 10 10 ?
Ga2 Ga4 Ga1 97.43(9) 13_544 10 ?
Ga3 Ga4 Ga1 97.20(8) 4 10 ?
Ga3 Ga4 Ga1 128.68(5) . 10 ?
Ni1 Ga4 Ga1 60.93(8) 14_544 13_544 ?
Ni1 Ga4 Ga1 119.64(8) 11 13_544 ?
Ga2 Ga4 Ga1 97.43(9) 10 13_544 ?
Ga2 Ga4 Ga1 59.60(12) 13_544 13_544 ?
Ga3 Ga4 Ga1 128.68(5) 4 13_544 ?
Ga3 Ga4 Ga1 97.20(8) . 13_544 ?
Ga1 Ga4 Ga1 128.79(8) 10 13_544 ?
Ni1 Ga5 Ni1 134.34(14) 4_556 . ?
Ni1 Ga5 Ga5 109.63(6) 4_556 3 ?
Ni1 Ga5 Ga5 109.64(6) . 3 ?
Ni1 Ga5 Ga5 109.64(6) 4_556 2 ?
Ni1 Ga5 Ga5 109.63(6) . 2 ?
Ga5 Ga5 Ga5 60.0 3 2 ?
Ni1 Ga5 Ga6 56.08(7) 4_556 4_556 ?
Ni1 Ga5 Ga6 130.48(8) . 4_556 ?
Ga5 Ga5 Ga6 61.64(6) 3 4_556 ?
Ga5 Ga5 Ga6 105.76(5) 2 4_556 ?
Ni1 Ga5 Ga6 130.48(8) 4_556 . ?
Ni1 Ga5 Ga6 56.08(7) . . ?
Ga5 Ga5 Ga6 105.76(5) 3 . ?
Ga5 Ga5 Ga6 61.64(6) 2 . ?
Ga6 Ga5 Ga6 166.51(11) 4_556 . ?
Ni1 Ga5 Ga6 56.09(7) 4_556 6_556 ?
Ni1 Ga5 Ga6 130.47(8) . 6_556 ?
Ga5 Ga5 Ga6 105.76(5) 3 6_556 ?
Ga5 Ga5 Ga6 61.64(6) 2 6_556 ?
Ga6 Ga5 Ga6 96.59(12) 4_556 6_556 ?
Ga6 Ga5 Ga6 81.81(12) . 6_556 ?
Ni1 Ga5 Ga6 130.47(8) 4_556 3 ?
Ni1 Ga5 Ga6 56.09(7) . 3 ?
Ga5 Ga5 Ga6 61.64(6) 3 3 ?
Ga5 Ga5 Ga6 105.76(5) 2 3 ?
Ga6 Ga5 Ga6 81.81(12) 4_556 3 ?
Ga6 Ga5 Ga6 96.59(12) . 3 ?
Ga6 Ga5 Ga6 166.51(11) 6_556 3 ?
Ni1 Ga5 Ho1 73.88(6) 4_556 7 ?
Ni1 Ga5 Ho1 74.19(7) . 7 ?
Ga5 Ga5 Ho1 165.15(3) 3 7 ?
Ga5 Ga5 Ho1 105.15(3) 2 7 ?
Ga6 Ga5 Ho1 127.44(7) 4_556 7 ?
Ga6 Ga5 Ho1 63.81(5) . 7 ?
Ga6 Ga5 Ho1 63.56(5) 6_556 7 ?
Ga6 Ga5 Ho1 127.71(7) 3 7 ?
Ni1 Ga5 Ho1 74.19(7) 4_556 16_545 ?
Ni1 Ga5 Ho1 73.88(6) . 16_545 ?
Ga5 Ga5 Ho1 105.15(3) 3 16_545 ?
Ga5 Ga5 Ho1 165.15(3) 2 16_545 ?
Ga6 Ga5 Ho1 63.81(4) 4_556 16_545 ?
Ga6 Ga5 Ho1 127.44(7) . 16_545 ?
Ga6 Ga5 Ho1 127.71(7) 6_556 16_545 ?
Ga6 Ga5 Ho1 63.56(5) 3 16_545 ?
Ho1 Ga5 Ho1 89.70(6) 7 16_545 ?
Ga5 Ho1 Ga5 120.0 15_554 13_444 ?
Ga5 Ho1 Ga5 120.0 15_554 14_544 ?
Ga5 Ho1 Ga5 120.0 13_444 14_544 ?
Ga5 Ho1 Ga6 78.65(4) 15_554 18_445 ?
```

```
Ga5 Ho1 Ga6 55.09(5) 13_444 18_445 ?
Ga5 Ho1 Ga6 140.74(6) 14_544 18_445 ?
Ga5 Ho1 Ga6 55.09(5) 15_554 16 ?
Ga5 Ho1 Ga6 140.74(6) 13_444 16 ?
Ga5 Ho1 Ga6 78.65(4) 14_544 16 ?
Ga6 Ho1 Ga6 88.03(9) 18_445 16 ?
Ga5 Ho1 Ga6 140.74(6) 15_554 17_545 ?
Ga5 Ho1 Ga6 78.65(4) 13_444 17_545 ?
Ga5 Ho1 Ga6 55.09(5) 14_544 17_545 ?
Ga6 Ho1 Ga6 88.03(9) 18_445 17_545 ?
Ga6 Ho1 Ga6 88.03(9) 16 17_545 ?
Ga5 Ho1 Ga6 78.49(4) 15_554 13_444 ?
Ga5 Ho1 Ga6 54.98(4) 13_444 13_444 ?
Ga5 Ho1 Ga6 140.19(6) 14_544 13_444 ?
Ga6 Ho1 Ga6 73.55(11) 18_445 13_444 ?
Ga6 Ho1 Ga6 132.78(5) 16 13_444 ?
Ga6 Ho1 Ga6 132.78(5) 17_545 13_444 ?
Ga5 Ho1 Ga6 54.98(4) 15_554 15_554 ?
Ga5 Ho1 Ga6 140.19(6) 13_444 15_554 ?
Ga5 Ho1 Ga6 78.49(4) 14_544 15_554 ?
Ga6 Ho1 Ga6 132.78(5) 18_445 15_554 ?
Ga6 Ho1 Ga6 73.55(11) 16 15_554 ?
Ga6 Ho1 Ga6 132.78(5) 17_545 15_554 ?
Ga6 Ho1 Ga6 87.66(9) 13_444 15_554 ?
Ga5 Ho1 Ga6 140.19(6) 15_554 14_544 ?
Ga5 Ho1 Ga6 78.49(4) 13_444 14_544 ?
Ga5 Ho1 Ga6 54.98(4) 14_544 14_544 ?
Ga6 Ho1 Ga6 132.78(5) 18_445 14_544 ?
Ga6 Ho1 Ga6 132.78(5) 16 14_544 ?
Ga6 Ho1 Ga6 73.55(11) 17_545 14_544 ?
Ga6 Ho1 Ga6 87.66(9) 13_444 14_544 ?
Ga6 Ho1 Ga6 87.66(9) 15_554 14_544 ?
Ga5 Ho1 Ga3 89.833(15) 15_554 . ?
Ga5 Ho1 Ga3 89.833(15) 13_444 . ?
Ga5 Ho1 Ga3 89.833(15) 14_544 . ?
Ga6 Ho1 Ga3 126.64(6) 18_445 . ?
Ga6 Ho1 Ga3 126.64(6) 16 . ?
Ga6 Ho1 Ga3 126.64(6) 17_545 . ?
Ga6 Ho1 Ga3 53.09(6) 13_444 . ?
Ga6 Ho1 Ga3 53.09(6) 15_554 . ?
Ga6 Ho1 Ga3 53.10(6) 14_544 . ?
Ga5 Ho1 Ga2 90.167(15) 15_554 . ?
Ga5 Ho1 Ga2 90.167(15) 13_444 . ?
Ga5 Ho1 Ga2 90.167(15) 14_544 . ?
Ga6 Ho1 Ga2 53.36(6) 18_445 . ?
Ga6 Ho1 Ga2 53.36(6) 16 . ?
Ga6 Ho1 Ga2 53.36(6) 17_545 . ?
Ga6 Ho1 Ga2 126.91(6) 13_444 . ?
Ga6 Ho1 Ga2 126.91(6) 15_554 . ?
Ga6 Ho1 Ga2 126.90(6) 14_544 . ?
Ga3 Ho1 Ga2 180.0 . . ?
Ga5 Ho1 Ni1 45.52(4) 15_554 17 ?
Ga5 Ho1 Ni1 100.21(4) 13_444 17 ?
Ga5 Ho1 Ni1 121.96(5) 14_544 17 ?
Ga6 Ho1 Ni1 45.21(5) 18_445 17 ?
Ga6 Ho1 Ni1 45.86(5) 16 17 ?
Ga6 Ho1 Ni1 100.36(8) 17_545 17 ?
Ga6 Ho1 Ni1 96.49(7) 13_444 17 ?
Ga6 Ho1 Ni1 96.96(6) 15_554 17 ?
Ga6 Ho1 Ni1 173.90(7) 14_544 17 ?
Ga3 Ho1 Ni1 132.99(5) . 17 ?
Ga2 Ho1 Ni1 47.01(5) . 17 ?
Ga4 Ni1 Ga5 156.01(11) 9 . ?
Ga4 Ni1 Ga6 101.21(12) 9 2_655 ?
Ga5 Ni1 Ga6 102.78(14) . 2_655 ?
Ga4 Ni1 Ga6 99.30(12) 9 . ?
Ga5 Ni1 Ga6 69.01(10) . . ?
Ga6 Ni1 Ga6 118.48(14) 2_655 . ?
Ga4 Ni1 Ga6 99.30(13) 9 3 ?
Ga5 Ni1 Ga6 69.00(10) . 3 ?
Ga6 Ni1 Ga6 118.46(14) 2_655 3 ?
Ga6 Ni1 Ga6 114.27(12) . 3 ?
Ga4 Ni1 Ga3 68.89(11) 9 7 ?
Ga5 Ni1 Ga3 121.02(12) . 7 ?
Ga6 Ni1 Ga3 67.71(8) 2_655 7 ?
Ga6 Ni1 Ga3 67.24(8) . 7 ?
Ga6 Ni1 Ga3 168.00(17) 3 7 ?
Ga4 Ni1 Ga2 68.47(10) 9 16_545 ?
Ga5 Ni1 Ga2 121.40(11) . 16_545 ?
Ga6 Ni1 Ga2 67.85(8) 2_655 16_545 ?
Ga6 Ni1 Ga2 167.58(17) . 16_545 ?
Ga6 Ni1 Ga2 67.38(8) 3 16_545 ?
Ga3 Ni1 Ga2 108.48(11) 7 16_545 ?
Ga4 Ni1 Ga1 68.28(11) 9 . ?
Ga5 Ni1 Ga1 87.73(11) . . ?
Ga6 Ni1 Ga1 169.49(18) 2_655 . ?
Ga6 Ni1 Ga1 65.07(7) . . ?
Ga6 Ni1 Ga1 65.07(8) 3 . ?
Ga3 Ni1 Ga1 107.01(11) 7 . ?
Ga2 Ni1 Ga1 106.77(11) 16_545 . ?
Ga4 Ni1 Ho1 133.55(9) 9 16_545 ?
Ga5 Ni1 Ho1 60.60(7) . 16_545 ?
Ga6 Ni1 Ho1 62.07(9) 2_655 16_545 ?
Ga6 Ni1 Ho1 127.05(13) . 16_545 ?
Ga6 Ni1 Ho1 61.83(9) 3 16_545 ?
Ga3 Ni1 Ho1 127.71(9) 7 16_545 ?
Ga2 Ni1 Ho1 65.09(9) 16_545 16_545 ?
Ga1 Ni1 Ho1 124.86(9) . 16_545 ?
Ga4 Ni1 Ho1 133.77(9) 9 7 ?
Ga5 Ni1 Ho1 60.40(7) . 7 ?
Ga6 Ni1 Ho1 62.13(9) 2_655 7 ?
Ga6 Ni1 Ho1 61.89(9) . 7 ?
Ga6 Ni1 Ho1 126.82(13) 3 7 ?
Ga3 Ni1 Ho1 64.89(9) 7 7 ?
Ga2 Ni1 Ho1 127.96(9) 16_545 7 ?
Ga1 Ni1 Ho1 124.85(9) . 7 ?
Ho1 Ni1 Ho1 79.35(6) 16_545 7 ?
Ni1 Ga6 Ni1 115.64(13) 3_665 . ?
Ni1 Ga6 Ni1 115.66(13) 3_665 2 ?
Ni1 Ga6 Ni1 119.92(13) . 2 ?
Ni1 Ga6 Ga1 140.54(15) 3_665 . ?
Ni1 Ga6 Ga1 60.40(7) . . ?
Ni1 Ga6 Ga1 60.39(7) 2 . ?
Ni1 Ga6 Ga5 133.87(13) 3_665 . ?
Ni1 Ga6 Ga5 54.91(8) . . ?
Ni1 Ga6 Ga5 104.33(10) 2 . ?
Ga1 Ga6 Ga5 79.02(7) . . ?
Ni1 Ga6 Ga5 133.88(13) 3_665 2 ?
Ni1 Ga6 Ga5 104.34(10) . 2 ?
Ni1 Ga6 Ga5 54.91(8) 2 2 ?
Ga1 Ga6 Ga5 79.02(7) . 2 ?
Ga5 Ga6 Ga5 56.72(10) . 2 ?
Ni1 Ga6 Ga3 58.58(7) 3_665 7 ?
Ni1 Ga6 Ga3 58.27(7) . 7 ?
Ni1 Ga6 Ga3 140.53(15) 2 7 ?
Ga1 Ga6 Ga3 98.23(10) . 7 ?
Ga5 Ga6 Ga3 103.08(8) . 7 ?
Ga5 Ga6 Ga3 159.80(10) 2 7 ?
Ni1 Ga6 Ga2 58.64(7) 3_665 16 ?
Ni1 Ga6 Ga2 140.16(16) . 16 ?
Ni1 Ga6 Ga2 58.32(7) 2 16 ?
Ga1 Ga6 Ga2 97.99(10) . 16 ?
Ga5 Ga6 Ga2 160.04(10) . 16 ?
Ga5 Ga6 Ga2 103.32(8) 2 16 ?
Ga3 Ga6 Ga2 96.88(10) 7 16 ?
Ni1 Ga6 Ho1 72.72(8) 3_665 16 ?
Ni1 Ga6 Ho1 153.20(15) . 16 ?
Ni1 Ga6 Ho1 72.31(8) 2 16 ?
Ga1 Ga6 Ho1 130.41(7) . 16 ?
Ga5 Ga6 Ho1 100.20(11) . 16 ?
Ga5 Ga6 Ho1 61.35(7) 2 16 ?
Ga3 Ga6 Ho1 129.19(7) 7 16 ?
Ga2 Ga6 Ho1 66.53(7) 16 16 ?
Ni1 Ga6 Ho1 72.82(8) 3_665 7 ?
```

```
Ni1 Ga6 Ho1 72.42(8) . 7 ?
Ni1 Ga6 Ho1 152.94(15) 2 7 ?
Ga1 Ga6 Ho1 130.45(7) . 7 ?
Ga5 Ga6 Ho1 61.21(7) . 7 ?
Ga5 Ga6 Ho1 99.95(11) 2 7 ?
Ga3 Ga6 Ho1 66.42(7) 7 7 ?
Ga2 Ga6 Ho1 129.40(7) 16 7 ?
Ho1 Ga6 Ho1 87.25(9) 16 7 ?

_diffrn_measured_fraction_theta_max    0.990
_diffrn_reflns_theta_full              29.93
_diffrn_measured_fraction_theta_full   0.990
_refine_diff_density_max    7.668
_refine_diff_density_min   -6.035
_refine_diff_density_rms    1.038
```

A2.5 $ErNi_3Ga_9$

```
data_erni3ga9

_audit_creation_method            SHELXL-97
_chemical_name_systematic
;
 ?
;
_chemical_name_common             ?
_chemical_melting_point           ?
_chemical_formula_moiety          ?
_chemical_formula_sum
 'Er Ga9 Ni3'
_chemical_formula_weight          970.87

loop_
 _atom_type_symbol
 _atom_type_description
 _atom_type_scat_dispersion_real
 _atom_type_scat_dispersion_imag
 _atom_type_scat_source
 'Ni'  'Ni'   0.3393   1.1124
 'International Tables Vol C Tables 4.2.6.8
and 6.1.1.4'
 'Ga'  'Ga'   0.2307   1.6083
 'International Tables Vol C Tables 4.2.6.8
and 6.1.1.4'
 'Er'  'Er'  -0.2586   4.9576
 'International Tables Vol C Tables 4.2.6.8
and 6.1.1.4'

_symmetry_cell_setting            ?
_symmetry_space_group_name_H-M    ?

loop_
 _symmetry_equiv_pos_as_xyz
 'x, y, z'
 '-y, x-y, z'
 '-x+y, -x, z'
 'x-y, -y, -z'
 '-x, -x+y, -z'
 'y, x, -z'
 'x+2/3, y+1/3, z+1/3'
 '-y+2/3, x-y+1/3, z+1/3'
 '-x+y+2/3, -x+1/3, z+1/3'
 'x-y+2/3, -y+1/3, -z+1/3'
 '-x+2/3, -x+y+1/3, -z+1/3'
 'y+2/3, x+1/3, -z+1/3'
 'x+1/3, y+2/3, z+2/3'
 '-y+1/3, x-y+2/3, z+2/3'
 '-x+y+1/3, -x+2/3, z+2/3'
 'x-y+1/3, -y+2/3, -z+2/3'
 '-x+1/3, -x+y+2/3, -z+2/3'
 'y+1/3, x+2/3, -z+2/3'

_cell_length_a                    7.237(5)
_cell_length_b                    7.237(5)
_cell_length_c                    27.422(2)
_cell_angle_alpha                 90.00
_cell_angle_beta                  90.00
_cell_angle_gamma                 120.00
_cell_volume                      1243.8(12)
_cell_formula_units_Z             6
_cell_measurement_temperature     298(2)
_cell_measurement_reflns_used     ?
_cell_measurement_theta_min       ?
_cell_measurement_theta_max       ?

_exptl_crystal_description        ?
_exptl_crystal_colour             ?
_exptl_crystal_size_max           0.05
_exptl_crystal_size_mid           0.03
_exptl_crystal_size_min           0.03
_exptl_crystal_density_meas       ?
_exptl_crystal_density_diffrn     7.777
_exptl_crystal_density_method            'not
measured'
_exptl_crystal_F_000              2586
_exptl_absorpt_coefficient_mu     45.254
_exptl_absorpt_correction_type    ?
_exptl_absorpt_correction_T_min   0.2106
_exptl_absorpt_correction_T_max   0.3975
_exptl_absorpt_process_details    ?

_exptl_special_details
;
 ?
;

_diffrn_ambient_temperature       298(2)
_diffrn_radiation_wavelength      0.71073
_diffrn_radiation_type            MoK\a
_diffrn_radiation_source               'fine-
focus sealed tube'
_diffrn_radiation_monochromator   graphite
_diffrn_measurement_device_type   ?
_diffrn_measurement_method        ?
_diffrn_detector_area_resol_mean  ?
_diffrn_standards_number          ?
_diffrn_standards_interval_count  ?
_diffrn_standards_interval_time   ?
_diffrn_standards_decay_%         ?
_diffrn_reflns_number             1200
_diffrn_reflns_av_R_equivalents   0.0920
_diffrn_reflns_av_sigmaI/netI     0.0912
_diffrn_reflns_limit_h_min        -10
_diffrn_reflns_limit_h_max        7
_diffrn_reflns_limit_k_min        -8
_diffrn_reflns_limit_k_max        10
_diffrn_reflns_limit_l_min        -38
_diffrn_reflns_limit_l_max        26
_diffrn_reflns_theta_min          3.57
_diffrn_reflns_theta_max          30.17
_reflns_number_total              656
_reflns_number_gt                 595
_reflns_threshold_expression      >2sigma(I)

_computing_data_collection        ?
_computing_cell_refinement        ?
_computing_data_reduction         ?
_computing_structure_solution     ?
_computing_structure_refinement    'SHELXL-97
(Sheldrick, 1997)'
_computing_molecular_graphics     ?
_computing_publication_material   ?

_refine_special_details
;
 Refinement of F^2^ against ALL reflections.
The weighted R-factor wR and
 goodness  of  fit  S  are  based  on  F^2^,
conventional R-factors R are based
 on F, with F set to zero for negative F^2^.
The threshold expression of
 F^2^  >  2sigma(F^2^)  is  used  only  for
calculating R-factors(gt) etc. and is
 not relevant to the choice of reflections
for refinement.  R-factors based
```

```
 on  F^2^  are  statistically  about  twice  as
large as those based on F, and R-
 factors  based  on  ALL  data  will  be  even
larger.
;

_refine_ls_structure_factor_coef  Fsqd
_refine_ls_matrix_type            full
_refine_ls_weighting_scheme       calc
_refine_ls_weighting_details
 'calc
w=1/[\s^2^(Fo^2^)+(0.1624P)^2^+12.9839P]
where P=(Fo^2^+2Fc^2^)/3'
_atom_sites_solution_primary      direct
_atom_sites_solution_secondary    difmap
_atom_sites_solution_hydrogens    geom
_refine_ls_hydrogen_treatment     mixed
_refine_ls_extinction_method      SHELXL
_refine_ls_extinction_coef        0.0087(11)
_refine_ls_extinction_expression
 'Fc^*^=kFc[1+0.001xFc^2^\l^3^/sin(2\q)]^-
1/4^'
_refine_ls_abs_structure_details
 'Flack  H  D  (1983),  Acta  Cryst.  A39,  876-
881'
_refine_ls_abs_structure_Flack    -0.15(19)
_refine_ls_number_reflns          656
_refine_ls_number_parameters      45
_refine_ls_number_restraints      0
_refine_ls_R_factor_all           0.0884
_refine_ls_R_factor_gt            0.0849
_refine_ls_wR_factor_ref          0.2266
_refine_ls_wR_factor_gt           0.2197
_refine_ls_goodness_of_fit_ref    1.085
_refine_ls_restrained_S_all       1.085
_refine_ls_shift/su_max           0.000
_refine_ls_shift/su_mean          0.000

loop_
 _atom_site_label
 _atom_site_type_symbol
 _atom_site_fract_x
 _atom_site_fract_y
 _atom_site_fract_z
 _atom_site_U_iso_or_equiv
 _atom_site_adp_type
 _atom_site_occupancy
 _atom_site_symmetry_multiplicity
 _atom_site_calc_flag
 _atom_site_refinement_flags
 _atom_site_disorder_assembly
 _atom_site_disorder_group
Er1  Er  0.0000  0.0000  0.16693(3)  0.0129(6)
Uani 0.88 3 d SP . .
Er2  Er  0.0000  0.0000  0.5000  0.0129(6)  Uani
0.25 6 d SP . .
Ga5  Ga  0.2065(5)  0.0000  0.5000  0.0156(8)
Uani 0.76 2 d SP . .
Ga7 Ga 0.188(3) 0.002(2) 0.1667(3) 0.0156(8)
Uani 0.12 1 d P . .
Ga1  Ga  0.0000  0.0000  0.38434(18)  0.0175(9)
Uani 1 3 d S . .
Ga2  Ga  0.0000  0.0000  0.28359(18)  0.0170(9)
Uani 1 3 d S . .
Ga3  Ga  0.0000  0.0000  0.05016(18)  0.0170(9)
Uani 1 3 d S . .
Ga4  Ga  0.3335(3)  0.0000  0.0000  0.0178(10)
Uani 1 2 d S . .
Ni1   Ni   0.3331(3)   0.0046(3)   0.08472(16)
0.0136(9) Uani 1 1 d . . .
Ga6   Ga   0.3337(3)   0.3361(3)   0.10063(19)
0.0159(8) Uani 1 1 d . . .

loop_
 _atom_site_aniso_label
 _atom_site_aniso_U_11
 _atom_site_aniso_U_22
 _atom_site_aniso_U_33
 _atom_site_aniso_U_23
 _atom_site_aniso_U_13
 _atom_site_aniso_U_12
Er1  0.0172(7)  0.0172(7)  0.0044(8)  0.000
0.000 0.0086(3)
Er2  0.0172(7)  0.0172(7)  0.0044(8)  0.000
0.000 0.0086(3)
Ga5   0.0200(14)   0.0234(19)   0.0045(12)   -
0.0016(13) -0.0008(7) 0.0117(9)
Ga7   0.0200(14)   0.0234(19)   0.0045(12)   -
0.0016(13) -0.0008(7) 0.0117(9)
Ga1  0.0211(13)  0.0211(13)  0.010(2)  0.000
0.000 0.0105(7)
Ga2  0.0211(13)  0.0211(13)  0.009(2)  0.000
0.000 0.0106(7)
Ga3  0.0210(13)  0.0210(13)  0.009(2)  0.000
0.000 0.0105(7)
Ga4 0.0238(15) 0.0247(16) 0.005(2) 0.0000(6)
0.0000(3) 0.0124(8)
Ni1    0.0179(15)    0.0182(15)    0.0044(18)
0.0004(5) -0.0005(6) 0.0088(9)
Ga6   0.0182(14)   0.0180(14)   0.0114(15)   -
0.0013(6) -0.0008(6) 0.0090(9)

_geom_special_details
;
 All  esds  (except  the  esd  in  the  dihedral
angle between two l.s. planes)
 are  estimated  using  the  full  covariance
matrix.  The cell esds are taken
 into account individually in the estimation
of esds in distances, angles
 and  torsion  angles;  correlations  between
esds in cell parameters are only
 used  when  they  are  defined  by  crystal
symmetry.  An approximate (isotropic)
 treatment  of  cell  esds  is  used  for
estimating esds involving l.s. planes.
;

loop_
 _geom_bond_atom_site_label_1
 _geom_bond_atom_site_label_2
 _geom_bond_distance
 _geom_bond_site_symmetry_2
 _geom_bond_publ_flag
Er1 Ga7 1.35(2) 3 ?
Er1 Ga7 1.35(2) 2 ?
Er1 Ga7 1.35(2) . ?
Er1 Ga5 2.979(3) 15_554 ?
Er1 Ga5 2.979(3) 13_444 ?
Er1 Ga5 2.979(3) 14_544 ?
Er1 Ga6 3.018(4) 12_445 ?
Er1 Ga6 3.018(4) 11 ?
Er1 Ga6 3.018(4) 10_455 ?
Er1 Ga6 3.030(4) 2 ?
Er1 Ga6 3.030(4) 3 ?
Er1 Ga6 3.030(4) . ?
Er2 Ga5 1.494(4) 3 ?
Er2 Ga5 1.494(4) 2 ?
Er2 Ga5 1.494(4) . ?
Er2 Ga6 3.001(4) 7_445 ?
Er2 Ga6 3.001(4) 18_445 ?
Er2 Ga6 3.001(4) 16 ?
Er2 Ga6 3.001(4) 8 ?
Er2 Ga6 3.001(4) 9_455 ?
```

Er2 Ga6 3.001(4) 17_545 ?
Er2 Ga7 3.09(2) 17 ?
Er2 Ga7 3.09(2) 9 ?
Er2 Ga7 3.09(2) 8_445 ?
Ga5 Ga7 1.72(2) 9 ?
Ga5 Ga7 1.72(2) 18_545 ?
Ga5 Ni1 2.440(4) 9 ?
Ga5 Ni1 2.441(4) 18_545 ?
Ga5 Ga5 2.589(6) 3 ?
Ga5 Ga5 2.589(6) 2 ?
Ga5 Ga6 2.767(4) 16 ?
Ga5 Ga6 2.767(4) 7_445 ?
Ga5 Ga6 2.769(4) 17_545 ?
Ga5 Ga6 2.769(4) 8 ?
Ga5 Er1 2.979(3) 7 ?
Ga7 Ga5 1.72(2) 14_544 ?
Ga7 Ga7 1.82(4) 11 ?
Ga7 Ga7 2.34(4) 3 ?
Ga7 Ga7 2.34(4) 2 ?
Ga7 Ni1 2.478(13) 11 ?
Ga7 Ni1 2.479(12) . ?
Ga7 Ga6 2.769(13) 11 ?
Ga7 Ga6 2.772(14) . ?
Ga7 Ga6 2.776(14) 12_445 ?
Ga7 Ga6 2.781(13) 3 ?
Ga7 Er1 3.074(19) 10 ?
Ga1 Ni1 2.615(4) 9 ?
Ga1 Ni1 2.615(4) 8_445 ?
Ga1 Ni1 2.615(4) 7_455 ?
Ga1 Ga6 2.753(4) 7_445 ?
Ga1 Ga6 2.753(4) 8 ?
Ga1 Ga6 2.753(4) 9_455 ?
Ga1 Ga2 2.763(10) . ?
Ga1 Ga4 2.788(3) 9 ?
Ga1 Ga4 2.788(3) 8_445 ?
Ga1 Ga4 2.788(3) 7_455 ?
Ga2 Ni1 2.581(4) 11 ?
Ga2 Ni1 2.581(4) 12_445 ?
Ga2 Ni1 2.581(4) 10_455 ?
Ga2 Ga4 2.771(3) 9 ?
Ga2 Ga4 2.771(3) 8_445 ?
Ga2 Ga4 2.771(3) 7_455 ?
Ga2 Ga6 2.793(4) 12_445 ?
Ga2 Ga6 2.793(4) 11 ?
Ga2 Ga6 2.793(4) 10_455 ?
Ga3 Ni1 2.575(4) . ?
Ga3 Ni1 2.575(4) 2 ?
Ga3 Ni1 2.575(4) 3 ?
Ga3 Ga3 2.751(10) 4 ?
Ga3 Ga4 2.778(3) 3 ?
Ga3 Ga4 2.778(3) 2 ?
Ga3 Ga4 2.778(3) . ?
Ga3 Ga6 2.791(4) . ?
Ga3 Ga6 2.791(4) 2 ?
Ga3 Ga6 2.791(4) 3 ?
Ga4 Ni1 2.323(4) 4 ?
Ga4 Ni1 2.323(4) . ?
Ga4 Ga2 2.771(3) 10 ?
Ga4 Ga2 2.771(3) 13_544 ?
Ga4 Ga3 2.778(3) 4 ?
Ga4 Ga1 2.788(3) 10 ?
Ga4 Ga1 2.788(3) 13_544 ?
Ni1 Ga6 2.436(3) . ?
Ni1 Ga5 2.441(4) 14_544 ?
Ni1 Ga6 2.459(3) 2_655 ?
Ni1 Ga6 2.460(3) 3 ?
Ni1 Ga7 2.478(13) 11 ?
Ni1 Ga2 2.581(4) 10 ?
Ni1 Ga1 2.615(4) 13_544 ?
Ni1 Er1 3.280(4) 10 ?
Ga6 Ni1 2.459(3) 3_665 ?
Ga6 Ni1 2.460(3) 2 ?
Ga6 Ga1 2.753(4) 13_554 ?
Ga6 Ga5 2.767(4) 13_554 ?
Ga6 Ga7 2.769(13) 11 ?
Ga6 Ga5 2.769(4) 15_554 ?
Ga6 Ga7 2.776(14) 12 ?
Ga6 Ga7 2.781(13) 2 ?
Ga6 Ga2 2.793(4) 10 ?

loop_
_geom_angle_atom_site_label_1
_geom_angle_atom_site_label_2
_geom_angle_atom_site_label_3
_geom_angle
_geom_angle_site_symmetry_1
_geom_angle_site_symmetry_3
_geom_angle_publ_flag
Ga7 Er1 Ga7 119.998(9) 3 2 ?
Ga7 Er1 Ga7 119.998(7) 3 . ?
Ga7 Er1 Ga7 119.998(9) 2 . ?
Ga7 Er1 Ga5 136.1(6) 3 15_554 ?
Ga7 Er1 Ga5 16.1(6) 2 15_554 ?
Ga7 Er1 Ga5 103.9(6) . 15_554 ?
Ga7 Er1 Ga5 16.1(6) 3 13_444 ?
Ga7 Er1 Ga5 103.9(6) 2 13_444 ?
Ga7 Er1 Ga5 136.1(6) . 13_444 ?
Ga5 Er1 Ga5 120.0 15_554 13_444 ?
Ga7 Er1 Ga5 103.9(6) 3 14_544 ?
Ga7 Er1 Ga5 136.1(6) 2 14_544 ?
Ga7 Er1 Ga5 16.1(6) . 14_544 ?
Ga5 Er1 Ga5 119.999(1) 15_554 14_544 ?
Ga5 Er1 Ga5 120.0 13_444 14_544 ?
Ga7 Er1 Ga6 66.4(5) 3 12_445 ?
Ga7 Er1 Ga6 143.6(4) 2 12_445 ?
Ga7 Er1 Ga6 66.7(6) . 12_445 ?
Ga5 Er1 Ga6 140.59(8) 15_554 12_445 ?
Ga5 Er1 Ga6 78.81(5) 13_444 12_445 ?
Ga5 Er1 Ga6 54.96(6) 14_544 12_445 ?
Ga7 Er1 Ga6 143.6(4) 3 11 ?
Ga7 Er1 Ga6 66.7(6) 2 11 ?
Ga7 Er1 Ga6 66.4(5) . 11 ?
Ga5 Er1 Ga6 54.96(6) 15_554 11 ?
Ga5 Er1 Ga6 140.59(8) 13_444 11 ?
Ga5 Er1 Ga6 78.81(5) 14_544 11 ?
Ga6 Er1 Ga6 87.96(12) 12_445 11 ?
Ga7 Er1 Ga6 66.7(6) 3 10_455 ?
Ga7 Er1 Ga6 66.4(5) 2 10_455 ?
Ga7 Er1 Ga6 143.6(4) . 10_455 ?
Ga5 Er1 Ga6 78.81(5) 15_554 10_455 ?
Ga5 Er1 Ga6 54.96(6) 13_444 10_455 ?
Ga5 Er1 Ga6 140.59(8) 14_544 10_455 ?
Ga6 Er1 Ga6 87.96(12) 12_445 10_455 ?
Ga6 Er1 Ga6 87.95(12) 11 10_455 ?
Ga7 Er1 Ga6 66.5(5) 3 2 ?
Ga7 Er1 Ga6 66.1(6) 2 2 ?
Ga7 Er1 Ga6 142.9(4) . 2 ?
Ga5 Er1 Ga6 78.63(5) 15_554 2 ?
Ga5 Er1 Ga6 54.88(6) 13_444 2 ?
Ga5 Er1 Ga6 140.18(8) 14_544 2 ?
Ga6 Er1 Ga6 132.83(6) 12_445 2 ?
Ga6 Er1 Ga6 132.75(6) 11 2 ?
Ga6 Er1 Ga6 73.57(16) 10_455 2 ?
Ga7 Er1 Ga6 66.1(6) 3 3 ?
Ga7 Er1 Ga6 142.9(4) 2 3 ?
Ga7 Er1 Ga6 66.5(5) . 3 ?
Ga5 Er1 Ga6 140.18(8) 15_554 3 ?
Ga5 Er1 Ga6 78.63(5) 13_444 3 ?
Ga5 Er1 Ga6 54.88(6) 14_544 3 ?
Ga6 Er1 Ga6 73.57(16) 12_445 3 ?
Ga6 Er1 Ga6 132.83(6) 11 3 ?
Ga6 Er1 Ga6 132.75(6) 10_455 3 ?
Ga6 Er1 Ga6 87.70(12) 2 3 ?
Ga7 Er1 Ga6 142.9(4) 3 . ?

```
Ga7 Er1 Ga6 66.5(5) 2 . ?
Ga7 Er1 Ga6 66.1(6) . . ?
Ga5 Er1 Ga6 54.88(6) 15_554 . ?
Ga5 Er1 Ga6 140.18(8) 13_444 . ?
Ga5 Er1 Ga6 78.63(5) 14_544 . ?
Ga6 Er1 Ga6 132.75(6) 12_445 . ?
Ga6 Er1 Ga6 73.57(16) 11 . ?
Ga6 Er1 Ga6 132.83(6) 10_455 . ?
Ga6 Er1 Ga6 87.70(12) 2 . ?
Ga6 Er1 Ga6 87.70(12) 3 . ?
Ga5 Er2 Ga5 120.000(2) 3 2 ?
Ga5 Er2 Ga5 120.000(2) 3 . ?
Ga5 Er2 Ga5 120.000(5) 2 . ?
Ga5 Er2 Ga6 66.54(5) 3 7_445 ?
Ga5 Er2 Ga6 142.89(8) 2 7_445 ?
Ga5 Er2 Ga6 66.46(4) . 7_445 ?
Ga5 Er2 Ga6 66.54(5) 3 18_445 ?
Ga5 Er2 Ga6 66.46(4) 2 18_445 ?
Ga5 Er2 Ga6 142.89(8) . 18_445 ?
Ga6 Er2 Ga6 133.08(9) 7_445 18_445 ?
Ga5 Er2 Ga6 142.89(8) 3 16 ?
Ga5 Er2 Ga6 66.54(5) 2 16 ?
Ga5 Er2 Ga6 66.46(4) . 16 ?
Ga6 Er2 Ga6 132.92(9) 7_445 16 ?
Ga6 Er2 Ga6 87.36(12) 18_445 16 ?
Ga5 Er2 Ga6 142.89(8) 3 8 ?
Ga5 Er2 Ga6 66.46(4) 2 8 ?
Ga5 Er2 Ga6 66.54(5) . 8 ?
Ga6 Er2 Ga6 87.36(12) 7_445 8 ?
Ga6 Er2 Ga6 132.92(9) 18_445 8 ?
Ga6 Er2 Ga6 74.22(17) 16 8 ?
Ga5 Er2 Ga6 66.46(4) 3 9_455 ?
Ga5 Er2 Ga6 66.54(5) 2 9_455 ?
Ga5 Er2 Ga6 142.89(8) . 9_455 ?
Ga6 Er2 Ga6 87.36(12) 7_445 9_455 ?
Ga6 Er2 Ga6 74.22(17) 18_445 9_455 ?
Ga6 Er2 Ga6 133.08(9) 16 9_455 ?
Ga6 Er2 Ga6 87.36(12) 8 9_455 ?
Ga5 Er2 Ga6 66.46(4) 3 17_545 ?
Ga5 Er2 Ga6 142.89(8) 2 17_545 ?
Ga5 Er2 Ga6 66.54(5) . 17_545 ?
Ga6 Er2 Ga6 74.22(17) 7_445 17_545 ?
Ga6 Er2 Ga6 87.36(12) 18_445 17_545 ?
Ga6 Er2 Ga6 87.36(12) 16 17_545 ?
Ga6 Er2 Ga6 133.08(9) 8 17_545 ?
Ga6 Er2 Ga6 132.92(9) 9_455 17_545 ?
Ga5 Er2 Ga7 137.2(3) 3 17 ?
Ga5 Er2 Ga7 17.2(3) 2 17 ?
Ga5 Er2 Ga7 102.8(3) . 17 ?
Ga6 Er2 Ga7 139.6(2) 7_445 17 ?
Ga6 Er2 Ga7 79.8(3) 18_445 17 ?
Ga6 Er2 Ga7 54.3(3) 16 17 ?
Ga6 Er2 Ga7 54.2(3) 8 17 ?
Ga6 Er2 Ga7 79.8(3) 9_455 17 ?
Ga6 Er2 Ga7 139.7(2) 17_545 17 ?
Ga5 Er2 Ga7 137.2(3) 3 9 ?
Ga5 Er2 Ga7 102.8(3) 2 9 ?
Ga5 Er2 Ga7 17.2(3) . 9 ?
Ga6 Er2 Ga7 79.8(3) 7_445 9 ?
Ga6 Er2 Ga7 139.6(2) 18_445 9 ?
Ga6 Er2 Ga7 54.2(3) 16 9 ?
Ga6 Er2 Ga7 54.3(3) 8 9 ?
Ga6 Er2 Ga7 139.7(2) 9_455 9 ?
Ga6 Er2 Ga7 79.8(3) 17_545 9 ?
Ga7 Er2 Ga7 85.7(7) 17 9 ?
Ga5 Er2 Ga7 17.2(3) 3 8_445 ?
Ga5 Er2 Ga7 137.2(4) 2 8_445 ?
Ga5 Er2 Ga7 102.8(3) . 8_445 ?
Ga6 Er2 Ga7 54.3(3) 7_445 8_445 ?
Ga6 Er2 Ga7 79.8(3) 18_445 8_445 ?
Ga6 Er2 Ga7 139.6(2) 16 8_445 ?
Ga6 Er2 Ga7 139.7(2) 8 8_445 ?
Ga6 Er2 Ga7 79.8(3) 9_455 8_445 ?
Ga6 Er2 Ga7 54.2(3) 17_545 8_445 ?
Ga7 Er2 Ga7 154.3(7) 17 8_445 ?
Ga7 Er2 Ga7 120.001(3) 9 8_445 ?
Er2 Ga5 Ga7 148.0(5) . 9 ?
Er2 Ga5 Ga7 148.0(6) . 18_545 ?
Ga7 Ga5 Ga7 63.9(11) 9 18_545 ?
Er2 Ga5 Ni1 112.96(10) . 9 ?
Ga7 Ga5 Ni1 70.7(3) 9 9 ?
Ga7 Ga5 Ni1 70.7(3) 18_545 9 ?
Er2 Ga5 Ni1 112.96(10) . 18_545 ?
Ga7 Ga5 Ni1 70.7(3) 9 18_545 ?
Ga7 Ga5 Ni1 70.7(3) 18_545 18_545 ?
Ni1 Ga5 Ni1 134.1(2) 9 18_545 ?
Er2 Ga5 Ga5 30.0 . 3 ?
Ga7 Ga5 Ga5 178.0(5) 9 3 ?
Ga7 Ga5 Ga5 118.0(5) 18_545 3 ?
Ni1 Ga5 Ga5 109.76(9) 9 3 ?
Ni1 Ga5 Ga5 109.73(9) 18_545 3 ?
Er2 Ga5 Ga5 30.000(1) . 2 ?
Ga7 Ga5 Ga5 118.0(5) 9 2 ?
Ga7 Ga5 Ga5 178.0(5) 18_545 2 ?
Ni1 Ga5 Ga5 109.73(9) 9 2 ?
Ni1 Ga5 Ga5 109.76(9) 18_545 2 ?
Ga5 Ga5 Ga5 60.0 3 2 ?
Er2 Ga5 Ga6 83.86(8) . 16 ?
Ga7 Ga5 Ga6 72.2(5) 9 16 ?
Ga7 Ga5 Ga6 119.2(4) 18_545 16 ?
Ni1 Ga5 Ga6 130.08(11) 9 16 ?
Ni1 Ga5 Ga6 55.92(9) 18_545 16 ?
Ga5 Ga5 Ga6 106.36(8) 3 16 ?
Ga5 Ga5 Ga6 62.17(8) 2 16 ?
Er2 Ga5 Ga6 83.86(8) . 7_445 ?
Ga7 Ga5 Ga6 119.2(4) 9 7_445 ?
Ga7 Ga5 Ga6 72.2(5) 18_545 7_445 ?
Ni1 Ga5 Ga6 55.92(9) 9 7_445 ?
Ni1 Ga5 Ga6 130.08(11) 18_545 7_445 ?
Ga5 Ga5 Ga6 62.17(8) 3 7_445 ?
Ga5 Ga5 Ga6 106.36(8) 2 7_445 ?
Ga6 Ga5 Ga6 167.72(16) 16 7_445 ?
Er2 Ga5 Ga6 83.79(8) . 17_545 ?
Ga7 Ga5 Ga6 119.2(4) 9 17_545 ?
Ga7 Ga5 Ga6 72.3(5) 18_545 17_545 ?
Ni1 Ga5 Ga6 130.14(11) 9 17_545 ?
Ni1 Ga5 Ga6 55.93(9) 18_545 17_545 ?
Ga5 Ga5 Ga6 62.09(8) 3 17_545 ?
Ga5 Ga5 Ga6 106.30(8) 2 17_545 ?
Ga6 Ga5 Ga6 96.96(17) 16 17_545 ?
Ga6 Ga5 Ga6 81.71(17) 7_445 17_545 ?
Er2 Ga5 Ga6 83.79(8) . 8 ?
Ga7 Ga5 Ga6 72.3(5) 9 8 ?
Ga7 Ga5 Ga6 119.2(4) 18_545 8 ?
Ni1 Ga5 Ga6 55.93(9) 9 8 ?
Ni1 Ga5 Ga6 130.14(11) 18_545 8 ?
Ga5 Ga5 Ga6 106.30(8) 3 8 ?
Ga5 Ga5 Ga6 62.09(8) 2 8 ?
Ga6 Ga5 Ga6 81.71(17) 16 8 ?
Ga6 Ga5 Ga6 96.96(17) 7_445 8 ?
Ga6 Ga5 Ga6 167.57(16) 17_545 8 ?
Er2 Ga5 Er1 135.47(5) . 7 ?
Ga7 Ga5 Er1 12.6(6) 9 7 ?
Ga7 Ga5 Er1 76.5(5) 18_545 7 ?
Ni1 Ga5 Er1 73.96(9) 9 7 ?
Ni1 Ga5 Er1 73.74(9) 18_545 7 ?
Ga5 Ga5 Er1 165.47(5) 3 7 ?
Ga5 Ga5 Er1 105.47(5) 2 7 ?
Ga6 Ga5 Er1 63.24(6) 16 7 ?
Ga6 Ga5 Er1 127.07(10) 7_445 7 ?
Ga6 Ga5 Er1 126.91(10) 17_545 7 ?
Ga6 Ga5 Er1 63.49(6) 8 7 ?
Er1 Ga7 Ga5 151.3(11) . 14_544 ?
Er1 Ga7 Ga7 150.6(6) . 11 ?
```

```
Ga5 Ga7 Ga7 58.0(5) 14_544 11 ?
Er1 Ga7 Ga7 30.001(4) . 3 ?
Ga5 Ga7 Ga7 121.3(11) 14_544 3 ?
Ga7 Ga7 Ga7 179.4(7) 11 3 ?
Er1 Ga7 Ga7 30.001(4) . 2 ?
Ga5 Ga7 Ga7 178.7(11) 14_544 2 ?
Ga7 Ga7 Ga7 120.6(7) 11 2 ?
Ga7 Ga7 Ga7 60.000(1) 3 2 ?
Er1 Ga7 Ni1 114.7(6) . 11 ?
Ga5 Ga7 Ni1 68.3(5) 14_544 11 ?
Ga7 Ga7 Ni1 68.4(6) 11 11 ?
Ga7 Ga7 Ni1 111.5(5) 3 11 ?
Ga7 Ga7 Ni1 111.4(5) 2 11 ?
Er1 Ga7 Ni1 115.2(7) . . ?
Ga5 Ga7 Ni1 68.3(5) 14_544 . ?
Ga7 Ga7 Ni1 68.4(6) 11 . ?
Ga7 Ga7 Ni1 111.4(5) 3 . ?
Ga7 Ga7 Ni1 111.3(5) 2 . ?
Ni1 Ga7 Ni1 130.1(9) 11 . ?
Er1 Ga7 Ga6 87.1(7) . 11 ?
Ga5 Ga7 Ga6 113.9(7) 14_544 11 ?
Ga7 Ga7 Ga6 70.9(5) 11 11 ?
Ga7 Ga7 Ga6 109.6(6) 3 11 ?
Ga7 Ga7 Ga6 65.2(7) 2 11 ?
Ni1 Ga7 Ga6 55.0(2) 11 11 ?
Ni1 Ga7 Ga6 127.7(6) . 11 ?
Er1 Ga7 Ga6 87.5(7) . . ?
Ga5 Ga7 Ga6 113.7(7) 14_544 . ?
Ga7 Ga7 Ga6 70.7(5) 11 . ?
Ga7 Ga7 Ga6 109.7(6) 3 . ?
Ga7 Ga7 Ga6 65.3(7) 2 . ?
Ni1 Ga7 Ga6 127.7(6) 11 . ?
Ni1 Ga7 Ga6 55.0(2) . . ?
Ga6 Ga7 Ga6 81.6(4) 11 . ?
Er1 Ga7 Ga6 86.8(7) . 12_445 ?
Ga5 Ga7 Ga6 71.6(5) 14_544 12_445 ?
Ga7 Ga7 Ga6 114.7(6) 11 12_445 ?
Ga7 Ga7 Ga6 64.9(7) 3 12_445 ?
Ga7 Ga7 Ga6 109.4(6) 2 12_445 ?
Ni1 Ga7 Ga6 55.5(2) 11 12_445 ?
Ni1 Ga7 Ga6 127.9(7) . 12_445 ?
Ga6 Ga7 Ga6 98.2(3) 11 12_445 ?
Ga6 Ga7 Ga6 174.3(9) . 12_445 ?
Er1 Ga7 Ga6 87.1(7) . 3 ?
Ga5 Ga7 Ga6 71.5(5) 14_544 3 ?
Ga7 Ga7 Ga6 114.6(6) 11 3 ?
Ga7 Ga7 Ga6 64.9(7) 3 3 ?
Ga7 Ga7 Ga6 109.4(6) 2 3 ?
Ni1 Ga7 Ga6 127.9(7) 11 3 ?
Ni1 Ga7 Ga6 55.4(2) . 3 ?
Ga6 Ga7 Ga6 174.2(9) 11 3 ?
Ga6 Ga7 Ga6 98.2(3) . 3 ?
Ga6 Ga7 Ga6 81.3(4) 12_445 3 ?
Er1 Ga7 Er1 138.2(9) . 10 ?
Ga5 Ga7 Er1 70.5(6) 14_544 10 ?
Ga7 Ga7 Er1 12.4(4) 11 10 ?
Ga7 Ga7 Er1 168.2(9) 3 10 ?
Ga7 Ga7 Er1 108.2(9) 2 10 ?
Ni1 Ga7 Er1 71.7(5) 11 10 ?
Ni1 Ga7 Er1 71.5(5) . 10 ?
Ga6 Ga7 Er1 62.2(3) 11 10 ?
Ga6 Ga7 Er1 61.9(3) . 10 ?
Ga6 Ga7 Er1 123.1(6) 12_445 10 ?
Ga6 Ga7 Er1 122.9(6) 3 10 ?
Ni1 Ga1 Ni1 108.22(15) 9 8_445 ?
Ni1 Ga1 Ni1 108.22(15) 9 7_455 ?
Ni1 Ga1 Ni1 108.21(15) 8_445 7_455 ?
Ni1 Ga1 Ga6 54.44(8) 9 7_445 ?
Ni1 Ga1 Ga6 54.48(8) 8_445 7_445 ?
Ni1 Ga1 Ga6 129.7(2) 7_455 7_445 ?
Ni1 Ga1 Ga6 54.48(8) 9 8 ?
Ni1 Ga1 Ga6 129.7(2) 8_445 8 ?
Ni1 Ga1 Ga6 54.44(8) 7_455 8 ?
Ga6 Ga1 Ga6 97.68(15) 7_445 8 ?
Ni1 Ga1 Ga6 129.7(2) 9 9_455 ?
Ni1 Ga1 Ga6 54.44(8) 8_445 9_455 ?
Ni1 Ga1 Ga6 54.47(8) 7_455 9_455 ?
Ga6 Ga1 Ga6 97.68(15) 7_445 9_455 ?
Ga6 Ga1 Ga6 97.68(15) 8 9_455 ?
Ni1 Ga1 Ga2 110.70(15) 9 . ?
Ni1 Ga1 Ga2 110.70(15) 8_445 . ?
Ni1 Ga1 Ga2 110.70(15) 7_455 . ?
Ga6 Ga1 Ga2 119.62(12) 7_445 . ?
Ga6 Ga1 Ga2 119.62(12) 8 . ?
Ga6 Ga1 Ga2 119.62(12) 9_455 . ?
Ni1 Ga1 Ga4 50.81(10) 9 9 ?
Ni1 Ga1 Ga4 125.53(8) 8_445 9 ?
Ni1 Ga1 Ga4 125.64(8) 7_455 9 ?
Ga6 Ga1 Ga4 82.59(7) 7_445 9 ?
Ga6 Ga1 Ga4 82.70(8) 8 9 ?
Ga6 Ga1 Ga4 179.50(19) 9_455 9 ?
Ga2 Ga1 Ga4 59.89(9) . 9 ?
Ni1 Ga1 Ga4 125.64(8) 9 8_445 ?
Ni1 Ga1 Ga4 50.81(10) 8_445 8_445 ?
Ni1 Ga1 Ga4 125.53(8) 7_455 8_445 ?
Ga6 Ga1 Ga4 82.70(8) 7_445 8_445 ?
Ga6 Ga1 Ga4 179.50(19) 8 8_445 ?
Ga6 Ga1 Ga4 82.59(7) 9_455 8_445 ?
Ga2 Ga1 Ga4 59.89(9) . 8_445 ?
Ga4 Ga1 Ga4 97.03(12) 9 8_445 ?
Ni1 Ga1 Ga4 125.53(8) 9 7_455 ?
Ni1 Ga1 Ga4 125.64(8) 8_445 7_455 ?
Ni1 Ga1 Ga4 50.81(10) 7_455 7_455 ?
Ga6 Ga1 Ga4 179.50(19) 7_445 7_455 ?
Ga6 Ga1 Ga4 82.59(7) 8 7_455 ?
Ga6 Ga1 Ga4 82.70(8) 9_455 7_455 ?
Ga2 Ga1 Ga4 59.89(9) . 7_455 ?
Ga4 Ga1 Ga4 97.03(12) 9 7_455 ?
Ga4 Ga1 Ga4 97.03(12) 8_445 7_455 ?
Ni1 Ga1 Er2 69.30(15) 9 . ?
Ni1 Ga1 Er2 69.30(15) 8_445 . ?
Ni1 Ga1 Er2 69.30(15) 7_455 . ?
Ga6 Ga1 Er2 60.38(12) 7_445 . ?
Ga6 Ga1 Er2 60.38(12) 8 . ?
Ga6 Ga1 Er2 60.38(12) 9_455 . ?
Ga2 Ga1 Er2 180.0 . . ?
Ga4 Ga1 Er2 120.11(9) 9 . ?
Ga4 Ga1 Er2 120.11(9) 8_445 . ?
Ga4 Ga1 Er2 120.11(9) 7_455 . ?
Ni1 Ga2 Ni1 107.04(16) 11 12_445 ?
Ni1 Ga2 Ni1 107.04(16) 11 10_455 ?
Ni1 Ga2 Ni1 107.03(16) 12_445 10_455 ?
Ni1 Ga2 Ga1 111.81(15) 11 . ?
Ni1 Ga2 Ga1 111.81(15) 12_445 . ?
Ni1 Ga2 Ga1 111.81(15) 10_455 . ?
Ni1 Ga2 Ga4 51.31(10) 11 9 ?
Ni1 Ga2 Ga4 125.29(7) 12_445 9 ?
Ni1 Ga2 Ga4 126.60(8) 10_455 9 ?
Ga1 Ga2 Ga4 60.50(9) . 9 ?
Ni1 Ga2 Ga4 126.60(8) 11 8_445 ?
Ni1 Ga2 Ga4 51.31(10) 12_445 8_445 ?
Ni1 Ga2 Ga4 125.29(7) 10_455 8_445 ?
Ga1 Ga2 Ga4 60.51(9) . 8_445 ?
Ga4 Ga2 Ga4 97.84(12) 9 8_445 ?
Ni1 Ga2 Ga4 125.29(7) 11 7_455 ?
Ni1 Ga2 Ga4 126.59(8) 12_445 7_455 ?
Ni1 Ga2 Ga4 51.31(10) 10_455 7_455 ?
Ga1 Ga2 Ga4 60.51(9) . 7_455 ?
Ga4 Ga2 Ga4 97.84(12) 9 7_455 ?
Ga4 Ga2 Ga4 97.84(12) 8_445 7_455 ?
Ni1 Ga2 Ga6 54.27(8) 11 12_445 ?
Ni1 Ga2 Ga6 53.74(8) 12_445 12_445 ?
Ni1 Ga2 Ga6 128.2(2) 10_455 12_445 ?
Ga1 Ga2 Ga6 119.97(12) . 12_445 ?
```

Ga4 Ga2 Ga6 82.17(8) 9 12_445 ?
Ga4 Ga2 Ga6 82.76(8) 8_445 12_445 ?
Ga4 Ga2 Ga6 179.39(16) 7_455 12_445 ?
Ni1 Ga2 Ga6 53.74(8) 11 11 ?
Ni1 Ga2 Ga6 128.2(2) 12_445 11 ?
Ni1 Ga2 Ga6 54.27(8) 10_455 11 ?
Ga1 Ga2 Ga6 119.97(12) . 11 ?
Ga4 Ga2 Ga6 82.76(8) 9 11 ?
Ga4 Ga2 Ga6 179.39(16) 8_445 11 ?
Ga4 Ga2 Ga6 82.17(8) 7_455 11 ?
Ga6 Ga2 Ga6 97.23(16) 12_445 11 ?
Ni1 Ga2 Ga6 128.2(2) 11 10_455 ?
Ni1 Ga2 Ga6 54.27(8) 12_445 10_455 ?
Ni1 Ga2 Ga6 53.74(8) 10_455 10_455 ?
Ga1 Ga2 Ga6 119.97(12) . 10_455 ?
Ga4 Ga2 Ga6 179.39(16) 9 10_455 ?
Ga4 Ga2 Ga6 82.17(8) 8_445 10_455 ?
Ga4 Ga2 Ga6 82.76(8) 7_455 10_455 ?
Ga6 Ga2 Ga6 97.23(16) 12_445 10_455 ?
Ga6 Ga2 Ga6 97.22(16) 11 10_455 ?
Ni1 Ga2 Er1 68.19(15) 11 . ?
Ni1 Ga2 Er1 68.19(15) 12_445 . ?
Ni1 Ga2 Er1 68.19(15) 10_455 . ?
Ga1 Ga2 Er1 180.0 . . ?
Ga4 Ga2 Er1 119.50(9) 9 . ?
Ga4 Ga2 Er1 119.49(9) 8_445 . ?
Ga4 Ga2 Er1 119.49(9) 7_455 . ?
Ga6 Ga2 Er1 60.03(12) 12_445 . ?
Ga6 Ga2 Er1 60.03(12) 11 . ?
Ga6 Ga2 Er1 60.03(12) 10_455 . ?
Ni1 Ga3 Ni1 107.27(16) . 2 ?
Ni1 Ga3 Ni1 107.27(16) . 3 ?
Ni1 Ga3 Ni1 107.27(16) 2 3 ?
Ni1 Ga3 Ga3 111.59(15) . 4 ?
Ni1 Ga3 Ga3 111.59(15) 2 4 ?
Ni1 Ga3 Ga3 111.59(15) 3 4 ?
Ni1 Ga3 Ga4 126.48(6) . 3 ?
Ni1 Ga3 Ga4 125.28(6) 2 3 ?
Ni1 Ga3 Ga4 51.28(10) 3 3 ?
Ga3 Ga3 Ga4 60.32(9) 4 3 ?
Ni1 Ga3 Ga4 125.28(6) . 2 ?
Ni1 Ga3 Ga4 51.28(10) 2 2 ?
Ni1 Ga3 Ga4 126.48(6) 3 2 ?
Ga3 Ga3 Ga4 60.32(9) 4 2 ?
Ga4 Ga3 Ga4 97.60(12) 3 2 ?
Ni1 Ga3 Ga4 51.28(10) . . ?
Ni1 Ga3 Ga4 126.48(6) 2 . ?
Ni1 Ga3 Ga4 125.28(6) 3 . ?
Ga3 Ga3 Ga4 60.32(9) 4 . ?
Ga4 Ga3 Ga4 97.60(12) 3 . ?
Ga4 Ga3 Ga4 97.60(12) 2 . ?
Ni1 Ga3 Ga6 53.83(8) . . ?
Ni1 Ga3 Ga6 54.40(8) 2 . ?
Ni1 Ga3 Ga6 128.7(2) 3 . ?
Ga3 Ga3 Ga6 119.72(12) 4 . ?
Ga4 Ga3 Ga6 179.68(9) 3 . ?
Ga4 Ga3 Ga6 82.19(7) 2 . ?
Ga4 Ga3 Ga6 82.67(7) . . ?
Ni1 Ga3 Ga6 128.7(2) . 2 ?
Ni1 Ga3 Ga6 53.83(8) 2 2 ?
Ni1 Ga3 Ga6 54.40(8) 3 2 ?
Ga3 Ga3 Ga6 119.72(12) 4 2 ?
Ga4 Ga3 Ga6 82.19(7) 3 2 ?
Ga4 Ga3 Ga6 82.67(7) 2 2 ?
Ga4 Ga3 Ga6 179.68(9) . 2 ?
Ga6 Ga3 Ga6 97.54(16) . 2 ?
Ni1 Ga3 Ga6 54.40(8) . 3 ?
Ni1 Ga3 Ga6 128.7(2) 2 3 ?
Ni1 Ga3 Ga6 53.83(8) 3 3 ?
Ga3 Ga3 Ga6 119.72(12) 4 3 ?
Ga4 Ga3 Ga6 82.67(7) 3 3 ?
Ga4 Ga3 Ga6 179.68(9) 2 3 ?
Ga4 Ga3 Ga6 82.19(7) . 3 ?
Ga6 Ga3 Ga6 97.54(16) . 3 ?
Ga6 Ga3 Ga6 97.54(16) 2 3 ?
Ni1 Ga3 Er1 68.41(15) . . ?
Ni1 Ga3 Er1 68.41(15) 2 . ?
Ni1 Ga3 Er1 68.41(15) 3 . ?
Ga3 Ga3 Er1 180.0 4 . ?
Ga4 Ga3 Er1 119.68(9) 3 . ?
Ga4 Ga3 Er1 119.68(9) 2 . ?
Ga4 Ga3 Er1 119.68(9) . . ?
Ga6 Ga3 Er1 60.28(12) . . ?
Ga6 Ga3 Er1 60.28(12) 2 . ?
Ga6 Ga3 Er1 60.28(12) 3 . ?
Ni1 Ga4 Ni1 179.02(15) 4 . ?
Ni1 Ga4 Ga2 120.36(11) 4 10 ?
Ni1 Ga4 Ga2 60.13(10) . 10 ?
Ni1 Ga4 Ga2 60.13(10) 4 13_544 ?
Ni1 Ga4 Ga2 120.36(11) . 13_544 ?
Ga2 Ga4 Ga2 128.45(10) 10 13_544 ?
Ni1 Ga4 Ga3 59.84(11) 4 4 ?
Ni1 Ga4 Ga3 119.19(13) . 4 ?
Ga2 Ga4 Ga3 128.43(6) 10 4 ?
Ga2 Ga4 Ga3 97.70(12) 13_544 4 ?
Ni1 Ga4 Ga3 119.19(13) 4 . ?
Ni1 Ga4 Ga3 59.84(11) . . ?
Ga2 Ga4 Ga3 97.70(12) 10 . ?
Ga2 Ga4 Ga3 128.43(6) 13_544 . ?
Ga3 Ga4 Ga3 59.36(19) 4 . ?
Ni1 Ga4 Ga1 60.75(10) 4 10 ?
Ni1 Ga4 Ga1 119.73(11) . 10 ?
Ga2 Ga4 Ga1 59.61(18) 10 10 ?
Ga2 Ga4 Ga1 97.48(12) 13_544 10 ?
Ga3 Ga4 Ga1 97.30(12) 4 10 ?
Ga3 Ga4 Ga1 128.60(6) . 10 ?
Ni1 Ga4 Ga1 119.73(11) 4 13_544 ?
Ni1 Ga4 Ga1 60.75(10) . 13_544 ?
Ga2 Ga4 Ga1 97.48(12) 10 13_544 ?
Ga2 Ga4 Ga1 59.61(18) 13_544 13_544 ?
Ga3 Ga4 Ga1 128.60(6) 4 13_544 ?
Ga3 Ga4 Ga1 97.30(12) . 13_544 ?
Ga1 Ga4 Ga1 128.79(10) 10 13_544 ?
Ga4 Ni1 Ga6 101.18(15) . . ?
Ga4 Ni1 Ga5 156.17(13) . 14_544 ?
Ga6 Ni1 Ga5 102.65(19) . 14_544 ?
Ga4 Ni1 Ga6 99.72(17) . 2_655 ?
Ga6 Ni1 Ga6 117.80(15) . 2_655 ?
Ga5 Ni1 Ga6 68.78(13) 14_544 2_655 ?
Ga4 Ni1 Ga6 99.82(16) . 3 ?
Ga6 Ni1 Ga6 118.04(15) . 3 ?
Ga5 Ni1 Ga6 68.82(13) 14_544 3 ?
Ga6 Ni1 Ga6 114.87(13) 2_655 3 ?
Ga4 Ni1 Ga7 155.4(5) . 11 ?
Ga6 Ni1 Ga7 68.6(4) . 11 ?
Ga5 Ni1 Ga7 41.0(5) 14_544 11 ?
Ga6 Ni1 Ga7 68.4(4) 2_655 11 ?
Ga6 Ni1 Ga7 104.7(5) 3 11 ?
Ga4 Ni1 Ga7 155.6(5) . . ?
Ga6 Ni1 Ga7 68.7(4) . . ?
Ga5 Ni1 Ga7 41.0(5) 14_544 . ?
Ga6 Ni1 Ga7 104.7(5) 2_655 . ?
Ga6 Ni1 Ga7 68.5(4) 3 . ?
Ga7 Ni1 Ga7 43.2(9) 11 . ?
Ga4 Ni1 Ga3 68.89(16) . . ?
Ga6 Ni1 Ga3 67.62(9) . . ?
Ga5 Ni1 Ga3 121.12(16) 14_544 . ?
Ga6 Ni1 Ga3 168.5(3) 2_655 . ?
Ga6 Ni1 Ga3 67.28(9) 3 . ?
Ga7 Ni1 Ga3 122.6(4) 11 . ?
Ga7 Ni1 Ga3 86.7(5) . . ?
Ga4 Ni1 Ga2 68.56(15) . 10 ?
Ga6 Ni1 Ga2 67.58(9) . 10 ?
Ga5 Ni1 Ga2 121.25(16) 14_544 10 ?

```
Ga6 Ni1 Ga2 67.27(9) 2_655 10 ?
Ga6 Ni1 Ga2 168.3(2) 3 10 ?
Ga7 Ni1 Ga2 86.8(5) 11 10 ?
Ga7 Ni1 Ga2 122.8(4) . 10 ?
Ga3 Ni1 Ga2 108.26(17) . 10 ?
Ga4 Ni1 Ga1 68.44(15) . 13_544 ?
Ga6 Ni1 Ga1 169.6(3) . 13_544 ?
Ga5 Ni1 Ga1 87.74(16) 14_544 13_544 ?
Ga6 Ni1 Ga1 65.63(9) 2_655 13_544 ?
Ga6 Ni1 Ga1 65.62(9) 3 13_544 ?
Ga7 Ni1 Ga1 120.8(4) 11 13_544 ?
Ga7 Ni1 Ga1 120.9(4) . 13_544 ?
Ga3 Ni1 Ga1 107.22(16) . 13_544 ?
Ga2 Ni1 Ga1 107.03(16) 10 13_544 ?
Ga4 Ni1 Er1 133.42(10) . 10 ?
Ga6 Ni1 Er1 61.66(11) . 10 ?
Ga5 Ni1 Er1 60.68(10) 14_544 10 ?
Ga6 Ni1 Er1 61.50(11) 2_655 10 ?
Ga6 Ni1 Er1 126.69(18) 3 10 ?
Ga7 Ni1 Er1 22.0(5) 11 10 ?
Ga7 Ni1 Er1 62.7(4) . 10 ?
Ga3 Ni1 Er1 127.26(12) . 10 ?
Ga2 Ni1 Er1 64.87(12) 10 10 ?
Ga1 Ni1 Er1 125.11(11) 13_544 10 ?
Ga4 Ni1 Er1 133.75(11) . . ?
Ga6 Ni1 Er1 61.81(11) . . ?
Ga5 Ni1 Er1 60.54(11) 14_544 . ?
Ga6 Ni1 Er1 126.48(18) 2_655 . ?
Ga6 Ni1 Er1 61.64(11) 3 . ?
Ga7 Ni1 Er1 62.6(4) 11 . ?
Ga7 Ni1 Er1 21.8(5) . . ?
Ga3 Ni1 Er1 64.87(13) . . ?
Ga2 Ni1 Er1 127.38(11) 10 . ?
Ga1 Ni1 Er1 125.17(11) 13_544 . ?
Er1 Ni1 Er1 79.00(10) 10 . ?
Ni1 Ga6 Ni1 115.99(14) . 3_665 ?
Ni1 Ga6 Ni1 115.75(14) . 2 ?
Ni1 Ga6 Ni1 118.97(15) 3_665 2 ?
Ni1 Ga6 Ga1 140.1(2) . 13_554 ?
Ni1 Ga6 Ga1 59.92(9) 3_665 13_554 ?
Ni1 Ga6 Ga1 59.91(9) 2 13_554 ?
Ni1 Ga6 Ga5 134.67(17) . 13_554 ?
Ni1 Ga6 Ga5 55.30(11) 3_665 13_554 ?
Ni1 Ga6 Ga5 103.64(12) 2 13_554 ?
Ga1 Ga6 Ga5 78.86(10) 13_554 13_554 ?
Ni1 Ga6 Ga7 56.4(3) . 11 ?
Ni1 Ga6 Ga7 99.1(5) 3_665 11 ?
Ni1 Ga6 Ga7 136.3(4) 2 11 ?
Ga1 Ga6 Ga7 156.3(5) 13_554 11 ?
Ga5 Ga6 Ga7 79.9(4) 13_554 11 ?
Ni1 Ga6 Ga5 134.52(17) . 15_554 ?
Ni1 Ga6 Ga5 103.65(13) 3_665 15_554 ?
Ni1 Ga6 Ga5 55.26(11) 2 15_554 ?
Ga1 Ga6 Ga5 78.82(10) 13_554 15_554 ?
Ga5 Ga6 Ga5 55.75(15) 13_554 15_554 ?
Ga7 Ga6 Ga5 97.6(3) 11 15_554 ?
Ni1 Ga6 Ga7 56.4(3) . . ?
Ni1 Ga6 Ga7 136.4(4) 3_665 . ?
Ni1 Ga6 Ga7 98.9(5) 2 . ?
Ga1 Ga6 Ga7 156.2(4) 13_554 . ?
Ga5 Ga6 Ga7 97.5(3) 13_554 . ?
Ga7 Ga6 Ga7 38.5(9) 11 . ?
Ga5 Ga6 Ga7 79.8(4) 15_554 . ?
Ni1 Ga6 Ga7 99.3(5) . 12 ?
Ni1 Ga6 Ga7 56.1(3) 3_665 12 ?
Ni1 Ga6 Ga7 138.3(4) 2 12 ?
Ga1 Ga6 Ga7 106.5(4) 13_554 12 ?
Ga5 Ga6 Ga7 36.2(5) 13_554 12 ?
Ga7 Ga6 Ga7 49.9(9) 11 12 ?
Ga5 Ga6 Ga7 84.3(4) 15_554 12 ?
Ga7 Ga6 Ga7 81.62(13) . 12 ?
Ni1 Ga6 Ga7 99.2(5) . 2 ?
Ni1 Ga6 Ga7 138.3(4) 3_665 2 ?
Ni1 Ga6 Ga7 56.0(3) 2 2 ?
Ga1 Ga6 Ga7 106.4(4) 13_554 2 ?
Ga5 Ga6 Ga7 84.3(4) 13_554 2 ?
Ga7 Ga6 Ga7 81.59(13) 11 2 ?
Ga5 Ga6 Ga7 36.2(5) 15_554 2 ?
Ga7 Ga6 Ga7 49.8(8) . 2 ?
Ga7 Ga6 Ga7 98.4(4) 12 2 ?
Ni1 Ga6 Ga3 58.55(8) . . ?
Ni1 Ga6 Ga3 140.0(2) 3_665 . ?
Ni1 Ga6 Ga3 58.32(8) 2 . ?
Ga1 Ga6 Ga3 97.81(16) 13_554 . ?
Ga5 Ga6 Ga3 159.29(13) 13_554 . ?
Ga7 Ga6 Ga3 105.7(4) 11 . ?
Ga5 Ga6 Ga3 103.55(11) 15_554 . ?
Ga7 Ga6 Ga3 77.2(3) . . ?
Ga7 Ga6 Ga3 155.5(4) 12 . ?
Ga7 Ga6 Ga3 77.0(3) 2 . ?
Ni1 Ga6 Ga2 58.68(9) . 10 ?
Ni1 Ga6 Ga2 58.46(9) 3_665 10 ?
Ni1 Ga6 Ga2 139.8(2) 2 10 ?
Ga1 Ga6 Ga2 97.76(16) 13_554 10 ?
Ga5 Ga6 Ga2 103.82(11) 13_554 10 ?
Ga7 Ga6 Ga2 77.4(3) 11 10 ?
Ga5 Ga6 Ga2 159.56(13) 15_554 10 ?
Ga7 Ga6 Ga2 105.9(4) . 10 ?
Ga7 Ga6 Ga2 77.3(3) 12 10 ?
Ga7 Ga6 Ga2 155.6(4) 2 10 ?
Ga3 Ga6 Ga2 96.87(15) . 10 ?

_diffrn_measured_fraction_theta_max    0.870
_diffrn_reflns_theta_full              30.17
_diffrn_measured_fraction_theta_full   0.870
_refine_diff_density_max    8.534
_refine_diff_density_min   -9.969
_refine_diff_density_rms    1.431
```

A2.6 $TmNi_3Ga_9$

```
data_tmni3ga9

_audit_creation_method            SHELXL-97
_chemical_name_systematic
;
 ?
;
_chemical_name_common             ?
_chemical_melting_point           ?
_chemical_formula_moiety          ?
_chemical_formula_sum
 'Ga9 Ni3 Tm'
_chemical_formula_weight          972.54

loop_
 _atom_type_symbol
 _atom_type_description
 _atom_type_scat_dispersion_real
 _atom_type_scat_dispersion_imag
 _atom_type_scat_source
 'Ni'  'Ni'   0.3393   1.1124
 'International Tables Vol C Tables 4.2.6.8
and 6.1.1.4'
 'Ga'  'Ga'   0.2307   1.6083
 'International Tables Vol C Tables 4.2.6.8
and 6.1.1.4'
 'Tm'  'Tm'  -0.3139   5.2483
 'International Tables Vol C Tables 4.2.6.8
and 6.1.1.4'

_symmetry_cell_setting            ?
_symmetry_space_group_name_H-M    ?

loop_
 _symmetry_equiv_pos_as_xyz
 'x, y, z'
 '-y, x-y, z'
 '-x+y, -x, z'
 'x-y, -y, -z'
 '-x, -x+y, -z'
 'y, x, -z'
 'x+2/3, y+1/3, z+1/3'
 '-y+2/3, x-y+1/3, z+1/3'
 '-x+y+2/3, -x+1/3, z+1/3'
 'x-y+2/3, -y+1/3, -z+1/3'
 '-x+2/3, -x+y+1/3, -z+1/3'
 'y+2/3, x+1/3, -z+1/3'
 'x+1/3, y+2/3, z+2/3'
 '-y+1/3, x-y+2/3, z+2/3'
 '-x+y+1/3, -x+2/3, z+2/3'
 'x-y+1/3, -y+2/3, -z+2/3'
 '-x+1/3, -x+y+2/3, -z+2/3'
 'y+1/3, x+2/3, -z+2/3'

_cell_length_a                    7.2307(4)
_cell_length_b                    7.2307(4)
_cell_length_c                    27.399(2)
_cell_angle_alpha                 90.00
_cell_angle_beta                  90.00
_cell_angle_gamma                 120.00
_cell_volume
1240.60(14)
_cell_formula_units_Z             6
_cell_measurement_temperature     298(2)
_cell_measurement_reflns_used     ?
_cell_measurement_theta_min       ?
_cell_measurement_theta_max       ?

_exptl_crystal_description        ?
_exptl_crystal_colour             ?
_exptl_crystal_size_max           0.05
_exptl_crystal_size_mid           0.03
_exptl_crystal_size_min           0.03
_exptl_crystal_density_meas       ?
_exptl_crystal_density_diffrn     7.810
_exptl_crystal_density_method           'not
measured'
_exptl_crystal_F_000              2592
_exptl_absorpt_coefficient_mu     45.950
_exptl_absorpt_correction_type    ?
_exptl_absorpt_correction_T_min   0.2072
_exptl_absorpt_correction_T_max   0.3929
_exptl_absorpt_process_details    ?

_exptl_special_details
;
 ?
;

_diffrn_ambient_temperature       298(2)
_diffrn_radiation_wavelength      0.71073
_diffrn_radiation_type            MoK\a
_diffrn_radiation_source              'fine-
focus sealed tube'
_diffrn_radiation_monochromator   graphite
_diffrn_measurement_device_type   ?
_diffrn_measurement_method        ?
_diffrn_detector_area_resol_mean  ?
_diffrn_standards_number          ?
_diffrn_standards_interval_count  ?
_diffrn_standards_interval_time   ?
_diffrn_standards_decay_%         ?
_diffrn_reflns_number             2086
_diffrn_reflns_av_R_equivalents   0.0807
_diffrn_reflns_av_sigmaI/netI     0.0691
_diffrn_reflns_limit_h_min        -8
_diffrn_reflns_limit_h_max        9
_diffrn_reflns_limit_k_min        -10
_diffrn_reflns_limit_k_max        8
_diffrn_reflns_limit_l_min        -24
_diffrn_reflns_limit_l_max        38
_diffrn_reflns_theta_min          3.34
_diffrn_reflns_theta_max          29.93
_reflns_number_total              806
_reflns_number_gt                 659
_reflns_threshold_expression      >2sigma(I)

_computing_data_collection        ?
_computing_cell_refinement        ?
_computing_data_reduction         ?
_computing_structure_solution     ?
_computing_structure_refinement    'SHELXL-97
(Sheldrick, 1997)'
_computing_molecular_graphics     ?
_computing_publication_material   ?

_refine_special_details
;
 Refinement of F^2^ against ALL reflections.
The weighted R-factor wR and
 goodness of fit S are based on F^2^,
conventional R-factors R are based
 on F, with F set to zero for negative F^2^.
The threshold expression of
 F^2^ > 2sigma(F^2^) is used only for
calculating R-factors(gt) etc. and is
 not relevant to the choice of reflections
for refinement.  R-factors based
```

```
 on F^2^ are statistically about twice as
large as those based on F, and R-
 factors based on ALL data will be even
larger.
;

_refine_ls_structure_factor_coef  Fsqd
_refine_ls_matrix_type            full
_refine_ls_weighting_scheme       calc
_refine_ls_weighting_details
 'calc
w=1/[\s^2^(Fo^2^)+(0.0631P)^2^+0.0000P]
where P=(Fo^2^+2Fc^2^)/3'
_atom_sites_solution_primary      direct
_atom_sites_solution_secondary    difmap
_atom_sites_solution_hydrogens    geom
_refine_ls_hydrogen_treatment     mixed
_refine_ls_extinction_method      SHELXL
_refine_ls_extinction_coef        0.0041(2)
_refine_ls_extinction_expression
 'Fc^*^=kFc[1+0.001xFc^2^\l^3^/sin(2\q)]^-
1/4^'
_refine_ls_abs_structure_details
 'Flack H D (1983), Acta Cryst. A39, 876-
881'
_refine_ls_abs_structure_Flack    -0.09(8)
_refine_ls_number_reflns          806
_refine_ls_number_parameters      45
_refine_ls_number_restraints      0
_refine_ls_R_factor_all           0.0634
_refine_ls_R_factor_gt            0.0469
_refine_ls_wR_factor_ref          0.1253
_refine_ls_wR_factor_gt           0.1111
_refine_ls_goodness_of_fit_ref    1.062
_refine_ls_restrained_S_all       1.062
_refine_ls_shift/su_max           0.000
_refine_ls_shift/su_mean          0.000

loop_
 _atom_site_label
 _atom_site_type_symbol
 _atom_site_fract_x
 _atom_site_fract_y
 _atom_site_fract_z
 _atom_site_U_iso_or_equiv
 _atom_site_adp_type
 _atom_site_occupancy
 _atom_site_symmetry_multiplicity
 _atom_site_calc_flag
 _atom_site_refinement_flags
 _atom_site_disorder_assembly
 _atom_site_disorder_group
Ga1 Ga 0.0000 0.0000 0.38492(9) 0.0070(5)
Uani 1 3 d S . .
Ga2 Ga 0.0000 0.0000 0.28290(9) 0.0070(5)
Uani 1 3 d S . .
Ga3 Ga 0.0000 0.0000 0.05084(9) 0.0068(5)
Uani 1 3 d S . .
Ga4 Ga 0.3334(2) 0.0000 0.0000 0.0088(5)
Uani 1 2 d S . .
Tm1 Tm 0.0000 0.0000 0.16694(3) 0.0053(3)
Uani 0.88 3 d SP . .
Tm2 Tm 0.0000 0.0000 0.5000 0.0053(3) Uani
0.25 6 d SP . .
Ni1 Ni 0.3375(2) -0.0003(2) 0.41838(8)
0.0052(5) Uani 1 1 d . . .
Ga6 Ga 0.3331(2) 0.3356(2) 0.10125(9)
0.0063(4) Uani 1 1 d . . .
Ga5 Ga 0.2099(3) 0.0000 0.5000 0.0062(6)
Uani 0.76 2 d SP . .
Ga7 Ga 0.2126(19) 0.0014(17) 0.1671(4)
0.0062(6) Uani 0.12 1 d P . .

loop_
 _atom_site_aniso_label
 _atom_site_aniso_U_11
 _atom_site_aniso_U_22
 _atom_site_aniso_U_33
 _atom_site_aniso_U_23
 _atom_site_aniso_U_13
 _atom_site_aniso_U_12
Ga1 0.0061(7) 0.0061(7) 0.0086(11) 0.000
0.000 0.0031(3)
Ga2 0.0064(7) 0.0064(7) 0.0083(10) 0.000
0.000 0.0032(3)
Ga3 0.0059(7) 0.0059(7) 0.0086(11) 0.000
0.000 0.0029(3)
Ga4 0.0113(8) 0.0120(9) 0.0034(11) -
0.0002(6) -0.0001(3) 0.0060(5)
Tm1 0.0042(4) 0.0042(4) 0.0077(6) 0.000
0.000 0.00208(18)
Tm2 0.0042(4) 0.0042(4) 0.0077(6) 0.000
0.000 0.00208(18)
Ni1 0.0051(8) 0.0052(8) 0.0049(9) -0.0004(5)
0.0005(5) 0.0023(6)
Ga6 0.0047(8) 0.0054(8) 0.0092(7) -0.0004(6)
0.0002(6) 0.0029(6)
Ga5 0.0052(8) 0.0041(11) 0.0090(12)
0.0013(10) 0.0007(5) 0.0020(5)
Ga7 0.0052(8) 0.0041(11) 0.0090(12)
0.0013(10) 0.0007(5) 0.0020(5)

_geom_special_details
;
 All esds (except the esd in the dihedral
angle between two l.s. planes)
 are estimated using the full covariance
matrix.  The cell esds are taken
 into account individually in the estimation
of esds in distances, angles
 and torsion angles; correlations between
esds in cell parameters are only
 used when they are defined by crystal
symmetry.  An approximate (isotropic)
 treatment of cell esds is used for
estimating esds involving l.s. planes.
;

loop_
 _geom_bond_atom_site_label_1
 _geom_bond_atom_site_label_2
 _geom_bond_distance
 _geom_bond_site_symmetry_2
 _geom_bond_publ_flag
Ga1 Ni1 2.6077(18) 2 ?
Ga1 Ni1 2.6077(18) . ?
Ga1 Ni1 2.6077(18) 3 ?
Ga1 Ga6 2.753(2) 7_445 ?
Ga1 Ga6 2.753(2) 8 ?
Ga1 Ga6 2.753(2) 9_455 ?
Ga1 Ga4 2.7939(15) 9 ?
Ga1 Ga4 2.7940(15) 8_445 ?
Ga1 Ga4 2.7940(15) 7_455 ?
Ga1 Ga2 2.795(4) . ?
Ga1 Tm2 3.153(3) . ?
Ga2 Ni1 2.5744(19) 17 ?
Ga2 Ni1 2.5744(19) 16_445 ?
Ga2 Ni1 2.5744(19) 18_545 ?
Ga2 Ga4 2.7782(14) 9 ?
Ga2 Ga4 2.7783(14) 8_445 ?
Ga2 Ga4 2.7783(14) 7_455 ?
Ga2 Ga6 2.792(2) 12_445 ?
Ga2 Ga6 2.792(2) 11 ?
Ga2 Ga6 2.792(2) 10_455 ?
```

```
Ga2 Tm1 3.177(3) . ?
Ga3 Ni1 2.5733(19) 15_554 ?
Ga3 Ni1 2.5733(19) 13_444 ?
Ga3 Ni1 2.5733(19) 14_544 ?
Ga3 Ga4 2.7839(19) 3 ?
Ga3 Ga4 2.7839(19) 2 ?
Ga3 Ga4 2.7839(19) . ?
Ga3 Ga6 2.784(2) . ?
Ga3 Ga6 2.784(2) 3 ?
Ga3 Ga6 2.784(2) 2 ?
Ga3 Ga3 2.786(5) 4 ?
Ga3 Tm1 3.181(3) . ?
Ga4 Ni1 2.330(2) 14_544 ?
Ga4 Ni1 2.330(2) 11 ?
Ga4 Ga2 2.7783(14) 10 ?
Ga4 Ga2 2.7783(14) 13_544 ?
Ga4 Ga3 2.7839(19) 4 ?
Ga4 Ga1 2.7940(15) 10 ?
Ga4 Ga1 2.7940(15) 13_544 ?
Tm1 Ga7 1.532(13) 3 ?
Tm1 Ga7 1.532(13) 2 ?
Tm1 Ga7 1.532(13) . ?
Tm1 Ga7 2.943(12) 11 ?
Tm1 Ga7 2.943(12) 12_445 ?
Tm1 Ga7 2.943(12) 10_455 ?
Tm1 Ga5 2.9590(17) 15_554 ?
Tm1 Ga5 2.9590(18) 13_444 ?
Tm1 Ga5 2.9590(18) 14_544 ?
Tm1 Ga6 3.007(2) 12_445 ?
Tm1 Ga6 3.007(2) 11 ?
Tm1 Ga6 3.007(2) 10_455 ?
Tm2 Ga5 1.518(3) 3 ?
Tm2 Ga5 1.518(2) 2 ?
Tm2 Ga5 1.518(2) . ?
Tm2 Ga7 2.955(12) 17 ?
Tm2 Ga7 2.955(12) 9 ?
Tm2 Ga7 2.955(12) 16_445 ?
Tm2 Ga7 2.955(12) 8_445 ?
Tm2 Ga7 2.955(12) 7_455 ?
Tm2 Ga7 2.955(12) 18_545 ?
Tm2 Ga6 2.9902(19) 7_445 ?
Tm2 Ga6 2.9902(19) 18_445 ?
Tm2 Ga6 2.9902(19) 16 ?
Ni1 Ga4 2.330(2) 9 ?
Ni1 Ga7 2.385(11) 18_545 ?
Ni1 Ga7 2.409(11) 9 ?
Ni1 Ga5 2.419(2) . ?
Ni1 Ga6 2.4368(17) 9 ?
Ni1 Ga6 2.4575(17) 7_445 ?
Ni1 Ga6 2.4587(17) 8 ?
Ni1 Ga3 2.5733(19) 7 ?
Ni1 Ga2 2.5744(19) 16_545 ?
Ni1 Tm1 3.2702(19) 16_545 ?
Ni1 Tm1 3.2831(19) 7 ?
Ga6 Ni1 2.4368(17) 14_544 ?
Ga6 Ni1 2.4575(17) 13_554 ?
Ga6 Ni1 2.4586(17) 15_554 ?
Ga6 Ga1 2.753(2) 13_554 ?
Ga6 Ga5 2.759(2) 15_554 ?
Ga6 Ga5 2.760(2) 13_554 ?
Ga6 Ga7 2.769(11) 11 ?
Ga6 Ga7 2.769(11) 12 ?
Ga6 Ga7 2.782(11) 2 ?
Ga6 Ga7 2.783(11) . ?
Ga6 Ga2 2.792(2) 10 ?
Ga5 Ga7 1.538(13) 9 ?
Ga5 Ga7 1.538(13) 18_545 ?
Ga5 Ni1 2.419(2) 4_556 ?
Ga5 Ga5 2.629(4) 3 ?
Ga5 Ga5 2.629(4) 2 ?
Ga5 Ga6 2.759(2) 17_545 ?
Ga5 Ga6 2.759(2) 8 ?
Ga5 Ga6 2.760(2) 16 ?
Ga5 Ga6 2.760(2) 7_445 ?
Ga5 Tm1 2.9590(18) 7 ?
Ga7 Ga7 1.51(2) 11 ?
Ga7 Ga5 1.538(13) 14_544 ?
Ga7 Ni1 2.385(11) 18_545 ?
Ga7 Ni1 2.409(11) 14_544 ?
Ga7 Ga7 2.65(2) 3 ?
Ga7 Ga7 2.65(2) 2 ?
Ga7 Ga6 2.769(11) 11 ?
Ga7 Ga6 2.769(11) 12_445 ?
Ga7 Ga6 2.782(11) 3 ?
Ga7 Tm1 2.943(12) 10 ?

loop_
 _geom_angle_atom_site_label_1
 _geom_angle_atom_site_label_2
 _geom_angle_atom_site_label_3
 _geom_angle
 _geom_angle_site_symmetry_1
 _geom_angle_site_symmetry_3
 _geom_angle_publ_flag
Ni1 Ga1 Ni1 108.33(7) 2 . ?
Ni1 Ga1 Ni1 108.33(7) 2 3 ?
Ni1 Ga1 Ni1 108.33(7) . 3 ?
Ni1 Ga1 Ga6 129.79(11) 2 7_445 ?
Ni1 Ga1 Ga6 54.49(5) . 7_445 ?
Ni1 Ga1 Ga6 54.51(4) 3 7_445 ?
Ni1 Ga1 Ga6 54.49(5) 2 8 ?
Ni1 Ga1 Ga6 54.51(4) . 8 ?
Ni1 Ga1 Ga6 129.79(11) 3 8 ?
Ga6 Ga1 Ga6 97.68(8) 7_445 8 ?
Ni1 Ga1 Ga6 54.51(4) 2 9_455 ?
Ni1 Ga1 Ga6 129.79(11) . 9_455 ?
Ni1 Ga1 Ga6 54.49(4) 3 9_455 ?
Ga6 Ga1 Ga6 97.68(8) 7_445 9_455 ?
Ga6 Ga1 Ga6 97.68(8) 8 9_455 ?
Ni1 Ga1 Ga4 125.53(5) 2 9 ?
Ni1 Ga1 Ga4 50.97(5) . 9 ?
Ni1 Ga1 Ga4 125.60(5) 3 9 ?
Ga6 Ga1 Ga4 82.84(4) 7_445 9 ?
Ga6 Ga1 Ga4 82.81(5) 8 9 ?
Ga6 Ga1 Ga4 179.23(9) 9_455 9 ?
Ni1 Ga1 Ga4 125.60(5) 2 8_445 ?
Ni1 Ga1 Ga4 125.53(5) . 8_445 ?
Ni1 Ga1 Ga4 50.97(5) 3 8_445 ?
Ga6 Ga1 Ga4 82.81(5) 7_445 8_445 ?
Ga6 Ga1 Ga4 179.23(9) 8 8_445 ?
Ga6 Ga1 Ga4 82.84(4) 9_455 8_445 ?
Ga4 Ga1 Ga4 96.67(6) 9 8_445 ?
Ni1 Ga1 Ga4 50.97(5) 2 7_455 ?
Ni1 Ga1 Ga4 125.60(5) . 7_455 ?
Ni1 Ga1 Ga4 125.53(5) 3 7_455 ?
Ga6 Ga1 Ga4 179.23(9) 7_445 7_455 ?
Ga6 Ga1 Ga4 82.84(4) 8 7_455 ?
Ga6 Ga1 Ga4 82.80(5) 9_455 7_455 ?
Ga4 Ga1 Ga4 96.67(6) 9 7_455 ?
Ga4 Ga1 Ga4 96.67(6) 8_445 7_455 ?
Ni1 Ga1 Ga2 110.59(7) 2 . ?
Ni1 Ga1 Ga2 110.59(7) . . ?
Ni1 Ga1 Ga2 110.59(7) 3 . ?
Ga6 Ga1 Ga2 119.62(6) 7_445 . ?
Ga6 Ga1 Ga2 119.62(6) 8 . ?
Ga6 Ga1 Ga2 119.62(6) 9_455 . ?
Ga4 Ga1 Ga2 59.61(5) 9 . ?
Ga4 Ga1 Ga2 59.61(5) 8_445 . ?
Ga4 Ga1 Ga2 59.61(5) 7_455 . ?
Ni1 Ga1 Tm2 69.41(7) 2 . ?
Ni1 Ga1 Tm2 69.41(7) . . ?
Ni1 Ga1 Tm2 69.41(7) 3 . ?
Ga6 Ga1 Tm2 60.38(6) 7_445 . ?
Ga6 Ga1 Tm2 60.38(6) 8 . ?
```

```
Ga6 Ga1 Tm2 60.38(6) 9_455 . ?
Ga4 Ga1 Tm2 120.39(5) 9 . ?
Ga4 Ga1 Tm2 120.39(5) 8_445 . ?
Ga4 Ga1 Tm2 120.39(5) 7_455 . ?
Ga2 Ga1 Tm2 180.0 . . ?
Ni1 Ga2 Ni1 107.24(7) 17 16_445 ?
Ni1 Ga2 Ni1 107.24(7) 17 18_545 ?
Ni1 Ga2 Ni1 107.24(7) 16_445 18_545 ?
Ni1 Ga2 Ga4 126.45(5) 17 9 ?
Ni1 Ga2 Ga4 125.37(5) 16_445 9 ?
Ni1 Ga2 Ga4 51.45(5) 18_545 9 ?
Ni1 Ga2 Ga4 125.37(5) 17 8_445 ?
Ni1 Ga2 Ga4 51.45(5) 16_445 8_445 ?
Ni1 Ga2 Ga4 126.45(5) 18_545 8_445 ?
Ga4 Ga2 Ga4 97.40(6) 9 8_445 ?
Ni1 Ga2 Ga4 51.45(5) 17 7_455 ?
Ni1 Ga2 Ga4 126.45(5) 16_445 7_455 ?
Ni1 Ga2 Ga4 125.37(5) 18_545 7_455 ?
Ga4 Ga2 Ga4 97.40(6) 9 7_455 ?
Ga4 Ga2 Ga4 97.40(6) 8_445 7_455 ?
Ni1 Ga2 Ga6 128.47(11) 17 12_445 ?
Ni1 Ga2 Ga6 53.83(4) 16_445 12_445 ?
Ni1 Ga2 Ga6 54.33(5) 18_545 12_445 ?
Ga4 Ga2 Ga6 82.43(4) 9 12_445 ?
Ga4 Ga2 Ga6 82.87(5) 8_445 12_445 ?
Ga4 Ga2 Ga6 179.70(6) 7_455 12_445 ?
Ni1 Ga2 Ga6 54.33(5) 17 11 ?
Ni1 Ga2 Ga6 128.47(11) 16_445 11 ?
Ni1 Ga2 Ga6 53.83(4) 18_545 11 ?
Ga4 Ga2 Ga6 82.87(5) 9 11 ?
Ga4 Ga2 Ga6 179.70(6) 8_445 11 ?
Ga4 Ga2 Ga6 82.43(4) 7_455 11 ?
Ga6 Ga2 Ga6 97.30(8) 12_445 11 ?
Ni1 Ga2 Ga6 53.83(4) 17 10_455 ?
Ni1 Ga2 Ga6 54.33(5) 16_445 10_455 ?
Ni1 Ga2 Ga6 128.47(11) 18_545 10_455 ?
Ga4 Ga2 Ga6 179.70(6) 9 10_455 ?
Ga4 Ga2 Ga6 82.43(4) 8_445 10_455 ?
Ga4 Ga2 Ga6 82.87(5) 7_455 10_455 ?
Ga6 Ga2 Ga6 97.29(8) 12_445 10_455 ?
Ga6 Ga2 Ga6 97.29(8) 11 10_455 ?
Ni1 Ga2 Ga1 111.62(7) 17 . ?
Ni1 Ga2 Ga1 111.62(7) 16_445 . ?
Ni1 Ga2 Ga1 111.62(7) 18_545 . ?
Ga4 Ga2 Ga1 60.17(5) 9 . ?
Ga4 Ga2 Ga1 60.17(5) 8_445 . ?
Ga4 Ga2 Ga1 60.17(5) 7_455 . ?
Ga6 Ga2 Ga1 119.91(6) 12_445 . ?
Ga6 Ga2 Ga1 119.91(6) 11 . ?
Ga6 Ga2 Ga1 119.91(6) 10_455 . ?
Ni1 Ga2 Tm1 68.38(7) 17 . ?
Ni1 Ga2 Tm1 68.38(7) 16_445 . ?
Ni1 Ga2 Tm1 68.38(7) 18_545 . ?
Ga4 Ga2 Tm1 119.83(5) 9 . ?
Ga4 Ga2 Tm1 119.83(5) 8_445 . ?
Ga4 Ga2 Tm1 119.83(5) 7_455 . ?
Ga6 Ga2 Tm1 60.09(6) 12_445 . ?
Ga6 Ga2 Tm1 60.09(6) 11 . ?
Ga6 Ga2 Tm1 60.09(6) 10_455 . ?
Ga1 Ga2 Tm1 180.0 . . ?
Ni1 Ga3 Ni1 107.52(7) 15_554 13_444 ?
Ni1 Ga3 Ni1 107.52(7) 15_554 14_544 ?
Ni1 Ga3 Ni1 107.52(7) 13_444 14_544 ?
Ni1 Ga3 Ga4 125.26(4) 15_554 3 ?
Ni1 Ga3 Ga4 51.39(5) 13_444 3 ?
Ni1 Ga3 Ga4 126.40(4) 14_544 3 ?
Ni1 Ga3 Ga4 51.39(5) 15_554 2 ?
Ni1 Ga3 Ga4 126.40(4) 13_444 2 ?
Ni1 Ga3 Ga4 125.26(4) 14_544 2 ?
Ga4 Ga3 Ga4 97.15(6) 3 2 ?
Ni1 Ga3 Ga4 126.40(4) 15_554 . ?
Ni1 Ga3 Ga4 125.26(4) 13_444 . ?
Ni1 Ga3 Ga4 51.39(5) 14_544 . ?
Ga4 Ga3 Ga4 97.15(6) 3 . ?
Ga4 Ga3 Ga4 97.15(6) 2 . ?
Ni1 Ga3 Ga6 54.46(5) 15_554 . ?
Ni1 Ga3 Ga6 128.90(11) 13_444 . ?
Ni1 Ga3 Ga6 53.93(4) 14_544 . ?
Ga4 Ga3 Ga6 179.58(8) 3 . ?
Ga4 Ga3 Ga6 82.43(4) 2 . ?
Ga4 Ga3 Ga6 82.90(4) . . ?
Ni1 Ga3 Ga6 128.90(11) 15_554 3 ?
Ni1 Ga3 Ga6 53.93(4) 13_444 3 ?
Ni1 Ga3 Ga6 54.46(5) 14_544 3 ?
Ga4 Ga3 Ga6 82.90(4) 3 3 ?
Ga4 Ga3 Ga6 179.58(8) 2 3 ?
Ga4 Ga3 Ga6 82.43(4) . 3 ?
Ga6 Ga3 Ga6 97.52(8) . 3 ?
Ni1 Ga3 Ga6 53.93(4) 15_554 2 ?
Ni1 Ga3 Ga6 54.46(5) 13_444 2 ?
Ni1 Ga3 Ga6 128.90(11) 14_544 2 ?
Ga4 Ga3 Ga6 82.43(4) 3 2 ?
Ga4 Ga3 Ga6 82.90(4) 2 2 ?
Ga4 Ga3 Ga6 179.58(8) . 2 ?
Ga6 Ga3 Ga6 97.52(8) . 2 ?
Ga6 Ga3 Ga6 97.52(8) 3 2 ?
Ni1 Ga3 Ga3 111.36(7) 15_554 4 ?
Ni1 Ga3 Ga3 111.36(7) 13_444 4 ?
Ni1 Ga3 Ga3 111.36(7) 14_544 4 ?
Ga4 Ga3 Ga3 59.98(5) 3 4 ?
Ga4 Ga3 Ga3 59.98(5) 2 4 ?
Ga4 Ga3 Ga3 59.98(5) . 4 ?
Ga6 Ga3 Ga3 119.74(6) . 4 ?
Ga6 Ga3 Ga3 119.74(6) 3 4 ?
Ga6 Ga3 Ga3 119.74(6) 2 4 ?
Ni1 Ga3 Tm1 68.64(7) 15_554 . ?
Ni1 Ga3 Tm1 68.64(7) 13_444 . ?
Ni1 Ga3 Tm1 68.64(7) 14_544 . ?
Ga4 Ga3 Tm1 120.02(5) 3 . ?
Ga4 Ga3 Tm1 120.02(5) 2 . ?
Ga4 Ga3 Tm1 120.02(5) . . ?
Ga6 Ga3 Tm1 60.26(6) . . ?
Ga6 Ga3 Tm1 60.26(6) 3 . ?
Ga6 Ga3 Tm1 60.26(6) 2 . ?
Ga3 Ga3 Tm1 180.0 4 . ?
Ni1 Ga4 Ni1 179.31(11) 14_544 11 ?
Ni1 Ga4 Ga2 59.75(6) 14_544 10 ?
Ni1 Ga4 Ga2 120.59(6) 11 10 ?
Ni1 Ga4 Ga2 120.59(6) 14_544 13_544 ?
Ni1 Ga4 Ga2 59.76(6) 11 13_544 ?
Ga2 Ga4 Ga2 128.59(7) 10 13_544 ?
Ni1 Ga4 Ga3 119.68(8) 14_544 4 ?
Ni1 Ga4 Ga3 59.63(6) 11 4 ?
Ga2 Ga4 Ga3 128.64(4) 10 4 ?
Ga2 Ga4 Ga3 97.28(5) 13_544 4 ?
Ni1 Ga4 Ga3 59.63(6) 14_544 . ?
Ni1 Ga4 Ga3 119.68(8) 11 . ?
Ga2 Ga4 Ga3 97.27(5) 10 . ?
Ga2 Ga4 Ga3 128.64(4) 13_544 . ?
Ga3 Ga4 Ga3 60.05(10) 4 . ?
Ni1 Ga4 Ga1 119.97(6) 14_544 10 ?
Ni1 Ga4 Ga1 60.38(6) 11 10 ?
Ga2 Ga4 Ga1 60.22(8) 10 10 ?
Ga2 Ga4 Ga1 97.04(6) 13_544 10 ?
Ga3 Ga4 Ga1 96.91(5) 4 10 ?
Ga3 Ga4 Ga1 128.79(4) . 10 ?
Ni1 Ga4 Ga1 60.38(6) 14_544 13_544 ?
Ni1 Ga4 Ga1 119.97(6) 11 13_544 ?
Ga2 Ga4 Ga1 97.04(6) 10 13_544 ?
Ga2 Ga4 Ga1 60.22(8) 13_544 13_544 ?
Ga3 Ga4 Ga1 128.79(4) 4 13_544 ?
Ga3 Ga4 Ga1 96.91(5) . 13_544 ?
Ga1 Ga4 Ga1 128.90(7) 10 13_544 ?
Ga7 Tm1 Ga7 119.999(6) 3 2 ?
```

```
Ga7 Tm1 Ga7 119.999(5) 3 . ?
Ga7 Tm1 Ga7 119.999(6) 2 . ?
Ga7 Tm1 Ga7 134.7(3) 3 11 ?
Ga7 Tm1 Ga7 105.3(3) 2 11 ?
Ga7 Tm1 Ga7 14.7(3) . 11 ?
Ga7 Tm1 Ga7 14.7(3) 3 12_445 ?
Ga7 Tm1 Ga7 134.7(3) 2 12_445 ?
Ga7 Tm1 Ga7 105.3(3) . 12_445 ?
Ga7 Tm1 Ga7 119.997(5) 11 12_445 ?
Ga7 Tm1 Ga7 105.3(3) 3 10_455 ?
Ga7 Tm1 Ga7 14.7(3) 2 10_455 ?
Ga7 Tm1 Ga7 134.7(3) . 10_455 ?
Ga7 Tm1 Ga7 119.995(6) 11 10_455 ?
Ga7 Tm1 Ga7 119.995(6) 12_445 10_455 ?
Ga7 Tm1 Ga5 135.5(4) 3 15_554 ?
Ga7 Tm1 Ga5 15.5(4) 2 15_554 ?
Ga7 Tm1 Ga5 104.5(4) . 15_554 ?
Ga7 Tm1 Ga5 89.8(2) 11 15_554 ?
Ga7 Tm1 Ga5 150.2(2) 12_445 15_554 ?
Ga7 Tm1 Ga5 30.2(2) 10_455 15_554 ?
Ga7 Tm1 Ga5 15.5(4) 3 13_444 ?
Ga7 Tm1 Ga5 104.5(4) 2 13_444 ?
Ga7 Tm1 Ga5 135.5(4) . 13_444 ?
Ga7 Tm1 Ga5 150.2(2) 11 13_444 ?
Ga7 Tm1 Ga5 30.2(2) 12_445 13_444 ?
Ga7 Tm1 Ga5 89.8(2) 10_455 13_444 ?
Ga5 Tm1 Ga5 120.0 15_554 13_444 ?
Ga7 Tm1 Ga5 104.5(4) 3 14_544 ?
Ga7 Tm1 Ga5 135.5(4) 2 14_544 ?
Ga7 Tm1 Ga5 15.5(4) . 14_544 ?
Ga7 Tm1 Ga5 30.2(2) 11 14_544 ?
Ga7 Tm1 Ga5 89.8(2) 12_445 14_544 ?
Ga7 Tm1 Ga5 150.2(2) 10_455 14_544 ?
Ga5 Tm1 Ga5 120.0 15_554 14_544 ?
Ga5 Tm1 Ga5 120.0 13_444 14_544 ?
Ga7 Tm1 Ga6 66.2(4) 3 12_445 ?
Ga7 Tm1 Ga6 143.4(4) 2 12_445 ?
Ga7 Tm1 Ga6 66.2(4) . 12_445 ?
Ga7 Tm1 Ga6 78.0(2) 11 12_445 ?
Ga7 Tm1 Ga6 55.8(2) 12_445 12_445 ?
Ga7 Tm1 Ga6 141.5(2) 10_455 12_445 ?
Ga5 Tm1 Ga6 141.00(5) 15_554 12_445 ?
Ga5 Tm1 Ga6 78.44(4) 13_444 12_445 ?
Ga5 Tm1 Ga6 55.10(4) 14_544 12_445 ?
Ga7 Tm1 Ga6 143.4(4) 3 11 ?
Ga7 Tm1 Ga6 66.2(4) 2 11 ?
Ga7 Tm1 Ga6 66.2(4) . 11 ?
Ga7 Tm1 Ga6 55.8(2) 11 11 ?
Ga7 Tm1 Ga6 141.5(2) 12_445 11 ?
Ga7 Tm1 Ga6 78.0(2) 10_455 11 ?
Ga5 Tm1 Ga6 55.10(4) 15_554 11 ?
Ga5 Tm1 Ga6 141.00(5) 13_444 11 ?
Ga5 Tm1 Ga6 78.44(4) 14_544 11 ?
Ga6 Tm1 Ga6 88.36(6) 12_445 11 ?
Ga7 Tm1 Ga6 66.2(4) 3 10_455 ?
Ga7 Tm1 Ga6 66.2(4) 2 10_455 ?
Ga7 Tm1 Ga6 143.4(4) . 10_455 ?
Ga7 Tm1 Ga6 141.5(2) 11 10_455 ?
Ga7 Tm1 Ga6 78.0(2) 12_445 10_455 ?
Ga7 Tm1 Ga6 55.8(2) 10_455 10_455 ?
Ga5 Tm1 Ga6 78.44(4) 15_554 10_455 ?
Ga5 Tm1 Ga6 55.10(4) 13_444 10_455 ?
Ga5 Tm1 Ga6 141.00(5) 14_544 10_455 ?
Ga6 Tm1 Ga6 88.36(6) 12_445 10_455 ?
Ga6 Tm1 Ga6 88.36(6) 11 10_455 ?
Ga5 Tm2 Ga5 120.000(1) 3 2 ?
Ga5 Tm2 Ga5 120.000(1) 3 . ?
Ga5 Tm2 Ga5 120.000(3) 2 . ?
Ga5 Tm2 Ga7 134.8(2) 3 17 ?
Ga5 Tm2 Ga7 14.8(2) 2 17 ?
Ga5 Tm2 Ga7 105.2(2) . 17 ?
Ga5 Tm2 Ga7 134.8(2) 3 9 ?
Ga5 Tm2 Ga7 105.2(2) 2 9 ?
Ga5 Tm2 Ga7 14.8(2) . 9 ?
Ga7 Tm2 Ga7 90.4(5) 17 9 ?
Ga5 Tm2 Ga7 14.8(2) 3 16_445 ?
Ga5 Tm2 Ga7 105.2(2) 2 16_445 ?
Ga5 Tm2 Ga7 134.8(2) . 16_445 ?
Ga7 Tm2 Ga7 119.999(4) 17 16_445 ?
Ga7 Tm2 Ga7 149.6(5) 9 16_445 ?
Ga5 Tm2 Ga7 14.8(2) 3 8_445 ?
Ga5 Tm2 Ga7 134.8(2) 2 8_445 ?
Ga5 Tm2 Ga7 105.2(2) . 8_445 ?
Ga7 Tm2 Ga7 149.6(5) 17 8_445 ?
Ga7 Tm2 Ga7 119.999(4) 9 8_445 ?
Ga7 Tm2 Ga7 29.6(5) 16_445 8_445 ?
Ga5 Tm2 Ga7 105.2(2) 3 7_455 ?
Ga5 Tm2 Ga7 14.8(2) 2 7_455 ?
Ga5 Tm2 Ga7 134.8(2) . 7_455 ?
Ga7 Tm2 Ga7 29.6(5) 17 7_455 ?
Ga7 Tm2 Ga7 119.998(9) 9 7_455 ?
Ga7 Tm2 Ga7 90.4(5) 16_445 7_455 ?
Ga7 Tm2 Ga7 119.998(7) 8_445 7_455 ?
Ga5 Tm2 Ga7 105.2(2) 3 18_545 ?
Ga5 Tm2 Ga7 134.8(2) 2 18_545 ?
Ga5 Tm2 Ga7 14.8(2) . 18_545 ?
Ga7 Tm2 Ga7 119.998(9) 17 18_545 ?
Ga7 Tm2 Ga7 29.6(5) 9 18_545 ?
Ga7 Tm2 Ga7 119.998(7) 16_445 18_545 ?
Ga7 Tm2 Ga7 90.4(5) 8_445 18_545 ?
Ga7 Tm2 Ga7 149.6(5) 7_455 18_545 ?
Ga5 Tm2 Ga6 66.39(3) 3 7_445 ?
Ga5 Tm2 Ga6 143.17(4) 2 7_445 ?
Ga5 Tm2 Ga6 66.43(3) . 7_445 ?
Ga7 Tm2 Ga6 140.5(2) 17 7_445 ?
Ga7 Tm2 Ga6 78.1(2) 9 7_445 ?
Ga7 Tm2 Ga6 77.7(2) 16_445 7_445 ?
Ga7 Tm2 Ga6 55.8(2) 8_445 7_445 ?
Ga7 Tm2 Ga6 140.9(2) 7_455 7_445 ?
Ga7 Tm2 Ga6 55.5(2) 18_545 7_445 ?
Ga5 Tm2 Ga6 66.39(3) 3 18_445 ?
Ga5 Tm2 Ga6 66.43(3) 2 18_445 ?
Ga5 Tm2 Ga6 143.17(4) . 18_445 ?
Ga7 Tm2 Ga6 78.1(2) 17 18_445 ?
Ga7 Tm2 Ga6 140.5(2) 9 18_445 ?
Ga7 Tm2 Ga6 55.8(2) 16_445 18_445 ?
Ga7 Tm2 Ga6 77.7(2) 8_445 18_445 ?
Ga7 Tm2 Ga6 55.5(2) 7_455 18_445 ?
Ga7 Tm2 Ga6 140.9(2) 18_545 18_445 ?
Ga6 Tm2 Ga6 132.77(6) 7_445 18_445 ?
Ga5 Tm2 Ga6 143.17(4) 3 16 ?
Ga5 Tm2 Ga6 66.39(3) 2 16 ?
Ga5 Tm2 Ga6 66.43(3) . 16 ?
Ga7 Tm2 Ga6 55.8(2) 17 16 ?
Ga7 Tm2 Ga6 55.5(2) 9 16 ?
Ga7 Tm2 Ga6 140.9(2) 16_445 16 ?
Ga7 Tm2 Ga6 140.5(2) 8_445 16 ?
Ga7 Tm2 Ga6 77.7(2) 7_455 16 ?
Ga7 Tm2 Ga6 78.1(2) 18_545 16 ?
Ga6 Tm2 Ga6 132.86(6) 7_445 16 ?
Ga6 Tm2 Ga6 87.77(6) 18_445 16 ?
Ga4 Ni1 Ga7 159.2(3) 9 18_545 ?
Ga4 Ni1 Ga7 159.3(3) 9 9 ?
Ga7 Ni1 Ga7 36.8(5) 18_545 9 ?
Ga4 Ni1 Ga5 156.81(9) 9 . ?
Ga7 Ni1 Ga5 37.3(3) 18_545 . ?
Ga7 Ni1 Ga5 37.1(3) 9 . ?
Ga4 Ni1 Ga6 101.26(8) 9 9 ?
Ga7 Ni1 Ga6 70.1(3) 18_545 9 ?
Ga7 Ni1 Ga6 70.1(3) 9 9 ?
Ga5 Ni1 Ga6 101.94(10) . 9 ?
Ga4 Ni1 Ga6 100.05(9) 9 7_445 ?
Ga7 Ni1 Ga6 69.7(3) 18_545 7_445 ?
Ga7 Ni1 Ga6 100.6(3) 9 7_445 ?
```

```
Ga5 Ni1 Ga6 68.92(7) . 7_445 ?
Ga6 Ni1 Ga6 117.81(11) 9 7_445 ?
Ga4 Ni1 Ga6 99.97(8) 9 8 ?
Ga7 Ni1 Ga6 100.8(3) 18_545 8 ?
Ga7 Ni1 Ga6 69.7(3) 9 8 ?
Ga5 Ni1 Ga6 68.87(7) . 8 ?
Ga6 Ni1 Ga6 117.60(11) 9 8 ?
Ga6 Ni1 Ga6 114.97(10) 7_445 8 ?
Ga4 Ni1 Ga3 68.98(8) 9 7 ?
Ga7 Ni1 Ga3 121.1(3) 18_545 7 ?
Ga7 Ni1 Ga3 90.3(3) 9 7 ?
Ga5 Ni1 Ga3 120.67(8) . 7 ?
Ga6 Ni1 Ga3 67.46(6) 9 7 ?
Ga6 Ni1 Ga3 168.93(11) 7_445 7 ?
Ga6 Ni1 Ga3 67.15(6) 8 7 ?
Ga4 Ni1 Ga2 68.79(7) 9 16_545 ?
Ga7 Ni1 Ga2 90.5(3) 18_545 16_545 ?
Ga7 Ni1 Ga2 121.3(3) 9 16_545 ?
Ga5 Ni1 Ga2 121.01(8) . 16_545 ?
Ga6 Ni1 Ga2 67.64(6) 9 16_545 ?
Ga6 Ni1 Ga2 67.35(6) 7_445 16_545 ?
Ga6 Ni1 Ga2 168.68(11) 8 16_545 ?
Ga3 Ni1 Ga2 108.38(8) 7 16_545 ?
Ga4 Ni1 Ga1 68.65(7) 9 . ?
Ga7 Ni1 Ga1 119.4(3) 18_545 . ?
Ga7 Ni1 Ga1 119.3(3) 9 . ?
Ga5 Ni1 Ga1 88.16(9) . . ?
Ga6 Ni1 Ga1 169.90(11) 9 . ?
Ga6 Ni1 Ga1 65.77(6) 7_445 . ?
Ga6 Ni1 Ga1 65.76(6) 8 . ?
Ga3 Ni1 Ga1 107.37(8) 7 . ?
Ga2 Ni1 Ga1 107.34(8) 16_545 . ?
Ga4 Ni1 Tm1 133.37(7) 9 16_545 ?
Ga7 Ni1 Tm1 25.9(3) 18_545 16_545 ?
Ga7 Ni1 Tm1 60.2(3) 9 16_545 ?
Ga5 Ni1 Tm1 60.50(5) . 16_545 ?
Ga6 Ni1 Tm1 61.55(6) 9 16_545 ?
Ga6 Ni1 Tm1 61.40(6) 7_445 16_545 ?
Ga6 Ni1 Tm1 126.62(8) 8 16_545 ?
Ga3 Ni1 Tm1 127.02(6) 7 16_545 ?
Ga2 Ni1 Tm1 64.58(6) 16_545 16_545 ?
Ga1 Ni1 Tm1 125.18(7) . 16_545 ?
Ga4 Ni1 Tm1 133.45(7) 9 7 ?
Ga7 Ni1 Tm1 60.1(3) 18_545 7 ?
Ga7 Ni1 Tm1 25.9(3) 9 7 ?
Ga5 Ni1 Tm1 60.28(5) . 7 ?
Ga6 Ni1 Tm1 61.52(6) 9 7 ?
Ga6 Ni1 Tm1 126.46(8) 7_445 7 ?
Ga6 Ni1 Tm1 61.36(6) 8 7 ?
Ga3 Ni1 Tm1 64.48(6) 7 7 ?
Ga2 Ni1 Tm1 127.17(6) 16_545 7 ?
Ga1 Ni1 Tm1 125.08(7) . 7 ?
Tm1 Ni1 Tm1 79.14(4) 16_545 7 ?
Ni1 Ga6 Ni1 115.76(10) 14_544 13_554 ?
Ni1 Ga6 Ni1 115.97(11) 14_544 15_554 ?
Ni1 Ga6 Ni1 118.65(10) 13_554 15_554 ?
Ni1 Ga6 Ga1 139.89(10) 14_544 13_554 ?
Ni1 Ga6 Ga1 59.74(6) 13_554 13_554 ?
Ni1 Ga6 Ga1 59.73(6) 15_554 13_554 ?
Ni1 Ga6 Ga5 134.55(10) 14_544 15_554 ?
Ni1 Ga6 Ga5 104.16(8) 13_554 15_554 ?
Ni1 Ga6 Ga5 54.89(6) 15_554 15_554 ?
Ga1 Ga6 Ga5 78.83(6) 13_554 15_554 ?
Ni1 Ga6 Ga5 134.43(9) 14_544 13_554 ?
Ni1 Ga6 Ga5 54.89(6) 13_554 13_554 ?
Ni1 Ga6 Ga5 104.14(8) 15_554 13_554 ?
Ga1 Ga6 Ga5 78.81(6) 13_554 13_554 ?
Ga5 Ga6 Ga5 56.91(11) 15_554 13_554 ?
Ni1 Ga6 Ga7 54.1(2) 14_544 11 ?
Ni1 Ga6 Ga7 102.8(3) 13_554 11 ?
Ni1 Ga6 Ga7 133.9(3) 15_554 11 ?
Ga1 Ga6 Ga7 160.0(3) 13_554 11 ?
Ga5 Ga6 Ga7 97.8(2) 15_554 11 ?
Ga5 Ga6 Ga7 82.8(3) 13_554 11 ?
Ni1 Ga6 Ga7 103.1(3) 14_544 12 ?
Ni1 Ga6 Ga7 53.9(2) 13_554 12 ?
Ni1 Ga6 Ga7 135.6(3) 15_554 12 ?
Ga1 Ga6 Ga7 102.7(3) 13_554 12 ?
Ga5 Ga6 Ga7 82.9(2) 15_554 12 ?
Ga5 Ga6 Ga7 32.3(3) 13_554 12 ?
Ga7 Ga6 Ga7 57.3(5) 11 12 ?
Ni1 Ga6 Ga7 103.2(3) 14_544 2 ?
Ni1 Ga6 Ga7 135.4(3) 13_554 2 ?
Ni1 Ga6 Ga7 54.3(2) 15_554 2 ?
Ga1 Ga6 Ga7 102.9(3) 13_554 2 ?
Ga5 Ga6 Ga7 32.2(3) 15_554 2 ?
Ga5 Ga6 Ga7 82.6(2) 13_554 2 ?
Ga7 Ga6 Ga7 82.45(9) 11 2 ?
Ga7 Ga6 Ga7 98.1(3) 12 2 ?
Ni1 Ga6 Ga7 54.5(2) 14_544 . ?
Ni1 Ga6 Ga7 133.6(3) 13_554 . ?
Ni1 Ga6 Ga7 102.9(3) 15_554 . ?
Ga1 Ga6 Ga7 159.9(3) 13_554 . ?
Ga5 Ga6 Ga7 82.6(2) 15_554 . ?
Ga5 Ga6 Ga7 97.4(2) 13_554 . ?
Ga7 Ga6 Ga7 31.6(5) 11 . ?
Ga7 Ga6 Ga7 82.43(9) 12 . ?
Ga7 Ga6 Ga7 57.0(5) 2 . ?
Ni1 Ga6 Ga3 58.61(6) 14_544 . ?
Ni1 Ga6 Ga3 139.84(10) 13_554 . ?
Ni1 Ga6 Ga3 58.39(6) 15_554 . ?
Ga1 Ga6 Ga3 97.85(8) 13_554 . ?
Ga5 Ga6 Ga3 103.04(7) 15_554 . ?
Ga5 Ga6 Ga3 159.94(9) 13_554 . ?
Ga7 Ga6 Ga3 102.1(3) 11 . ?
Ga7 Ga6 Ga3 159.3(3) 12 . ?
Ga7 Ga6 Ga3 78.8(2) 2 . ?
Ga7 Ga6 Ga3 78.8(2) . . ?
Ni1 Ga6 Ga2 58.52(6) 14_544 10 ?
Ni1 Ga6 Ga2 58.32(6) 13_554 10 ?
Ni1 Ga6 Ga2 139.67(10) 15_554 10 ?
Ga1 Ga6 Ga2 97.68(7) 13_554 10 ?
Ga5 Ga6 Ga2 159.99(9) 15_554 10 ?
Ga5 Ga6 Ga2 103.09(7) 13_554 10 ?
Ga7 Ga6 Ga2 78.6(2) 11 10 ?
Ga7 Ga6 Ga2 78.6(2) 12 10 ?
Ga7 Ga6 Ga2 159.3(3) 2 10 ?
Ga7 Ga6 Ga2 102.4(3) . 10 ?
Ga3 Ga6 Ga2 96.96(7) . 10 ?
Tm2 Ga5 Ga7 150.5(4) . 9 ?
Tm2 Ga5 Ga7 150.5(4) . 18_545 ?
Ga7 Ga5 Ga7 58.9(8) 9 18_545 ?
Tm2 Ga5 Ni1 112.43(7) . 4_556 ?
Ga7 Ga5 Ni1 70.1(4) 9 4_556 ?
Ga7 Ga5 Ni1 71.1(4) 18_545 4_556 ?
Tm2 Ga5 Ni1 112.43(7) . . ?
Ga7 Ga5 Ni1 71.1(4) 9 . ?
Ga7 Ga5 Ni1 70.1(4) 18_545 . ?
Ni1 Ga5 Ni1 135.14(13) 4_556 . ?
Tm2 Ga5 Ga5 30.0 . 3 ?
Ga7 Ga5 Ga5 179.3(4) 9 3 ?
Ga7 Ga5 Ga5 120.6(4) 18_545 3 ?
Ni1 Ga5 Ga5 109.32(6) 4_556 3 ?
Ni1 Ga5 Ga5 109.27(6) . 3 ?
Tm2 Ga5 Ga5 30.0 . 2 ?
Ga7 Ga5 Ga5 120.6(4) 9 2 ?
Ga7 Ga5 Ga5 179.3(4) 18_545 2 ?
Ni1 Ga5 Ga5 109.27(6) 4_556 2 ?
Ni1 Ga5 Ga5 109.32(6) . 2 ?
Ga5 Ga5 Ga5 60.0 3 2 ?
Tm2 Ga5 Ga6 83.33(6) . 17_545 ?
Ga7 Ga5 Ga6 117.7(4) 9 17_545 ?
Ga7 Ga5 Ga6 74.7(4) 18_545 17_545 ?
Ni1 Ga5 Ga6 56.24(5) 4_556 17_545 ?
```

```
Ni1 Ga5 Ga6 130.12(6) . 17_545 ?
Ga5 Ga5 Ga6 61.57(6) 3 17_545 ?
Ga5 Ga5 Ga6 105.97(6) 2 17_545 ?
Tm2 Ga5 Ga6 83.33(6) . 8 ?
Ga7 Ga5 Ga6 74.7(4) 9 8 ?
Ga7 Ga5 Ga6 117.7(4) 18_545 8 ?
Ni1 Ga5 Ga6 130.12(6) 4_556 8 ?
Ni1 Ga5 Ga6 56.24(5) . 8 ?
Ga5 Ga5 Ga6 105.96(6) 3 8 ?
Ga5 Ga5 Ga6 61.56(6) 2 8 ?
Ga6 Ga5 Ga6 166.66(12) 17_545 8 ?
Tm2 Ga5 Ga6 83.29(6) . 16 ?
Ga7 Ga5 Ga6 74.2(4) 9 16 ?
Ga7 Ga5 Ga6 118.4(4) 18_545 16 ?
Ni1 Ga5 Ga6 56.19(5) 4_556 16 ?
Ni1 Ga5 Ga6 130.20(6) . 16 ?
Ga5 Ga5 Ga6 105.93(5) 3 16 ?
Ga5 Ga5 Ga6 61.52(6) 2 16 ?
Ga6 Ga5 Ga6 97.40(9) 17_545 16 ?
Ga6 Ga5 Ga6 81.03(9) 8 16 ?
Tm2 Ga5 Ga6 83.29(6) . 7_445 ?
Ga7 Ga5 Ga6 118.4(4) 9 7_445 ?
Ga7 Ga5 Ga6 74.2(4) 18_545 7_445 ?
Ni1 Ga5 Ga6 130.20(6) 4_556 7_445 ?
Ni1 Ga5 Ga6 56.19(5) . 7_445 ?
Ga5 Ga5 Ga6 61.52(6) 3 7_445 ?
Ga5 Ga5 Ga6 105.93(5) 2 7_445 ?
Ga6 Ga5 Ga6 81.03(9) 17_545 7_445 ?
Ga6 Ga5 Ga6 97.40(9) 8 7_445 ?
Ga6 Ga5 Ga6 166.59(12) 16 7_445 ?
Tm2 Ga5 Tm1 135.14(3) . 7 ?
Ga7 Ga5 Tm1 15.4(4) 9 7 ?
Ga7 Ga5 Tm1 74.3(4) 18_545 7 ?
Ni1 Ga5 Tm1 74.13(6) 4_556 7 ?
Ni1 Ga5 Tm1 74.48(6) . 7 ?
Ga5 Ga5 Tm1 165.14(3) 3 7 ?
Ga5 Ga5 Tm1 105.14(3) 2 7 ?
Ga6 Ga5 Tm1 127.63(8) 17_545 7 ?
Ga6 Ga5 Tm1 63.52(4) 8 7 ?
Ga6 Ga5 Tm1 63.33(4) 16 7 ?
Ga6 Ga5 Tm1 127.91(8) 7_445 7 ?
Ga7 Ga7 Tm1 150.3(4) 11 . ?
Ga7 Ga7 Ga5 60.6(4) 11 14_544 ?
Tm1 Ga7 Ga5 149.1(8) . 14_544 ?
Ga7 Ga7 Ni1 72.5(8) 11 18_545 ?
Tm1 Ga7 Ni1 111.3(6) . 18_545 ?
Ga5 Ga7 Ni1 72.5(4) 14_544 18_545 ?
Ga7 Ga7 Ni1 70.8(8) 11 14_544 ?
Tm1 Ga7 Ni1 110.9(6) . 14_544 ?
Ga5 Ga7 Ni1 71.8(4) 14_544 14_544 ?
Ni1 Ga7 Ni1 137.8(6) 18_545 14_544 ?
Ga7 Ga7 Ga7 179.0(8) 11 3 ?
Tm1 Ga7 Ga7 30.000(3) . 3 ?
Ga5 Ga7 Ga7 119.1(8) 14_544 3 ?
Ni1 Ga7 Ga7 108.4(3) 18_545 3 ?
Ni1 Ga7 Ga7 108.3(3) 14_544 3 ?
Ga7 Ga7 Ga7 120.3(4) 11 2 ?
Tm1 Ga7 Ga7 30.000(2) . 2 ?
Ga5 Ga7 Ga7 179.0(7) 14_544 2 ?
Ni1 Ga7 Ga7 108.1(3) 18_545 2 ?
Ni1 Ga7 Ga7 107.9(3) 14_544 2 ?
Ga7 Ga7 Ga7 60.0 3 2 ?
Ga7 Ga7 Ga6 74.7(6) 11 11 ?
Tm1 Ga7 Ga6 83.4(5) . 11 ?
Ga5 Ga7 Ga6 119.6(6) 14_544 11 ?
Ni1 Ga7 Ga6 55.8(2) 18_545 11 ?
Ni1 Ga7 Ga6 129.6(4) 14_544 11 ?
Ga7 Ga7 Ga6 106.1(3) 3 11 ?
Ga7 Ga7 Ga6 61.4(4) 2 11 ?
Ga7 Ga7 Ga6 119.1(7) 11 12_445 ?
Tm1 Ga7 Ga6 83.4(4) . 12_445 ?
Ga5 Ga7 Ga6 73.5(4) 14_544 12_445 ?
Ni1 Ga7 Ga6 56.4(2) 18_545 12_445 ?
Ni1 Ga7 Ga6 130.3(4) 14_544 12_445 ?
Ga7 Ga7 Ga6 61.4(4) 3 12_445 ?
Ga7 Ga7 Ga6 106.1(3) 2 12_445 ?
Ga6 Ga7 Ga6 98.4(3) 11 12_445 ?
Ga7 Ga7 Ga6 117.6(7) 11 3 ?
Tm1 Ga7 Ga6 83.2(5) . 3 ?
Ga5 Ga7 Ga6 73.0(4) 14_544 3 ?
Ni1 Ga7 Ga6 130.6(4) 18_545 3 ?
Ni1 Ga7 Ga6 56.0(2) 14_544 3 ?
Ga7 Ga7 Ga6 61.5(4) 3 3 ?
Ga7 Ga7 Ga6 106.0(3) 2 3 ?
Ga6 Ga7 Ga6 166.7(5) 11 3 ?
Ga6 Ga7 Ga6 80.5(3) 12_445 3 ?
Ga7 Ga7 Ga6 73.7(6) 11 . ?
Tm1 Ga7 Ga6 83.2(5) . . ?
Ga5 Ga7 Ga6 118.8(6) 14_544 . ?
Ni1 Ga7 Ga6 130.0(4) 18_545 . ?
Ni1 Ga7 Ga6 55.4(2) 14_544 . ?
Ga7 Ga7 Ga6 106.0(3) 3 . ?
Ga7 Ga7 Ga6 61.5(4) 2 . ?
Ga6 Ga7 Ga6 80.4(3) 11 . ?
Ga6 Ga7 Ga6 166.6(5) 12_445 . ?
Ga6 Ga7 Ga6 97.6(3) 3 . ?
Ga7 Ga7 Tm1 14.9(2) 11 10 ?
Tm1 Ga7 Tm1 135.4(6) . 10 ?
Ga5 Ga7 Tm1 75.5(4) 14_544 10 ?
Ni1 Ga7 Tm1 75.3(3) 18_545 10 ?
Ni1 Ga7 Tm1 74.6(3) 14_544 10 ?
Ga7 Ga7 Tm1 165.4(6) 3 10 ?
Ga7 Ga7 Tm1 105.4(6) 2 10 ?
Ga6 Ga7 Tm1 63.6(2) 11 10 ?
Ga6 Ga7 Tm1 128.2(4) 12_445 10 ?
Ga6 Ga7 Tm1 127.3(4) 3 10 ?
Ga6 Ga7 Tm1 63.3(2) . 10 ?

_diffrn_measured_fraction_theta_max    0.998
_diffrn_reflns_theta_full              29.93
_diffrn_measured_fraction_theta_full   0.998
_refine_diff_density_max    4.590
_refine_diff_density_min   -4.110
_refine_diff_density_rms    0.683
```

A2.7 $YbNi_3Ga_9$

```
data_ybni3ga9

_audit_creation_method            SHELXL-97
_chemical_name_systematic
;
 ?
;
_chemical_name_common             ?
_chemical_melting_point           ?
_chemical_formula_moiety          ?
_chemical_formula_sum
 'Ga9 Ni3 Yb'
_chemical_formula_weight          976.65

loop_
 _atom_type_symbol
 _atom_type_description
 _atom_type_scat_dispersion_real
 _atom_type_scat_dispersion_imag
 _atom_type_scat_source
 'Ni'  'Ni'   0.3393   1.1124
 'International Tables Vol C Tables 4.2.6.8
and 6.1.1.4'
 'Ga'  'Ga'   0.2307   1.6083
 'International Tables Vol C Tables 4.2.6.8
and 6.1.1.4'
 'Yb'  'Yb'  -0.3850   5.5486
 'International Tables Vol C Tables 4.2.6.8
and 6.1.1.4'

_symmetry_cell_setting            ?
_symmetry_space_group_name_H-M    ?

loop_
 _symmetry_equiv_pos_as_xyz
 'x, y, z'
 '-y, x-y, z'
 '-x+y, -x, z'
 'x-y, -y, -z'
 '-x, -x+y, -z'
 'y, x, -z'
 'x+2/3, y+1/3, z+1/3'
 '-y+2/3, x-y+1/3, z+1/3'
 '-x+y+2/3, -x+1/3, z+1/3'
 'x-y+2/3, -y+1/3, -z+1/3'
 '-x+2/3, -x+y+1/3, -z+1/3'
 'y+2/3, x+1/3, -z+1/3'
 'x+1/3, y+2/3, z+2/3'
 '-y+1/3, x-y+2/3, z+2/3'
 '-x+y+1/3, -x+2/3, z+2/3'
 'x-y+1/3, -y+2/3, -z+2/3'
 '-x+1/3, -x+y+2/3, -z+2/3'
 'y+1/3, x+2/3, -z+2/3'

_cell_length_a                    7.2265(2)
_cell_length_b                    7.2265(2)
_cell_length_c                    27.5290(9)
_cell_angle_alpha                 90.00
_cell_angle_beta                  90.00
_cell_angle_gamma                 120.00
_cell_volume                      1245.02(6)
_cell_formula_units_Z             6
_cell_measurement_temperature     293(2)
_cell_measurement_reflns_used     ?
_cell_measurement_theta_min       ?
_cell_measurement_theta_max       ?

_exptl_crystal_description        ?
_exptl_crystal_colour             ?
_exptl_crystal_size_max           ?
_exptl_crystal_size_mid           ?
_exptl_crystal_size_min           ?
_exptl_crystal_density_meas       ?
_exptl_crystal_density_diffrn     7.816
_exptl_crystal_density_method           'not
measured'
_exptl_crystal_F_000              2598
_exptl_absorpt_coefficient_mu     46.365
_exptl_absorpt_correction_type    ?
_exptl_absorpt_correction_T_min   ?
_exptl_absorpt_correction_T_max   ?
_exptl_absorpt_process_details    ?

_exptl_special_details
;
 ?
;

_diffrn_ambient_temperature       293(2)
_diffrn_radiation_wavelength      0.71073
_diffrn_radiation_type            MoK\a
_diffrn_radiation_source              'fine-
focus sealed tube'
_diffrn_radiation_monochromator   graphite
_diffrn_measurement_device_type   ?
_diffrn_measurement_method        ?
_diffrn_detector_area_resol_mean  ?
_diffrn_standards_number          ?
_diffrn_standards_interval_count  ?
_diffrn_standards_interval_time   ?
_diffrn_standards_decay_%         ?
_diffrn_reflns_number             1311
_diffrn_reflns_av_R_equivalents   0.0348
_diffrn_reflns_av_sigmaI/netI     0.0561
_diffrn_reflns_limit_h_min        -10
_diffrn_reflns_limit_h_max        10
_diffrn_reflns_limit_k_min        -8
_diffrn_reflns_limit_k_max        8
_diffrn_reflns_limit_l_min        -32
_diffrn_reflns_limit_l_max        38
_diffrn_reflns_theta_min          3.34
_diffrn_reflns_theta_max          30.00
_reflns_number_total              810
_reflns_number_gt                 725
_reflns_threshold_expression      >2sigma(I)

_computing_data_collection        ?
_computing_cell_refinement        ?
_computing_data_reduction         ?
_computing_structure_solution     ?
_computing_structure_refinement    'SHELXL-97
(Sheldrick, 1997)'
_computing_molecular_graphics     ?
_computing_publication_material   ?

_refine_special_details
;
 Refinement of F^2^ against ALL reflections.
The weighted R-factor wR and
 goodness  of  fit  S  are  based  on  F^2^,
conventional R-factors R are based
 on F, with F set to zero for negative F^2^.
The threshold expression of
 F^2^  >  2sigma(F^2^)  is  used  only  for
calculating R-factors(gt) etc. and is
 not relevant to the choice of reflections
for refinement.  R-factors based
 on  F^2^  are  statistically  about  twice  as
large as those based on F, and R-
```

```
 factors  based  on  ALL  data  will  be  even
larger.
;

_refine_ls_structure_factor_coef  Fsqd
_refine_ls_matrix_type            full
_refine_ls_weighting_scheme       calc
_refine_ls_weighting_details
 'calc
w=1/[\s^2^(Fo^2^)+(0.0495P)^2^+0.0000P]
where P=(Fo^2^+2Fc^2^)/3'
_atom_sites_solution_primary      direct
_atom_sites_solution_secondary    difmap
_atom_sites_solution_hydrogens    geom
_refine_ls_hydrogen_treatment     mixed
_refine_ls_extinction_method      SHELXL
_refine_ls_extinction_coef
0.00147(10)
_refine_ls_extinction_expression
 'Fc^*^=kFc[1+0.001xFc^2^\l^3^/sin(2\q)]^-
1/4^'
_refine_ls_abs_structure_details
 'Flack  H  D  (1983),  Acta  Cryst.  A39,  876-
881'
_refine_ls_abs_structure_Flack    -0.07(5)
_refine_ls_number_reflns          810
_refine_ls_number_parameters      53
_refine_ls_number_restraints      0
_refine_ls_R_factor_all           0.0432
_refine_ls_R_factor_gt            0.0389
_refine_ls_wR_factor_ref          0.0914
_refine_ls_wR_factor_gt           0.0890
_refine_ls_goodness_of_fit_ref    1.042
_refine_ls_restrained_S_all       1.042
_refine_ls_shift/su_max           0.000
_refine_ls_shift/su_mean          0.000

loop_
 _atom_site_label
 _atom_site_type_symbol
 _atom_site_fract_x
 _atom_site_fract_y
 _atom_site_fract_z
 _atom_site_U_iso_or_equiv
 _atom_site_adp_type
 _atom_site_occupancy
 _atom_site_symmetry_multiplicity
 _atom_site_calc_flag
 _atom_site_refinement_flags
 _atom_site_disorder_assembly
 _atom_site_disorder_group
Ga1  Ga  0.0000  0.0000  0.38460(7)  0.0079(3)
Uani 1 3 d S . .
Ga2  Ga  0.0000  0.0000  0.28302(7)  0.0075(3)
Uani 1 3 d S . .
Ga3  Ga  0.0000  0.0000  0.05077(7)  0.0077(3)
Uani 1 3 d S . .
Ga4  Ga  0.33292(13)  0.0000  0.0000  0.0110(4)
Uani 1 2 d S . .
Yb1  Yb  0.0000  0.0000  0.166828(16)  0.0064(2)
Uani 0.88 3 d SP . .
Yb2  Yb  0.0000  0.0000  0.5000  0.0036(6)  Uani
0.25 6 d SP . .
Ni1  Ni  0.33742(14)  0.00004(15)  0.41809(6)
0.0059(4) Uani 1 1 d . . .
Ga6  Ga  0.33332(14)  0.33582(14)  0.10093(7)
0.0078(3) Uani 1 1 d . . .
Ga5  Ga  0.2106(2)  0.0000  0.5000  0.0068(4)
Uani 0.76 2 d SP . .
Ga7  Ga  0.2146(12)  0.0002(10)  0.16657(19)
0.0059(19) Uani 0.12 1 d P . .
```

```
loop_
 _atom_site_aniso_label
 _atom_site_aniso_U_11
 _atom_site_aniso_U_22
 _atom_site_aniso_U_33
 _atom_site_aniso_U_23
 _atom_site_aniso_U_13
 _atom_site_aniso_U_12
Ga1  0.0095(5)  0.0095(5)  0.0046(8)  0.000
0.000 0.0048(2)
Ga2  0.0090(5)  0.0090(5)  0.0045(8)  0.000
0.000 0.0045(2)
Ga3  0.0091(5)  0.0091(5)  0.0051(8)  0.000
0.000 0.0045(2)
Ga4 0.0156(5) 0.0152(6) 0.0018(10) 0.0002(3)
0.00009(17) 0.0076(3)
Yb1  0.0074(2)  0.0074(2)  0.0044(4)  0.000
0.000 0.00370(12)
Yb2  0.0040(7)  0.0040(7)  0.0029(16)  0.000
0.000 0.0020(4)
Ni1  0.0072(6)  0.0078(6)  0.0025(9)  0.0001(3)
0.0010(3) 0.0036(4)
Ga6 0.0082(6) 0.0087(6) 0.0068(6) -0.0011(3)
-0.0004(3) 0.0045(4)
Ga5 0.0094(6) 0.0080(7) 0.0026(10) 0.0005(7)
0.0003(3) 0.0040(4)
Ga7  0.010(3)  0.002(3)  0.001(5)  0.005(3)
0.003(2) -0.002(2)

_geom_special_details
;
 All  esds  (except  the  esd  in  the  dihedral
angle between two l.s. planes)
 are  estimated  using  the  full  covariance
matrix.  The cell esds are taken
 into account individually in the estimation
of esds in distances, angles
 and  torsion  angles;  correlations  between
esds in cell parameters are only
 used  when  they  are  defined  by  crystal
symmetry.  An approximate (isotropic)
 treatment  of  cell  esds  is  used  for
estimating esds involving l.s. planes.
;

loop_
 _geom_bond_atom_site_label_1
 _geom_bond_atom_site_label_2
 _geom_bond_distance
 _geom_bond_site_symmetry_2
 _geom_bond_publ_flag
Ga1 Ni1 2.6067(13) 3 ?
Ga1 Ni1 2.6067(13) . ?
Ga1 Ni1 2.6067(13) 2 ?
Ga1 Ga6 2.7542(14) 7_445 ?
Ga1 Ga6 2.7542(14) 8 ?
Ga1 Ga6 2.7542(14) 9_455 ?
Ga1 Ga4 2.7930(11) 9 ?
Ga1 Ga4 2.7930(11) 8_445 ?
Ga1 Ga4 2.7930(11) 7_455 ?
Ga1 Ga2 2.796(4) . ?
Ga1 Yb2 3.1770(19) . ?
Ga2 Ni1 2.5754(13) 17 ?
Ga2 Ni1 2.5754(13) 16_445 ?
Ga2 Ni1 2.5754(13) 18_545 ?
Ga2 Ga4 2.7800(10) 9 ?
Ga2 Ga4 2.7800(10) 8_445 ?
Ga2 Ga4 2.7800(10) 7_455 ?
Ga2 Ga6 2.7905(14) 12_445 ?
Ga2 Ga6 2.7906(14) 11 ?
Ga2 Ga6 2.7906(14) 10_455 ?
Ga2 Yb1 3.199(2) . ?
```

```
Ga3 Ni1 2.5703(13) 15_554 ?
Ga3 Ni1 2.5703(13) 13_444 ?
Ga3 Ni1 2.5703(13) 14_544 ?
Ga3 Ga4 2.7824(13) 3 ?
Ga3 Ga4 2.7824(13) . ?
Ga3 Ga4 2.7824(13) 2 ?
Ga3 Ga6 2.7842(14) . ?
Ga3 Ga6 2.7842(14) 2 ?
Ga3 Ga6 2.7842(14) 3 ?
Ga3 Ga3 2.796(4) 4 ?
Ga3 Yb1 3.195(2) . ?
Ga4 Ni1 2.3333(17) 14_544 ?
Ga4 Ni1 2.3333(17) 11 ?
Ga4 Ga2 2.7800(10) 10 ?
Ga4 Ga2 2.7800(10) 13_544 ?
Ga4 Ga3 2.7824(13) 4 ?
Ga4 Ga1 2.7930(11) 10 ?
Ga4 Ga1 2.7930(11) 13_544 ?
Yb1 Ga7 1.550(8) 3 ?
Yb1 Ga7 1.550(8) 2 ?
Yb1 Ga7 1.550(8) . ?
Yb1 Ga7 2.933(7) 11 ?
Yb1 Ga7 2.933(7) 12_445 ?
Yb1 Ga7 2.933(7) 10_455 ?
Yb1 Ga5 2.9537(11) 15_554 ?
Yb1 Ga5 2.9537(11) 13_444 ?
Yb1 Ga5 2.9538(11) 14_544 ?
Yb1 Ga6 3.0176(14) 12_445 ?
Yb1 Ga6 3.0176(14) 11 ?
Yb1 Ga6 3.0176(14) 10_455 ?
Yb2 Ga5 1.5221(16) 3 ?
Yb2 Ga5 1.5221(16) 2 ?
Yb2 Ga5 1.5221(16) . ?
Yb2 Ga7 2.935(8) 17 ?
Yb2 Ga7 2.935(8) 9 ?
Yb2 Ga7 2.935(8) 16_445 ?
Yb2 Ga7 2.935(8) 8_445 ?
Yb2 Ga7 2.935(8) 18_545 ?
Yb2 Ga7 2.935(8) 7_455 ?
Yb2 Ga6 2.9985(14) 7_445 ?
Yb2 Ga6 2.9985(14) 18_445 ?
Yb2 Ga6 2.9986(14) 16 ?
Ni1 Ga4 2.3333(17) 9 ?
Ni1 Ga7 2.405(6) 9 ?
Ni1 Ga7 2.410(6) 18_545 ?
Ni1 Ga5 2.4339(17) . ?
Ni1 Ga6 2.4384(11) 9 ?
Ni1 Ga6 2.4554(11) 8 ?
Ni1 Ga6 2.4558(10) 7_445 ?
Ni1 Ga3 2.5703(13) 7 ?
Ni1 Ga2 2.5754(13) 16_545 ?
Ni1 Yb1 3.2861(13) 16_545 ?
Ni1 Yb1 3.2919(13) 7 ?
Ga6 Ni1 2.4384(11) 14_544 ?
Ga6 Ni1 2.4553(10) 15_554 ?
Ga6 Ni1 2.4558(10) 13_554 ?
Ga6 Ga1 2.7542(14) 13_554 ?
Ga6 Ga5 2.7692(15) 15_554 ?
Ga6 Ga5 2.7693(15) 13_554 ?
Ga6 Ga7 2.780(6) 2 ?
Ga6 Ga7 2.784(6) 12 ?
Ga6 Ga2 2.7905(14) 10 ?
Ga6 Ga7 2.793(6) . ?
Ga6 Ga7 2.797(6) 11 ?
Ga5 Ga7 1.513(9) 9 ?
Ga5 Ga7 1.513(9) 18_545 ?
Ga5 Ni1 2.4339(17) 4_556 ?
Ga5 Ga5 2.636(3) 3 ?
Ga5 Ga5 2.636(3) 2 ?
Ga5 Ga6 2.7693(15) 17_545 ?
Ga5 Ga6 2.7693(15) 8 ?
Ga5 Ga6 2.7693(15) 16 ?
Ga5 Ga6 2.7693(15) 7_445 ?
Ga5 Yb1 2.9537(11) 7 ?
Ga7 Ga7 1.486(16) 11 ?
Ga7 Ga5 1.513(9) 14_544 ?
Ga7 Ni1 2.405(6) 14_544 ?
Ga7 Ni1 2.410(6) 18_545 ?
Ga7 Ga7 2.684(15) 3 ?
Ga7 Ga7 2.684(14) 2 ?
Ga7 Ga6 2.780(6) 3 ?
Ga7 Ga6 2.784(6) 12_445 ?
Ga7 Ga6 2.797(6) 11 ?
Ga7 Yb1 2.933(7) 10 ?

loop_
 _geom_angle_atom_site_label_1
 _geom_angle_atom_site_label_2
 _geom_angle_atom_site_label_3
 _geom_angle
 _geom_angle_site_symmetry_1
 _geom_angle_site_symmetry_3
 _geom_angle_publ_flag
Ni1 Ga1 Ni1 108.20(6) 3 . ?
Ni1 Ga1 Ni1 108.20(6) 3 2 ?
Ni1 Ga1 Ni1 108.20(6) . 2 ?
Ni1 Ga1 Ga6 54.43(3) 3 7_445 ?
Ni1 Ga1 Ga6 54.45(3) . 7_445 ?
Ni1 Ga1 Ga6 129.52(9) 2 7_445 ?
Ni1 Ga1 Ga6 129.52(9) 3 8 ?
Ni1 Ga1 Ga6 54.43(3) . 8 ?
Ni1 Ga1 Ga6 54.44(3) 2 8 ?
Ga6 Ga1 Ga6 97.49(6) 7_445 8 ?
Ni1 Ga1 Ga6 54.45(3) 3 9_455 ?
Ni1 Ga1 Ga6 129.52(9) . 9_455 ?
Ni1 Ga1 Ga6 54.43(3) 2 9_455 ?
Ga6 Ga1 Ga6 97.49(6) 7_445 9_455 ?
Ga6 Ga1 Ga6 97.49(6) 8 9_455 ?
Ni1 Ga1 Ga4 125.66(3) 3 9 ?
Ni1 Ga1 Ga4 51.06(4) . 9 ?
Ni1 Ga1 Ga4 125.56(3) 2 9 ?
Ga6 Ga1 Ga4 82.93(3) 7_445 9 ?
Ga6 Ga1 Ga4 82.85(3) 8 9 ?
Ga6 Ga1 Ga4 179.41(7) 9_455 9 ?
Ni1 Ga1 Ga4 51.06(4) 3 8_445 ?
Ni1 Ga1 Ga4 125.57(3) . 8_445 ?
Ni1 Ga1 Ga4 125.66(3) 2 8_445 ?
Ga6 Ga1 Ga4 82.85(3) 7_445 8_445 ?
Ga6 Ga1 Ga4 179.41(7) 8 8_445 ?
Ga6 Ga1 Ga4 82.93(3) 9_455 8_445 ?
Ga4 Ga1 Ga4 96.73(5) 9 8_445 ?
Ni1 Ga1 Ga4 125.56(3) 3 7_455 ?
Ni1 Ga1 Ga4 125.66(3) . 7_455 ?
Ni1 Ga1 Ga4 51.06(4) 2 7_455 ?
Ga6 Ga1 Ga4 179.41(7) 7_445 7_455 ?
Ga6 Ga1 Ga4 82.93(3) 8 7_455 ?
Ga6 Ga1 Ga4 82.85(3) 9_455 7_455 ?
Ga4 Ga1 Ga4 96.73(5) 9 7_455 ?
Ga4 Ga1 Ga4 96.72(5) 8_445 7_455 ?
Ni1 Ga1 Ga2 110.71(5) 3 . ?
Ni1 Ga1 Ga2 110.71(5) . . ?
Ni1 Ga1 Ga2 110.71(5) 2 . ?
Ga6 Ga1 Ga2 119.76(5) 7_445 . ?
Ga6 Ga1 Ga2 119.76(5) 8 . ?
Ga6 Ga1 Ga2 119.76(5) 9_455 . ?
Ga4 Ga1 Ga2 59.65(3) 9 . ?
Ga4 Ga1 Ga2 59.65(3) 8_445 . ?
Ga4 Ga1 Ga2 59.65(3) 7_455 . ?
Ni1 Ga1 Yb2 69.29(5) 3 . ?
Ni1 Ga1 Yb2 69.29(5) . . ?
Ni1 Ga1 Yb2 69.29(5) 2 . ?
Ga6 Ga1 Yb2 60.24(5) 7_445 . ?
Ga6 Ga1 Yb2 60.24(5) 8 . ?
Ga6 Ga1 Yb2 60.24(5) 9_455 . ?
```

```
Ga4 Ga1 Yb2 120.35(3) 9 . ?
Ga4 Ga1 Yb2 120.35(3) 8_445 . ?
Ga4 Ga1 Yb2 120.35(3) 7_455 . ?
Ga2 Ga1 Yb2 180.0 . . ?
Ni1 Ga2 Ni1 107.26(6) 17 16_445 ?
Ni1 Ga2 Ni1 107.26(6) 17 18_545 ?
Ni1 Ga2 Ni1 107.26(6) 16_445 18_545 ?
Ni1 Ga2 Ga4 126.38(3) 17 9 ?
Ni1 Ga2 Ga4 125.43(3) 16_445 9 ?
Ni1 Ga2 Ga4 51.49(4) 18_545 9 ?
Ni1 Ga2 Ga4 125.43(3) 17 8_445 ?
Ni1 Ga2 Ga4 51.49(4) 16_445 8_445 ?
Ni1 Ga2 Ga4 126.38(3) 18_545 8_445 ?
Ga4 Ga2 Ga4 97.33(5) 9 8_445 ?
Ni1 Ga2 Ga4 51.49(4) 17 7_455 ?
Ni1 Ga2 Ga4 126.38(3) 16_445 7_455 ?
Ni1 Ga2 Ga4 125.44(3) 18_545 7_455 ?
Ga4 Ga2 Ga4 97.33(5) 9 7_455 ?
Ga4 Ga2 Ga4 97.33(5) 8_445 7_455 ?
Ni1 Ga2 Ga6 128.45(9) 17 12_445 ?
Ni1 Ga2 Ga6 53.87(3) 16_445 12_445 ?
Ni1 Ga2 Ga6 54.29(3) 18_545 12_445 ?
Ga4 Ga2 Ga6 82.51(3) 9 12_445 ?
Ga4 Ga2 Ga6 82.91(3) 8_445 12_445 ?
Ga4 Ga2 Ga6 179.73(4) 7_455 12_445 ?
Ni1 Ga2 Ga6 54.29(3) 17 11 ?
Ni1 Ga2 Ga6 128.45(9) 16_445 11 ?
Ni1 Ga2 Ga6 53.87(3) 18_545 11 ?
Ga4 Ga2 Ga6 82.91(3) 9 11 ?
Ga4 Ga2 Ga6 179.73(4) 8_445 11 ?
Ga4 Ga2 Ga6 82.51(3) 7_455 11 ?
Ga6 Ga2 Ga6 97.25(6) 12_445 11 ?
Ni1 Ga2 Ga6 53.87(3) 17 10_455 ?
Ni1 Ga2 Ga6 54.29(3) 16_445 10_455 ?
Ni1 Ga2 Ga6 128.45(9) 18_545 10_455 ?
Ga4 Ga2 Ga6 179.73(4) 9 10_455 ?
Ga4 Ga2 Ga6 82.51(3) 8_445 10_455 ?
Ga4 Ga2 Ga6 82.91(3) 7_455 10_455 ?
Ga6 Ga2 Ga6 97.25(6) 12_445 10_455 ?
Ga6 Ga2 Ga6 97.25(6) 11 10_455 ?
Ni1 Ga2 Ga1 111.60(5) 17 . ?
Ni1 Ga2 Ga1 111.60(5) 16_445 . ?
Ni1 Ga2 Ga1 111.60(5) 18_545 . ?
Ga4 Ga2 Ga1 60.11(3) 9 . ?
Ga4 Ga2 Ga1 60.11(3) 8_445 . ?
Ga4 Ga2 Ga1 60.11(3) 7_455 . ?
Ga6 Ga2 Ga1 119.95(5) 12_445 . ?
Ga6 Ga2 Ga1 119.95(5) 11 . ?
Ga6 Ga2 Ga1 119.95(5) 10_455 . ?
Ni1 Ga2 Yb1 68.40(5) 17 . ?
Ni1 Ga2 Yb1 68.40(5) 16_445 . ?
Ni1 Ga2 Yb1 68.40(5) 18_545 . ?
Ga4 Ga2 Yb1 119.89(3) 9 . ?
Ga4 Ga2 Yb1 119.89(3) 8_445 . ?
Ga4 Ga2 Yb1 119.89(3) 7_455 . ?
Ga6 Ga2 Yb1 60.05(5) 12_445 . ?
Ga6 Ga2 Yb1 60.05(5) 11 . ?
Ga6 Ga2 Yb1 60.05(5) 10_455 . ?
Ga1 Ga2 Yb1 180.0 . . ?
Ni1 Ga3 Ni1 107.54(6) 15_554 13_444 ?
Ni1 Ga3 Ni1 107.54(6) 15_554 14_544 ?
Ni1 Ga3 Ni1 107.54(6) 13_444 14_544 ?
Ni1 Ga3 Ga4 125.32(3) 15_554 3 ?
Ni1 Ga3 Ga4 51.50(4) 13_444 3 ?
Ni1 Ga3 Ga4 126.36(3) 14_544 3 ?
Ni1 Ga3 Ga4 126.36(3) 15_554 . ?
Ni1 Ga3 Ga4 125.32(3) 13_444 . ?
Ni1 Ga3 Ga4 51.50(4) 14_544 . ?
Ga4 Ga3 Ga4 96.98(5) 3 . ?
Ni1 Ga3 Ga4 51.50(4) 15_554 2 ?
Ni1 Ga3 Ga4 126.36(3) 13_444 2 ?
Ni1 Ga3 Ga4 125.32(3) 14_544 2 ?
Ga4 Ga3 Ga4 96.98(5) 3 2 ?
Ga4 Ga3 Ga4 96.98(5) . 2 ?
Ni1 Ga3 Ga6 54.41(3) 15_554 . ?
Ni1 Ga3 Ga6 128.93(9) 13_444 . ?
Ni1 Ga3 Ga6 54.00(3) 14_544 . ?
Ga4 Ga3 Ga6 179.46(6) 3 . ?
Ga4 Ga3 Ga6 82.98(3) . . ?
Ga4 Ga3 Ga6 82.50(3) 2 . ?
Ni1 Ga3 Ga6 54.00(3) 15_554 2 ?
Ni1 Ga3 Ga6 54.41(3) 13_444 2 ?
Ni1 Ga3 Ga6 128.93(9) 14_544 2 ?
Ga4 Ga3 Ga6 82.50(3) 3 2 ?
Ga4 Ga3 Ga6 179.46(6) . 2 ?
Ga4 Ga3 Ga6 82.98(3) 2 2 ?
Ga6 Ga3 Ga6 97.54(6) . 2 ?
Ni1 Ga3 Ga6 128.93(9) 15_554 3 ?
Ni1 Ga3 Ga6 54.00(3) 13_444 3 ?
Ni1 Ga3 Ga6 54.41(3) 14_544 3 ?
Ga4 Ga3 Ga6 82.98(3) 3 3 ?
Ga4 Ga3 Ga6 82.50(3) . 3 ?
Ga4 Ga3 Ga6 179.46(6) 2 3 ?
Ga6 Ga3 Ga6 97.54(6) . 3 ?
Ga6 Ga3 Ga6 97.54(6) 2 3 ?
Ni1 Ga3 Ga3 111.34(5) 15_554 4 ?
Ni1 Ga3 Ga3 111.34(5) 13_444 4 ?
Ni1 Ga3 Ga3 111.34(5) 14_544 4 ?
Ga4 Ga3 Ga3 59.84(4) 3 4 ?
Ga4 Ga3 Ga3 59.84(4) . 4 ?
Ga4 Ga3 Ga3 59.84(4) 2 4 ?
Ga6 Ga3 Ga3 119.73(5) . 4 ?
Ga6 Ga3 Ga3 119.73(5) 2 4 ?
Ga6 Ga3 Ga3 119.73(5) 3 4 ?
Ni1 Ga3 Yb1 68.66(5) 15_554 . ?
Ni1 Ga3 Yb1 68.66(5) 13_444 . ?
Ni1 Ga3 Yb1 68.66(5) 14_544 . ?
Ga4 Ga3 Yb1 120.16(4) 3 . ?
Ga4 Ga3 Yb1 120.16(4) . . ?
Ga4 Ga3 Yb1 120.16(4) 2 . ?
Ga6 Ga3 Yb1 60.27(5) . . ?
Ga6 Ga3 Yb1 60.27(5) 2 . ?
Ga6 Ga3 Yb1 60.27(5) 3 . ?
Ga3 Ga3 Yb1 180.0 4 . ?
Ni1 Ga4 Ni1 179.41(6) 14_544 11 ?
Ni1 Ga4 Ga2 59.72(4) 14_544 10 ?
Ni1 Ga4 Ga2 120.57(4) 11 10 ?
Ni1 Ga4 Ga2 120.57(4) 14_544 13_544 ?
Ni1 Ga4 Ga2 59.73(4) 11 13_544 ?
Ga2 Ga4 Ga2 128.52(4) 10 13_544 ?
Ni1 Ga4 Ga3 119.86(5) 14_544 4 ?
Ni1 Ga4 Ga3 59.55(4) 11 4 ?
Ga2 Ga4 Ga3 128.74(3) 10 4 ?
Ga2 Ga4 Ga3 97.19(4) 13_544 4 ?
Ni1 Ga4 Ga3 59.55(4) 14_544 . ?
Ni1 Ga4 Ga3 119.86(5) 11 . ?
Ga2 Ga4 Ga3 97.19(4) 10 . ?
Ga2 Ga4 Ga3 128.74(3) 13_544 . ?
Ga3 Ga4 Ga3 60.31(7) 4 . ?
Ni1 Ga4 Ga1 119.95(4) 14_544 10 ?
Ni1 Ga4 Ga1 60.34(4) 11 10 ?
Ga2 Ga4 Ga1 60.23(6) 10 10 ?
Ga2 Ga4 Ga1 96.95(5) 13_544 10 ?
Ga3 Ga4 Ga1 96.89(4) 4 10 ?
Ga3 Ga4 Ga1 128.87(3) . 10 ?
Ni1 Ga4 Ga1 60.34(4) 14_544 13_544 ?
Ni1 Ga4 Ga1 119.95(4) 11 13_544 ?
Ga2 Ga4 Ga1 96.95(5) 10 13_544 ?
Ga2 Ga4 Ga1 60.23(6) 13_544 13_544 ?
Ga3 Ga4 Ga1 128.87(3) 4 13_544 ?
Ga3 Ga4 Ga1 96.89(4) . 13_544 ?
Ga1 Ga4 Ga1 128.77(4) 10 13_544 ?
Ga7 Yb1 Ga7 119.998(4) 3 2 ?
Ga7 Yb1 Ga7 119.998(4) 3 . ?
```

Ga7 Yb1 Ga7 119.998(4) 2 . ?
Ga7 Yb1 Ga7 134.65(18) 3 11 ?
Ga7 Yb1 Ga7 105.35(18) 2 11 ?
Ga7 Yb1 Ga7 14.65(18) . 11 ?
Ga7 Yb1 Ga7 14.65(18) 3 12_445 ?
Ga7 Yb1 Ga7 134.65(18) 2 12_445 ?
Ga7 Yb1 Ga7 105.35(18) . 12_445 ?
Ga7 Yb1 Ga7 120.0 11 12_445 ?
Ga7 Yb1 Ga7 105.35(18) 3 10_455 ?
Ga7 Yb1 Ga7 14.65(18) 2 10_455 ?
Ga7 Yb1 Ga7 134.65(18) . 10_455 ?
Ga7 Yb1 Ga7 120.000(2) 11 10_455 ?
Ga7 Yb1 Ga7 119.999(2) 12_445 10_455 ?
Ga7 Yb1 Ga5 135.1(2) 3 15_554 ?
Ga7 Yb1 Ga5 15.1(2) 2 15_554 ?
Ga7 Yb1 Ga5 104.9(2) . 15_554 ?
Ga7 Yb1 Ga5 90.22(16) 11 15_554 ?
Ga7 Yb1 Ga5 149.78(16) 12_445 15_554 ?
Ga7 Yb1 Ga5 29.78(16) 10_455 15_554 ?
Ga7 Yb1 Ga5 15.1(2) 3 13_444 ?
Ga7 Yb1 Ga5 104.9(2) 2 13_444 ?
Ga7 Yb1 Ga5 135.1(2) . 13_444 ?
Ga7 Yb1 Ga5 149.78(16) 11 13_444 ?
Ga7 Yb1 Ga5 29.77(16) 12_445 13_444 ?
Ga7 Yb1 Ga5 90.22(16) 10_455 13_444 ?
Ga5 Yb1 Ga5 120.0 15_554 13_444 ?
Ga7 Yb1 Ga5 104.9(2) 3 14_544 ?
Ga7 Yb1 Ga5 135.1(2) 2 14_544 ?
Ga7 Yb1 Ga5 15.1(2) . 14_544 ?
Ga7 Yb1 Ga5 29.78(16) 11 14_544 ?
Ga7 Yb1 Ga5 90.22(16) 12_445 14_544 ?
Ga7 Yb1 Ga5 149.78(16) 10_455 14_544 ?
Ga5 Yb1 Ga5 120.0 15_554 14_544 ?
Ga5 Yb1 Ga5 120.0 13_444 14_544 ?
Ga7 Yb1 Ga6 66.8(2) 3 12_445 ?
Ga7 Yb1 Ga6 143.51(19) 2 12_445 ?
Ga7 Yb1 Ga6 66.3(2) . 12_445 ?
Ga7 Yb1 Ga6 77.53(14) 11 12_445 ?
Ga7 Yb1 Ga6 55.97(13) 12_445 12_445 ?
Ga7 Yb1 Ga6 140.96(12) 10_455 12_445 ?
Ga5 Yb1 Ga6 140.65(4) 15_554 12_445 ?
Ga5 Yb1 Ga6 78.43(2) 13_444 12_445 ?
Ga5 Yb1 Ga6 55.25(3) 14_544 12_445 ?
Ga7 Yb1 Ga6 143.51(19) 3 11 ?
Ga7 Yb1 Ga6 66.3(2) 2 11 ?
Ga7 Yb1 Ga6 66.8(2) . 11 ?
Ga7 Yb1 Ga6 55.97(13) 11 11 ?
Ga7 Yb1 Ga6 140.96(12) 12_445 11 ?
Ga7 Yb1 Ga6 77.53(14) 10_455 11 ?
Ga5 Yb1 Ga6 55.25(3) 15_554 11 ?
Ga5 Yb1 Ga6 140.65(4) 13_444 11 ?
Ga5 Yb1 Ga6 78.43(2) 14_544 11 ?
Ga6 Yb1 Ga6 87.88(5) 12_445 11 ?
Ga7 Yb1 Ga6 66.3(2) 3 10_455 ?
Ga7 Yb1 Ga6 66.8(2) 2 10_455 ?
Ga7 Yb1 Ga6 143.51(19) . 10_455 ?
Ga7 Yb1 Ga6 140.96(12) 11 10_455 ?
Ga7 Yb1 Ga6 77.53(14) 12_445 10_455 ?
Ga7 Yb1 Ga6 55.97(13) 10_455 10_455 ?
Ga5 Yb1 Ga6 78.43(2) 15_554 10_455 ?
Ga5 Yb1 Ga6 55.25(3) 13_444 10_455 ?
Ga5 Yb1 Ga6 140.65(4) 14_544 10_455 ?
Ga6 Yb1 Ga6 87.88(5) 12_445 10_455 ?
Ga6 Yb1 Ga6 87.88(5) 11 10_455 ?
Ga5 Yb2 Ga5 120.000(1) 3 2 ?
Ga5 Yb2 Ga5 120.000(1) 3 . ?
Ga5 Yb2 Ga5 120.000(2) 2 . ?
Ga5 Yb2 Ga7 134.67(14) 3 17 ?
Ga5 Yb2 Ga7 14.67(14) 2 17 ?
Ga5 Yb2 Ga7 105.33(14) . 17 ?
Ga5 Yb2 Ga7 134.67(14) 3 9 ?
Ga5 Yb2 Ga7 105.33(14) 2 9 ?
Ga5 Yb2 Ga7 14.67(14) . 9 ?
Ga7 Yb2 Ga7 90.7(3) 17 9 ?
Ga5 Yb2 Ga7 14.67(14) 3 16_445 ?
Ga5 Yb2 Ga7 105.33(14) 2 16_445 ?
Ga5 Yb2 Ga7 134.67(15) . 16_445 ?
Ga7 Yb2 Ga7 120.001(2) 17 16_445 ?
Ga7 Yb2 Ga7 149.3(3) 9 16_445 ?
Ga5 Yb2 Ga7 14.67(14) 3 8_445 ?
Ga5 Yb2 Ga7 134.67(15) 2 8_445 ?
Ga5 Yb2 Ga7 105.33(14) . 8_445 ?
Ga7 Yb2 Ga7 149.3(3) 17 8_445 ?
Ga7 Yb2 Ga7 120.001(1) 9 8_445 ?
Ga7 Yb2 Ga7 29.3(3) 16_445 8_445 ?
Ga5 Yb2 Ga7 105.33(14) 3 18_545 ?
Ga5 Yb2 Ga7 134.67(15) 2 18_545 ?
Ga5 Yb2 Ga7 14.67(14) . 18_545 ?
Ga7 Yb2 Ga7 120.000(5) 17 18_545 ?
Ga7 Yb2 Ga7 29.3(3) 9 18_545 ?
Ga7 Yb2 Ga7 119.999(4) 16_445 18_545 ?
Ga7 Yb2 Ga7 90.7(3) 8_445 18_545 ?
Ga5 Yb2 Ga7 105.33(14) 3 7_455 ?
Ga5 Yb2 Ga7 14.67(14) 2 7_455 ?
Ga5 Yb2 Ga7 134.67(15) . 7_455 ?
Ga7 Yb2 Ga7 29.3(3) 17 7_455 ?
Ga7 Yb2 Ga7 120.000(5) 9 7_455 ?
Ga7 Yb2 Ga7 90.7(3) 16_445 7_455 ?
Ga7 Yb2 Ga7 119.999(4) 8_445 7_455 ?
Ga7 Yb2 Ga7 149.3(3) 18_545 7_455 ?
Ga5 Yb2 Ga6 66.50(2) 3 7_445 ?
Ga5 Yb2 Ga6 142.88(3) 2 7_445 ?
Ga5 Yb2 Ga6 66.506(19) . 7_445 ?
Ga7 Yb2 Ga6 140.52(11) 17 7_445 ?
Ga7 Yb2 Ga6 77.80(13) 9 7_445 ?
Ga7 Yb2 Ga6 77.86(13) 16_445 7_445 ?
Ga7 Yb2 Ga6 55.87(13) 8_445 7_445 ?
Ga7 Yb2 Ga6 55.95(12) 18_545 7_445 ?
Ga7 Yb2 Ga6 140.43(11) 7_455 7_445 ?
Ga5 Yb2 Ga6 66.50(2) 3 18_445 ?
Ga5 Yb2 Ga6 66.506(19) 2 18_445 ?
Ga5 Yb2 Ga6 142.88(3) . 18_445 ?
Ga7 Yb2 Ga6 77.80(13) 17 18_445 ?
Ga7 Yb2 Ga6 140.52(11) 9 18_445 ?
Ga7 Yb2 Ga6 55.87(13) 16_445 18_445 ?
Ga7 Yb2 Ga6 77.86(13) 8_445 18_445 ?
Ga7 Yb2 Ga6 140.43(11) 18_545 18_445 ?
Ga7 Yb2 Ga6 55.95(12) 7_455 18_445 ?
Ga6 Yb2 Ga6 133.01(4) 7_445 18_445 ?
Ga5 Yb2 Ga6 142.88(3) 3 16 ?
Ga5 Yb2 Ga6 66.50(2) 2 16 ?
Ga5 Yb2 Ga6 66.51(2) . 16 ?
Ga7 Yb2 Ga6 55.87(13) 17 16 ?
Ga7 Yb2 Ga6 55.95(12) 9 16 ?
Ga7 Yb2 Ga6 140.43(11) 16_445 16 ?
Ga7 Yb2 Ga6 140.52(11) 8_445 16 ?
Ga7 Yb2 Ga6 77.80(13) 18_545 16 ?
Ga7 Yb2 Ga6 77.86(14) 7_455 16 ?
Ga6 Yb2 Ga6 133.01(4) 7_445 16 ?
Ga6 Yb2 Ga6 87.34(5) 18_445 16 ?
Ga4 Ni1 Ga7 159.7(2) 9 9 ?
Ga4 Ni1 Ga7 159.8(2) 9 18_545 ?
Ga7 Ni1 Ga7 36.0(3) 9 18_545 ?
Ga4 Ni1 Ga5 157.21(6) 9 . ?
Ga7 Ni1 Ga5 36.4(2) 9 . ?
Ga7 Ni1 Ga5 36.4(2) 18_545 . ?
Ga4 Ni1 Ga6 101.21(6) 9 9 ?
Ga7 Ni1 Ga6 70.43(17) 9 9 ?
Ga7 Ni1 Ga6 70.44(17) 18_545 9 ?
Ga5 Ni1 Ga6 101.59(8) . 9 ?
Ga4 Ni1 Ga6 100.04(6) 9 8 ?
Ga7 Ni1 Ga6 69.77(17) 9 8 ?
Ga7 Ni1 Ga6 100.1(2) 18_545 8 ?
Ga5 Ni1 Ga6 69.00(5) . 8 ?

Ga6 Ni1 Ga6 117.68(7) 9 8 ?
Ga4 Ni1 Ga6 100.14(6) 9 7_445 ?
Ga7 Ni1 Ga6 100.1(2) 9 7_445 ?
Ga7 Ni1 Ga6 69.78(17) 18_545 7_445 ?
Ga5 Ni1 Ga6 68.99(5) . 7_445 ?
Ga6 Ni1 Ga6 117.67(7) 9 7_445 ?
Ga6 Ni1 Ga6 114.96(6) 8 7_445 ?
Ga4 Ni1 Ga3 68.95(6) 9 7 ?
Ga7 Ni1 Ga3 90.8(2) 9 7 ?
Ga7 Ni1 Ga3 121.00(16) 18_545 7 ?
Ga5 Ni1 Ga3 120.62(6) . 7 ?
Ga6 Ni1 Ga3 67.48(4) 9 7 ?
Ga6 Ni1 Ga3 67.24(4) 8 7 ?
Ga6 Ni1 Ga3 169.00(9) 7_445 7 ?
Ga4 Ni1 Ga2 68.79(6) 9 16_545 ?
Ga7 Ni1 Ga2 121.25(16) 9 16_545 ?
Ga7 Ni1 Ga2 91.1(2) 18_545 16_545 ?
Ga5 Ni1 Ga2 120.85(6) . 16_545 ?
Ga6 Ni1 Ga2 67.58(4) 9 16_545 ?
Ga6 Ni1 Ga2 168.74(9) 8 16_545 ?
Ga6 Ni1 Ga2 67.33(4) 7_445 16_545 ?
Ga3 Ni1 Ga2 108.35(6) 7 16_545 ?
Ga4 Ni1 Ga1 68.60(6) 9 . ?
Ga7 Ni1 Ga1 119.16(17) 9 . ?
Ga7 Ni1 Ga1 119.14(17) 18_545 . ?
Ga5 Ni1 Ga1 88.60(6) . . ?
Ga6 Ni1 Ga1 169.81(10) 9 . ?
Ga6 Ni1 Ga1 65.84(4) 8 . ?
Ga6 Ni1 Ga1 65.84(4) 7_445 . ?
Ga3 Ni1 Ga1 107.39(6) 7 . ?
Ga2 Ni1 Ga1 107.25(6) 16_545 . ?
Ga4 Ni1 Yb1 133.61(4) 9 16_545 ?
Ga7 Ni1 Yb1 59.68(17) 9 16_545 ?
Ga7 Ni1 Yb1 26.26(19) 18_545 16_545 ?
Ga5 Ni1 Yb1 60.00(4) . 16_545 ?
Ga6 Ni1 Yb1 61.53(4) 9 16_545 ?
Ga6 Ni1 Yb1 126.31(7) 8 16_545 ?
Ga6 Ni1 Yb1 61.41(4) 7_445 16_545 ?
Ga3 Ni1 Yb1 126.94(5) 7 16_545 ?
Ga2 Ni1 Yb1 64.83(5) 16_545 16_545 ?
Ga1 Ni1 Yb1 125.22(4) . 16_545 ?
Ga4 Ni1 Yb1 133.63(4) 9 7 ?
Ga7 Ni1 Yb1 26.1(2) 9 7 ?
Ga7 Ni1 Yb1 59.55(17) 18_545 7 ?
Ga5 Ni1 Yb1 59.90(4) . 7 ?
Ga6 Ni1 Yb1 61.56(4) 9 7 ?
Ga6 Ni1 Yb1 61.44(4) 8 7 ?
Ga6 Ni1 Yb1 126.19(7) 7_445 7 ?
Ga3 Ni1 Yb1 64.68(5) 7 7 ?
Ga2 Ni1 Yb1 127.10(5) 16_545 7 ?
Ga1 Ni1 Yb1 125.22(5) . 7 ?
Yb1 Ni1 Yb1 78.73(3) 16_545 7 ?
Ni1 Ga6 Ni1 115.85(7) 14_544 15_554 ?
Ni1 Ga6 Ni1 115.86(7) 14_544 13_554 ?
Ni1 Ga6 Ni1 118.61(7) 15_554 13_554 ?
Ni1 Ga6 Ga1 139.72(9) 14_544 13_554 ?
Ni1 Ga6 Ga1 59.72(4) 15_554 13_554 ?
Ni1 Ga6 Ga1 59.72(4) 13_554 13_554 ?
Ni1 Ga6 Ga5 134.26(7) 14_544 15_554 ?
Ni1 Ga6 Ga5 55.14(4) 15_554 15_554 ?
Ni1 Ga6 Ga5 104.30(6) 13_554 15_554 ?
Ga1 Ga6 Ga5 79.25(4) 13_554 15_554 ?
Ni1 Ga6 Ga5 134.26(7) 14_544 13_554 ?
Ni1 Ga6 Ga5 104.30(6) 15_554 13_554 ?
Ni1 Ga6 Ga5 55.13(4) 13_554 13_554 ?
Ga1 Ga6 Ga5 79.25(4) 13_554 13_554 ?
Ga5 Ga6 Ga5 56.85(7) 15_554 13_554 ?
Ni1 Ga6 Ga7 103.56(18) 14_544 2 ?
Ni1 Ga6 Ga7 54.27(14) 15_554 2 ?
Ni1 Ga6 Ga7 135.01(17) 13_554 2 ?
Ga1 Ga6 Ga7 102.74(16) 13_554 2 ?
Ga5 Ga6 Ga7 31.63(19) 15_554 2 ?
Ga5 Ga6 Ga7 82.15(14) 13_554 2 ?
Ni1 Ga6 Ga7 103.57(18) 14_544 12 ?
Ni1 Ga6 Ga7 134.97(17) 15_554 12 ?
Ni1 Ga6 Ga7 54.35(14) 13_554 12 ?
Ga1 Ga6 Ga7 102.77(16) 13_554 12 ?
Ga5 Ga6 Ga7 82.08(15) 15_554 12 ?
Ga5 Ga6 Ga7 31.61(19) 13_554 12 ?
Ga7 Ga6 Ga7 97.24(19) 2 12 ?
Ni1 Ga6 Ga3 58.52(4) 14_544 . ?
Ni1 Ga6 Ga3 58.35(4) 15_554 . ?
Ni1 Ga6 Ga3 139.81(9) 13_554 . ?
Ga1 Ga6 Ga3 97.76(6) 13_554 . ?
Ga5 Ga6 Ga3 103.05(5) 15_554 . ?
Ga5 Ga6 Ga3 159.90(6) 13_554 . ?
Ga7 Ga6 Ga3 79.13(14) 2 . ?
Ga7 Ga6 Ga3 159.44(17) 12 . ?
Ni1 Ga6 Ga2 58.55(4) 14_544 10 ?
Ni1 Ga6 Ga2 139.58(9) 15_554 10 ?
Ni1 Ga6 Ga2 58.38(4) 13_554 10 ?
Ga1 Ga6 Ga2 97.61(6) 13_554 10 ?
Ga5 Ga6 Ga2 160.03(6) 15_554 10 ?
Ga5 Ga6 Ga2 103.19(5) 13_554 10 ?
Ga7 Ga6 Ga2 159.61(17) 2 10 ?
Ga7 Ga6 Ga2 79.40(15) 12 10 ?
Ga3 Ga6 Ga2 96.91(6) . 10 ?
Ni1 Ga6 Ga7 54.23(15) 14_544 . ?
Ni1 Ga6 Ga7 103.27(18) 15_554 . ?
Ni1 Ga6 Ga7 133.40(17) 13_554 . ?
Ga1 Ga6 Ga7 160.31(18) 13_554 . ?
Ga5 Ga6 Ga7 82.59(15) 15_554 . ?
Ga5 Ga6 Ga7 97.15(14) 13_554 . ?
Ga7 Ga6 Ga7 57.6(3) 2 . ?
Ga7 Ga6 Ga7 82.09(6) 12 . ?
Ga3 Ga6 Ga7 78.92(14) . . ?
Ga2 Ga6 Ga7 102.06(17) 10 . ?
Ni1 Ga6 Ga7 54.31(14) 14_544 11 ?
Ni1 Ga6 Ga7 133.36(17) 15_554 11 ?
Ni1 Ga6 Ga7 103.27(18) 13_554 11 ?
Ga1 Ga6 Ga7 160.26(18) 13_554 11 ?
Ga5 Ga6 Ga7 97.06(13) 15_554 11 ?
Ga5 Ga6 Ga7 82.53(15) 13_554 11 ?
Ga7 Ga6 Ga7 82.09(6) 2 11 ?
Ga7 Ga6 Ga7 57.5(3) 12 11 ?
Ga3 Ga6 Ga7 101.95(17) . 11 ?
Ga2 Ga6 Ga7 79.18(13) 10 11 ?
Ga7 Ga6 Ga7 30.8(3) . 11 ?
Ga7 Ga5 Ga7 58.9(5) 9 18_545 ?
Ga7 Ga5 Yb2 150.6(2) 9 . ?
Ga7 Ga5 Yb2 150.6(3) 18_545 . ?
Ga7 Ga5 Ni1 71.0(2) 9 4_556 ?
Ga7 Ga5 Ni1 70.8(2) 18_545 4_556 ?
Yb2 Ga5 Ni1 112.11(4) . 4_556 ?
Ga7 Ga5 Ni1 70.8(2) 9 . ?
Ga7 Ga5 Ni1 71.0(2) 18_545 . ?
Yb2 Ga5 Ni1 112.11(4) . . ?
Ni1 Ga5 Ni1 135.78(9) 4_556 . ?
Ga7 Ga5 Ga5 179.4(3) 9 3 ?
Ga7 Ga5 Ga5 120.6(3) 18_545 3 ?
Yb2 Ga5 Ga5 30.0 . 3 ?
Ni1 Ga5 Ga5 109.02(4) 4_556 3 ?
Ni1 Ga5 Ga5 109.03(4) . 3 ?
Ga7 Ga5 Ga5 120.6(2) 9 2 ?
Ga7 Ga5 Ga5 179.4(3) 18_545 2 ?
Yb2 Ga5 Ga5 30.0 . 2 ?
Ni1 Ga5 Ga5 109.03(4) 4_556 2 ?
Ni1 Ga5 Ga5 109.02(4) . 2 ?
Ga5 Ga5 Ga5 60.0 3 2 ?
Ga7 Ga5 Ga6 118.1(2) 9 17_545 ?
Ga7 Ga5 Ga6 74.6(2) 18_545 17_545 ?
Yb2 Ga5 Ga6 83.23(4) . 17_545 ?
Ni1 Ga5 Ga6 55.87(4) 4_556 17_545 ?
Ni1 Ga5 Ga6 130.54(4) . 17_545 ?

Ga5 Ga5 Ga6 61.58(4) 3 17_545 ?
Ga5 Ga5 Ga6 105.76(4) 2 17_545 ?
Ga7 Ga5 Ga6 74.6(2) 9 8 ?
Ga7 Ga5 Ga6 118.1(2) 18_545 8 ?
Yb2 Ga5 Ga6 83.22(4) . 8 ?
Ni1 Ga5 Ga6 130.54(4) 4_556 8 ?
Ni1 Ga5 Ga6 55.87(4) . 8 ?
Ga5 Ga5 Ga6 105.76(4) 3 8 ?
Ga5 Ga5 Ga6 61.58(4) 2 8 ?
Ga6 Ga5 Ga6 166.45(7) 17_545 8 ?
Ga7 Ga5 Ga6 74.7(2) 9 16 ?
Ga7 Ga5 Ga6 118.0(2) 18_545 16 ?
Yb2 Ga5 Ga6 83.22(4) . 16 ?
Ni1 Ga5 Ga6 55.88(4) 4_556 16 ?
Ni1 Ga5 Ga6 130.52(4) . 16 ?
Ga5 Ga5 Ga6 105.76(4) 3 16 ?
Ga5 Ga5 Ga6 61.57(4) 2 16 ?
Ga6 Ga5 Ga6 96.78(7) 17_545 16 ?
Ga6 Ga5 Ga6 81.61(7) 8 16 ?
Ga7 Ga5 Ga6 118.0(2) 9 7_445 ?
Ga7 Ga5 Ga6 74.7(2) 18_545 7_445 ?
Yb2 Ga5 Ga6 83.22(4) . 7_445 ?
Ni1 Ga5 Ga6 130.52(4) 4_556 7_445 ?
Ni1 Ga5 Ga6 55.88(4) . 7_445 ?
Ga5 Ga5 Ga6 61.57(4) 3 7_445 ?
Ga5 Ga5 Ga6 105.76(3) 2 7_445 ?
Ga6 Ga5 Ga6 81.61(7) 17_545 7_445 ?
Ga6 Ga5 Ga6 96.78(7) 8 7_445 ?
Ga6 Ga5 Ga6 166.45(7) 16 7_445 ?
Ga7 Ga5 Yb1 15.5(3) 9 7 ?
Ga7 Ga5 Yb1 74.4(2) 18_545 7 ?
Yb2 Ga5 Yb1 135.07(2) . 7 ?
Ni1 Ga5 Yb1 74.47(4) 4_556 7 ?
Ni1 Ga5 Yb1 74.63(4) . 7 ?
Ga5 Ga5 Yb1 165.07(2) 3 7 ?
Ga5 Ga5 Yb1 105.07(2) 2 7 ?
Ga6 Ga5 Yb1 127.63(5) 17_545 7 ?
Ga6 Ga5 Yb1 63.67(3) 8 7 ?
Ga6 Ga5 Yb1 63.54(3) 16 7 ?
Ga6 Ga5 Yb1 127.78(5) 7_445 7 ?
Ga7 Ga7 Ga5 60.6(2) 11 14_544 ?
Ga7 Ga7 Yb1 150.1(2) 11 . ?
Ga5 Ga7 Yb1 149.4(5) 14_544 . ?
Ga7 Ga7 Ni1 72.2(4) 11 14_544 ?
Ga5 Ga7 Ni1 72.8(3) 14_544 14_544 ?
Yb1 Ga7 Ni1 110.8(3) . 14_544 ?
Ga7 Ga7 Ni1 71.8(4) 11 18_545 ?
Ga5 Ga7 Ni1 72.7(2) 14_544 18_545 ?
Yb1 Ga7 Ni1 110.2(3) . 18_545 ?
Ni1 Ga7 Ni1 138.9(4) 14_544 18_545 ?
Ga7 Ga7 Ga7 179.8(4) 11 3 ?
Ga5 Ga7 Ga7 119.4(5) 14_544 3 ?
Yb1 Ga7 Ga7 30.001(2) . 3 ?
Ni1 Ga7 Ga7 108.0(2) 14_544 3 ?
Ni1 Ga7 Ga7 108.0(2) 18_545 3 ?
Ga7 Ga7 Ga7 120.1(2) 11 2 ?
Ga5 Ga7 Ga7 179.4(5) 14_544 2 ?
Yb1 Ga7 Ga7 30.001(2) . 2 ?
Ni1 Ga7 Ga7 107.4(2) 14_544 2 ?
Ni1 Ga7 Ga7 107.4(2) 18_545 2 ?
Ga7 Ga7 Ga7 60.0 3 2 ?
Ga7 Ga7 Ga6 118.7(4) 11 3 ?
Ga5 Ga7 Ga6 73.8(2) 14_544 3 ?
Yb1 Ga7 Ga6 83.4(3) . 3 ?
Ni1 Ga7 Ga6 55.96(13) 14_544 3 ?
Ni1 Ga7 Ga6 131.1(3) 18_545 3 ?
Ga7 Ga7 Ga6 61.4(2) 3 3 ?
Ga7 Ga7 Ga6 105.8(2) 2 3 ?
Ga7 Ga7 Ga6 118.3(4) 11 12_445 ?
Ga5 Ga7 Ga6 73.7(2) 14_544 12_445 ?
Yb1 Ga7 Ga6 83.0(3) . 12_445 ?
Ni1 Ga7 Ga6 131.2(3) 14_544 12_445 ?
Ni1 Ga7 Ga6 55.87(12) 18_545 12_445 ?
Ga7 Ga7 Ga6 61.5(2) 3 12_445 ?
Ga7 Ga7 Ga6 105.8(2) 2 12_445 ?
Ga6 Ga7 Ga6 81.16(18) 3 12_445 ?
Ga7 Ga7 Ga6 74.7(3) 11 . ?
Ga5 Ga7 Ga6 119.5(3) 14_544 . ?
Yb1 Ga7 Ga6 82.9(3) . . ?
Ni1 Ga7 Ga6 55.34(12) 14_544 . ?
Ni1 Ga7 Ga6 130.0(3) 18_545 . ?
Ga7 Ga7 Ga6 105.5(2) 3 . ?
Ga7 Ga7 Ga6 61.0(3) 2 . ?
Ga6 Ga7 Ga6 97.42(18) 3 . ?
Ga6 Ga7 Ga6 166.0(3) 12_445 . ?
Ga7 Ga7 Ga6 74.4(3) 11 11 ?
Ga5 Ga7 Ga6 119.3(3) 14_544 11 ?
Yb1 Ga7 Ga6 82.6(3) . 11 ?
Ni1 Ga7 Ga6 130.1(3) 14_544 11 ?
Ni1 Ga7 Ga6 55.25(13) 18_545 11 ?
Ga7 Ga7 Ga6 105.5(2) 3 11 ?
Ga7 Ga7 Ga6 61.0(2) 2 11 ?
Ga6 Ga7 Ga6 166.0(3) 3 11 ?
Ga6 Ga7 Ga6 97.25(18) 12_445 11 ?
Ga6 Ga7 Ga6 80.71(18) . 11 ?
Ga7 Ga7 Yb1 15.29(15) 11 10 ?
Ga5 Ga7 Yb1 75.9(3) 14_544 10 ?
Yb1 Ga7 Yb1 134.8(4) . 10 ?
Ni1 Ga7 Yb1 75.26(19) 14_544 10 ?
Ni1 Ga7 Yb1 75.34(19) 18_545 10 ?
Ga7 Ga7 Yb1 164.8(4) 3 10 ?
Ga7 Ga7 Yb1 104.8(4) 2 10 ?
Ga6 Ga7 Yb1 128.0(3) 3 10 ?
Ga6 Ga7 Yb1 128.0(3) 12_445 10 ?
Ga6 Ga7 Yb1 63.55(13) . 10 ?
Ga6 Ga7 Yb1 63.63(14) 11 10 ?

_diffrn_measured_fraction_theta_max 0.980
_diffrn_reflns_theta_full 30.00
_diffrn_measured_fraction_theta_full 0.980
_refine_diff_density_max 4.106
_refine_diff_density_min -4.389
_refine_diff_density_rms 0.599

APPENDIX 3 – LETTERS OF PERMISSION

ELSEVIER LICENSE
TERMS AND CONDITIONS

Feb 01, 2010

Supplier	Elsevier Limited The Boulevard,Langford Lane Kidlington,Oxford,OX5 1GB,UK
Registered Company Number	1982084
Customer name	Kandace R Thomas
Customer address	232 Choppin Hall Baton Rouge, LA 70803
License Number	2360270048606
License date	Feb 01, 2010
Licensed content publisher	Elsevier
Licensed content publication	Journal of Crystal Growth
Licensed content title	Crystal growth and physical properties of Ln_2MGa_{12} (Ln=Pr, Nd, and Sm; M=Ni, Cu)
Licensed content author	Kandace R. Thomas, Jung Young Cho, Jasmine N. Millican, Richard D. Hembree, M. Moldovan, Amar Karki, D.P. Young, Julia Y. Chan
Licensed content date	28 December 2009
Volume number	n/a
Issue number	n/a
Pages	1
Type of Use	Thesis / Dissertation
Portion	Full article
Format	Both print and electronic

You are an author of the Elsevier article	Yes
Are you translating?	No
Order Reference Number	
Expected publication date	
Elsevier VAT number	GB 494 6272 12
Permissions price	0.00 USD
Value added tax 0.0%	0.00 USD
Total	0.00 USD

Terms and Conditions

INTRODUCTION

1. The publisher for this copyrighted material is Elsevier. By clicking "accept" in connection with completing this licensing transaction, you agree that the following terms and conditions apply to this transaction (along with the Billing and Payment terms and conditions established by Copyright Clearance Center, Inc. ("CCC"), at the time that you opened your Rightslink account and that are available at any time at http://myaccount.copyright.com).

GENERAL TERMS

2. Elsevier hereby grants you permission to reproduce the aforementioned material subject to the terms and conditions indicated.

3. Acknowledgement: If any part of the material to be used (for example, figures) has appeared in our publication with credit or acknowledgement to another source, permission must also be sought from that source. If such permission is not obtained then that material may not be included in your publication/copies. Suitable acknowledgement to the source must be made, either as a footnote or in a reference list at the end of your publication, as follows:

"Reprinted from Publication title, Vol /edition number, Author(s), Title of article / title of chapter, Pages No., Copyright (Year), with permission from Elsevier [OR APPLICABLE SOCIETY COPYRIGHT OWNER]." Also Lancet special credit - "Reprinted from The Lancet, Vol. number, Author(s), Title of article, Pages No., Copyright (Year), with permission from Elsevier."

4. Reproduction of this material is confined to the purpose and/or media for which permission is hereby given.

5. Altering/Modifying Material: Not Permitted. However figures and illustrations may be altered/adapted minimally to serve your work. Any other abbreviations, additions, deletions and/or any other alterations shall be made only with prior written authorization of Elsevier

Ltd. (Please contact Elsevier at permissions@elsevier.com)

6. If the permission fee for the requested use of our material is waived in this instance, please be advised that your future requests for Elsevier materials may attract a fee.

7. Reservation of Rights: Publisher reserves all rights not specifically granted in the combination of (i) the license details provided by you and accepted in the course of this licensing transaction, (ii) these terms and conditions and (iii) CCC's Billing and Payment terms and conditions.

8. License Contingent Upon Payment: While you may exercise the rights licensed immediately upon issuance of the license at the end of the licensing process for the transaction, provided that you have disclosed complete and accurate details of your proposed use, no license is finally effective unless and until full payment is received from you (either by publisher or by CCC) as provided in CCC's Billing and Payment terms and conditions. If full payment is not received on a timely basis, then any license preliminarily granted shall be deemed automatically revoked and shall be void as if never granted. Further, in the event that you breach any of these terms and conditions or any of CCC's Billing and Payment terms and conditions, the license is automatically revoked and shall be void as if never granted. Use of materials as described in a revoked license, as well as any use of the materials beyond the scope of an unrevoked license, may constitute copyright infringement and publisher reserves the right to take any and all action to protect its copyright in the materials.

9. Warranties: Publisher makes no representations or warranties with respect to the licensed material.

10. Indemnity: You hereby indemnify and agree to hold harmless publisher and CCC, and their respective officers, directors, employees and agents, from and against any and all claims arising out of your use of the licensed material other than as specifically authorized pursuant to this license.

11. No Transfer of License: This license is personal to you and may not be sublicensed, assigned, or transferred by you to any other person without publisher's written permission.

12. No Amendment Except in Writing: This license may not be amended except in a writing signed by both parties (or, in the case of publisher, by CCC on publisher's behalf).

13. Objection to Contrary Terms: Publisher hereby objects to any terms contained in any purchase order, acknowledgment, check endorsement or other writing prepared by you, which terms are inconsistent with these terms and conditions or CCC's Billing and Payment terms and conditions. These terms and conditions, together with CCC's Billing and Payment terms and conditions (which are incorporated herein), comprise the entire agreement between you and publisher (and CCC) concerning this licensing transaction. In the event of any conflict between your obligations established by these terms and conditions and those established by CCC's Billing and Payment terms and conditions, these terms and

conditions shall control.

14. Revocation: Elsevier or Copyright Clearance Center may deny the permissions described in this License at their sole discretion, for any reason or no reason, with a full refund payable to you. Notice of such denial will be made using the contact information provided by you. Failure to receive such notice will not alter or invalidate the denial. In no event will Elsevier or Copyright Clearance Center be responsible or liable for any costs, expenses or damage incurred by you as a result of a denial of your permission request, other than a refund of the amount(s) paid by you to Elsevier and/or Copyright Clearance Center for denied permissions.

LIMITED LICENSE

The following terms and conditions apply only to specific license types:

15. **Translation**: This permission is granted for non-exclusive world **English** rights only unless your license was granted for translation rights. If you licensed translation rights you may only translate this content into the languages you requested. A professional translator must perform all translations and reproduce the content word for word preserving the integrity of the article. If this license is to re-use 1 or 2 figures then permission is granted for non-exclusive world rights in all languages.

16. **Website**: The following terms and conditions apply to electronic reserve and author websites:
Electronic reserve: If licensed material is to be posted to website, the web site is to be password-protected and made available only to bona fide students registered on a relevant course if:
This license was made in connection with a course,
This permission is granted for 1 year only. You may obtain a license for future website posting,
All content posted to the web site must maintain the copyright information line on the bottom of each image,
A hyper-text must be included to the Homepage of the journal from which you are licensing at http://www.sciencedirect.com/science/journal/xxxxx or the Elsevier homepage for books at http://www.elsevier.com , and
Central Storage: This license does not include permission for a scanned version of the material to be stored in a central repository such as that provided by Heron/XanEdu.

17. **Author website** for journals with the following additional clauses:

All content posted to the web site must maintain the copyright information line on the bottom of each image, and
he permission granted is limited to the personal version of your paper. You are not allowed to download and post the published electronic version of your article (whether PDF or HTML, proof or final version), nor may you scan the printed edition to create an electronic version,

A hyper-text must be included to the Homepage of the journal from which you are licensing at http://www.sciencedirect.com/science/journal/xxxxx , As part of our normal production process, you will receive an e-mail notice when your article appears on Elsevier's online service ScienceDirect (www.sciencedirect.com). That e-mail will include the article's Digital Object Identifier (DOI). This number provides the electronic link to the published article and should be included in the posting of your personal version. We ask that you wait until you receive this e-mail and have the DOI to do any posting.
Central Storage: This license does not include permission for a scanned version of the material to be stored in a central repository such as that provided by Heron/XanEdu.

18. **Author website** for books with the following additional clauses:
Authors are permitted to place a brief summary of their work online only.
A hyper-text must be included to the Elsevier homepage at http://www.elsevier.com

All content posted to the web site must maintain the copyright information line on the bottom of each image
You are not allowed to download and post the published electronic version of your chapter, nor may you scan the printed edition to create an electronic version.
Central Storage: This license does not include permission for a scanned version of the material to be stored in a central repository such as that provided by Heron/XanEdu.

19. **Website** (regular and for author): A hyper-text must be included to the Homepage of the journal from which you are licensing at http://www.sciencedirect.com/science/journal/xxxxx. or for books to the Elsevier homepage at http://www.elsevier.com

20. **Thesis/Dissertation**: If your license is for use in a thesis/dissertation your thesis may be submitted to your institution in either print or electronic form. Should your thesis be published commercially, please reapply for permission. These requirements include permission for the Library and Archives of Canada to supply single copies, on demand, of the complete thesis and include permission for UMI to supply single copies, on demand, of the complete thesis. Should your thesis be published commercially, please reapply for permission.

21. **Other Conditions**: Please note that as one of the Authors of this article, you retain the right to include the journal article, in full or in part, in a thesis or dissertation. You do not require permission to do so.

v1.6

Gratis licenses (referencing $0 in the Total field) are free. Please retain this printable license for your reference. No payment is required.

If you would like to pay for this license now, please remit this license along with your payment made payable to "COPYRIGHT CLEARANCE CENTER" otherwise you will be invoiced within 48 hours of the license date. Payment should be in the form of a check or money order referencing your account number and this invoice number RLNK10728386.
Once you receive your invoice for this order, you may pay your invoice by credit card. Please follow instructions provided at that time.

Make Payment To:
Copyright Clearance Center
Dept 001
P.O. Box 843006
Boston, MA 02284-3006

If you find copyrighted material related to this license will not be used and wish to cancel, please contact us referencing this license number 2360270048606 and noting the reason for cancellation.

Questions? customercare@copyright.com or +1-877-622-5543 (toll free in the US) or +1-978-646-2777.

VITA

Kandace Renee Thomas was born in August 1983 to her parents, Shermaine M. Thomas and Kemp Thomas, III, in Baton Rouge, Louisiana. She has a large, mixed family that consists of three older brothers, two older sisters, two younger sisters, and two younger brothers. Kandace graduated high school in 2001 from Scotlandville Magnet High School in Baton Rouge, Louisiana. She continued her education at Southern University and A&M College and earned a Bachelor of Science degree in chemistry in 2005.

Kandace began her graduate career at Louisiana State University and A&M College in 2005. Her dissertation work will be completed under the direction of Dr. Julia Chan on the study of ternary intermetallic systems. Kandace has earned several fellowships and awards during her graduate career: supplemental Bridge to Doctoral Fellowship (2005–2007), Bridge to Doctoral Fellowship (2007-2008), Graduate Alliance for Education in Louisiana Supplement (2008), Sigma-Xi Grant-in-Aid Award (2009), and the Louisiana State University GK-12 Fellowship (2009-2010). She has attended and presented at several conferences: Southern Regional Education Board Meeting in Arlington, Virginia (2005), 57th Annual Meeting of Nobel Laureates in Lindau, Germany (2007), International Center for Materials Research – Jawaharlal Nehru Centre for Advanced Scientific Research Winter School in Bangalore, India (2007), National Science Foundation Joint Annual Meeting in Washington, D.C. (2007 and 2008), Gordon Research Conference: Solid State Chemistry in New London, New Hampshire (2008), and Summer School on Methods and Applications of Neutron Spectroscopy at the National Institute for Standards and Technology Center for Neutron Research in Gaithersburg, Maryland (2009). During her time in the LSU Chemistry Department she served as an officer on the 2006-2007 Chemistry Graduate Student Council and volunteered numerous times for K-12 science education outreach.

Kandace will graduate from Louisiana State University in December 2010 and will be awarded a Doctor of Philosophy degree in chemistry.